# Elucidating the spatial organization and control of information processing in cell signalling networks: *from network and enzymatic building blocks to concrete systems*

A thesis presented for the degree of

Doctor of Philosophy of the University of London

and the

Diploma of Imperial College

by

**Aiman Alam Nazki**

Department of Chemical Engineering

Imperial College

180 Queen's Gate, London SW7 2AZ

FEBRUARY 20, 2015

I certify that this thesis, and the research to which it refers, are the product of my own work, and that any ideas or quotations from the work of other people, published or otherwise, are fully acknowledged in accordance with the standard referencing practices of the discipline.

Signed:

# Copyright

# Abstract

Cells function and survive by making decisions in response to dynamic environments. The core controllers of decision-making are highly complex intracellular networks of proteins and genes, which harbour sophisticated information processing capabilities. The effect of spatial organization and control of signaling networks is typically ignored. However, the role of space in signalling networks is being increasingly recognized. While there are some experimental and modelling efforts that incorporate spatial aspects in specific cellular contexts, the role of spatial regulation of signalling across different cell networks remains largely unexplored.

In this thesis, we utilize a combination of mathematical modeling, systems engineering and *in silico* synthetic approaches to understand the spatial organization and control of signaling networks at multiple levels. We examine spatial effects in representative networks and enzymatic building blocks, including typical network modules, covalent modification cycles and enzymatic modification cascades and pathways. We complement these studies by dissecting the role of spatial regulation in the concrete context of the *Caulobacter* cell cycle, which involves specific combinations of these building blocks. In another investigation, we examine the organization of spatially regulated signaling networks underlying chemotaxis.

We explicitly examine the effects of diffusion and its interplay with spatially varying signals and localization/compartmentalization of signalling entities and gain key insights into the interplay of these factors. At the network level, examining typical network modules reveals how introduction of diffusion/global entities may significantly distort temporal characteristics and introduce new types of signal transduction characteristics. At the enzymatic level, dissecting spatial regulation in enzymatic modules highlights the subtle effect and new facets that arise due to the interweaving of cycle kinetics and diffusion. The various ways in which spatial compartmentalization affects pathway behaviour is revealed in the study of various types of signaling pathways. The study of spatial regulation of these enzymatic/network building blocks provides a systematic basis for understanding how spatial control can affect the spatiotemporal interactions driving *Caulobacter* cell cycle and we use an *in-silico* synthetic approach to create a platform for further understanding the functioning of the networks controlling this process. In a different study, we use a design approach to shed light on different signalling configurations of chemotactic networks that allow cells to exhibit both attractive and repulsive behaviour, in light of known signalling

characteristics seen in cells.

Our results uncover the various capabilities, constraints and trade-offs associated with the spatial control of information processing in signalling networks, which come to the surface only if spatial factors are explicitly considered. Overall, using a focused multipronged approach reveals different facets of spatial regulation of signalling at multiple levels and in different contexts. Combining mathematical modelling, systems engineering and synthetic design approaches creates a powerful framework, which may be used to elucidate spatial control of information processing in multiple contexts and design synthetic systems that could fruitfully exploit spatial organization and regulation.

# Acknowledgements

First and foremost I would like to thank God for allowing me to embark on this journey of experiencing a postgraduate education.

There are of course many people I would like to thank. Dr. Krishnan, my supervisor, has given me the most interesting set of problems to work on. I would like to thank him for spending time teaching and advising me and also making my educational experience a holistic one. Most of all I would like to thank him for being a good person and for the extensive support that he has provided.

I am extremely grateful to my husband Tawseef for the love, kindness and support he has shown me. Thanks to him I have remained focused and balanced through out this process. Without him this journey would have been very isolating. I would like to thank the rest of my family- Appea for giving me excellent advice and encouragement and always being perceptive of my needs. My in-laws and my parents have given me boundless love and a strong shoulder to lean on.

My Imperial family has helped me tremendously in so many different aspects- from my research to my general well being. There are many people I would like to thank- a few are- Ios, Daniel, Cong, Phil and Naveed. I would like to thank Prof. Nilay Shah for his support as well.

Last but not the least- I would like to thank all my friends, especially Shikhs, Shams, LZM- for the laughs and for helping me keep my chin up!

# Table of contents

# List of Figures

# List of Tables

# List of papers

Some of the research presented in this thesis can also be found in the following list of publications:

- J. Krishnan and A. Alam-Nazki. An investigation of design principles underlying repulsive and attractive gradient sensing and their switching. *Journal of theoretical biology*, 2011, 273:80-99
- A. Alam-Nazki and J. Krishnan. An investigation of spatial signal transduction in cellular networks. *BMC Systems Biology*, 2012, 6:83.
- A. Alam-Nazki and J. Krishnan. Covalent Modification Cycles through the Spatial Prism. *Biophysical Journal*, 2013, 105:1720-1731.
- A. Alam-Nazki and J. Krishnan. Spatial control of chemical modification cascades and pathways. *Biophysical Journal, (under revision)*, 2014.

# Chapter 1

# Introduction

The survival of an organism is dictated by the behaviour of its cells. Cellular behaviour is driven by a multitude of cellular processes that are governed by a tightly orchestrated web of interacting biochemical/biomolecular networks. Some examples of fundamental cellular responses or processes are cell division, proliferation and growth. When networks malfunction, processes encounter problems, which may lead to the improper functioning of cells or even a diseased state for the organism. Hence understanding the structure and dynamics of biological networks is a vital area of research in biology and biological engineering and has wide ranging applications in therapeutics, health care and biotechnology.

The sheer number of entities interacting in any given biological network and the highly interconnected nature between different networks makes them extremely complex to discern as a whole. The interactions between entities are intricate, non-linear, may harbour stochastic characteristics and are spatially distributed. Unlike man-made networks, biological networks are a product of evolution; and the logic underlying their organization may not be easy to understand. Furthermore, these networks also have the ability to continually evolve (Purnick and Weiss, 2009). However given the important role of these networks, understanding how they are organized and function is an important goal in biological research (Marks et al., 2009).

Networks may be classified at different levels in the organism (at the level of cells, multi-cells, tissues, organs, etc.) but here our main focus is on intra-cellular networks. A key feature of cellular networks is that they integrate signals from the cells environment (or from within the cell) and process them to give the appropriate response- this is known as signal transduction. Understanding how cellular network interactions are organized gives

key insights into how information is processed from various signals and decisions are made. Signals maybe of various forms, for example chemical, electrical and mechanical. Chemotaxis is an example of a process where a cell makes a decision to migrate either towards or away from a chemical signal. The underlying chemotactic networks receive the signal, process the 'information' and enable the cell to respond accordingly. This may result in, for example, the cell moving away from a toxin or towards a food source, depending on the signal(s) encountered (Eisenbach et al., 2004).

The fibroblast growth factor (FGF) signalling network is an example where a multitude of outcomes are possible once signal information is received and processed (Turner and Grose, 2010). FGF signals are known to induce cell proliferation, migration or even attenuate the cell cycle. There may be a number of factors that determine the kind of response achieved, such as, the nature of the signal and the states of the external and internal environments of the cell. Furthermore, this signalling network interacts with multiple downstream signalling networks and these in turn may regulate different gene regulatory networks. This example illustrates that information processing that leads to decision making is dependent on a variety of factors and maybe controlled by a highly interconnected web of complex networks, which are organized at multiple levels within the cell.

Unraveling the complexity of cellular networks and the functioning of cellular processes is the main goal of the interdisciplinary field of research known as Systems Biology. The research arises through a combination of experiments and mathematical modelling/computational studies and associated theoretical work. The collaborative efforts of experimentalists and engineers/mathematicians/physicists/computational scientists are also an important aspect of how research is conducted in systems biology. The emphasis here is on developing models to predict behaviour and working in an iterative fashion with experimentalists to refine the model. Various theoretical methodologies and tools are used in this discipline, ranging from dynamical systems theory, systems engineering, control engineering and information theory, to biophysical approaches and stochastic analysis (and associated computational methodologies). Complementary approaches associated with bioinformatics utilize other computational tools to identify and screen for genes from large sets of experimental data (Klipp et al., 2013).

The mathematical models used are classified along different axes- for example networks may be modelled qualitatively or quantitatively; deterministically or by using a stochastic description and maybe treated as discrete or continuous. It is important to understand that a process or a network maybe described by more than one type of model and the choice

of model depends on the nature of the investigation and questions of interest. Different techniques are used in modelling signal transduction in networks; for example, if a deterministic approach is used then differential equations such as ODEs are employed and tools from dynamical systems may be used to analyse non-linear behaviour in the resulting model. Increasingly, a number of studies focus on stochastic descriptions (where the state of a variable is given in terms of probability distributions) to study signalling and gene regulatory networks.

These approaches are typically used to describe the properties of networks with respect to changes in time only (Tyson et al., 2003; Tyson and Novák, 2010). However the dependence on space, a variable equally important to time, is often ignored. Cells are often assumed to be well-stirred reactors or spatially homogenous and thus the spatial dimension of information processing in signal transduction is wiped out from the description of the network in the model. However, an inspection of the intracellular organization of cells immediately reveals that this is simply not the case.

A look at the signalling landscape reveals the myriad processes where the spatial dimension to information processing plays an important role. These processes are vitally important for cell function. At the level of cells, networks underlying processes such as chemotaxis, cytokinesis, calcium signalling, pole to pole communication in bacteria, shuttling of proteins and trafficking are all spatially organized (Berridge et al., 2000; Eisenbach et al., 2004; Nelson, 2003; Rappaport, 1971; Shapiro et al., 2009). Spatial architecture and landmarks play an important role in the functioning of networks underlying processes such as cell division, growth and cell polarity. At the level of tissues or multi-cellular level, the positions of neighbouring cells are important for correct cell to cell communication. Interestingly even in bacteria, which were effectively assumed to be well stirred vessels, a highly intricate spatial organization is present at the subcellular level (Goley, 2013), which plays an important role in various regulatory processes in bacteria. An example seen across different bacterial systems such as *E. coli* and *C. crescentus* is polar localization of signalling entities (Laloux and Jacobs-Wagner, 2014; Rudner and Losick, 2010). Spatiotemporal phenomena such as waves have also been observed in different bacterial systems (Loose et al., 2008; Shapiro et al., 2009).

These are only a few examples of how spatial organization of signal transduction plays a fundamental role in different processes. If its role is left unaccounted for, there will remain a significant gap in our fundamental understanding of these processes. In recent years, the importance of spatial organization and regulation of cellular processes is increasingly

being recognized in the signalling and related communities (Hurtley, 2009; Kholodenko, 2006; Kholodenko et al., 2010; Schwarz-Romond and Gorski, 2010). Understanding the spatial dimension to signalling is not without its challenges. Firstly, spatial signalling is a part of numerous processes in different biological systems with distinct biochemical details. Second, the quality of spatially resolved data does not match that of the available temporal data. However recently there has been a surge in the development and refinement of experimental techniques and tools and much progress is ongoing to increase the spatiotemporal resolution of these tools (Etoc et al., 2013; Lasker and Shapiro, 2014). Third, from a modelling/systems/theoretical point of view, considering the effects of space adds yet another layer of complexity to the analysis of network behaviour.

In addition to mechanistically investigating specific concrete cellular processes in detail, a broader framework, to understand spatial regulation in signalling is necessary. This would be relevant to different systems and processes and would aid in understanding fundamental aspects of spatial signalling as well. It would also be useful for synthetically engineering spatially organized networks.

In this thesis, we develop a multipronged approach through which we combine studies of spatial regulation and control of representative networks and concrete signalling networks. Through this multifaceted approach, we aim to illuminate the various roles of space in information processing in cellular networks.

Our initial study focuses on the spatial organization of signalling networks underlying chemotaxis, and later evolves to studying spatial organization in signalling networks in a broader context. Chemotaxis is an important process found in a wide range of systems from bacteria (e.g. *E. coli*) to eukaryotes (for e.g. mammalian white blood cells) and is an integral part of important phenomena such as tumour metastasis, development of the nervous system and the immune response. The study of chemotaxis is highly relevant for a number of applications including nerve regeneration after injury, development of therapeutics and understanding mechanisms of diseases like cancer (Eisenbach et al., 2004).

Chemoattraction is the focus of many experimental and modelling studies while chemorepulsion, where cells move away from stimuli, has been largely left unexplored. During our investigation of chemorepulsion, in an earlier study (Alam-Nazki and Krishnan, 2010), a survey of the literature showed that cell movement both, towards and away from the same or different signals had been repeatedly observed in experimental studies in various biological systems (for e.g. neurons and *E. coli* bacteria). However, there was no study dedicated to understanding how the underlying chemotactic networks are naturally organized to give

rise to both responses, in light of the known properties of signalling.

In Chapter 2, we develop an engineering design approach to understand how the underlying chemical networks are wired to give rise to opposite migratory decisions. This approach complements mechanistic modelling of signalling networks in individual cells types. Our aim is to isolate what type of network configurations may or may not allow for both attractive and repulsive behaviours. We also aim to gain insight into how signalling networks are naturally designed to give rise to such responses. The approach we employ acts a basis for developing synthetic engineering approaches to manipulate chemotactic behaviour in cells and furthermore our findings act as a platform to understand, in detail, chemotactic signalling networks in concrete systems.

Chemotaxis is known to involve spatially distributed signalling and typically modelling and experimental studies explicitly take this into consideration. However, this is not the case in most processes where spatial organization and control of signalling is naturally present. A survey of the literature reveals that a systematic multipronged approach to investigating patterns of spatial signalling across different kinds of networks and cell types is needed. In the studies discussed in Chapters 3, 4, 5 and 6, we examine the spatial organization and regulation of signalling at multiple levels- both at network and enzymatic levels. Spatial organization maybe present in a number of guises in signalling and spatial effects may arise through localization of network entities, via transport and due to the presence of graded signals.

In Chapter 3, we discuss the study in which we examine a series of widely recurring network modules; these are typically examined through ODEs. Our aim is to shed light on how spatial organization affects temporal information processing in these representative signalling networks. We examine the effect of spatially varying signals in combination with the effect of diffusive transport of network species to gain an understanding of the role of diffusion in different kinds of signalling networks.

In Chapter 4, a basic enzymatic building block known as the covalent modification cycle is examined through the spatial prism. Covalent modification cycles are basic building blocks of posttranslational modification of proteins (for example a protein may be modified via the addition of a chemical group such as a phosphate or an acyl group). In this part of the study, our aim is to gain insight into the interplay of spatial effects and kinetics at the level of a single modification cycle. We also dissect the role of diffusional transport of enzymes, substrates and complexes and study the effects on information processing in this basic module. Covalent modification cycles are building blocks of different kinds of

modification cascades with multiple levels.

Thus, our study naturally progresses from studying one enzymatic building block to the study of signalling cascades (Chapter 5). Different types of cascades are a common feature of cellular signalling networks and are paradigms for how information is processed during signalling. We systematically disentangle the effects of space in a variety of signalling cascades by examining the effects of localization or compartmentalization and diffusion of enzymes and substrates, in multiple variants of chemical modification cascades.

In our final study, we elucidate how spatial organization and control is integrated into signalling networks underlying the cell cycle in the bacterium *Caulobacter crescentus* (Chapter 6). Various spatial and temporal control mechanisms coordinate the signalling interactions and events in the cell cycle. Modification cycles with bifunctional and monofunctional enzymes are the basic building blocks of these networks. Using a systems approach, we first dissect the spatial regulation in these building blocks and then build on the insights obtained to investigate the spatiotemporal control of concrete signalling networks in the cell cycle. The spatial features we study here: dynamic localization, gradient formation and localization of entities and their interplay with diffusion are recurrently observed in signalling networks of different bacterial and eukaryotic organisms. Hence, the insights pertaining to these features have a broader relevance.

To summarize, we develop and utilize multipronged approaches in our investigations- starting with the concrete process of chemotaxis, and then moving on to studying networks, enzymatic building blocks, signalling cascades and finally network modules in the concrete context of *Caulobacter*. Such multipronged approaches provide an avenue for the systematic exploration of different facets of spatial organization in information processing in a broader context as well as for understanding spatial control of signalling networks in different types of cells.

# Chapter 2

# An investigation of design principles underlying repulsive and attractive gradient sensing and their switching

## 2.1 Introduction

Chemotaxis, the directed migration of cells in response to chemicals, is a fundamental cellular process with manifold applications ranging from wound healing, tumour metastasis to immune system function (Eisenbach et al., 2004). In these systems the external environment is sensed by the ligand binding to specific receptors on the cell surface. The sensing stage leads to the biasing or guiding of cell motility in appropriate directions. In bacterial cells like E.coli, the temporal sensing of the ligand leads to the regulation of the tumbling frequency of the flagellum. In the case of eukaryotic cells, the sensing typically leads to the intermediate step of polarization, the persistent localization of key signalling components to opposite ends of the cell leading to the establishment of an axis, which aids persistent movement.

Chemotaxis is of two types, attractive and repulsive. Chemoattraction has been intensively studied experimentally in bacteria, especially in *E.coli*, and also in eukaryotes such as *Dictyostelium*, neutrophils, fibroblasts to name a few. These studies have focussed not only on the qualitative aspects of migration, but also on the underlying signal transduction processes connecting receptor-ligand binding to motility. Some experimental studies have investigated chemorepulsion in systems such as *E.Coli, Dictyostelium*, neutrophils and T-

cells. Most of these studies have focussed on demonstrating the fact that cells are capable of chemorepulsion, and are not focussed in detail on the signal transduction (Keizer-Gunnink et al., 2007; Tharp et al., 2006). From the modelling perspective, a series of modelling efforts have been aimed at understanding signal transduction in chemoattraction in E.coli as well as eukaryotes (for example see (Iglesias and Devreotes, 2008; Tindall et al., 2008) for surveys of the relevant efforts). A mechanistic modelling study of chemorepulsive sensing in *Dictyostelium* was performed by us in a previous work (Alam-Nazki and Krishnan, 2010).

While different cells may exhibit chemoattraction or chemorepulsion, our focus will be on cells (primarily eukaryotic cells) which exhibit both chemoattraction and chemorepulsion. There are a number of examples of such cases: *Dictyostelium* (under similar conditions) exhibits chemoattraction to cAMP and chemorepulsion to 8CPT-cAMP (Keizer-Gunnink et al., 2007); growth cones can exhibit chemoattraction and chemorepulsion to the same chemical stimulus depending on other factors present in the external medium, or its internal state (Mueller, 1999; Song et al., 1998); leukocytes can exhibit chemoattraction and chemorepulsion to Interleukin-8 depending on the strength of the stimulus(Tharp et al., 2006). In this chapter we present a framework to examine the possible design principles and features in the underlying signalling networks which allow them to exhibit both chemoattraction and chemorepulsion.

In all these eukaryotic cells (and bacteria) it is expected that the main difference between chemoattraction and chemorepulsion lies in the sensory transduction stage. In general the chemoattractant and the chemorepellent may be different chemicals, and their receptors can be different. However the mechanism of motility in response to both these chemicals is expected to be the same. This involves the regulation of the actin cytoskeleton, by key proteins in the polarization process such as Rac, Rho and (where applicable) Cdc42. There are many natural questions which arise in trying to understand chemoattractive and chemorepulsive signalling in these systems. Is there a common upstream entity whose regulation acts as the key connection between attractive and repulsive sensing? Is the nature of signalling in these systems local or adaptive? Is an underlying spontaneous symmetry breaking mechanism (spontaneous rearrangement of signalling entities at the front and rear ends of the cell in the absence of pre-established asymmetric cues or uniform signals) involved? How does this affect the cell's capacity to exhibit both attractive and repulsive sensing?

Different aspects of attractive and repulsive signal transduction have been discussed in

the literature. In particular, experimental studies in *Dictyostelium* in chemorepulsion have led to a network model postulated. In this model, the experimentally observed opposite regulation of the enzyme PLC (a regulator of phosphoinositide lipids) by chemoattractant and chemorepellent respectively is postulated to be the key connection between chemoattraction and chemorepulsion from the perspective of signal transduction. Thus PLC is postulated to be a "polarity switch" in this system (Keizer-Gunnink et al., 2007). The notion of a "polarity switch" has been discussed elsewhere in the literature too (Huttenlocher and Poznansky, 2008). In systems like growth cones and T-cells, the fact that competing pathways are involved in the gradient sensing have been demonstrated experimentally. In this study, we will focus on primarily these two design aspects, how they could work to give attractive and repulsive migration in eukaryotic systems, and how this might depend on the qualitative aspects of signal transduction. In this manner we aim to develop a framework to examine and elucidate various issues regarding attractive and repulsive sensing and their transition. In particular an implicit focus is on the underlying design principles and network regulation which allow the network controlling attractive migration to be exploited/regulated/modified to give rise to repulsive migration in the same cell. We believe that these are natural issues to examine as a first step towards a detailed mechanistic understanding of attractive and repulsive migration in these systems.

At the outset we recognize that the details of signalling in different cells will be different. This is because of both differences in biochemical network details, as well as basic qualitative differences in the nature of cellular signal processing. In order to address these classes of questions, we will work with representative modules of signalling. These modules, taken from the literature, represent different essential characteristics observed. While these modules naturally do not capture all the biochemical signal transduction complexity, they provide key insights regarding sensing capabilities. These modules must be seen as being building blocks or representing individual pathways in the overall signal transduction. The detailed biochemical understanding of chemotactic response in these various systems needs the integration of various pathway behaviour, as well as qualitative understanding of the nature of signal processing. In these cases it is vital to obtain insights to the questions above to guide the building of detailed models. The nature of the analysis in this work is such that it is likely to be useful for a wide range of systems.

Attractive and repulsive migratory behaviour has been observed in different systems as mentioned. While the mechanistic understanding of signal transduction in these systems is far from complete, many important qualitative aspects of the behaviour in chemoattractive

signalling have been investigated. This aspect underlies our approach in this work: we aim to exploit these aspects along with the experimental studies on chemorepulsion to postulate and examine some key questions about how attractive and repulsive signalling occurs, which would provide useful insights as well as testable predictions. We believe that the use of qualitatively simplified models is much more appropriate in this context, as it allows us to focus on some key qualitative aspects and obtain transparent insights, without being distracted by the different mechanistic details and gaps to contend with in individual systems. In the building of detailed mechanistic models, one would have to deal with many unknown details which are somewhat tangential to the issue at hand and in many ways obscure the main points; further, one would have to then check what aspects of the detailed models gave rise to the relevant insights, and if this would still hold good if different biochemical variants were employed. Finally for the issue under consideration, any mechanistic model would necessarily incorporate some phenomenological descriptions. Overall our models incorporate succinctly and transparently certain hypotheses whose consequences can then be understood more easily. The investigations of this work should be seen as a first step in mechanistically investigating such issues in individual systems using a combination of modelling and focussed experiments.

This chapter is organized as follows. In the next section we present the representative modules we employ for our analysis. We then examine different network designs (upstream switch, competing effects) which can give rise to both attractive and repulsive biasing, and examine what the consequence of each possibility is, in light of different signal transduction scenarios. We then conclude with a synthesis of our results and a discussion of how the analysis might be applied and extended to other systems.

## 2.2 Models and Methods

We will examine different ways in which sensing occurs, and how the sensed signal may be propagated downstream. In this section we discuss the modules describing how the sensed signals are propagated. Our modules are intended to be compact representations of different characteristic signal transduction observed in different systems. For the most part we will be concerned with spatial signalling mechanisms. However purely temporal signalling mechanisms are also contained in two of the models (discussed later). In general, for the modules we consider, chemical signalling occurs through receptor-ligand binding where the receptors could be evenly distributed along the membrane, or localized in some

sub-region. For simplicity, all these modules are formulated on a 1-D spatial domain with periodic boundary conditions, representing the boundary of a cell. The main insights are unchanged by a change of domain or boundary conditions. Schematic diagrams of the three modules which we discuss are shown in Fig. 2.1. Our qualitatively simplified models are intended to capture key aspects of how sensed signals are connected to downstream components which regulate F-actin. Thus the output may be regarded as a representative biochemical "frontness" component or component which biases pseudopod extension (eg. $PIP_3$ or Rac).

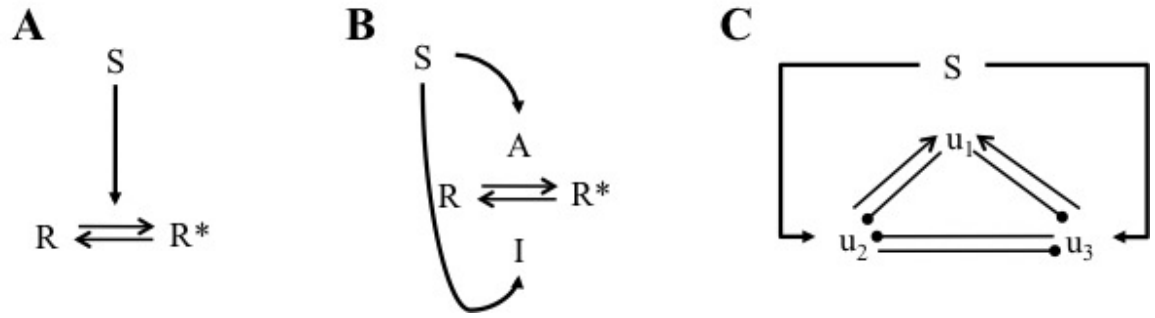


Figure 2.1: **Schematic diagrams of Local, Adaptive and Spontaneous Polarization modules.** (A). The local module contains an input signal labelled $S$ that regulates the response $R^*$. $R^*$ is capable of diffusing. (B). The adaptive module consists of an input signal that regulates an activator A and an inhibitor I which in turn regulate the response element R*. A and I may or may not diffuse. (C). In the spontaneous polarization module the input signal $S$ regulates two activators $u_2$ and $u_3$. These activators inhibit one another and upregulate the production of an inhibitor $u_1$. $u_1$ inhibits both $u_2$ and $u_3$ and diffuses as well (see text for details).

The first model involves a simple description of local regulation. Local regulation/biasing is the basis for description of migration in certain cell types (Arrieumerlou and Meyer, 2005), and can be expected to be important in cells which are already polarized with an existing pseudopod/front, driving the migration. In this model, a signal $S$ regulates the production of an active form of a response element $R^*$ from an inactive form $R$. The equations governing the response are given by

$$\begin{aligned} \frac{\partial R^*}{\partial t} &= (k_f + kS)R - k_r R^* + k_d \frac{\partial^2 R^*}{\partial \theta^2} \\ \frac{\partial R}{\partial t} &= -(k_f + kS)R + k_r R^* + k_d \frac{\partial^2 R}{\partial \theta^2} \end{aligned} \tag{2.1}$$

In the above equations $k_f$ and $k_r$ denote the rate constants for the constitutive conversion between inactive and active forms. $k$ is the rate constant involved in the signal mediated

conversion of inactive to active forms. Finally $k_d$ is the diffusion coefficient of the active and inactive forms (assumed equal for simplicity). The equations are written in dimensionless form, with $R + R^* = 1$ initially. By adding the above two equations we see that

$$\frac{\partial(R + R^*)}{dt} = k_d \frac{\partial^2(R^* + R)}{\partial\theta^2} \tag{2.2}$$

so that if $R + R^* = 1$ initially, this condition holds for all time and so we can write $R = 1 - R^*$. Note that the signal affects the forward reaction here. An exact analogue involves the signal causing the degradation of $R^*$ rather than the production. This results in

$$\frac{\partial R^*}{\partial t} = k_f(1 - R^*) - (k_r + kS)R^* + k_d \frac{\partial^2 R^*}{\partial\theta^2} \tag{2.3}$$

where the above conservation condition is explicitly incorporated. Note that in the above equation, restricting the signal to be homogeneous (or as occurring through localized receptors) and setting $k_d = 0$, we have a model of local temporal sensing.

The second model which we consider includes adaptation as an important ingredient of sensing. This is motivated by the demonstrated presence of adaptive signal transduction to different pathways such as PI3K and PTEN in *Dictyostelium*. It should be noted that the temporal adaptive behaviour is combined with a non-trivial spatial gradient sensing response. The essential ingredient for this to occur is some regulatory pathway which is not purely local, and could for instance be a highly diffusible element (Iglesias and Devreotes, 2008; Levchenko and Iglesias, 2002). Other ways of giving rise to similar effects through cytosolic pools is discussed in (Skupsky et al., 2005). For our purposes we will employ a compact model which gives rise to adaptive signalling and spatial responses. Since, we will be considering both attractive and repulsive responses, we choose a generalization of the local excitation global inhibition model developed previously (Krishnan, 2009). This involves a response element $R^*$ to be regulated by an activator and inhibitor both of which may be diffusible. For simplicity, we will assume the response element to be non-diffusible. Again, similar to the above, a conservation condition holds good between the inactive and active forms of the response element. Incorporating this, the governing equations for this

model are

$$\begin{aligned} \frac{\partial A}{\partial t} &= k_a S - k_{-a} A + k_{da} \frac{\partial^2 A}{\partial \theta^2} \\ \frac{\partial I}{\partial t} &= k_i S - k_{-i} I + k_{di} \frac{\partial^2 I}{\partial \theta^2} \\ \frac{\partial R^*}{\partial t} &= (k_f) A (1 - R^*) - k_r I R^* \end{aligned} \tag{2.4}$$

Here $A$ and $I$ denote the concentrations of activator and inhibitor respectively, while $R^*$ denotes the concentration of the response element. Here $k_a$ and $k_{-a}$ denote the activation and deactivation rate constants for the activating enzyme, while $k_i$ and $k_{-i}$ denote the activation and deactivation rate constants of the inhibiting enzyme. The activating and deactivating rate constants of the response element are denoted by $k_f$ and $k_r$ respectively. The diffusion coefficients of the activator and inhibitor are denoted by $k_{da}$ and $k_{di}$ respectively. In this case when $S$ is spatially homogeneous, the response $R^*$ is independent of S, as it depends on the ratio of A and I, both of which are proportional to S. Note that here too, by setting $k_{da} = k_{di} = 0$ and restricting the signal to be independent of space (or as occurring through localized reception) we have a case of purely temporal sensing with adaptation.

The third model embodies another characteristically different form of signal transduction which is observed in certain eukaryotic systems like leukocytes: spontaneous polarization. The model we employ for this purpose is based on the work of Narang (Narang, 2006) (which in turn in based conceptually on (Xu et al., 2003)), and involves spatial sensing with the special feature of spontaneous polarization induced by spatially homogeneous signals. In this model, the addition of a spatially homogeneous stimulus leads to symmetry breaking via a Turing instability, leading to a well defined front and back. For our purposes, the main features of interest in this model are that it leads to spontaneous symmetry breaking and also that the frontness and backness signals are present in an explicit manner. The fact that the symmetry breaks via a Turing instability is of much less relevance.

This model involves 3 components $u_1$ (the cytosolic inhibitor, also modelled in 1-D for simplicity), the frontness component $u_2$ (representative of Rac/Cdc42) and the backness component $u_3$ (representative of Rho). This model is based on the mutual inhibition of frontness and backness components both directly and through the upregulation of the intermediate cytosolic component $u_1$. The receptor signal upregulates both the frontness and

backness components. The model equations are

$$\begin{aligned}
\frac{\partial u_1}{\partial t} &= -u_1 + a_{12}u_2 + a_{13}u_3 + D_1\frac{\partial^2 u_1}{\partial \theta^2} \\
\frac{\partial u_2}{\partial t} &= \rho_2 u_2(S - a_{21}u_1 - a_{22}u_2 - a_{23}u_3) + D_2\frac{\partial^2 u_2}{\partial \theta^2} \\
\frac{\partial u_3}{\partial t} &= \rho_3 u_3(S - a_{31}u_1 - a_{32}u_2 - a_{33}u_3) + D_3\frac{\partial^2 u_3}{\partial \theta^2}
\end{aligned} \tag{2.5}$$

In the above equation, the regulation of cytosolic component $u_1$ by the frontness and backness components is described by the rate constants $a_{12}$ and $a_{13}$ respectively; the first term on the right hand side of the first equation describes the constitutive degradation of this cytosolic component, while $D_1$ describes its diffusion coefficient. In the second equation $a_{21}$ and $a_{23}$ are rate constants which depict the inhibitory effects of the cytosolic inhibitor and the backness component on the frontness component. The frontness component is regulated by the signal, but also involves constitutive degradation (associated with the term $a_{22}$). $D_2$ is the diffusion coefficient of the frontness component. The terms in the third equation are described in an exactly analogous fashion. $\rho_2$ and $\rho_3$ are scaling constants which arise when the equation is non-dimensionalized. Further details are given in (Narang, 2006). In the above equation, typically $u_1$ is highly diffusible. Note that the cytosolic pool $u_1$ is produced by both $u_2$ and $u_3$ and plays a role in inhibiting each of these components (see Fig. 2.1 for a schematic). A degradation of each component $u_2, u_3$ which is quadratic is assumed. The essential aspect of the interaction of $u_2$ and $u_3$ is similar to the Lotka-Volterra equation. The difference in diffusivities of the species plays a crucial role in the Turing mechanism. Analytical results demonstrating the presence of the instability, and dependence on parameters are presented in (Narang, 2006). While this model was originally formulated with Neumann boundary conditions, we will employ periodic boundary conditions. This introduces no qualitative difference.

The above models are analyzed both analytically and numerically: simulations are performed by discretizing space, and solving the resulting equations in MATLAB using the ODE solver ode15s. Sample parameter values are employed. In the case of both the adaptive and the Narang module, some comments must be made about the choice of parameters. In the adaptive module, a response whose gradient response parallels the upstream signal is achieved when $k_{da}/k_{-a} < k_{di}/k_{-i}$ and a repulsive response is observed in the opposite case. For specificity we choose parameter values which lie in the parameter region

$k_{da}/k_{-a} < k_{di}/k_{-i}$. Our main conclusions, being qualitative in nature, do not depend on the particular choice of parameters. In the Narang module, we employ a basal set of parameters taken from (Narang, 2006). In this module, under basal conditions, the spatially homogeneous state is stable, but may be destabilized (leading to an inhomogeneous state) when the signal level crosses a particular threshold. The resulting patterned state is reminiscent of a polarized cell, and depending on the choice of parameters in the module, the resulting state (just above the instability threshold) may be either representative of an attractive response (i.e. frontness component highest near maximum of signal) or that of a repulsive response (i.e. frontness component highest near minimum of signal). Again for specificity we choose parameters so that the attractive response is obtained. We will comment in detail on the role of the parameters in this system in the context of specific results (parameter values for the relevant figures are in Appendix A).

## 2.3 Results and Discussion

In this section, we present various results related to the ways in which repulsive and attractive response may be obtained in the same cellular system. In order to do this, we examine two basic mechanisms postulated and partly studied in the literature: one which postulated that chemorepulsive signalling is related to chemoattractive signalling, via the opposite regulation of a key upstream component, which is referred to as a polarity switch. The second scenario is one where upstream competing pathways play a crucial role in the cell exhibiting chemorepulsion and chemoattraction. This is based on such pathways being observed in growth cones, and similar effects being observed in neutrophils. However in no case has either scenario been examined carefully and systematically in light of the possible signal transduction which might occur. We will examine both scenarios, and pay particular attention to how these might work in different cells which have very different signal transduction characteristics. In order to do this, we examine how each of the scenarios described above would work to propagate signals downstream. This involves ing each of these scenarios upstream of each kind of signal propagation module. Analyzing each of these settings allows us to make robust conclusions regarding the roles of polarity switches and competing effects in spatial gradient sensing and chemotactic signalling. The computational results presented here are complemented by analytical work, which was presented in (Krishnan and Alam-Nazki, 2011) and is reproduced in this section.

Before we examine this, we first briefly analyze the different basic modules embodying

local/simple feedforward regulation, adaptive signal transduction and spontaneous polarization.

### 2.3.1 Response of signal propagation modules

We first investigate the simple local model (see Fig. 2.2A). The imposition of a linear gradient ($S = a + bcos\theta$ in terms of the angular co-ordinate) results in a response which essentially mirrors the input. This is the simplest kind of module. There are a few points to be noted even in this simple module. Firstly, the response is essentially proportional to the input when this module is far from saturation. Secondly, the basal reaction rate constants determine the range over which the response can vary at steady state. In general, if the relevant basal reaction rate constant (forward for attractive biasing, backward for repulsive biasing) is small relative to the basal reaction rate constant of the opposite reaction, then practically the entire range of response element concentrations can be exploited. Thirdly while the regulating reaction is assumed to follow mass-action kinetics, alternate mechanisms such as Michaelis-Menten kinetics can lead to a non-linear distortion of the input signal. Finally any threshold mechanism downstream can also lead to a sharpening or simple amplification of the response.

Very similar insights apply to a local module of repulsive sensing. Here again the presence of a basal backward reaction rate can restrict the range over which the response may vary in response to the signal. Here, the presence of a threshold mechanism downstream could lead to a sharp falling off of net output as a function of signal concentration. In both these cases the effect of increasing the diffusion coefficient of the response element is to reduce the amplitude of variation of the response. As this diffusion coefficient is made larger the gradient information is gradually lost.

We now turn to the adaptive module (Fig. 2.2B). Again as before, we investigate the case of a linear gradient. In the first case, we use parameters such that $k_{da}/k_{-a} < k_{di}/k_{-i}$. The simulations performed revealed an attractive biasing with a response maximum coincident with the input signal maximum. In general increasing the gradient strength increases the amplitude of the response, while a homogeneous signal of any magnitude keeps the response fixed. Further by varying the parameters, we see that the smaller the difference $k_{di}/k_{-i} - k_{da}/k_{-a}$ for a fixed input signal, the weaker the steady state gradient response. The presence of a downstream amplifying element allows for an amplification of this signal in such a way that the adaptation property is preserved (assuming this amplifying mech-

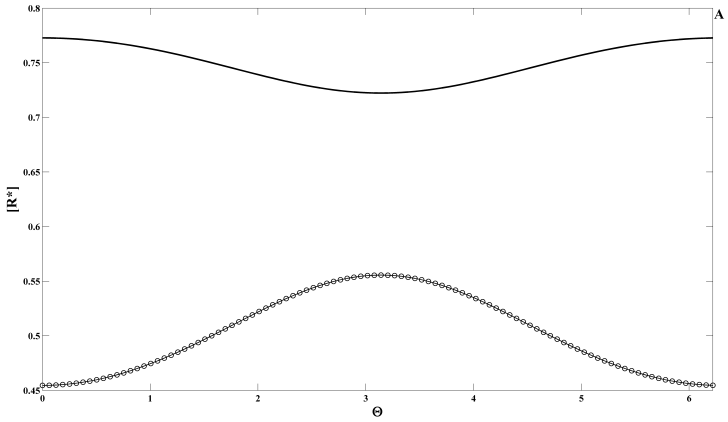


(A)

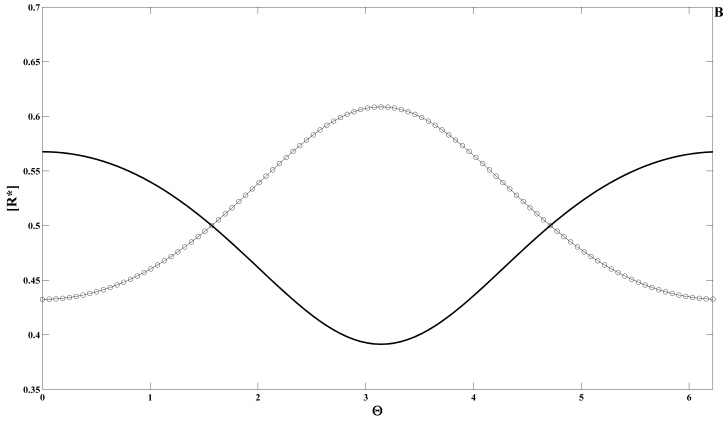


(B)

Figure 2.2: **Response of local and adaptive modules.** (A) For the local module, an attractive response (solid line) is seen when the external signal upregulates the response and repulsive (solid line with circles), when it is downregulated by the external signal. Here and in other diagrams, unless mentioned, the signal is $S = 1 + 0.4cos\theta$, with a maximum at $\theta = 0$. (B) The adaptive module response is attractive (solid line) when $k_{di}/k_{-i} - k_{da}/k_{-a}$ is positive. A repulsive response (solid line with circles) is achieved when this quantity is negative. For the repulsive response in the adaptive module, diffusivities of activator and inhibitor are interchanged.

anism is via a monostable threshold mechanism). For completeness we investigate the behaviour of the module in response to a signal when $k_{da}/k_{-a} > k_{di}/k_{-i}$. In this case the response of the module is to produce a repulsive biasing. The same conclusions regarding the positive biasing case above hold good here.

Finally we investigate the Narang module, when subject to a gradient (see Fig. 2.3). For the parameters employed, a clear polarized response representative of chemoattraction is obtained. When the gradient is relatively weak, both the frontness signal $u_2$ and the backness signal $u_3$ display localized responses. When the gradient is substantially strong we clearly see that the frontness signal $u_2$ and backness signal $u_3$ also develop localized profiles in response to the gradient, though the effect of the gradient leads to the frontness signal being sharply localized and the backness component displaying a weakly bi-modal response. The basis of the underlying mechanism of this module is spontaneous symmetry breaking, leading to polarized profiles (Narang, 2006). A similar simulation of this module with different parameter values and the same input signals, reveals polarized profiles for the frontness and backness components $u_2$ and $u_3$ respectively, which are representative of a chemorepulsive response. In this case, for strong gradients, the backness signal is more sharply localized. Further, this chemorepulsive response also involves a spontaneous symmetry breaking mechanism. Thus this module, for different choices of parameters can result in either a chemoattractive or a chemorepulsive mechanism with spontaneous symmetry breaking in homogeneous stimulation.

These three modules act as representative modules of signal propagation, embodying very different behaviour, but still producing/propagating attractive or repulsive biasing. It is worth pointing out, incidentally, that both the adaptive as well as the Narang models can exhibit both repulsive as well as attractive biasing simply by changing parameters. We will return to this point later in the chapter.

### 2.3.2 A polarity switch

In general it is worth noting that chemoattraction and chemorepulsion typically involve different chemical signals, and perhaps different receptors too. Therefore it is possible that chemoattractive behaviour and chemorepulsive behaviour could occur through very different pathways, involving qualitatively completely different mechanisms. In this subsection, we examine a scenario which has been postulated and discussed in the literature: the opposite regulation of a key upstream element by chemoattractant and chemorepellent

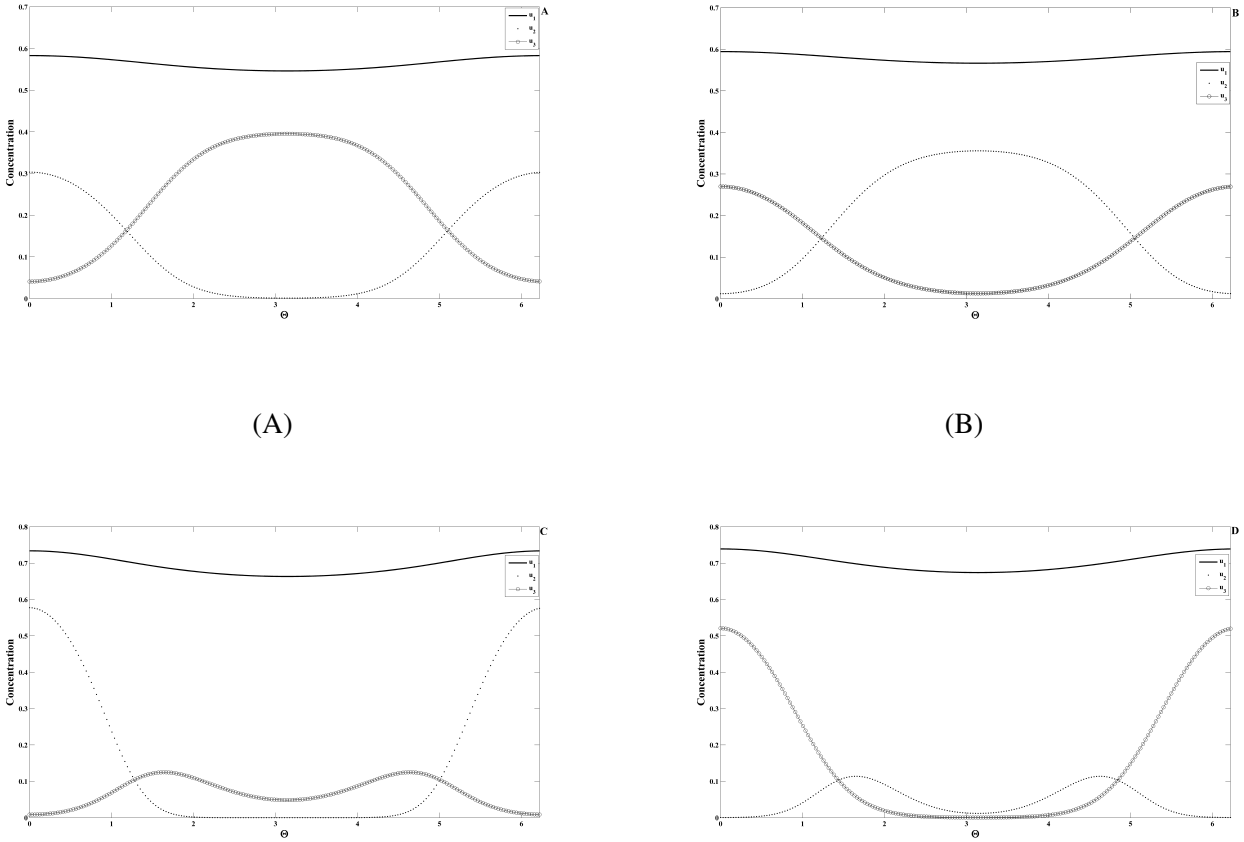


(A) (B)

(C) (D)

Figure 2.3: **Attractive and Repulsive responses from the spontaneous polarization module.** Attractive responses (A,C): The signal is $S = 1 + 0.05cos\theta$ (A) and $S = 1 + 0.4cos\theta$ (C). The inhibitor (solid line) and the two activators $u_2$ (dotted line) and $u_3$ (solid line with circles) are shown. The activator $u_2$ ("frontness pathway") is in phase with the signal. Repulsive responses (B,D): Again the same signals $S = 1 + 0.05cos\theta$ (B) and $S = 1 + 0.4cos\theta$ (D) are employed. The activator $u_3$ ("backness pathway") is now in phase with the signal.

is suggested to be the key to the opposite response in the system.

Here we will examine this possibility in more detail. In particular we will examine what such a simple polarity switch implies for the downstream response, and also what kind of signal transduction might be consistent with the possibility of a simple upstream polarity switch. In order to do this, we will examine how an upstream polarity switch would work along with essentially linear/simple feedforward signal transduction, adaptive signal

transduction and signalling involving spontaneous polarization.

In order to address this issue we revisit the above models. We expand these models somewhat to include an additional intermediate reaction whose output $S^*$ is the input to the module, rather than the receptor signal $S$ itself (see Fig. 2.4). Thus $S^*$ is the input to the module, and its dynamics are described by

$$dS^*/dt = (k_1 S + k_{f1})(1 - S^*) - k_{r1} S^* \tag{2.6}$$

in the case of activation, and

$$dS^*/dt = (k_{f1})(1 - S^*) - (k_1 S + k_{r1}) S^* \tag{2.7}$$

in the case of inhibition (note that it is assumed that $S_0 + S^* = 1$ where $S_0$ is the inactive form of $S^*$). In the above, $k_{f1}, k_{r1}$ are the basal activation and inactivation rate constants for the regulation of $S^*$. $k_1$ is the rate constant associated with the receptor mediated activation/deactivation of $S^*$. In other words, the receptor regulatory pathways act on the key upstream element $S^*$, and this upstream signal controls the regulatory dynamics of network. Thus $S^*$ plays the role of a potential polarity switch.

We can immediately make a few conclusions from the above model. Firstly we note that if $k_{f1} << k_{r1}$ then at basal levels higher concentrations of the inactive form of $S^*$ are present. A corresponding conclusion can be made when $k_{r1} << k_{f1}$. Now we investigate whether the reversal of regulation of this common element will effectively revert the nature of the downstream response. To do this we first note that if either of the rate constants $k_{r1}, k_{f1}$ is very small relative to the other, then this results in a basal value of $S^*$ either very small or close to saturation. This severely limits the dynamic range in one direction, and so in our simulations we will assume that both constants are of comparable magnitude, leading to an equilibrium neither too much to the left nor to the right.

We first investigate the local module. Fig. 2.5 compares the case where the activation in the common element is switched to inhibition. We see a clear switch in the downstream response from attraction to repulsion with local sensing. Another related point should be mentioned. If this local sensing module has a downstream threshold module (monostable,local) which leads to non-linear amplification, then the reverse regulation of $S^*$, even if it leads to a repulsive biasing cannot employ this threshold effect, as it generally pushes the response everywhere further away from the threshold.

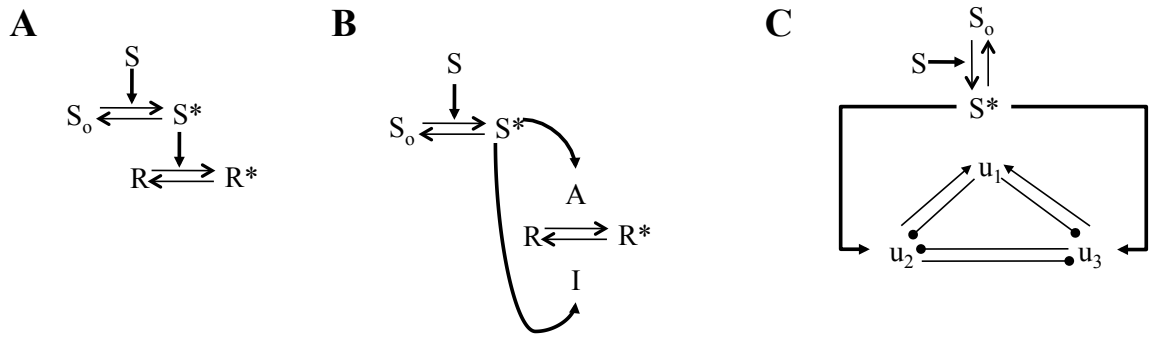


Figure 2.4: **Schematic of modules with extra element.** The figure shows the three modules with an extra element $S^*$ which may be activated or inhibited by the attractant and repellent respectively. Only the scenarios corresponding to the activation case are shown.

The conclusion from this study reveals that a simple polarity switch can lead to a reversal in downstream gradient response. However this comes at a price: the opposite regulation of a common upstream element means that any downstream (monostable) threshold can be employed only by one of the two opposite regulatory effects of the polarity switch. Nevertheless it is possible that such a scenario may work in cells which are already polarized and migrating through essentially local gradient response to pre-existing pseudopods/growing fronts (Arrieumerlou and Meyer, 2005; Krishnan and Iglesias, 2007).

We now investigate the effect of this reverse regulation of $S^*$ if the downstream module is an adaptive module. Fig. 2.5 shows the net result. The effect of the reversed regulation of $S^*$ results in the biasing being altered from attractive to repulsive behaviour. This is also seen by simple analytical results. We note here that the response to the adaptive module to a homogeneous signal is independent of the value of the input signal, or indeed of the basal value of $S^*$. We further note that both the spatial as well as temporal behaviour of the response are reversed. Thus in homogeneous stimulation, the response is switched from a transient jump to a transient depression before recovery to basal levels (an exploration of a "polarity switch" in the context of a purely temporal adaptive signalling model is made in Appendix A).

In summary, if the downstream signal transduction is adaptive (with spatial sensing), then an upstream polarity switch results in the downstream response being reversed, in a manner consistent with adaptation in homogeneous signalling. An implication of such downstream adaptive signalling is that it allows an upstream polarity switch to provide the appropriate downstream biasing in a way which keeps the mean value fixed. Thus, unlike in the simple local regulation, a polarity switch no longer implies that the downstream

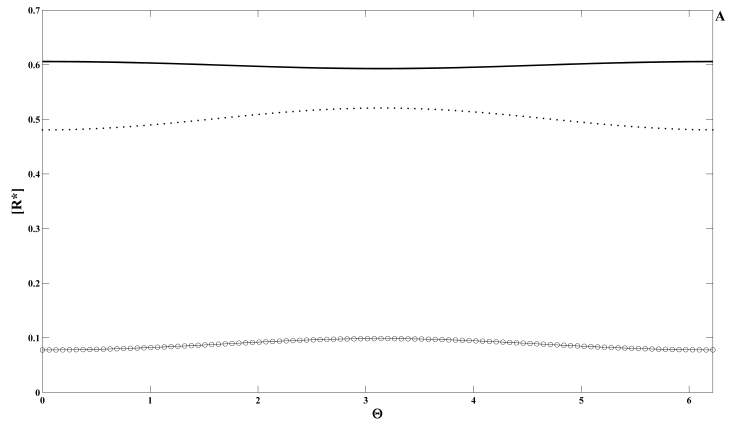


(A)

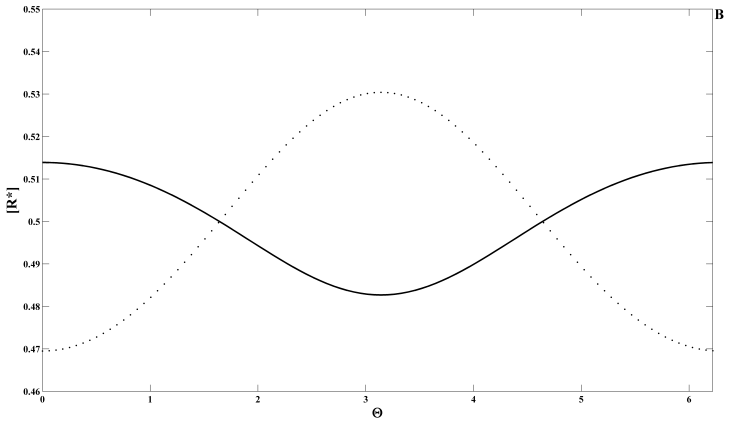


(B)

Figure 2.5: **Switching of local and adaptive modules by altering the behaviour of upstream components.** (A) In the local module the attractive (solid line) and the repulsive (dotted line) is achieved by positively or negatively regulating the upstream component by the external signal, respectively. If the kinetic constant $k_{f1}$ is decreased then the repulsive response (solid line with circles) is obtained that is overall reduced. (B) In the adaptive module the attractive (solid line) and the repulsive (dotted line) is achieved by positively or negatively regulating the upstream component by the external signal respectively. We notice that adaptive signalling downstream of a polarity switch, provides the opposite biasing without decreasing the overall response everywhere.

signal is regulated in opposite directions relative to basal values. This also means that any downstream monostable threshold may be accessed for both the opposite regulation of the polarity switch.

While we have used a specific module of adaptive signalling with spatial sensing, we note that this result is more general, and applies to any similar adaptive signalling which involves a global regulatory element, which serves to compensate for changes in the mean value of the upstream signal. Thus downstream adaptive signalling is in many ways advantageous for the functioning of a polarity switch.

We now examine how such an upstream polarity switch would work in conjunction with signalling involving spontaneous polarization (Fig. 2.6). Here too we find that changing the regulation of $S^*$ from activation to inhibition alters the nature of the downstream response from attractive to repulsive. However a closer look at the response reveals a rather different response when this signal is reversed, and in general the localization of $u_2$ and $u_3$ is much less sharp.

Some basic analysis of this module reveals the main difference. While the attractive response involves spontaneous polarization (via the Turing mechanism in this case) as a crucial ingredient in the gradient sensing response, switching the regulation of $S^*$ results in a situation where no spontaneous polarization is observed. Indeed, in this case, the parameters in the Narang module are regulated so as to move further away from the instability/spontaneous polarization threshold, rather than cross it. Thus the repulsive response obtained is qualitatively fundamentally different from the attractive response. Thus if the response to a chemorepellent involved a simple inhibition (as opposed to activation) of a common upstream component, this would necessarily involve a completely different kind of sensing response.

To complete one aspect of the analysis of the Narang module above, it is worth asking whether an alternate regulation of the upstream component $S^*$ would result in a chemorepulsive response which would also involve spontaneous polarization as a key ingredient. We show using one scenario that this is indeed possible. Indeed if the regulation of $S^*$ is locally inhibited by the signal, and simultaneously also activated by a signal which is related to the spatial average of the signal, this is indeed possible. This latter activation could be through some pathway involving highly diffusible components. To illustrate this point

we consider alternate regulation of $S^*$ as

$$\begin{aligned} dS^*/dt &= (k_{f1} + k_{11}A)(1 - S^*) - (k_1 S + k_{r1})S^* \\ dA/dt &= k_{fa}S^2 - k_{ba}A + k_{da}\frac{\partial^2 A}{\partial \theta^2} \end{aligned} \tag{2.8}$$

where $A$ refers to the additional pathway which is highly diffusible.

Now the results in Fig. 2.6C show that a repulsive response is indeed obtained, with a sharper localization of frontness and backness components. Some further analysis reveals that this indeed involves spontaneous symmetry breaking as an ingredient in the gradient response. A look at the above equation reveals the main issue: the spontaneous symmetry breaking involves pushing the input to the Narang module past a particular threshold. In this above modification, for a given input signal $S$ the gradient information causes the spatial biasing to be opposite to that of attraction. In addition, the regulation of the activation while providing no gradient information, allows for $S^*$ to be increased (even counteracting the decrease due to the local inhibition) so that the threshold may be crossed for strong enough input signals. The above combination of factors allows for a repulsive response which also exhibits spontaneous polarization in homogeneous signalling and is a basic ingredient in the gradient response.

In essence the above analysis suggests the following conclusions. A simple upstream polarity switch in a system which exhibits spontaneous polarization as a key element in the gradient response will indicate a pronounced difference in the attractive and repulsive responses. Firstly, no spontaneous polarization may be expected in homogeneous chemorepellent stimulation, and the gradient response is likely to indicate a much weaker polarization. Further it also suggests that a chemorepellent can even depolarize a cell. Thus for instance a homogeneous stimulation of chemoattractant can lead to spontaneous polarization; however if the cell is subsequently subjected to a homogeneous dose of chemorepellent of sufficient strength, then this has the effect of directly working against the chemoattractant, and regulating the upstream element in the opposite direction, and pushing it below the stability threshold of the downstream module. Thus, in such a case, a homogeneous stimulation of chemorepellent can depolarize a polarized cell.

While we have used the Narang module for illustrative purposes, we note that this conclusion holds for any similar module which exhibits spontaneous polarization due to some upstream regulation pushing it past the stability threshold. If the signalling to the

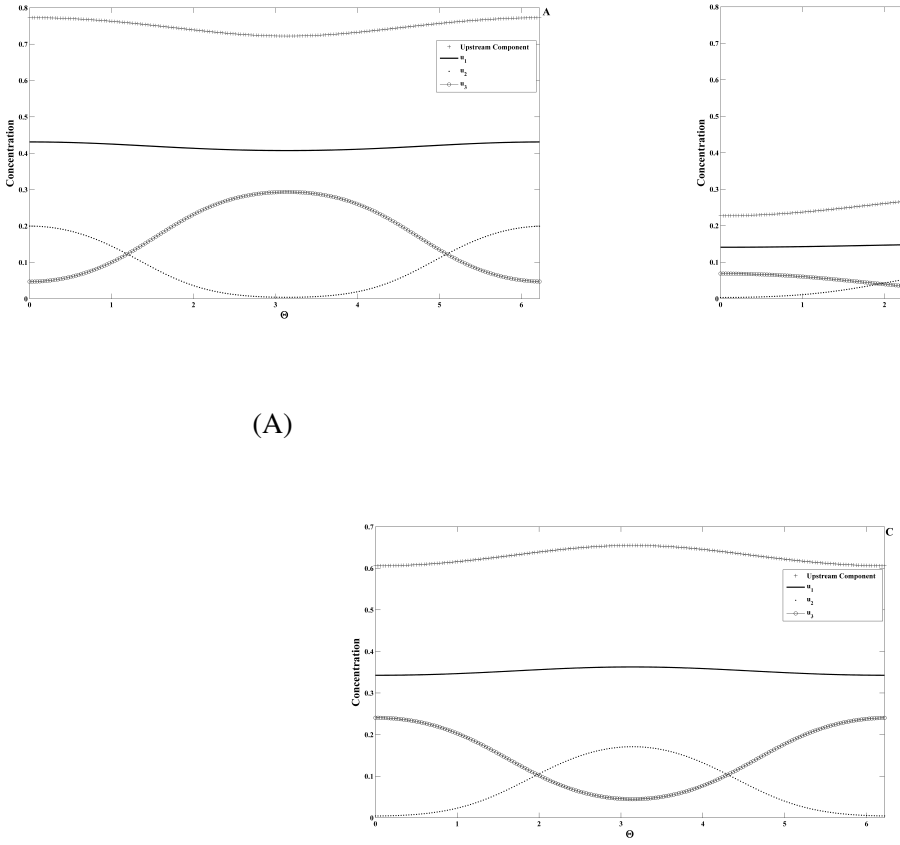


(A) (B)

(C)

Figure 2.6: **Switching of spontaneous polarization element by altering regulation of upstream components.** The upstream component (+sign), inhibitor $u_1$ (solid line) and the two activators $u_2$ (dotted line) and $u_3$ (solid line with circles) are shown. (A) The attractive and (B) the repulsive response is achieved by locally positively and locally negatively regulating the upstream component by the external signal, respectively, as is seen from the location of the frontness component $u_2$. Note that in (B), while a repulsive response is achieved, it is rather weak without a clear and sharp separation of frontness and backness components. (C) By altering the regulation of the upstream component to include dual activation (global) and inhibition (local) it is possible to obtain a repulsive response which makes use of the symmetry breaking mechanism that is the core of the attractive mechanism.

spontaneous polarization module occurs primarily through one pathway (for e.g. $PIP_3$) then the opposite regulation of this pathway by chemorepellent will necessarily push it away from the stability boundary. We will discuss the implications of this point later.

Taken together, our analysis reveals that while a simple upstream polarity switch can

result in the reversal of the biasing, the downstream signal transduction characteristics can play a crucial role in how such a switch might function to provide an opposite gradient sensing response.

### 2.3.3 Multiple and competing effects in gradient sensing

In the previous subsection, we examined how a so-called polarity switch could result in the reversal of the sensing but with very different characteristics. In this subsection, we examine a different scenario, also motivated directly by experiments, namely the possible presence of multiple and competing effects in gradient sensing. This is related to examining whether signal transduction to the same chemical can lead to attractive and repulsive responses under different conditions. We will consider the case of a gradient response being transduced by multiple pathways, in competition with one another.

Multiple competing effects are observed in very different cell signalling settings and related effects have been examined in the literature under the name hormesis (Calabrese, 2001, 2005). In the chemotactic context, the consideration of competing effects is very natural, since these have been observed in different systems, including growth cones and neutrophils (Song et al., 1998; Vianello et al., 2005). The exact details of how these competing effects are integrated in these systems is still being elucidated.

We aim to examine what the consequences of having competing pathways in gradient sensing are, and what kind of signal propagation possibilities can result. In order to do this we examine a model of competing pathways which is stripped down to its essential features. Thus we examine the parallel feedforward regulation of two pathways corresponding to species A and B whose respective total amounts are $A_{tot}, B_{tot}$. A and B represent the multiple elements in signal transduction. Both active A and B regulate a response element $R^*$ from its inactive form. For simplicity, the response element is assumed non-diffusible. This leads to the equations:

$$dR^*/dt = k_f(A + B)(R_{tot} - R^*) - k_r R^* \tag{2.9}$$

This equation describes the conversion to active form of the response element by the pathways A and B: the associated forward rate constant is $k_f$ and a constitutive backward reaction with rate constant $k_r$ is assumed. In the above description the total amount of active and inactive forms of the response element is a constant (and equal to $R_{tot}$) and this has

been explicitly incorporated in the dynamical description. Note that in general different rates may be assumed for the regulation of the forward reaction associated with A and B, but this effect can be captured essentially in the total amounts of A and B. The regulation of A by the signal leads to

$$\frac{dA}{dt} = (A_{tot} - A)(k_{fa} + k_a S) - (k_{ba})A + k_{da}\frac{\partial^2 A}{\partial \theta^2} \tag{2.10}$$

for the case where A is positively regulated by the signal. Note that A refers to the active form of the enzyme A. In this equation (and similarly below, Equation 2.11), $k_{fa}$ and $k_{ba}$ denote constitutive reaction rate constants for the activation and deactivation of the active form of A. $k_a$ denotes the rate constant associated with the upstream signal regulation of $A$ (in the above, this regulation occurs for the positive reaction). $k_{da}$ denotes the diffusion coefficient of the active form of A (assumed to be the same as that of the inactive form). Since the concentrations of the active and inactive forms satisfy a conservation condition (owing to the fact that there is only interconversion between active and inactive forms, and that their diffusion coefficients are equal), this is explicitly incorporated above. The equations for the other cases is presented below, in an exactly analogous notation. In the case of negative regulation of A by the signal, we have

$$\frac{dA}{dt} = (A_{tot} - A)(k_{fa}) - (k_{ba} + k_a S)A + k_{da}\frac{\partial^2 A}{\partial \theta^2} \tag{2.11}$$

In an exactly analogous way, the regulation of B by the signal leads to two possibilities:

$$\frac{dB}{dt} = (B_{tot} - B)(k_{fb} + k_b S) - k_{bb}B + k_{db}\frac{\partial^2 B}{\partial \theta^2} \tag{2.12}$$

in the case of activation and

$$\frac{dB}{dt} = (B_{tot} - B)(k_{fb}) - (k_{bb} + k_b S)B + k_{db}\frac{\partial^2 B}{\partial \theta^2} \tag{2.13}$$

in the case of inhibition.

This leads to four possible effects of the coregulation of the pathways: (i) Forward regulation of both A and B (ii) Backward regulation of both A and B (iii) Forward regulation of A and backward regulation of B and (iv) Backward regulation of A and forward regulation of B. We examine these in turn. A schematic diagram showing the positive regulation

of A and negative regulation of B is shown in Fig. 2.7.

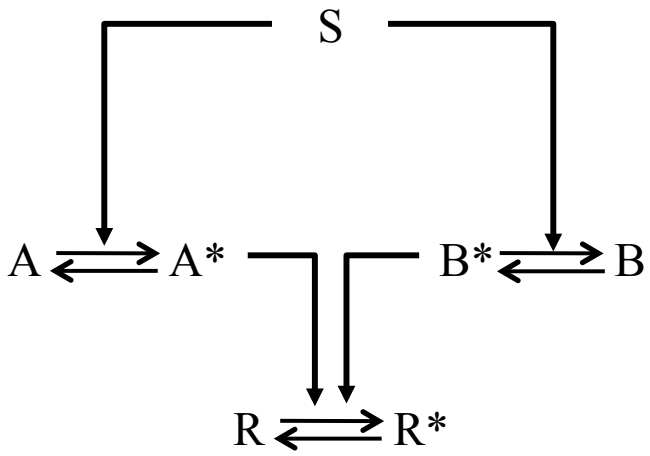


Figure 2.7: **Schematic diagram of competing pathways.** A schematic diagram of competing pathways with the signal mediating the forward regulation of A and the backward regulation of B are shown. A and B have additive effects in regulating a response element.

Sample simulations of each of these cases is shown in Fig. 2.8. In Fig. 2.8A we see the simple additive effects leading to positive biasing in a signal. In Fig. 2.8A we also see the parallel effects of two pathways leading to negative biasing. In Fig. 2.8B in contrast there is a competition between A and B, and the net effect is a positive biasing of the signal suggesting a dominance of A for the conditions considered. Also shown in this figure is a case of negative regulation of A and positive regulation of B resulting in the net negative biasing, suggesting the dominance of A under these conditions.

While the results of cases (i) and (ii) are intuitively obvious, the case of (iii) and (iv) are of interest. We will examine the case of (iii), which directly reflects the case of competing pathways in feedforward regulation. For simplicity, we start by considering A and B to be non-diffusible and the case where the basal forward rate constant $k_{fa}$ and the basal backward rate constant of B are zero. Further simulations exploring the competition between A and B are presented in Fig. 2.9.

The analysis discussed next was performed in (Krishnan and Alam-Nazki, 2011) and for convenience is reproduced below. The steady state response of the response $R^*$ is dependent on the spatial profile of $A + B$. It is a simple matter to see that

$$A + B = \frac{A_{tot}}{(1 + (k_{ba}/k_a S))} + \frac{B_{tot}}{(1 + k_b S/k_{fb})} \tag{2.14}$$

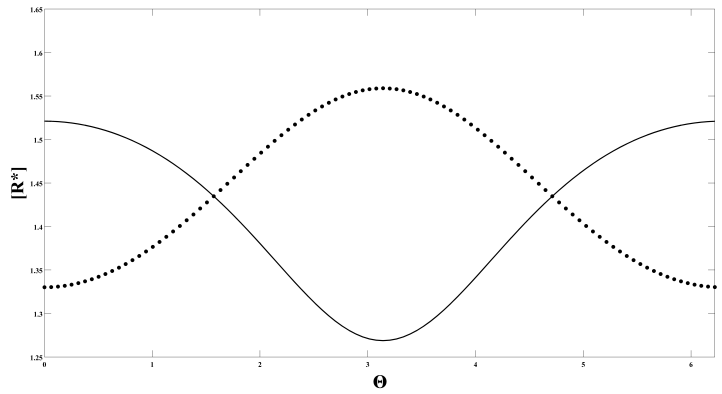


(A)

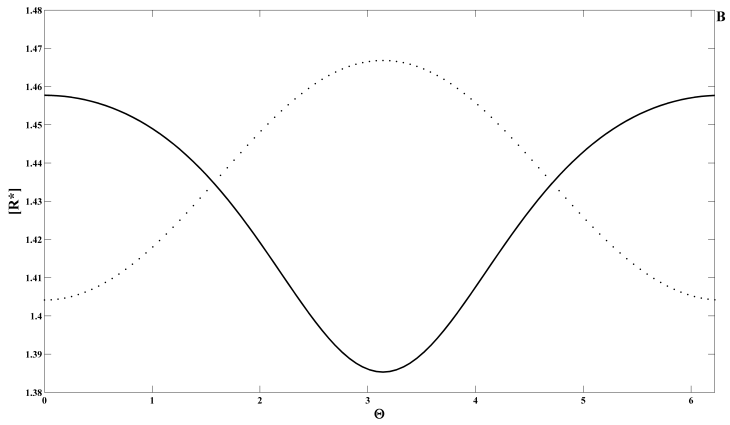


(B)

Figure 2.8: **Parallel local regulation of pathways.** This figure depicts certain qualitative aspects of the competition between pathways. (A) When both components $A$ and $B$ are positively regulated by the signal, an attractive response (solid line) is achieved. When both $A$ and $B$ are negatively regulated by the external signal a repulsive response (dotted line) is observed. (B) When $A$ is positively regulated by the signal and $B$ is negatively regulated by the signal an attractive response is achieved (solid line). And when $A$ is negatively regulated by the signal and $B$ is positively regulated by the signal a repulsive response is seen (dotted line).

The competing effects of the signal in each of the terms in the right hand side is clearly seen. In order to examine the nature of the response and its dependence on the signal, we examine when $(d/dS)(A+B)$ is greater than zero. We set $k_a/k_{ba} = K_1, k_b/k_{fb} = K_2$. Thus the variation of $A+B$ and hence the response with signal at steady state indicates positive biasing if

$$\frac{(1+K_1S)^2}{(1+K_2S)^2} \quad < \quad \frac{K_1A_{tot}}{K_2B_{tot}} \tag{2.15}$$

This equation reveals that depending on parameter values both positive and negative biasing may be obtained. In particular the left hand side is a monotonic function of S varying between 1 and $(K_1/K_2)^2$, while the right hand side depends on both the ratio $K_1/K_2$ as well as $A_{tot}/B_{tot}$.

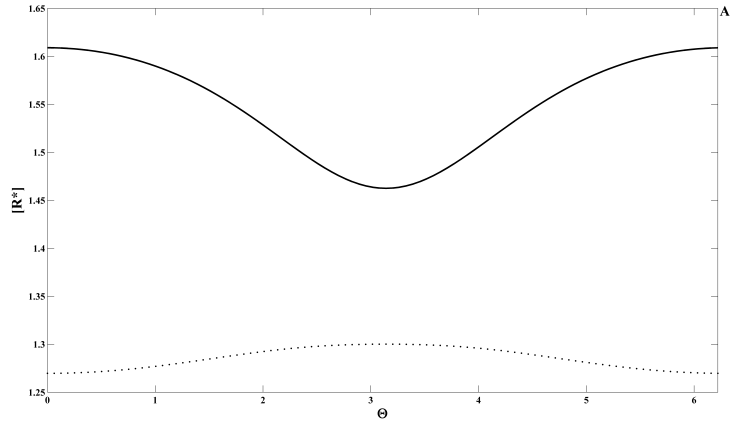


(A)

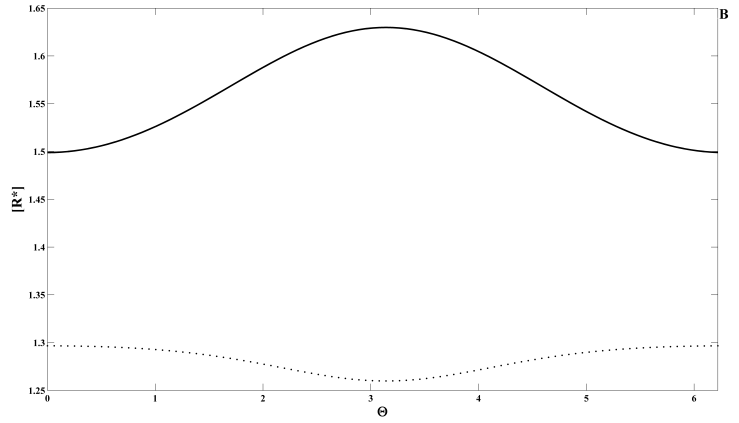


(B)

Figure 2.9: **Competition of pathways.** (A) *A* is positively regulated by the signal and *B* is negatively regulated by the signal. When the total amount of *A* is much greater than *B* (1.4 and 0.3, respectively) (solid line) an attractive response is achieved. However when the total amount of *B* is greater than *A* (0.7 and 0.6, respectively) (dotted line) then a repulsive response is achieved. (B) *A* is negatively regulated by the signal and *B* is positively regulated by the signal. In this scenario, the net sensing response is qualitatively the opposite of that of (A).

We can immediately infer a few important points from the above. Consider the hypo-

thetical situation of $K_1 = K_2$, in this case positive biasing is always obtained if $A_{tot} > B_{tot}$ and negative biasing is always obtained if the opposite inequality holds. This is intuitively obvious. However when $K_1$ and $K_2$ are different for a fixed $A_{tot}/B_{tot}$ neither too large not too small, the inequality above may be reversed at a fixed S. In this case, we have a switch from attractive to repulsive biasing as the signal strength crosses a particular level. The core of this effect is the competing effects of the pathways as well as saturation. This effect is explored in Fig. 2.10 and Fig. 2.11.

We now examine the effect of the presence of basal forward/backward reactions (i.e. $k_a, k_b > 0$). In this case the steady state for A+B is obtained as

$$A + B \;=\; A_{tot}/(1 + (k_{ba}/(k_{fa} + k_a S)) + B_{tot}/(1 + (k_{bb} + k_b S)/k_{fb}) \quad (2.16)$$

Here again, exactly as above one can examine when the response shows a positive biasing towards the signal. In this case, the condition above is replaced by

$$\frac{(1 + [(k_{fa} + k_a S)/k_{ba}])^2}{(1 + [(k_{bb} + k_b S)/k_{fb}])^2} \;<\; \frac{A_{tot} k_a / k_{ba}}{B_{tot} k_b / k_{fb}} \quad (2.17)$$

Again this equation can be analyzed explicitly to see if this inequality is reversed for a specific value of S. This reveals a critical value of signal mean value at which the gradient response may be reversed. If we define Q as

$$Q^2 \;=\; (A_{tot} k_a / k_{ba})/(B_{tot} k_b / k_{fb}) \quad (2.18)$$

then the critical mean value at which the gradient response is reversed is

$$S_{crit} \;=\; \frac{(1 + k_{fa}/k_{ba}) - (1 + k_{bb}/k_{fb})Q)}{k_b/k_{fb} Q - k_a/k_{ba}} \quad (2.19)$$

Fig. 2.10 shows different cases of the variation of the response when the pathways are subject to a homogeneous stimulus. In particular this reveals that the response can be either a monotonically increasing function of the signal strength, a monotonically decreasing function, an initially increasing function, which reaches a maximum and starts decreasing or an initially decreasing function which reaches a minimum and starts increasing. Since the pathways are non-diffusible these plots also provide information about the nature of the response in a gradient: this response can be either always a positive biasing, always a

negative biasing, or a response which can switch from a positive to a negative biasing at particular signal strengths.

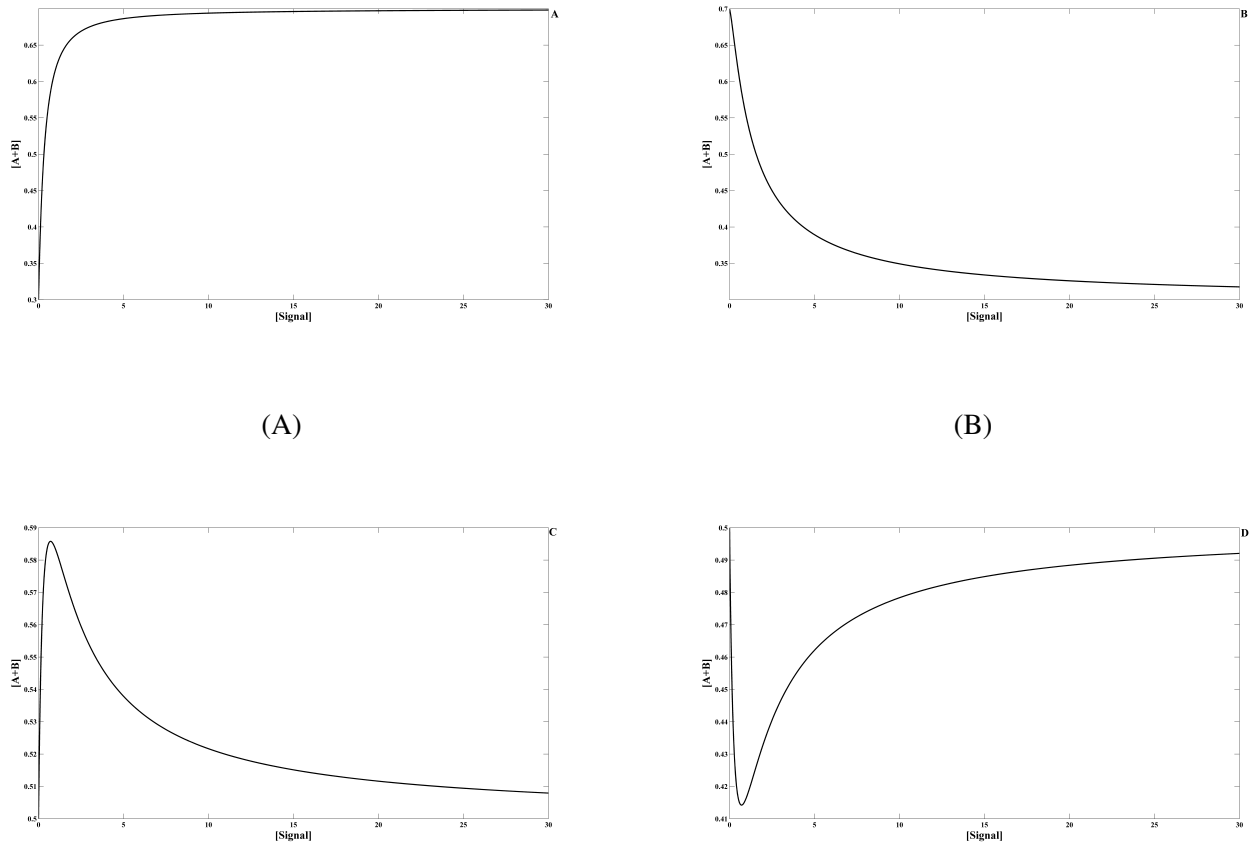


(A) (B)

(C) (D)

Figure 2.10: **The variation of response to homogeneous signals for the case of competing pathways.** In this case $A$ is activated and $B$ is inhibited by the signal. Different scenarios depicting the variation of response to the signal value (dose-response curve) are shown. For simplicity the total upstream signal $A + B$ regulating the response is plotted. (A) Response is a monotonically increasing function of signal value. (B) Response monotonically decreases (C) Response monotonically increases and then decreases. (D) Response monotonically decreases and then increases. In all these cases the slope of the curve provides information about the gradient response for weak gradients superimposed upon a mean value of signal corresponding to that location of the curve, in the case where the pathways are non-diffusible.

So far we have examined the response of the two competing pathways, and examined when the net response is biased towards and away from the signal. In the above analysis the species were assumed to be non-diffusible. In (Krishnan and Alam-Nazki, 2011), this

analysis was re-examined for the case where both A and B were diffusible.

The combined response of the pathways A and B in the case where both are non-diffusible, and where either or both may be diffusible raises some important points which we discuss now. Recall that from our previous discussion (when $A_{tot} > B_{tot}$) that when the signal S is increased, the combined response evolves in either a monotonic way across the entire range of signals or in a non-monotonic way. Thus the curve of the response vs signal provides crucial information. It also indicates the absolute range of response, which provides other useful information.

Now when the pathways A and B are diffusible, we may expect a perturbation of the results obtained for non-diffusible pathways. This is indeed the case when the diffusion coefficients of $A$ and $B$ are small. Examining the above expressions in some special cases proves illuminating. In particular, suppose A is highly diffusible $k_{da} \gg 1$ and B is hardly diffusible. Then it is easily seen that the gradient response is always repulsive–this is because it is pathway B which provides the gradient information. Now the behaviour of the total response in a homogeneous signal may either be monotonic (always increasing or always decreasing) or may even change sign as seen in the analysis above. However because of the effect of diffusion, the gradient response is always negative. When A is non-diffusible and B is highly diffusible, we have the opposite case and here the gradient response is always attractive whatever the variation of the response in homogeneous signals is.

The above point also indicates how, by virtue of diffusion, it is possible to substantially distort the results of the non-diffusive case and even essentially decouple the mean response and the gradient response. This point is very important when one notes that many threshold phenomena rely on the local concentration of a downstream element crossing a particular value. This analysis shows that it is possible to get different kinds of variation to homogeneous signals, both monotonic and non-monotonic, and have in some cases, a completely decoupled gradient response with two pathways. This also shows that in general one could have quite complex and unintuitive behaviour arising from this precise feature.

### 2.3.4 Downstream signal propagation

We now consider the effects of competing pathways on different kinds of downstream signal propagation. Firstly if there is simple local downstream regulation, then the main insights are contained in the analysis above. In particular, the possibility of the reversal of

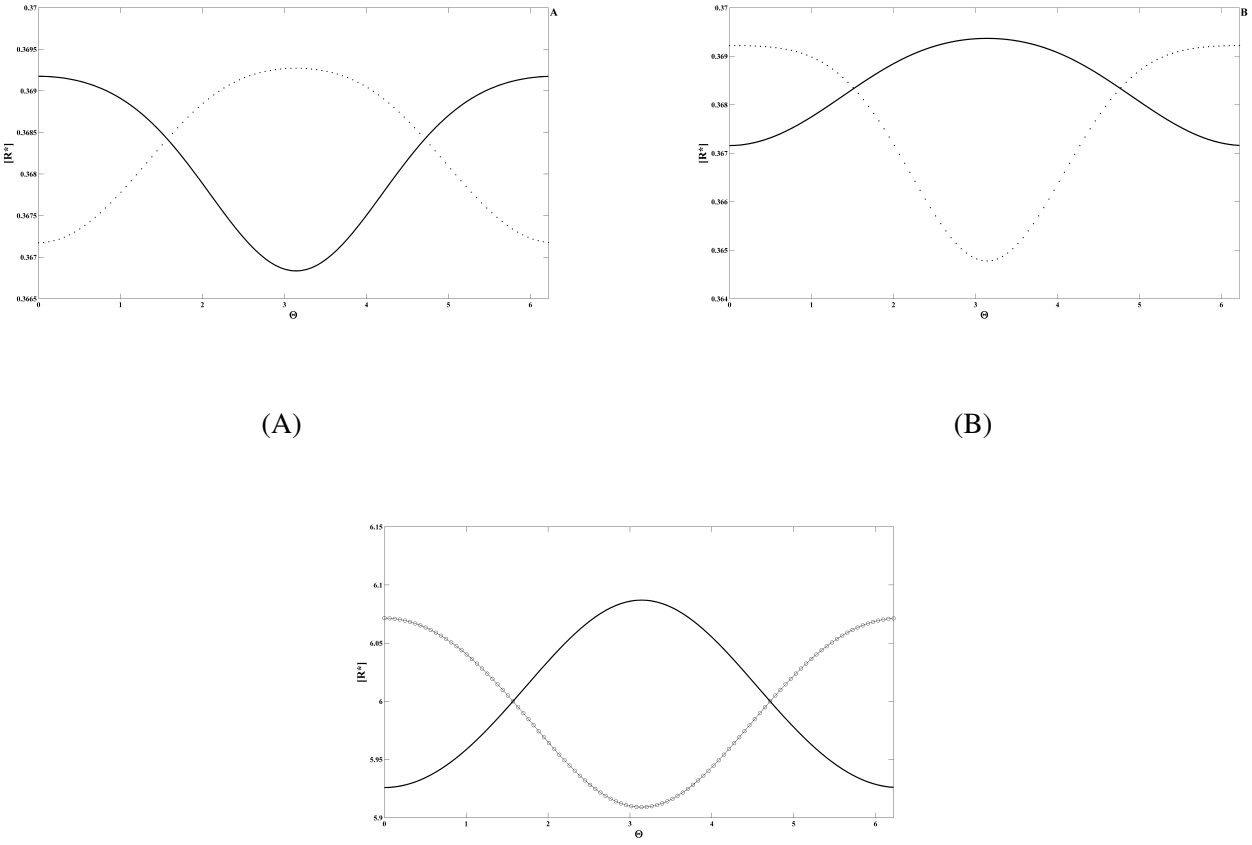


(A) (B)

(C)

Figure 2.11: **The gradient response for the case of competing local pathways.** This figure shows the qualitative effect of mean value of signal reversing the gradient response, and also the effects of the competing pathways. (A) *A* is positively regulated by the signal and *B* is negatively regulated by the signal and $A_{tot} = B_{tot}$. The response for the external signal $S = 0.5 + 0.1Cos\theta$ (solid line) and $1.0 + 0.2Cos\theta$ (dotted line) is shown. Here the mean value is changed keeping the relative gradient fixed. A reversal in the nature of the gradient response is observed. A similar qualitative effect is observed if the mean value is changed keeping the gradient strength fixed. (B) *B* is positively regulated by the signal and *A* is negatively regulated by the signal and $A_{tot} = B_{tot}$. The response for the external signal $S = 1 + 0.4Cos\theta$ (solid line) and $S = 2.0 + 0.4Cos\theta$ (dotted line) is shown. In this case, the mean value of the signal is varied keeping the gradient strength fixed. Again we see a switching in response. (C) The effect of varying the strengths of the competing pathways for a fixed signal is considered. *A* is positively regulated and *B* is negatively regulated by the signal $S = 1 + 0.2cos\theta$. Here the parameters $A_{tot}$ and $B_{tot}$ are varied and the qualitative effect of this change on the response is observed. A reversal in the gradient response is observed when we compare the case of $A_{tot} < B_{tot} = 2.0$ (solid line, repulsive response) and $B_{tot} < A_{tot} = 2.0$ (solid line with circles, attractive response).

a gradient response when the mean value of the signal is increased, exists. Now if there is downstream adaptive signalling then this can be analyzed by "connecting" the upstream competing pathways module with an adaptive module. In this case the downstream adaptive module simply acts to reset the level of the response without distorting the essential features of the gradient response. Thus a positive biasing is simply converted into another positive biasing response, with its level adjusted by the adaptive response, and similarly for a negative biasing. Other main features such as a reversal in gradient response also continue to hold good. Note that in this case both competing pathways are upstream of the adaptive signalling module.

We now examine the effect of a downstream module of spontaneous polarization in signal transduction with competing pathways. To illustrate this we "connect" the competing pathways module to the Narang module. Here the situation is a little more subtle. For the parameters in the Narang module chosen, the gradient response reflects that of the upstream signal. However the essential nature of the response also depends on whether the spontaneous polarization threshold has been crossed. It is simplest to examine the response in a weak gradient.

With this in mind, we first examine the nature of the response in homogeneous stimulation. Now if the input signal is homogeneous, we saw above that the response from the competing pathways module could either monotonically increase, increase and then decrease and reach an asymptotic value, monotonically decrease, or decrease and then increase. If the response monotonically decreases, then the threshold is never crossed and no (spontaneous) polarization occurs. Now if the response monotonically increases then it is possible that at some finite signal strength, the threshold is crossed, leading to spontaneous polarization. Any signal whose strength is above this value will always elicit such a response. If the response of the competing pathways module increases, reaches a maximum and then decreases, then if the maximum is above the spontaneous polarization threshold, spontaneous polarization will occur for a homogeneous signal of sufficiently high strength. Here however there exists the possibility that for signal of even higher strength, the response of the competing pathways module may decrease sufficiently so as to fall below the threshold of the spontaneous polarization threshold. This then means in response to a second stimulus of sufficiently high strength, depolarization may occur leaving an unpolarized cell.

We can build on these insights and consider the response of the combined modules to a weak gradient. To start with we consider the competing pathways to be essentially

non-diffusible. The response of the system then depends on the mean value of the signal. If the mean value of the signal is low then an attractive gradient response will be observed. However if the mean value is high enough, the system can exhibit a strongly polarized attractive response, by virtue of the fact that the spontaneous polarization threshold is crossed. However depending on the characteristics of the competing pathways module as discussed above, different kinds of responses may be observed. Essentially the mean value of the input signal (along with the characteristics of the competing pathways module) will determine if the threshold for spontaneous polarization is crossed or not. Further the slope of the curve of the response of the competing pathways module as a function of signal strength (in homogeneous signals) plotted above will determine whether the input to the spontaneous polarization module is co-aligned or counter-aligned to the gradient signal to the cell. Thus a monotonic curve above would correspond here to an attractive gradient response, with the additional feature of strong polarization if the threshold for spontaneous polarization is crossed. If the curve is non-monotonic then if the ascending part of the curve crosses the level corresponding to spontaneous polarization the response for signal levels where the curve is above the spontaneous polarization threshold will correspond to a highly polarized cell: the polarization of the cell will be co-aligned with the external gradient (i.e. frontness signal highest where signal is maximum) if the slope of the curve is positive, and the polarization and gradient response will be counter-aligned if the slope of the curve is negative. Thus to summarize, the response of the network to a weak gradient will depend on two factors which can be obtained from the curve: whether the response value for the competing pathways model is above or below the spontaneous polarization threshold, and also on the slope of the curve (see Fig. 2.12 for illustrative results).

Such analysis also follows for pathways which may be diffusible. The only point to note here is that the diffusivity of the pathways can affect the response, and this effect can be seen from the analytical results and the discussion above.

In summary if one considers a sequence of experiments where the cells are subject to signals where the mean value of a signal is changed keeping the gradient strength fixed, one could have different kinds of transitions. Thus overall rather subtle combinations of gradient response (with or without spontaneous polarization) may be obtained by competing effects in gradient sensing.

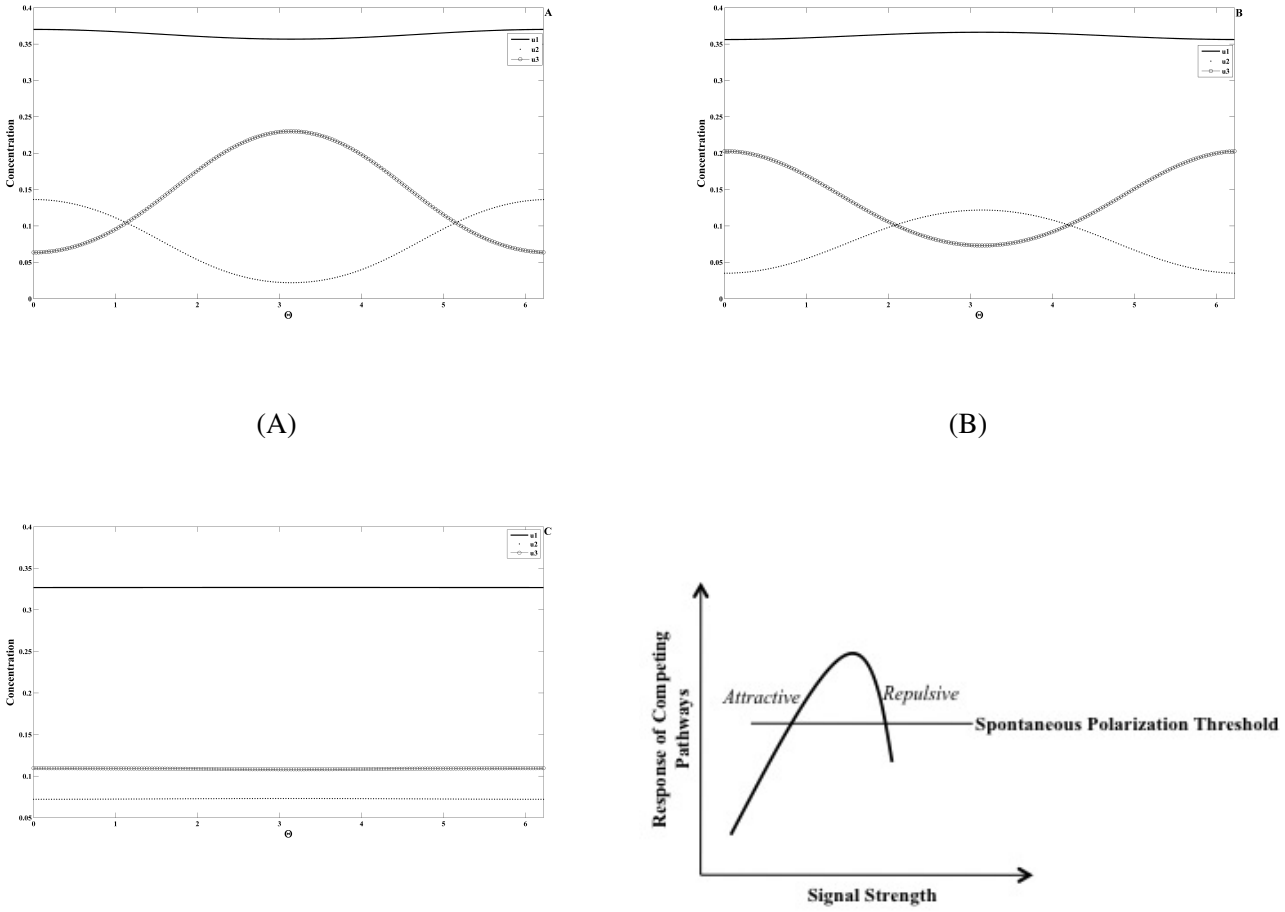


Figure 2.12: **The effect of spontaneous polarization downstream of competing pathways.** In this figure we consider the case of competing pathways *A* (positively) and *B* (negatively) regulated by the signal: The competing pathways regulate a response ($R^*$), which serves as the input to the spontaneous polarization module. The response of the combined system to three different gradient signals is shown: (A) $S = 0.3 + 0.03cos\theta$: the response is indicative of an attractive response ( frontness component $u_2$(dotted line) co-localized with the maximum of the signal) which makes use of the symmetry breaking mechanism: note that the polarization of frontness and backness are much stronger than the external signal. (B) $S = 5 + 0.03cos\theta$: here the response is representative of a repulsive response, which is also sharply polarized (and making use of the instability mechanism). (C) $S = 30 + 0.03cos\theta$: here the response is very weakly repulsive for the same gradient strength, and there is no sharp polarization of frontness and backness components. (D) A schematic of the dose-response curve for the competing non-diffusible pathways, labelling the implication of downstream spontaneous polarization for the overall gradient response. The slope of the curve indicates the nature of the gradient response, while its position relative to the spontaneous polarization line indicates whether that mechanism is employed in the gradient response.

## Modulating the effects of competing pathways

The above subsection examined the signal transduction arising from two competing pathways and the particular focus here was to characterize the response to a range of signal values. In this subsection, we build on this to address how these pathways may be modulated by factors other than the external signal itself. It should be noted that the two pathways involve different elements which may be modulated by the cells depending on their internal states (e.g. stage in the developmental cycle) or other factors in the growth or external medium (Nishiyama, 2003; Song et al., 1998). It is also possible that other signal transduction in the cell may involve sequestration/uptake of some elements in the pathways. We will assume that in all these cases, that the distortion to the pathways occurs at a fast time scale, and that the system has reached a steady state, where the system may now be characterized by new parameters $A_{tot}, B_{tot}$. Thus in effect these extra modulations change parameters of the network.

We first examine the case of the competing pathways module alone. We note that for any fixed set of parameters, the dose response curve of the network (for homogeneous stimuli) is either monotonically increasing, monotonically decreasing, initially increasing reaching a peak and then decreasing or initially decreasing reaching a minimum and then increasing. We note from this that a change/modulation in the strength of some pathway can completely change the dose response curve from any one of these four types to potentially any other type.

The implication of this point is the following. Changes in internal or external conditions can completely alter the nature of the dose response to the same signal. Thus even the gradient response of the cell can be completely changed by such modulation (see Fig.2.11C). Therefore it is possible–because of an altered internal state of the cell or other conditions in the medium– to completely alter the nature of the gradient response to the same signal, as well as how that depends on the signal level. For example a cell which could exhibit only an attractive response can exhibit an attractive response which is transformed into a repulsive response at higher signal values. Other transitions can likewise be possible. These effects are primarily because the balance of the competing effects can be altered.

Similar effects can be examined when one analyzes competing effects with downstream polarization. Here again, modulating the strengths of different pathways can completely alter whether attractive, repulsive or both responses may be obtained, just as discussed above. In addition the altering of parameters in the competing pathways module can also

alter the range of the dose response curve (even if the shape is not changed). This could have profound implications for whether the polarization threshold is crossed or not, for a fixed strength of the external signal. Thus the modulation of the strengths of the competing pathways could alter the gradient response from a highly polarized to a weakly polarized response, completely change the kind of gradient response (attractive or repulsive) or a combination of both.

The above indicates that while performing experiments and analysis on cellular response, one must be very careful in considering cells with essentially the same internal state as well as growth/external conditions. Differences in such effects can play important roles when non-trivial competing effects exist in gradient sensing, and even more so if symmetry breaking polarization mechanisms are additionally at play.

### 2.3.5 Spontaneous polarization and the attractive and repulsive response

In previous subsections, we analyzed the effect of signalling scenarios which could allow a cell to exhibit attractive and repulsive biasing and how this would work when the cell had the capacity to spontaneously polarize in homogeneous stimuli. Such behaviour is observed in different cells such as T-cells and neutrophils. In this subsection, we aim to flesh out in a little more detail, various relevant aspects. We start by noting that the polarization in these cells involves the RhoGTPase signalling circuit including Rac, Rho and (where applicable) Cdc42. Spontaneous polarization is expected to result primarily from the interaction of these components. From our perspective we expect that the difference in attractive and repulsive sensing is already manifest upstream of this circuit. In our analysis we have used a simplified model of spontaneous polarization, the Narang module, to analyze various issues.

Firstly, as examined above, if chemoattractant and chemorepellent regulate opposite reactions upstream then while stimulation of one of them can employ the spontaneous polarization (instability) mechanism, the other typically will not. While our analysis was based on the Narang module, it is basically valid for a polarization module with a single instability or non-linear dynamic threshold (e.g. (Dawes and Edelstein-Keshet, 2007; Jilkine et al., 2007)) with the regulation of a common single upstream component by attractant and repellent.

In the context of the Narang module, we note that the upstream signal regulates both frontness and backness elements, and hence there are two pathways controlled by the up-

stream signal. A natural next question to ask is whether a chemorepellent can regulate the same two pathways in different strengths to give rise to spontaneous polarization with chemorepulsion, given that spontaneous polarization is obtained in the chemoattractant regulation. In the Narang module, the parameters which are involved in the signal regulation of the polarity circuit are contained in the equations for $u_2$ and $u_3$. Changing the strength of the receptor regulation of the frontness component $u_2$ has the effect of proportionally changing the parameters $\rho_2, a_{21}, a_{22}, a_{23}$ while changing the receptor regulation of the backness component $u_3$ has the effect of proportionally changing $\rho_3, a_{31}, a_{32}, a_{33}$: this is related to how the original equations were non-dimensionalized (Narang, 2006). Now the condition of a Turing instability occurring giving rise to a polarized profile depends on the following condition: $0 < \frac{a_{22}}{a_{12}}(b_{32} - 1) < a_{21} - a_{31} < \frac{a_{33}}{a_{13}}(1 - b_{23})$ for the case where the polarity circuit is wired to give an attractive response relative to its input signal: $b_{23}b_{32} > 1$, with $b_{23} < 1$ and $b_{32} > 1$. Likewise when the polarity circuit has parameters which give a repulsive response: $b_{23}b_{32} > 1$ along with $b_{23} > 1$ and $b_{32} < 1$, the instability occurs if $\frac{a_{22}}{a_{12}}(b_{32} - 1) < a_{21} - a_{31} < \frac{a_{33}}{a_{13}}(1 - b_{23}) < 0$. In these equations $b_{23} = a_{23}/a_{22}$ and $b_{32} = a_{32}/a_{33}$. The point to note is that a change of the receptor regulatory pathways will affect the different parameters proportionally, as mentioned above, and hence leave the parameters $b_{23}, b_{32}$ fixed. Noting the conditions above we see that the intrinsic proclivity of the circuit to provide an attractive or repulsive response relative to its upstream signal is in fact not altered (since $b_{23}, b_{32}$ are fixed). The alteration of parameters $a_{31}, a_{21}$ may cause the above inequality to be violated, and hence the relevant instability giving the polarized state to be suppressed. In summary an alteration of the receptor regulatory pathways is not sufficient to yield an instability mechanism with the opposite gradient response.

It is of course possible that in other polarity circuits, the signal can regulate the polarity circuit in multiple locations, and a chemorepellent may regulate the polarity circuit in different locations, or with different differential strengths, to result in spontaneous polarization. However such a setting has to, of necessity, be more complex than a simple upstream switch.

In the above, we were examining the case of cells subject to either different chemicals or different mean values of the same chemical. On the other hand if the internal state of the polarity circuit itself is modulated, either by intrinsic factors, or other external elements in the medium then it is possible to change the behaviour of the polarity circuit completely. Thus such a change can allow for the Narang module to fundamentally change its response so that its response represents repulsion to the same gradient signal.

The analysis above suggests that if chemoattraction and chemorepulsion to different chemicals involves a single upstream polarity switch, then homogeneous doses of each cannot both elicit spontaneous polarization which further has implications for the gradient response. This immediately brings up the question: suppose both chemoattractant and chemorepellent elicit spontaneous polarization in a particular cellular system, what can we infer about the signalling? One possibility is that the chemoattractant and chemorepellent act to modulate the polarity circuit in more than one location, and possibly different locations. This would suggest that the polarity circuit regulation may be quite different (in a very non-trivial way) in the two cases and further do so in a way to give rise to opposite biasing and spontaneous polarization. A second possibility is that opposite biasing is obtained upstream of the polarity circuit, but the mean value of this upstream signal is compensated so that the oppositely biased input to the polarization module also crossed the instability threshold.

Another possibility is that the polarity circuit regulation by the attractant is distinct or only partially overlapping with that regulated by the repellent. Noting that different cells have multiple isoforms of Rac and other RhoGTPases, we see that it is quite plausible that attractants and repellents might regulate different forms of the same species. Thus different forms may be involved in different, or only partially overlapping polarity circuit interactions. In the context of the module we have analyzed, it is possible that two different isoforms of Rac (for e.g.) could result in two different polarity circuits, one which is intrinsically "tuned" to give an attractive response and the other to give a repulsive response. The chemoattractant would regulate one polarity circuit and the chemorepellent would regulate the other polarity circuit. This is a possible way for obtaining spontaneous polarization in homogeneous stimulation of both chemoattractant and chemorepellent.

### 2.3.6 Polarity switch and competing pathways

In previous subsections we examined both the polarity switch and competing pathways, and the resulting signal processing in each case. Here, we briefly examine another issue which connects these two aspects. Our discussion of a polarity switch was based on the opposite regulation of an upstream component by chemoattractant and chemorepellent. For completeness, we discuss how this could be realized if competing pathways exist. Thus we examine the following situation: suppose a chemoattractant regulates downstream signalling through two competing pathways, could a chemorepellent also regulate the two

competing pathways in the same manner but balanced differently to give rise to chemorepulsion?

Our analysis of the competing pathways immediately indicates that this is possible. Suppose A and B are the competing pathways (assumed non-diffusible for simplicity) then having a chemorepellent regulate these pathways amounts to changing the regulatory constants $k_a, k_b$. From our analysis above we see that a chemorepellent can regulate these competing pathways in a way in which the regulation of B is stronger than that of A, and this can result in a scenario corresponding to chemorepulsion. Furthermore, an analysis exactly along the previous lines suggests that since the response ends up below basal levels, any downstream spontaneous polarization mechanism will not be triggered in this case too.

An interesting point to note is that in this case both the $S = 0$ and the large $S$ limits asymptote to the same values for chemoattractant and chemorepellent (as is revealed by a simple analysis). Thus suppose the dose-response curve for a chemoattractant is monotonically increasing, then in the chemorepellent case, the curve would initially decrease (indicative of chemorepulsion) but have to eventually turn around and increase. Thus one could predict that a chemorepellent regulation of the same pathways would result in a transition from repulsion to attraction as the signal mean value is increased. This is because the faster kinetic regulation of pathway B (which makes it dominate for relatively small levels of signal) is compensated by the greater "capacity" (or relatively slower saturation) of pathway A at higher signal values. In general if in chemoattraction, the dose response curve is such that the large signal response is higher than the zero signal response, then the chemorepellent regulation of such competing pathways will involve a switch from repulsion to attraction as signal levels are increased.

## 2.4 Conclusions

Attractive and repulsive migration in response to different kinds of cues is widespread in both prokaryotic and eukaryotic systems. Chemoattraction and chemorepulsion are specific examples of this. Interestingly many cells exhibit both chemoattraction and chemorepulsion– in particular eukaryotic cells such as *Dictyostelium*, neutrophils, T-cells and neural growth cones all possess this feature. It is likely that these opposite migratory responses have evolved to allow the cellular systems to accomplish specific responses. While it may be anticipated that both these phenomena will be the focus of many detailed modelling studies, there are other questions which arise at the outset. What are the design principles and

features involved in the signalling networks of such cells which allow them to exhibit both chemoattractive and chemorepulsive responses? Are attractive and repulsive responses related by a simple upstream switch? How can an attractive response to a particular chemical be converted to a repulsive response? In this work we develop a framework to analyze these questions (all related to the qualitative nature of signal transduction) from a more general non-system specific perspective. We believe that this provides a platform and systems-skeleton for guiding the examination of these issues in different specific systems, using detailed modelling and focussed experiments.

We examined two design principles which may allow cells to exhibit both chemoattraction and chemorepulsion, both directly motivated by the biological literature. One is that chemoattraction and chemorepulsion are related by simply the opposite regulation of an upstream component by attractant and repellent respectively. The opposite regulation of active enzyme PLC in *Dictyostelium* by chemoattractant cAMP and chemorepellent 8-CPT cAMP has been found experimentally (Keizer-Gunnink et al., 2007). The other principle is that cellular signalling may have inbuilt competing effects upstream which allow it to exhibit both kinds of behaviour. Competing pathways (mediated by cAMP and cGMP) have been observed in neural growth cones, and are believed to be present in neutrophils and T-cells too (Song et al., 1998; Vianello et al., 2005). Competing effects could occur at the level of the receptor as well.

Eukaryotic cells typically sense their environment using a spatial sensing mechanism, and this leads the cell to polarize (form a persistent front and back) and migrate. Different biochemical players are involved in the sensing stage in different systems but they often involve phosphoinositide lipids. The polarization process involves a polarity circuit comprising the RhoGTPases such as Rac, Rho and Cdc42. The interactions between these players can vary from system to system. Chemotaxis in eukaryotic systems is highly subtle as it depends not only on the underlying signalling circuits but also on the internal state of the cell and whether it is already polarized (the effects of intrinsic polarization are discussed in (Krishnan and Iglesias, 2007)), and pseudopods are being formed. This can fundamentally affect how a cell responds and migrates in response to a chemical cue. Further, signal propagation in some systems involves adaptation to homogeneous signals, whereas in other systems (eg neutrophils) homogeneous stimulation can lead to spontaneous polarization.

We examined possible design principles involving attractive and repulsive signalling in light of the above complexities. We used qualitatively simplified, rather than detailed mechanistic models. This is because we seek to distill basic qualitative insights regard-

ing the issues under consideration. Building detailed mechanistic models would entail incorporating a lot of details, and contending with gaps in the mechanistic understanding which are tangential to and distracting from the focus of the work. Overall, the models which we employ (and combinations thereof) compactly encapsulate different possible qualitative signalling scenarios, and allow us to draw appropriate conclusions therefrom. The signalling characteristics we examined are simple feedforward local regulation (the simplest signal propagation), adaptive signalling and spontaneous polarization. All these kinds of behaviour are observed in different eukaryotic systems. In the case of adaptive signalling, the adaptive "layer" occurs in the sensing stage itself, while spontaneous polarization usually involves downstream signalling entities such as Rho GTPases. We examine these different signal propagation possibilities downstream of the individual configurations (Table 2.1).

| **Design Feature** | **Downstream Signal Transduction Mechanism** | | |
|---|---|---|---|
| | **Local Signalling** | **Adaptive Signalling** | **Spontaneous Polarization** |
| Polarity Switch: Relevant to different CA & CR chemical | Switched biasing possible. Effective switching for already polarized or moving cell. | Switched biasing. Preserve/enhance switch effect by resetting mean value. | Switch in gradient response with qualitatively different features. Spontaneous polarization in homogeneous dose of CA but not CR (or vice versa). Homogenous CR dose can depolarize polarized cell. |
| Competing Pathways: Relevant for the same chemical (CA & CR) | Switched gradient response as mean value of signal increased is possible. | Switched biasing (same as previous) | Switched gradient response as mean value of signal is increased, combined with employment or non-employment of instability mechanism. Different combinations of attractive & repulsive gradient responses with & without instability mechanisms possible, as the mean value of the signal is increased. |

Table 2.1: **Summary of Results** The different kinds of upstream mechanisms, the different downstream signalling effects, and the different kinds of switching which can result from any combination thereof are summarised compactly. CA and CR refer to the chemoattractant and chemorepellent, respectively.

In addition to providing basic qualitative insight, our models provide a framework for also understanding and appreciating any additional complexity which occurs in the signalling network wiring of actual systems.

**Polarity switch.** We note that cells may exhibit attractive and repulsive behaviour to either the same or different chemicals. Further this may depend either on the signal strength or the internal state of the cell (or external medium). The first case we examined was the polarity switch–this is especially appropriate for considering attraction and repulsion to different chemicals. We found that by having a single polarity switch, an overall reversal in the response could be obtained. However the main insight here is that repellent and attractant would be regulating particular entities (in absolute concentration) in opposite directions of basal levels. This means in particular than any downstream (monostable) thresholds which were triggered by one of the chemicals, would be inaccessible for the opposite case. Such a scenario may be however appropriate for signal transduction in already polarized cells (Arrieumerlou and Meyer, 2005), where an existing pseudopod/front may simply need to be biased appropriately to guide cell motion. This further suggests that a simple polarity switch, for its functioning, may need additional features relevant to the intrinsic state of the cell for its effective functioning (and also perhaps that this repulsive response may be actually utilized or needed by the cell only when it is polarized and moving). In direct contrast, downstream adaptive signalling actually enhances the role of a polarity switch, by resetting the baseline to exactly nullify the effect mentioned above.

If a single polarity switch occurs upstream of a spontaneous polarization module, then the analysis makes a direct non-trivial prediction: if a homogeneous stimulus of chemoattractant results in spontaneous polarization, then a homogeneous stimulus of chemorepellent will not. Furthermore, if a cell spontaneously polarizes in response to a homogeneous dose of chemoattractant, this can be reversed by a sufficiently high homogeneous dose of chemorepellent, resulting in an unpolarized cell. Thus if these predictions are invalidated experimentally this means that either there is no simple single polarity switch, or that the spontaneous polarization circuit is more complex (for example having bidirectional instability thresholds, none of which have been considered in modelling thus far). It should be emphasized that while a representative module was used in our analysis the conclusion is more broadly applicable to other modules which use spontaneous symmetry breaking mechanisms. Incidentally, certain cells may spontaneously polarize in response to other signals (eg. adhesive signals) when present homogeneously, and the conclusion here is that if the chemorepellent acts on an upstream element in an exactly opposite manner to

the triggering (eg adhesive) signal, then depolarization can occur for the same reasons as above.

In general it is also possible that in cells chemoattractant and chemorepellent independently switch the regulation of multiple parallel entities. This can result in a reversal in a gradient response, assuming that the entities are switched in the same way. If the regulation of the entities is itself in competition with one another, then switching their regulation is not of course guaranteed to switch the response (as this depends on the kinetics of the different regulation). Thus the observation of particular upstream entities whose regulation is switched does not necessarily imply that this is the source of the opposite response.

**Competing pathways.** The second scenario which we examined was the possibility that competing effects were naturally present in the gradient sensing network. Competing effects in signalling response is observed in diverse contexts in signalling, and at different levels, and is often studied in the context of hormesis. Analysis of this scenario reveals how this can naturally, under certain circumstances, reveal a reversal in the gradient response to the same signal, as the mean value of the signal is changed. Reversal of the gradient as the mean value is increased is observed both in the neutrophil response to the chemokine Interleukin-8 as well as the T-cell response to the chemokine SDF-1$\alpha$ (Poznansky et al., 2000; Tharp et al., 2006). It has been suggested that the gradient response reversal for high levels of chemokine may be a natural mechanism to prevent over-accumulation of cells at particular locations. If the degree of competition between pathways is increased, then such a reversed gradient response can occur at lower stimulus mean values (a prediction which can be tested in individual systems). However, having competing pathways does not guarantee the reversal of the response as signal mean value is increased. Further the effect of the presence of a spontaneous polarization circuit downstream of such a setting is that both spontaneous polarization (in homogeneous signals) and gradient reversal may be observed, and further by increasing the stimulus strength in homogeneous stimulation, a depolarization may occur. This has basic implications for the qualitative nature of the migratory response.

In our study, we notice that if a competing pathway structure exists, then it can be modulated by changes in the external or internal cellular environment so that a reversal of gradient response can be achieved even to the same gradient signal (and signal strength). Further by modulating the competing pathways it is possible to either suppress or produce or hasten the possibility of a gradient reversal as the signal mean value is increased. Noting that elements of these pathways in cells are affected by other factors and signalling we see

that it is possible for cells to use the same configuration under different stages of their life cycle, other internal or external conditions, to produce very different results. Reversal of gradient response by modulating the effects of competing pathways has been studied in neural growth cones, where both modulation of pathways as well as changes in the external environment have been made. Given the apparent widespread presence of competing effects in cell signalling, it is an intriguing possibility that this may be a common occurrence in chemotactic systems.

While we have examined the effect of the competition of simple competing pathways, the results can be altered by other factors. For instance if one of the pathways has an upstream threshold, then the smooth transition from (for eg.) attractive to repulsive response can be changed to a scenario where the attractive response weakens and plateaus off for a range of concentrations before a repulsive response kicks in. Further if the signal transduction involved in the competing pathways is fundamentally different, other scenarios may be observed. A competition between adaptive and local pathways can lead to a double switching as the mean value of the signal is increased (the analysis is done in (Krishnan and Alam-Nazki, 2011)).

**Spontaneous polarization.** The other issue which has emerged involves spontaneous polarization and the fact that spontaneous polarization (in the case of a simple polarity switch) may be observed in the case of chemoattraction or chemorepulsion but not both. The question then arises as to how a signalling network may be able to exhibit spontaneous polarization to both chemoattractants and chemorepellents. This could actually occur in different ways. One way is if chemoattractant and chemorepellent modulate different elements of the polarity circuit in a highly non-trivial way to result in spontaneous polarization for both chemoattractant and chemorepellent. A second possibility is that some global (diffusible) element upstream of the polarity circuit resets the regulation of common elements for chemoattractant and/or chemorepellent to ensure that chemorepellent may regulate the element (in mean value) in the same direction, while communicating an opposite gradient response. The other possibility is that while the signalling from each of these signals regulates the polarity circuit, they regulate different elements of the polarity circuit–an example of this could be the different isoforms of Rac or Rho which are observed in different cells. It is quite conceivable that signalling from the chemoattractant and chemorepellent may regulate different Rac isoforms, in fact, and in effect are regulating different or only partially overlapping polarity circuits. This could allow for chemoattractant and chemorepellent to both elicit their respective gradient responses as well as spontaneous polarization in ho-

mogeneous stimulation. Quite intriguingly, different Rac and Rho isoforms are observed both in the front and back of chemotaxing T-cells (Prof. Ridley, personal communication) suggesting possibly different roles for different isoforms of these RhoGTPases in some systems.

We have considered different mechanisms (polarity switch, competing pathways) upstream of adaptive and spontaneous polarization modules. Spontaneous polarization, involving Rho GTPases may be expected to be downstream of such effects, but adaptation may occur at the sensing level. Could adaptive signalling be upstream of the polarity switch/competing pathways? Adaptive signalling upstream of a polarity switch would still provide a reversal in the gradient response. Adaptive signalling upstream of competing pathways would however prevent the signal level dependent reversal in gradient response.

Our study strongly suggests a systematic effort to elucidating both attractive and repulsive responses in cells using both modelling and focussed experiments. In particular it is important to study the response of cells (both mobile and immobilized, where possible) to different stimuli (homogeneous,gradient) of both chemoattractant and chemorepellent: this includes a systematic study of the mean value and gradient strength of the stimulus and monitoring the response of components such as phosphoinositide lipids (or relevant components involved in gradient sensing), as well as the Rho GTPases. Care must be taken to ensure that cells are in essentially the same initial state. Building on this a systematic study of the effect of modulating different (especially competing) pathways biochemically would reveal important information. If a polarity switch is suspected, it is important to systematically examine and compare temporal and spatial behaviour of downstream components to different chemoattractant and chemorepellent stimuli. Our study serves as a basis for examining different characteristic signalling responses. It also suggests that based on the results of experimental investigations suggested, particular attention be paid in modelling how gradient sensing signalling regulates the Rho GTPases. A detailed elucidation of how individual cells are wired to exhibit attractive and repulsive responses would provide invaluable insight into the different kinds of control of cell migration pathways, the manner and conditions under which the cell would exhibit each of these responses, as well as the essential constraints involved in each case. It would also provide clues as to the contexts in which these responses are needed, as well as how the capacity to exhibit one response may have been built on the other.

In conclusion we have formulated a framework, from an implicit systems perspective, for analyzing some design principles which might allow cells to exhibit attractive and re-

pulsive response to either the same or different signals. In fact this framework would also provide insights in the case where the signals may be of different types (not necessarily chemical). Understanding this aspect of migrating cells would be a very convenient way of starting to examine how the cellular behaviour may be exploited or reversed. Noting that cells likely naturally have such capabilities through evolution, a careful exploitation of this aspect can allow for the control of directional migration even if various details of downstream signalling are not completely elucidated. This in turn could be of considerable use and set the stage for a systematic exploitation of this feature in biological, physiological, medical and synthetic contexts.

# Chapter 3

# An investigation of spatial signal transduction in cellular networks

## 3.1 Introduction

Cells consist of highly complex genetic and protein networks which allow them to respond to a variety of cues and make appropriate decisions. Thus much of the decision making in response to external cues, as well as the regulation and control of intracellular processes is achieved through complex, non-linear, and often sophisticated and subtle chemical signal processing (Bastein D. Gomperts, 2009). A considerable body of work has focussed on the understanding of signal transduction and gene regulatory networks underlying a number of important processes. Increasingly, and especially in the last decade, modelling is integrated with experimental work.

In a number of signal transduction settings, the focus is either on steady state or temporal aspects of the signalling. However in many of these cases, spatial aspects are present: for instance proteins have to diffuse to the correct location for the appropriate signalling event to occur; there may be trafficking and interchange of signalling components between different compartments; likewise similar issues arise even in gene regulation and genetic processes. In most of the studies of such processes, spatial aspects are ignored, even if acknowledged. The non-incorporation of spatial effects in some of these processes may be reasonable given that for the available (or measurable) information on the system, a simplified description of various steps is sufficient. However, even here, it is not always clear a priori what roles spatial effects play, and what their significance might be (eg see

(Kholodenko et al., 2010; Stelling and Kholodenko, 2009; Sturrock et al., 2011)).

There are a number of other intracellular processes where spatial effects play a highly non-trivial and even central role and certainly cannot be neglected. Examples of these processes include the chemotactic migration of eukaryotic cells, polarity generation and maintenance in a number of cell types such as fungi and epithelial cells, cytokinesis and the propagation of intracellular waves of calcium (Berridge et al., 2000; Eisenbach et al., 2004; Nelson, 2003; Rappaport, 1971). It is worth pointing out that important spatial processes including localization and wave propagation occur in bacteria itself (Loose et al., 2008; Shapiro et al., 2009). In all these processes the spatial aspects of the process combine with the complexity of the underlying networks and this makes them especially difficult to elucidate. In particular, it becomes necessary to ascertain and establish the spatial locations of multiple signalling components requiring appropriate spatiotemporal resolution and account for these aspects in modelling.

There has been an increasing interest in spatial signalling and an increasing awareness of the need to account for spatial effects in the signal transduction community (Hurtley, 2009; Schwarz-Romond and Gorski, 2010). Further there has been an acknowledgement that there is the need for appropriate understanding and conceptualization of various processes involved in spatial signalling (Kholodenko, 2006; Kholodenko et al., 2010).

In the modelling community there has been a history of modelling a number of specific intracellular and intercellular processes with spatial variation. In the recent past, modelling has focussed on spatial signal transduction in a number of contexts. One set of modelling efforts has dealt with modelling of networks which interpret gradients of chemical stimuli to make decisions: examples include gradient sensing in chemotaxis (eg. see (Alam-Nazki and Krishnan, 2010; Ma et al., 2004)) and pheromone sensing in yeast (Moore et al., 2008). Another set of modelling efforts has focussed on different aspects of cell polarization: this includes the dynamics of the Rho GTPase networks controlling migration (Dawes and Edelstein-Keshet, 2007), cell polarity involving autocrine EGFR signalling (Maly et al., 2004) and polarization of Cdc42 in budding yeast (Howell et al., 2009); related studies have modelled basic aspects of cell polarization incorporating stochastic effects and feedback and applied this to budding yeast polarization (Altschuler et al., 2008). Other studies have examined spatial effects in signalling which had been hitherto studied in purely temporal settings: these include studies of spatial effects in oscillating systems (Hes1 and p53-Mdm2) (Sturrock et al., 2011) and MAPK cascades (Zhao et al., 2011). Other models focus on spatial mechanisms coupling cell size and cell cycle (Vilela et al., 2010) and the

role of networks which provide spatial cues for cytokinesis specification (Padte et al., 2006) and self-organized microtubule assembly (Caudron et al., 2005). There is also a broader literature focussing on modelling self-organized behaviour at the cellular level (reviewed in (Karsenti, 2008)). These examples are a snapshot of some of the spatial signal transduction modelling in specific biological contexts and is by no means a complete list. These models exploit different spatial aspects of signalling elements which are embedded in intricate intracellular network interactions to explain certain phenomena in specific biological processes. What is lacking in the spatial signal transduction modelling literature, however, is a systematic analysis of how different types of network interactions can give rise to complex non-trivial spatial signal processing.

In this work we will develop a modelling and systems framework to elucidate certain aspects of spatial signalling. Thus we will be concerned with various aspects of spatial variation on one hand, and with aspects of the signalling on the other. This informs our approach in this study. Spatial signalling includes the natural complexity of signal transduction, with other aspects specific to spatial considerations. At the outset, while considering spatial signalling, we see that there are different ways in which spatial variation in signalling entities in a network can occur: (i) Some regulating signal or cue external to the cell or "upstream" of the network is spatially varying (ii) there is internal spatial variation of signalling entities for instance due to pre-existent asymmetries, spatial localization, compartmentalization or sequestration (iii) Self organized spatial or spatio-temporal behaviour (Karsenti, 2008). Classic examples of self-organized behaviour include the generation of patterns through Turing mechanisms and their variants (Gierer and Meinhardt, 1972; Turing, 1952). We of course note that depending on the signalling entities or process of interest, this distinction can differ: for instance in a process, a self-organized behaviour may result in spatial pattern formation, which combines with other signalling, and thus acts as a pre-existent or internal spatial variation for other interacting signalling processes. Further in a given process/system, different combinations of these factors might be important.

In this investigation we will elucidate certain aspects of spatial signal processing in the first case, namely spatially varying signals upstream of a given network. Our approach will be generic in nature and not process and/or system specific. While elucidating specific spatial signalling processes of course needs to include specific experimental investigations appropriately complemented by modelling, we will not attempt that here. This is because of the diversity of processes, the time-consuming and iterative nature of modelling, and the fact that quite a few details of the process depend on the system under consideration.

Our goal is to obtain insights into how spatial signals are transduced through different networks, which may be relevant in multiple contexts. In order to do this, we use as a basis a set of basic signal transduction networks or motifs. These networks are chosen because the dynamic behaviour they embody (eg. switch-like behaviour or oscillations) or their structure is widely observed in cell signalling settings. Noting that structure of course does not uniquely determine dynamic behaviour even qualitatively, we choose our basis set to represent essentially different kinds of signal processing which are observed. Thus the modules we will consider include coherent and incoherent feedforward, negative and positive feedback circuits (with no cooperativity), cyclic networks, monostable and bistable switches and oscillators. We then examine how these networks respond to spatially varying signals and further how the circuit response is affected by diffusion of individual elements. In this manner we develop a number of insights into how common basic signalling circuits process spatially varying signals and how diffusion may significantly affect the signal processing.

We believe that the use of simplified models is much more appropriate for the analysis we undertake here. It is worth pointing out that even in temporal signalling, while different signalling circuits vary considerably in details, there are some kinds of basic signalling patterns which occur repeatedly and the understanding of these basic elements has proven to be a good reference point for understanding additional complexities in signalling (Tyson et al., 2003). We adopt an analogous approach here. All the signalling circuits which we study include compact encapsulations of the signalling behaviour we wish to examine, while simultaneously allowing for exploration of the issues at hand. The nature of the analysis implies that it is possible to transfer such insights to more complex models with similar dynamic behaviour. We believe that such an approach will help in developing a basis for systematically understanding aspects of spatial signalling.

Our results provide non-trivial insights regarding temporal and spatial signal transduction and when particular temporal signal transduction characteristics may or may not be translated into spatial signalling characteristics. In particular, we find that having highly diffusible or global entities can either impose big constraints or create new capabilities in spatial signal transduction when compared to temporal signal transduction. For instance, such entities can strongly accentuate switching behavior in spatial signalling, or abolish the switching behaviour in spatial signals (in bistable switches). This aspect is explored in detail in multiple modules.

The chapter is organized as follows. In the next section, we detail the various models which we use for our investigations. In the following section, we present a series of re-

sults on how these circuits process spatial signals and how diffusion might play a role in modulating or affecting the response. The results are based on numerical and analytical work, some of which is detailed in the Appendix. We then conclude with a synthesis of the results.

## 3.2 Models and methods

In this section we present and discuss the models which we employ. Before proceeding to discuss the models in detail, we first discuss the goal of the work, and the logic for the choice of models.

The goal of this work is to examine certain aspects of spatial signalling driven by external or "upstream" signals through the investigation of representative network circuits, and to further elucidate in which regard the signal processing mirrors temporal signalling and where it is essentially different. Spatial signal transduction of course encompasses a wide variety of processes with all their underlying complexities, with details potentially varying significantly even from system to system. Our goal will therefore be to choose a class of representative signalling networks to investigate these issues. As has been mentioned earlier, the investigation and analysis of ubiquitously occurring signalling behaviour through basic minimal models has proven to be very useful in temporal signalling.

The models which we will examine are a suite of essentially minimal models which compactly describe qualitatively different signalling patterns. These are realized through networks of a small number of components. The models are chosen because they represent signalling and causal patterns which are observed or studied in temporal signalling (Alon, 2006a; Tyson et al., 2003). The models examined are (i) Coherent feedforward network (ii) Incoherent feedforward network (iii) Positive feedback regulation (iv) Negative feedback regulation (v) Cyclic network (vi) Monostable switches (vii) Bistable switches (viii) Oscillators (ix) Other switches (see Fig. 3.1).

These networks are all purely temporal networks to start with, and further have a clear input-output representation. While in some cases different parameters or reactions could alternatively be modulated by an input, we will regard the designated input as the primary input, since such other modulation either has essentially similar effects or otherwise predictable effects. Since we focus on spatial signalling we will assume that these networks are spatially distributed, and thus different components can diffuse.

We will especially focus on where spatial signalling in these networks may be essen-

tially different from temporal signalling. We will approach this as follows. For each network we will start with the case where each component is non-diffusible. We will examine the response to spatially varying signals to start with, as these are the most natural and basic ways in which spatial signal processing may occur. We will then examine the role of diffusion by examining how highly diffusible entities may distort the signal transduction in these networks, and explore what spatial analogues of these temporal signalling mechanisms may be. This will be done by considering the same classes of signals but also studying the effect of high diffusivities of network components. Taken together our studies will elucidate basic spatial processing and the significant changes introduced by highly diffusible or global components.

We now discuss the basic models which we will study. All of these are postulated on a 1-D spatial domain for simplicity. The 1-D domain could represent a membrane compartment or a slice of a cytosolic compartment or organelle. Since we are mainly considering effects of high diffusion, the essential results and insights in this study carry through to 2-D and 3-D domains as well. It should be noted that if examining spatial effects arising due to internal spatial variation due to structures within the cell then a 2-D or 3-D description would be required. However, for the purpose of our study, utilizing a 1-D description is sufficient. Further for specificity we will assume periodic boundary conditions, although most results are equally valid for other boundary conditions such as no-flux boundary conditions. Periodic boundary conditions imply that the spatial region for modelling is akin to a circle, with the two ends identified with one another. Since none of the results obtained actually relies on the boundaries of the spatial region under consideration, the effect of this choice of boundary condition is minimal.

In all modules the signal will be denoted by S while $R^*$ is a key response element of interest. We will allow each element to be diffusible (discussed later). We also note that all enzymatic reactions are described by mass action kinetics, unless specifically mentioned otherwise. In principle the reactions may be modelled via other kinetic descriptions; we have chosen to utilize the simplest descriptions (with the least amount of assumptions) of the causal patterns we are interested in studying in the modules.

In the equations below, the species with a '*' superscript denotes the active form and species term without this denotes the inactive form. $D_j$ is the diffusion coefficient for the species j. $\theta$ denotes the position of the species. In many of the circuits, the signalling model involves the interconversion between active and inactive forms a species, say $X$ and $X^*$. In these cases, when active and inactive forms are non-diffusible, the signalling leads to

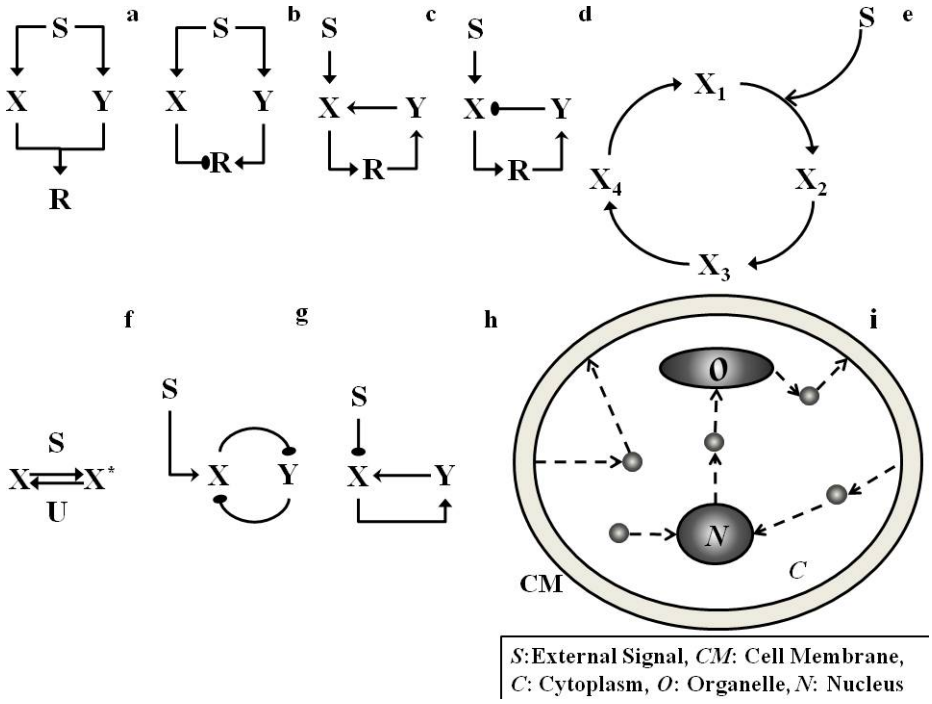


Figure 3.1: **Schematic diagrams of modules employed** The input $S$ is a spatial signal. (A) In the coherent feedforward module $S$ positively regulates (arrows denoted by filled arrowheads) $X$ and $Y$ which in turn positively modulate the response $R$. (B) Similar to (A) except $X$ inhibits the response element, representing one kind of incoherent feedforward circuit (see text). (C,D) In the positive (negative) feedback module $S$ leads to the activation of the response $R$ which subsequently activates (inhibits) $X$ via the intermediate feedback element $Y$. (E) A sample cyclic reaction network is shown. $S$ catalyzes (denoted by a sharp line arrowhead) the conversion of $X_1$ to $X_2$. (F) The monostable switch module consists of two enzymes $S$ and $U$ acting close to saturation and mediating the production and degradation of $X$. (G) The bistable switch module consists of a double negative feedback loop. $S$ regulates the production of $X$ and $X$ and $Y$ inhibit one another. (H) In the transcritical bifurcation module $X$ is inhibited by the signal and activates its own production via the feedback element $Y$. The oscillator module is realized from the topology in (D) with different non-linear interactions (see text). (I) A simple cross section of the cell is shown exhibiting a cell membrane (CM), cytoplasm (C), an organelle (O) and a nucleus (N). The small circles in the cell represent signalling molecules. Gradually graded as well as localized concentration profiles of different signalling entities naturally arise and are transduced through various complex networks which also include global coupling through diffusion.

conservation of total amount of $X + X^* = X_{tot}$. In such cases, we write only the equation for the rate of change of concentration of the active form $X^*$ in terms of $X^*$ and $X$ and this conservation will be used to eliminate $X$. This introduces an additional parameter $X_{tot}$. It may be noted that if $X$ and $X^*$ are diffusible (assumed to have the same diffusivity), then it is found that $X + X^*$ satisfies a homogeneous diffusion equation, and since $X + X^* = X_{tot}$ holds good initially everywhere, this continue to hold good for all time. Thus again, $X$ can be written in terms of $X^*$ and $X_{tot}$.

In the equations of the models 1-4 (coherent feedforward, incoherent feedforward, positive feedback, negative feedback) the kinetic constant $k_{ij}$ denotes the i species mediated conversion of species j to its active form (if the term is preceded by a positive sign) or inactive form (if the term is preceded by a negative sign), where $i = X$ or $Y$ or $R$ or $S$ and $j = X$ or $Y$ or $R$. $k_j$ and $k_{-j}$ denote the rate constants for the constitutive (basal) conversion between inactive and active forms for species j.

### 3.2.1 Coherent feedforward module

This module involves a signal regulating a response element through two parallel pathways, denoted by X and Y (with active forms denoted by $X^*$ and $Y^*$). Both $X^*$ and $Y^*$ additively regulate the production of $R^*$ in a positive way. The equations governing the coherent feedforward module are given by

$$\begin{aligned}
\frac{\partial X^*}{\partial t} &= (k_{sx}S + k_x)X - k_{-x}X^* + D_X\frac{\partial^2 X^*}{\partial \theta^2} \\
\frac{\partial Y^*}{\partial t} &= (k_{sy}S + k_y)Y - k_{-y}Y^* + D_Y\frac{\partial^2 Y^*}{\partial \theta^2} \\
\frac{\partial R^*}{\partial t} &= (k_{xr}X^* + k_{yr}Y^*)R + k_rR - k_{-r}R^* + D_R\frac{\partial^2 R^*}{\partial \theta^2}
\end{aligned} \tag{3.1}$$

In the above equations the parameters $k_{xr}$ and $k_{yr}$ were varied to modulate the strength of the associated pathways.

### 3.2.2 Incoherent feedforward module

Here, in contrast to the first module, the signal regulates the response element through two pathways X and Y which are in opposition to one another. Thus, we have Y positively regulating the production of the response element, while X negatively regulates it. There

are two ways in which this could be modelled. In one case, X inhibits the production of the response element (by for instance binding to and suppressing the enzymatic activity involved) while in the second case, X acts to enhance the deactivation/degradation of the response element. We choose the second case first, and subsequently consider the first case. The equations governing the incoherent feedforward module in the second case mentioned above (also see (Krishnan, 2009, 2011)) are given by

$$\begin{aligned}
\frac{\partial X^*}{\partial t} &= (k_{sx}S + k_x)X - k_{-x}X^* + D_X\frac{\partial^2 X^*}{\partial\theta^2} \\
\frac{\partial Y^*}{\partial t} &= (k_{sy}S + k_y)Y - k_{-y}Y^* + D_Y\frac{\partial^2 Y^*}{\partial\theta^2} \\
\frac{\partial R^*}{\partial t} &= k_{yr}Y^*R - k_{xr}X^*R^* + k_rR - k_{-r}R^* + D_R\frac{\partial^2 R^*}{\partial\theta^2}
\end{aligned} \tag{3.2}$$

Here X is the inhibitor and Y is the activator. In this module $k_{sx}, k_{-x}, k_{xr}, k_{sy}, k_{-y}$ and $k_{yr}$ are modulated to achieve different scenarios where either X or Y is regulated more strongly.

We also consider another type of incoherent feedforward module where the signal S modulates X positively and Y negatively. Both X and Y additively regulate the activation of $R^*$.

$$\begin{aligned}
\frac{\partial X^*}{\partial t} &= (k_{sx}S + k_x)X - k_{-x}X^* + D_X\frac{\partial^2 X^*}{\partial\theta^2} \\
\frac{\partial Y^*}{\partial t} &= k_yY - (k_{sy}S + k_{-y})Y^* + D_Y\frac{\partial^2 Y^*}{\partial\theta^2} \\
\frac{\partial R^*}{\partial t} &= (k_{xr}X^* + k_{yr}Y^*)R - k_{-r}R^* + D_R\frac{\partial^2 R^*}{\partial\theta^2}
\end{aligned} \tag{3.3}$$

The difference in this module is in the equation for the response element, where both $X^*$ and $Y^*$ positively regulate the response element and in that the Y pathway is inhibited by the signal (for simplicity here the basal constant $k_r$ is assumed to be zero.

The previous two modules were feedforward modules. We now examine modules with feedback as a key element.

### 3.2.3 Positive feedback module

The equations governing the Positive Feedback module are given by

$$\begin{aligned}
\frac{\partial X^*}{\partial t} &= (k_{sx}S + k_x)X - k_{-x}X^* + k_{yx}XY^* + D_X\frac{\partial^2 X^*}{\partial \theta^2} \\
\frac{\partial R^*}{\partial t} &= (k_{xr}X^* + k_r)R - k_{-r}R^* + D_R\frac{\partial^2 R^*}{\partial \theta^2} \\
\frac{\partial Y^*}{\partial t} &= (k_{ry}R^* + k_y)Y - k_{-y}Y^* + D_Y\frac{\partial^2 Y^*}{\partial \theta^2}
\end{aligned} \tag{3.4}$$

This module describes the signal regulating an element $X^*$ which regulates the response $R^*$. Additionally $R^*$ can positively regulate the production of the active form of X, through the production of another element Y. Y is the intermediate feedback element. Since we focus on spatial aspects and diffusion, we explicitly describe the dynamics of this intermediate feedback element. The parameter of particular interest here is the one associated with the feedback- $k_{yx}$. Note that the positive feedback described here involves no cooperativity.

### 3.2.4 Negative feedback module

The negative feedback module is an analogue of the positive feedback module except that the response negatively regulates the production of the upstream element $X^*$. Again, here, we model that by having $R^*$ enhancing the degradation of $X^*$. The equations governing the Negative Feedback module are given by

$$\begin{aligned}
\frac{\partial X^*}{\partial t} &= (k_{sx}S + k_x)X - k_{-x}X^* - k_{yx}X^*Y^* + D_X\frac{\partial^2 X^*}{\partial \theta^2} \\
\frac{\partial R^*}{\partial t} &= (k_{xr}X^* + k_r)R - k_{-r}R^* + D_R\frac{\partial^2 R^*}{\partial \theta^2} \\
\frac{\partial Y^*}{\partial t} &= (k_{ry}R^* + k_y)Y - k_{-y}Y^* + D_Y\frac{\partial^2 Y^*}{\partial \theta^2}
\end{aligned} \tag{3.5}$$

Y is the intermediate feedback element as before. The main parameter varied here is the one associated with the feedback - $k_{yx}$.

### 3.2.5 Cyclic module

We consider an irreversible cyclic module, involving $n$ species where the concentration of the ith species is denoted by $X_i$. The reactions are irreversible and it is assumed that the signal regulates the conversion of $X_1$ to $X_2$, without loss of generality. We note that this cyclic module includes as a special case, the simple reversible interconversion of two species (with one of the reactions regulated by the signal), which is realized when $n = 2$. This is the simplest reversible signalling network one can consider for spatial signal processing. The equations governing the irreversible cyclic reaction network module are given by

$$\begin{aligned}
\frac{\partial X_1}{\partial t} &= k_n X_n - k_1 X_1 S + D_1 \frac{\partial^2 X_1}{\partial \theta^2} \\
\frac{\partial X_2}{\partial t} &= k_1 X_1 S - k_2 X_2 + D_2 \frac{\partial^2 X_2}{\partial \theta^2} \\
\frac{\partial X_i}{\partial t} &= k_{i-1} X_{i-1} - k_i X_i + D_i \frac{\partial^2 X_i}{\partial \theta^2} (i = 3, 4...n)
\end{aligned} \tag{3.6}$$

In the above equation $k_i$ is the rate constant associated with the conversion from $X_i$ to the next member in the cycle. In the case of the conversion of $X_1$, the presence of the external signal is written explicitly, so that while all $k_i$ for $i > 1$ are first order rate constants, $k_1$ is actually a second order rate constant, with $k_1 S$ being the corresponding first order rate constant.

The subsequent modules we examine are examples of modules which embody highly non-linear signal processing.

### 3.2.6 Monostable switches

While monostable switches may be realized in quite different ways, for example through combination of the effects of different stages as in MAP Kinase cascades (Ferrell, 1996), we consider another case which has been studied and used widely. This is the Goldbeter-Koshland module (Goldbeter and Koshland, 1981), which involves a reversible reaction pair with enzymes involved in each reaction acting close to saturation. The equations gov-

erning this module are given by

$$\begin{aligned}\frac{\partial X^*}{\partial t} &= \frac{k_{sx}SX}{K_{M1}+X} - \frac{k_r X^* U}{K_{M2}+X^*} + D_{X^*}\frac{\partial^2 X^*}{\partial \theta^2} \\ \frac{\partial X}{\partial t} &= \frac{-k_{sx}SX}{K_{M1}+X} + \frac{k_r X^* U}{K_{M2}+X^*} + D_X\frac{\partial^2 X}{\partial \theta^2}\end{aligned} \tag{3.7}$$

In the above equations the signal $S$ is the enzyme which catalyzes the production of $X^*$ and the enzyme $U$ catalyzes its degradation. $k_{sx}$ denotes the rate constant for the signal mediated production of $X^*$. The Michaelis Menten kinetic constants $K_{M1}$ and $K_{M2}$ are associated with the enzymes S and U, respectively. $k_r$ is the rate constant associated with the backward reaction.

### 3.2.7 Bistable switches

The subsequent module we consider is a very different kind of switch, which is also ubiquitously observed in cell signalling — the bistable switch. A bistable switch is typically achieved by positive feedback (Ferrell and Xiong, 2001), with co-operativity/non-linearity in the feedback regulation. The positive feedback could be realized by for instance the mutual activation/positive regulation of two elements, or alternatively through the mutual inhibition of two elements. We will present the mutual inhibition case, and discuss the similarities/differences with the mutual activation module later.

The equations governing the mutual inhibition bistable switch module are given by

$$\begin{aligned}\frac{\partial X^*}{\partial t} &= k_0 + k_1 S - k_2 X^* - k_{21} X^* Y^* + D_X\frac{\partial^2 X^*}{\partial \theta^2} \\ \frac{\partial Y^*}{\partial t} &= \frac{-k_3 X^* Y^*}{K_{M3}+Y^*} + \frac{k_4 Y}{K_{M4}+Y} + D_Y\frac{\partial^2 Y^*}{\partial \theta^2}\end{aligned} \tag{3.8}$$

The above model is a sample bistable circuit analyzed in (Tyson et al., 2003). In that paper the equation for $Y^*$ has been written explicitly as a Goldbeter Koshland switch-like function, by invoking a quasi-steady state approximation. Here we have written this in the fully expanded form- using Michaelis Menten kinetics, explicitly describing the dynamics of the two species. In the above equation, $k_0$ is the basal rate constant for the production of species $X^*$. $k_1$ denotes the rate constant for the signal mediated production of $X^*$. $k_2$ and $k_4$ denote the basal inactivation and activation rate constants for species $X$ and $Y$, respectively and in each case, the associated reaction is independent of the other species.

$k_{21}$ and $k_3$ are the kinetic rate constants associated with the mutual inhibition of species $X^*$ and $Y^*$ respectively. The Michaelis Menten kinetic constants $K_{M3}$ and $K_{M4}$ are associated with the degradation and production of $Y^*$ respectively. This module has the property of bistability, i.e. it has two stable steady state values for a particular range of the signal values and an unstable steady state as well. The fact that a substantial signal range is associated with bistability, is readily confirmed by doing bifurcation analysis of this module with the signal as a parameter. Such analysis is performed in (Tyson et al., 2003).

### 3.2.8 Oscillator module

The module we examine is one of negative feedback leading to oscillations (studied in (Tyson et al., 2003)). This is an example of a module where the strong nonlinear negative feedback is capable of generating oscillations. It should be noted that there is no explicit delay in this system.

The equations governing the Negative Feedback Oscillator module are given by

$$\begin{aligned}
\frac{\partial X^*}{\partial t} &= k_0 + k_1 S - k_2 X^* - k_{21} X^* Y^* + D_X \frac{\partial^2 X^*}{\partial \theta^2} \\
\frac{\partial R^*}{\partial t} &= \frac{k_3 X^* R}{K_{M3} + R} - \frac{k_4 R^*}{K_{M4} + R^*} + D_R \frac{\partial^2 R^*}{\partial \theta^2} \\
\frac{\partial Y^*}{\partial t} &= \frac{k_5 R^* Y}{K_{M5} + Y} - \frac{k_6 Y^*}{K_{M6} + Y^*} + D_Y \frac{\partial^2 Y^*}{\partial \theta^2}
\end{aligned} \tag{3.9}$$

In this module, the signal is relayed through the element $X^*$ and $R^*$ is the response. The negative feedback pathway involves the response inhibiting $X^*$ via an intermediate element $Y^*$ (rate constant $k_{21}$).

In the above equations $k_0$ is the basal rate constant for the production of species X. $k_1$ denotes the rate constant for the signal mediated production of $X^*$. $k_2, k_4$ and $k_6$ denote the basal inactivation rate constants for the species $X^*, R^*$ and $Y^*$ respectively. $k_3$ and $k_5$ denote the rate constants associated with the conversion of the species $R^*$ and $Y^*$, respectively, from their inactive to active forms (catalyzed by $X^*$ and $R^*$ respectively). The Michaelis Menten kinetic constants $K_{M3}$ and $K_{M4}$ are associated with the production and degradation of $R^*$, respectively. The Michaelis Menten kinetic constants $K_{M5}$ and $K_{M6}$ are associated with the production and degradation of $Y^*$, respectively. This three-component module consists of a negative feedback and for a critical range of values of the signal (held fixed), gives rise to a sustained oscillatory response. The lower and upper limits of the

signal range where oscillations occur are associated with Hopf bifurcation points and at these points the steady state response undergoes a change in stability and oscillations are generated via supercritical Hopf bifurcations.

### 3.2.9 Choice of parameters

We briefly comment on the choice of parameters in the modules which we employ. An advantage of using relatively simple models is that the parametric dependence of these models can be fairly easily mapped out. As discussed above, our model analysis will first consider the response of the network to representative spatial signals, where all elements are essentially non-diffusible. Then we examine the effects of diffusion. With regard to kinetic parameters we make a representative choice of kinetic parameters in such a way that these kinetic parameters represent the typical behaviour of the module. Our aim in this investigation is to focus on the spatial aspects of signalling and not get bogged down in various auxiliary analysis. If in certain modules, there are different representative parameter regimes with qualitatively different behaviour, we will analyze them separately. In the case of the non-linear dynamic modules, for the basal parameter values (which have already been considered and analyzed before), bifurcation analysis in the parameter S yields robust non-trivial parameter regimes of desired behaviour (eg. bistability, oscillations). Overall our approach is to keep auxiliary parameters in the background with the understanding that they are a reasonable choice of parameters to represent the module signalling behaviour.

We also discuss the effects of diffusion. The modules have different elements all of which may diffuse. Our main goal is to find qualitative changes introduced by diffusion and strong diffusion in particular. With that in mind, when we consider the effect of diffusion, we do so one species at a time, and choose a high enough diffusion coefficient for the domain size and time scales of interest that the element may be regarded as highly diffusible. The other species will be considered to be (essentially) non-diffusible. In this manner we will obtain clear cut qualitative signatures of the effect of highly diffusible elements in signal processing. We will not attempt to study thoroughly the effects of various diffusivities over their entire range (this will be done subsequently). We mention that the global regulation introduced by such highly diffusible components could also result from components which are exchanged between compartments, one where spatial signal transduction occurs, and another essentially well-mixed compartment which exchanges material with it.

The results involve performing simulations in MATLAB using ode15s. The partial differential equations were discretized using finite difference equations and the results checked by doubling the discretization. As complementary work, bifurcation/sensitivity analysis of the kinetic equations was performed using MATCONT.

## 3.3 Results and Discussion

In this section, we present results on the analysis of the models employed. For each module, we present two sets of results. The first relates to how the modules process spatial signals such as spatially graded signals and localized signals. Both kinds of signals are repeatedly encountered and may be generically expected in intracellular signalling. In this case the elements of the network are regarded as essentially non-diffusible. We analyze this separately firstly because it is the most natural way in which spatial signalling may arise, and secondly because it forms a basis for examining what happens when individual elements may be highly diffusible. Only steady state input signals will be examined here. We subsequently build on these results to examine what happens when individual elements may be highly diffusible. Here we will primarily focus on cases where non-trivial spatial signal transduction occurs in the network.

To perform the analysis, we use a combination of numerical simulations, bifurcation and sensitivity analysis and analytical results (analytical results were discussed in (Alam-Nazki and Krishnan, 2012)). Taken together the results provide insights into the spatial signal transduction capabilities of such networks, and the role of high diffusivity of individual elements in altering/distorting the local temporal signal transduction of the individual temporal modules. We build on our studies to interpret our findings in terms of implications for cell signalling associated with those modules. In particular we focus on the capabilities and constraints associated with these modules, in spatial signalling, and also on situations where spatial signal processing is essentially different from temporal signalling. We discuss these at the end of each module subsection (parameter values for each figure are in Appendix B).

### 3.3.1 Coherent Feedforward Module

In the coherent feedforward module there are two distinct pathways involving species X and Y driving the production of the response. Here we will consider the case where the

pathways are of two different strengths but similar saturation capabilities, so as to avoid dealing with additional and rather tangential issues such as saturation in the current context.

First we will examine the case when none of the elements diffuse. When a gradient signal input (a linear gradient which amounts to a cosine signal) is applied the response essentially mirrors the input (Fig. 3.2). When a localized signal input is applied to the module, the response is localized at the location of the input signal. Both these results are understood simply in terms of parallel feedforward effects in the coherent feedforward module.

Next we examined the case when one of the elements involved in the feedforward pathways is highly diffusible. Thus $X$ and $Y$ are made highly diffusible (one at a time) and the response to the aforementioned signals is again observed. The module response is qualitatively similar to the signal and has weaker spatial variation when compared to the case when none of the elements are diffusible (Fig. 3.2). For the case illustrated in Fig. 3.2, $k_{xr} > k_{yr}$, i.e. the mediation of the production of $R^*$ by species $X$ is stronger relative to the $Y$ mediated production of $R^*$. Thus, when the $X$ pathway is made highly diffusible then the spatial variation of $R^*$ is weaker relative to the case where the $Y$ pathway is highly diffusible. It is interesting to note here that in the localized response, when $X$ is highly diffusible, the baseline concentration of the response is higher than the case when none of the elements diffuse. This is because the pathway involving species X conveys global information about the input signal, which results in an increase in response everywhere. It is also seen that when the stronger pathway is the highly diffusible one, this results in a higher increase in the "background " level of the output. These results may further be consolidated by analytical results (discussed in (Alam-Nazki and Krishnan, 2012)). The analysis shows that a coherent feedforward network gives rise to an output which is a combination of the direct effect of the signal through one pathway, and the global average of the signal through another pathway. It is the latter effect which results in an elevated level everywhere, even when the signal is relatively localized.

## Biological relevance

Our analysis reveals that if the two feedforward pathway elements are non-diffusible, then the coherent feedforward pathway provides a degree of redundancy with regard to signal transduction, which is also relevant to spatial signalling. If one of the pathways is diffusible, we find that only one pathway conveys spatial information, and thus the redundancy in

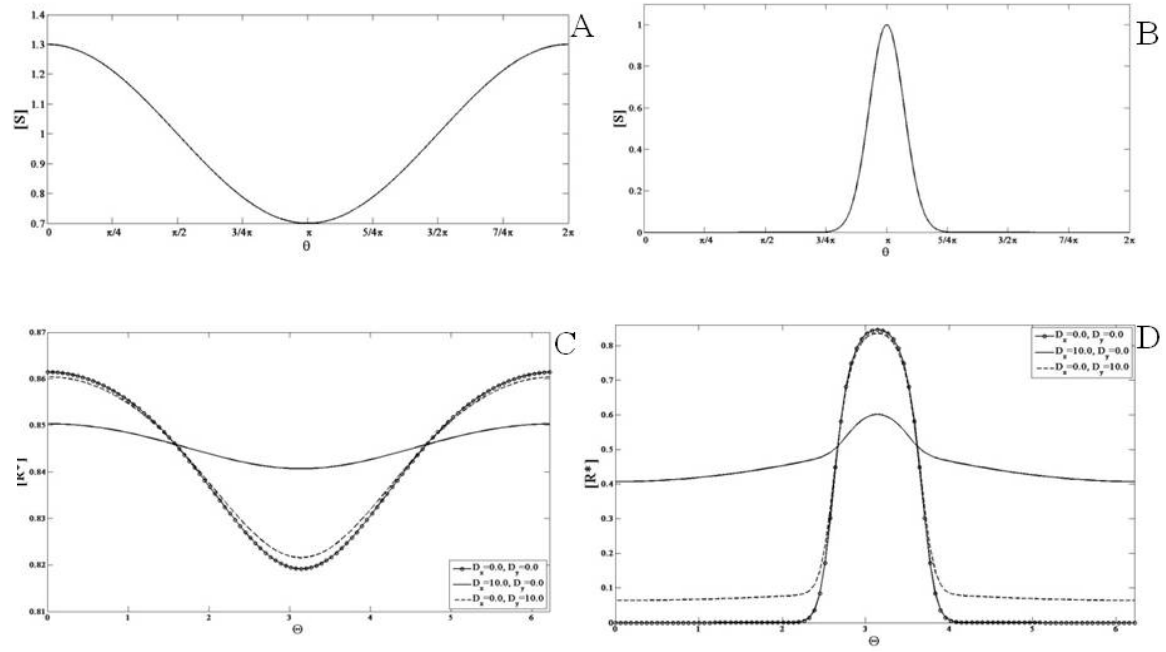


Figure 3.2: **Response of the Coherent Feedforward module.** An example of the (A) gradient signal input and the (B) localized signal input used in the analysis is shown (as a function of the domain position). In this and other simulations the graded signal has a cosine variation and is of the form $S = a + bcos\theta$. The localized signal is of the form $a + Aexp(x - x_o)/\alpha$ (refer to supplementary material for parameter values for all the figures). The module is subjected to a (C) gradient signal input and a (D) localized signal input and the response is shown for either when none of the elements are diffusible (solid line with circles) or when the $X$ pathway (solid line) or the $Y$ pathway (dashed line) is highly diffusible. The scenario where pathway $X$ is stronger than pathway $Y$ is shown here. In each case the response qualitatively mirrors the signal. When $X$ diffuses, the spatial variation of the response is weaker than when $Y$ diffuses. In both these cases, the response element exhibits weaker spatial variation when compared to the non-diffusible case.

temporal signalling is lost in spatial signal transduction. This feature could be considered either a capability or a constraint, depending on the context.

A number of examples of the coherent feedforward module can be seen in protein signaling networks. These include the regulation of cyclin A by E2F in the cell cycle (Tyson and Novák, 2010) and the activation of Akt by the PDGF receptor via distinct PI3K isoforms (Park et al., 2003). An example of the coherent feedforward network with a global element is found embedded in the signaling pathways leading to the activation of the enzyme PKC (Krauss, 2008) through the signalling pathway associated with PLC. When PLC is activated it catalyzes the hydrolysis of $PIP_2$ into Diacyl glycerol (DAG) and Inositol-3,4,5-trisphosphate ($InsP_3$). DAG remains in the membrane and activates PKC and enhances its translocation to and association with the membrane. $InsP_3$ diffuses into

the cytoplasm and initiates the release of calcium ions in the cytosol, which in turn also activate PKC and promote its attachment to the membrane, and hence acts as the global regulator.

### 3.3.2 Incoherent Feedforward Module

We now examine the first type of incoherent feedforward module which has two pathways in competition with one another. This module consists of an activator $Y$ and an inhibitor $X$ that mediate the activation and inhibition of $R^*$. In our study of the incoherent feedforward module, we first modulate the strength and kinetics of these two pathways and observe the response of the module when none of the elements diffuse. In our study we will assume that the total amount of enzymes X and Y are the same. We first consider the situation, where the regulation of the X pathway is stronger than that of the Y pathway. Simulations of the module when subject to a gradual gradient reveal that the steady state concentration profile of the response indeed varies spatially and is qualitatively opposite to that of the signal (Fig. 3.3). This is simply understood by the fact that the pathway inhibiting the response is stronger than that of the activating pathway. Similarly in response to a localized Gaussian input signal, the module exhibits a localized dip for exactly the same reason. If the activating pathway were made stronger, then the response of the module to a gradient would be qualitatively similar to that of the input, again simply reflecting the dominance of the activating pathway over the inhibiting pathway. We note in passing that if both pathways are of equal strength, then their effects exactly cancel out, resulting in a spatially homogeneous steady state output even for spatially varying input.

Next, we examined the case where one of the species was highly diffusible (see Fig. 3.3). When the inhibitor is highly diffusible, the response of the module when subject to a gradual gradient mirrors the signal. This is irrespective of which of the two pathways has stronger kinetic regulation by the signal. This is understood by noting that only the activating pathway is conveying spatial information. There is a further difference in comparison to the non-diffusible case considered above. When the signal range is not too high (so that both pathways are far from saturation), the response has the feature that a spatially homogeneous signal leads to a steady state which is very insensitive to the level of the signal. Thus the module exhibits adaptive behaviour in a homogeneous stimulus (this is true irrespective of the diffusivity of the species). Therefore this module has the characteristic of providing a gradient response, while exhibiting adaptive behaviour in homogeneous stimuli. This

means that the gradient response essentially varies about a fixed mean value (at least when the signal is not high). Thus in this case the module shows similar behaviour to the so-called Local Excitation Global Inhibition module (Levchenko and Iglesias, 2002). More importantly, having a diffusible entity provides a clear contrast between temporal and spatial signalling characteristics: an adaptive response is seen in spatially homogeneous (i.e. temporal) signals, but not in spatial gradients.

If the activator is diffusible, then the module exhibits a response in a gradual gradient, which is opposite to the input simply because spatial gradient information is conveyed only through the inhibitor. This is a module which also exhibits a gradient response along with adaptive behaviour in homogeneous stimuli, with the difference that the gradient response is counter-aligned with the input. The analytical reasoning behind these results was laid out in (Alam-Nazki and Krishnan, 2012).

Finally we briefly examine the second type of incoherent feedforward module (see Fig. 3.3).

An analysis of such an incoherent feedforward module reveals that for wide ranges of parameters, the behaviour is as follows: the response of the module to a spatially homogeneous stimulus is biphasic (Krishnan and Alam-Nazki, 2011). This has the following implications for spatial signalling: if the network (with all elements non-diffusible) is subject to a gradient, then the response can completely switch from being co-aligned to being counter-aligned (or vice versa) as the mean value of the signal is changed.

Next we consider the case where one of the elements in the network is highly diffusible. If the dominant pathway X is highly diffusible, then the spatial information from the signal will only be conveyed through the non-diffusible pathway- Y. Thus the response will be counter-aligned to the signal and this continues to hold good even when the mean value is changed. Thus having one pathway being diffusible, completely abolishes the possibility of switching in gradient response. This again underscores the difference between steady state temporal and spatial responses, and demonstrates how having a diffusible element acts as a constraint (if a reversal in response is desired, as has been suggested in migratory responses) or a capability (preventing a reversal in spatial response, inspite of a biphasic steady state response to temporal stimuli).

**Biological relevance** We have just seen how having global entities in incoherent feedforward networks can prevent reversal of responses as the mean value of the driving signal is increased, and that it can also prevent adaptation in spatially varying signals. The incoherent feedforward signalling network is observed or implicated in multiple biological

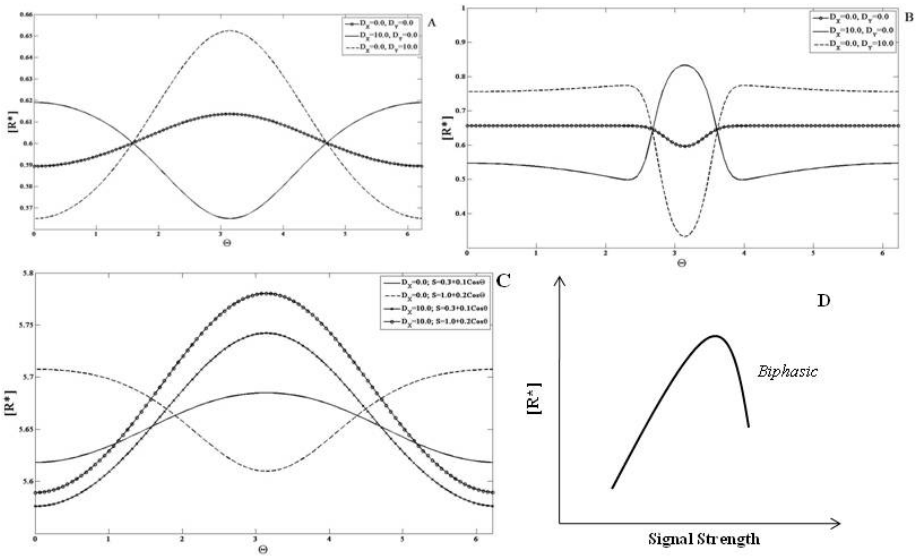


Figure 3.3: **Response of the Incoherent Feedforward modules.** The first incoherent feedforward module (see text) is subjected to a (A) gradient signal and a (B) localized signal input. In the case illustrated here pathway $X$ (inhibitor) is stronger than pathway $Y$ (activator). When none of the pathways are diffusible (solid line with circles) the response is qualitatively opposite to that of the signal. When pathway $X$ is highly diffusible (solid line), the response mirrors the signal profile. On the other hand when the activator pathway is highly diffusible (dashed line) the response is qualitatively opposite to the signal. Thus, having a diffusible element allows for the response to show greater spatial contrast. (C) The second module (eq. 3, see text) is subjected to gradient signals. In the case illustrated here pathway X (inhibitor) is stronger than pathway Y (activator). When none of the pathways are diffusible, the response of the module switches from being qualitatively similar to the signal (solid line) to being qualitatively opposite (dashed line) to that of the signal as the mean value of the signal is increased. When pathway X is highly diffusible, the response mirrors the signal profile even if the mean value of the signal is increased (solid line with circles and solid line with x markers). Thus, the presence of a diffusible element prevents the switch in spatial biasing of the response. (D) A schematic of the biphasic response is shown- here the response increases and then decreases as the value of the (temporal or homogenous) signal increases.

processes, including axon growth cone turning (involving pathways controlled by cAMP and cGMP) and hormesis or the biphasic dose response of fibroblasts to chemical agents (Calabrese, 2001; Nishiyama, 2003). Incoherent feedforward loops with diffusible entities have been used to model the PI3K and PTEN pathways underlying gradient sensing in Dictyostelium chemotaxis (Ma et al., 2004).

### 3.3.3 Positive Feedback Module

We now examine the positive feedback module. Note that the element involved in the positive feedback regulation is Y. Of particular interest in this case, will be the effect of the strength of the positive feedback. In this module, if all elements are non-diffusible, when a gradient signal input is applied, the response of the module $R^*$ is also a gradient co-aligned with the signal (Fig. 3.4). Next, we observe the change in the steady state concentration profile of the response when the feedback constant $k_{yx}$ is varied, keeping the input signal fixed. As this parameter is increased, the concentration of the response is elevated at every spatial location. We then applied a localized signal input and observed the response of the module. The response obtained is localized as well.

Next, we analyzed the response of the module when the intermediate feedback element, $Y$, is highly diffusible. When the input to the module is a gradient signal, the response is a gradient signal which is co-aligned with the input signal (Fig. 3.4) which when compared to the response in the previous analysis has a more spread out profile. Similarly, when the feedback constant $k_{yx}$ was increased, the concentration of the response everywhere increased and the resulting spatial profiles are more spread out relative to the case when the feedback element does not diffuse. Similar observations hold for the localized signal input.

These results were complemented by analytical results shown in (Alam-Nazki and Krishnan, 2012).

The analysis showed that when $Y^*$ is highly diffusible, it is spatially uniform and acts as a positive feedback mediator. Thus this circuit is an example of a global positive feedback circuit, with the feedback element being uniform and spread out everywhere. It is precisely this which leads to an elevation in response everywhere.

It is also worth pointing out that in this module, if the response element was the highly diffusible element, then it would not exhibit any spatial variation at steady state. Likewise if the element X was highly diffusible, then again the response would again exhibit no spatial variation at steady state.

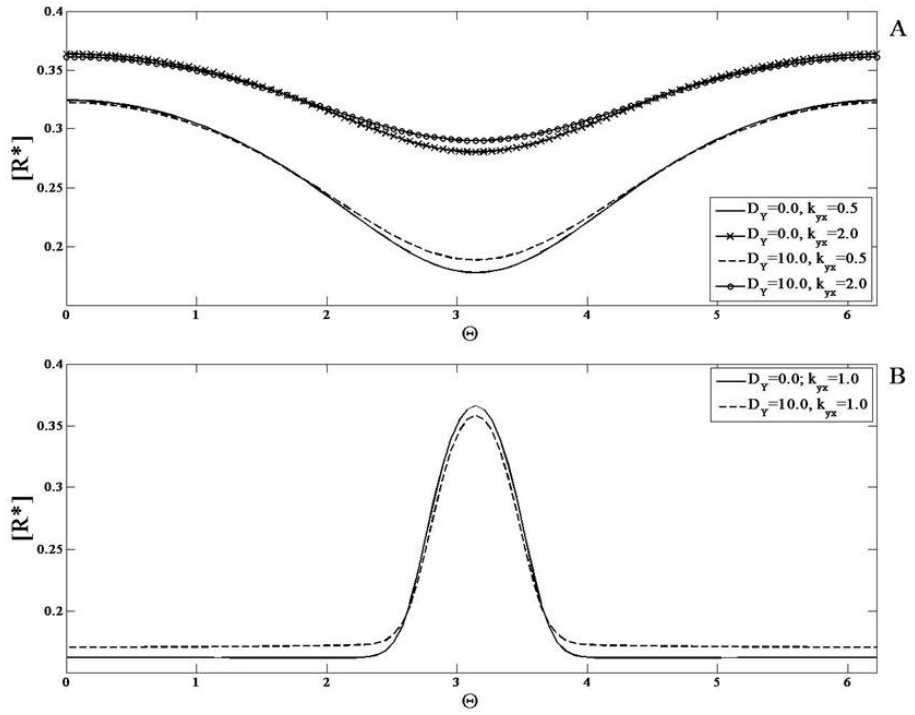


Figure 3.4: **Response of the Positive Feedback module.** This module is simulated with a (A) gradient signal and a (B) localized signal input and the effect of the feedback strength is analyzed for non-diffusible species and a highly diffusible feedback element. (A) $R^*$ is shown for (non-diffusible case) $k_{yx} = 0.5$ (solid line) and 2.0 (solid line with x markers) and (diffusible case) $k_{yx} = 0.5$ (dashed line) and 2.0 (solid line with circles). (B) $R^*$ is shown for (the non-diffusible case) $k_{yx} = 1.0$ (solid line) and (the diffusible case) $k_{yx} = 1.0$ (dashed line). The response qualitatively mirrors the signal. As the feedback constant $k_{yx}$ increases, the total concentration of the response increases everywhere. When the feedback element is highly diffusible, the spatial profile of $R^*$ shows weaker spatial variation.

## Biological relevance

Having a global element mediating the positive feedback acts to actually weaken the spatial contrast in the response. Positive feedback interactions are ubiquitously observed in signaling networks, including in different classes of MAPK cascades (Ferrell and Machleder, 1998). Signaling associated with calcium ions showcase examples of positive feedback networks with a global feedback interaction: PLC leads to the generation of $IP_3$ in the cyotosol which via calcium ions acts to further activate $IP_3$ (Meyer and Stryer, 1988). A simple positive feedback circuit combined with stochastic effects has been used to model polarization for budding yeast (Altschuler et al., 2008).

### 3.3.4 Negative Feedback Module

We first consider the case when none of the elements in the module are diffusible. A gradient signal input is applied to the module and the response obtained has a similar variation (Fig. 3.5). Next, the feedback constant $k_{yx}$ is varied and as it increases, the total concentration of the response decreases everywhere. This is due to the property of the negative feedback present in this module. A localized signal was also applied to the module and similar observations hold.

The negative feedback module is capable of exhibiting the property of adaptation - i.e. when a (homogeneous) step signal is applied to the module, a transient increase is observed in the response before it is reset at or close to its original value (Behar et al., 2007). In the case of this simple negative feedback module, an imperfect adaptive response is observed, where the response does not decrease to its original value, but to a value a little higher (Fig. 3.5). This is an example of an underadaptive response.

We then consider the case that the intermediate feedback element Y is highly diffusible. When a gradient signal input is applied to this module, the observed behaviour is counter-intuitive and interesting. The response exhibits greater spatial contrast than the response when Y does not diffuse (Fig. 3.5). This is due to the global negative feedback. As the feedback constant $k_{yx}$ is increased, the concentration of the response everywhere decreases. Similar insights hold for the case when the signal is localized.

This may be understood as follows. A greater contrast in the diffusible case occurs because the inhibiting effect is global, acting in concert with a spatially varying activation. This module with global negative feedback is in some respects a feedback analogue of an incoherent feedforward module with a diffusible inhibitor. In the latter case, a gradient response is seen along with adaptation in homogeneous stimuli. In this module too, a partial adaptive response is observed, with the global negative feedback (the analogue of a diffusible inhibitor in an incoherent feedforward pathway) enhancing the spatial contrast.

The analytical reasoning underlying the above results are discussed in (Alam-Nazki and Krishnan, 2012)

The analysis indicated that while negative feedback by itself tends to reduce the response locally and hence can be expected to reduce spatial variation in response to a spatial signal, a global negative feedback in fact accentuates the gradient response. This is also in contrast to the global positive feedback, which acted to smudge the response.

While we only concentrate on spatial signals in this study it should be noted that a

negative feedback network can also exhibit an adaptive (perhaps partial) response to homogenous signal inputs. Again this indicates how having a diffusible element leads to a qualitative difference in the spatial steady state response when compared to the temporal steady state response (the spatial response is accentuated and distinctly non-adaptive).

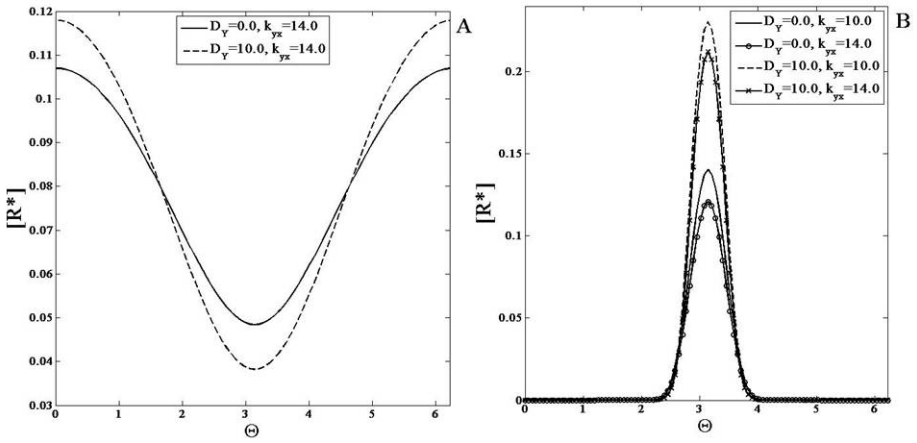


Figure 3.5: **Response of the Negative Feedback module.** This module is simulated with a (A) gradient signal and a (B) localized signal input. The response of the module when the feedback strength is varied is shown for when the feedback element $Y$ is non-diffusible and highly diffusible. (A) $R^*$ is shown for (non-diffusible case) $k_{yx} = 14.0$ (solid line) and (diffusible case) $k_{yx} = 14.0$ (dashed line). (B) $R^*$ is shown for (the non-diffusible case) $k_{yx} = 10.0$ (solid line) and 14.0 (solid line with circles) and (the diffusible case) $k_{yx} = 10.0$ (dashed line) and 14.0 (solid line with x markers). The response exhibits a profile qualitatively similar to the signal but the concentration everywhere is reduced due to the negative feedback. As the feedback constant $k_{yx}$ increases, the total concentration of the response decreases everywhere. The spatial profile of $R^*$ in the diffusible case shows stronger spatial variation than the corresponding non-diffusible case.

## Biological relevance

The fact that a ubiquitously occurring feature such as negative feedback can have such a result suggests that cells might make use of negative feedback, or perhaps a multiplicity of negative feedbacks to achieve sharp spatial responses, and further that negative feedback may combine with the natural complexity of cell signalling networks to robustly organize spatial responses. Further such global negative feedback can combine adaptive (perhaps partial) response in temporal stimuli, with distinct non-adaptive response in spatial signalling.

Global negative feedback interactions are observed in calcium signaling pathways (Krauss, 2008). One example is when the G-Protein $G_q$ activates PLC$\beta$ which in turn hydrolyses $PIP_2$ into Inositol-3,4,5-trisphosphate ($InsP_3$). $InsP_3$ stimulates release of $Ca^{2+}$ into the cy-

toplasm. Regulators of G Protein signaling (RGS) inhibit $G_q$ signalling and are activated by high concentrations of $Ca^{2+}$ in the cytosol. A distinct example of the negative feedback network is in the EGFR autocrine signalling circuit, and has been used as a basis for modelling polarization responses (Maly et al., 2004).

### 3.3.5 Cyclic Module

We now examine the cyclic module: this module involves $n$ species (labelled from 1 to n) in an irreversible cycle, with non-zero conversion rates. A signal, which is spatially inhomogeneous regulates the conversion of species 1 to 2. Every other conversion rate is spatially homogeneous. The case $n = 2$ reduces to a simple reversible reaction, with the signal regulating one reaction.

We first consider the response of the cyclic module to spatially varying signals with all species non-diffusible. For purposes of simulations, a cycle with $n = 4$ was considered. When a gradient signal is applied as mentioned, we find that at steady state, all the species except $X_1$ show a graded response which is qualitatively the same (with same gradient features) as the external signal while $X_1$ shows a graded response opposite to that of the signal. The same conclusions also hold good for a localized signal (with a background level which is non-zero) (see Fig. 3.6).

We now consider the possibility that one of the elements is diffusible. We consider this in two stages. In the first case $X_1$ is highly diffusible. At steady state, $X_1$ attains a flat profile with no spatial variation, while the other elements all exhibit a graded response which mirrors that of the signal, but which is in some respects more pronounced than in the case of non-diffusible elements. Then we examine the case where one of the other elements is highly diffusible. From the structure of the network, we expect that if species $k$ is diffusible then it will attain a flat steady-state profile, and all other species from $k + 1$ to $n$ (i.e. downstream of it, and not directly regulated by the signal) will also attain homogeneous profiles at steady state. This is indeed what is observed. What is more interesting is the fact that all species from 2 to $k$ also attain homogeneous profiles. In fact only species 1 exhibits an inhomogeneous profile (see Fig. 3.7). In other words only the species directly regulated by the signal exhibits an inhomogeneous spatial profile at steady state, even if only one other species is highly diffusible. The analytical results for the cyclic network are shown in (Alam-Nazki and Krishnan, 2012), which also explain the reason for this result.

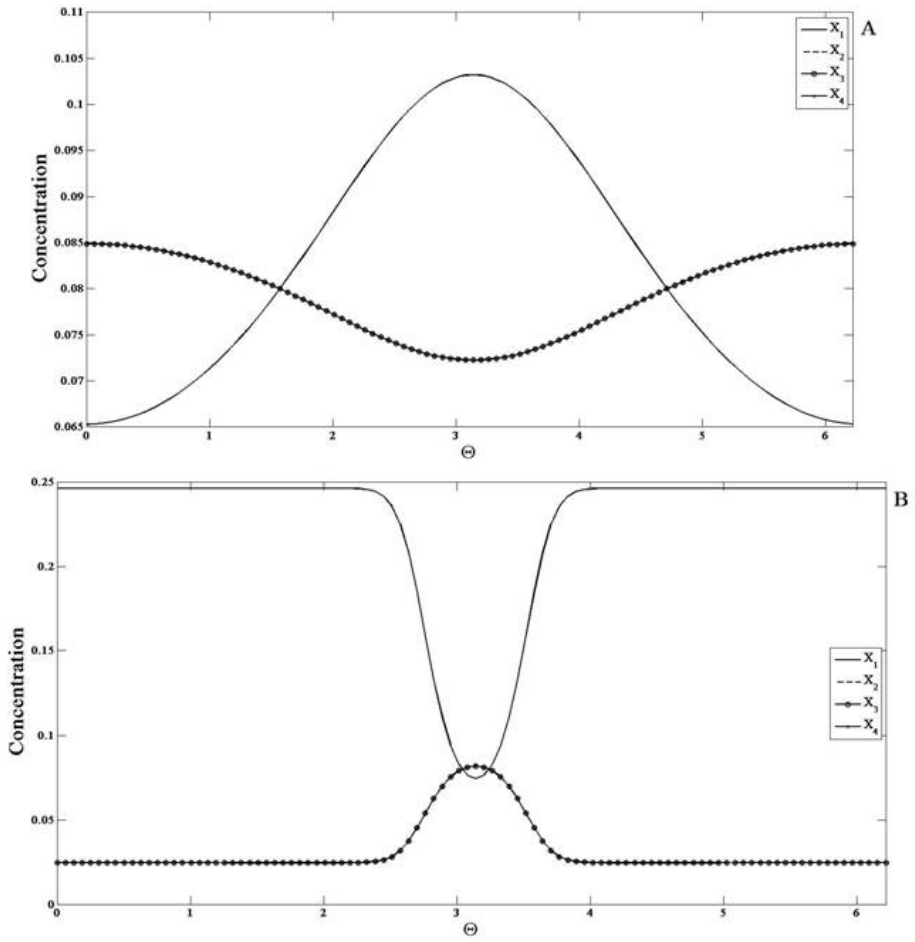


Figure 3.6: **Response of the Cyclic Reaction network module.** $X_1$ (solid line), $X_2$ (dashed line), $X_3$ (solid line with circles) and $X_4$ (solid line with dots) are shown for when the module (all elements non-diffusible) is subjected to a (A) gradient signal and a (B) localized signal input. Note that the profiles of $X_2$, $X_3$ and $X_4$ are coincident for the parameters chosen. The concentration profile of $X_1$ is qualitatively opposite to that of the signal while $X_2$, $X_3$ and $X_4$ are qualitatively similar to the input.

## Biological relevance

We have analysed both a purely local cyclic network and a cyclic network with a highly diffusible/global component. An interesting insight revealed from our analysis was that when particular elements in the cyclic network are highly diffusible, both "upstream" and "downstream" elements show a spatially homogenous response to a spatial signal. This indicates that in such networks, if individual elements exhibit inhomogeneous spatial profiles then direct spatial regulation needs to be present at one or more locations in the cycle.

Cyclic networks form a part of the intracellular signalling network of the cell. Numer-

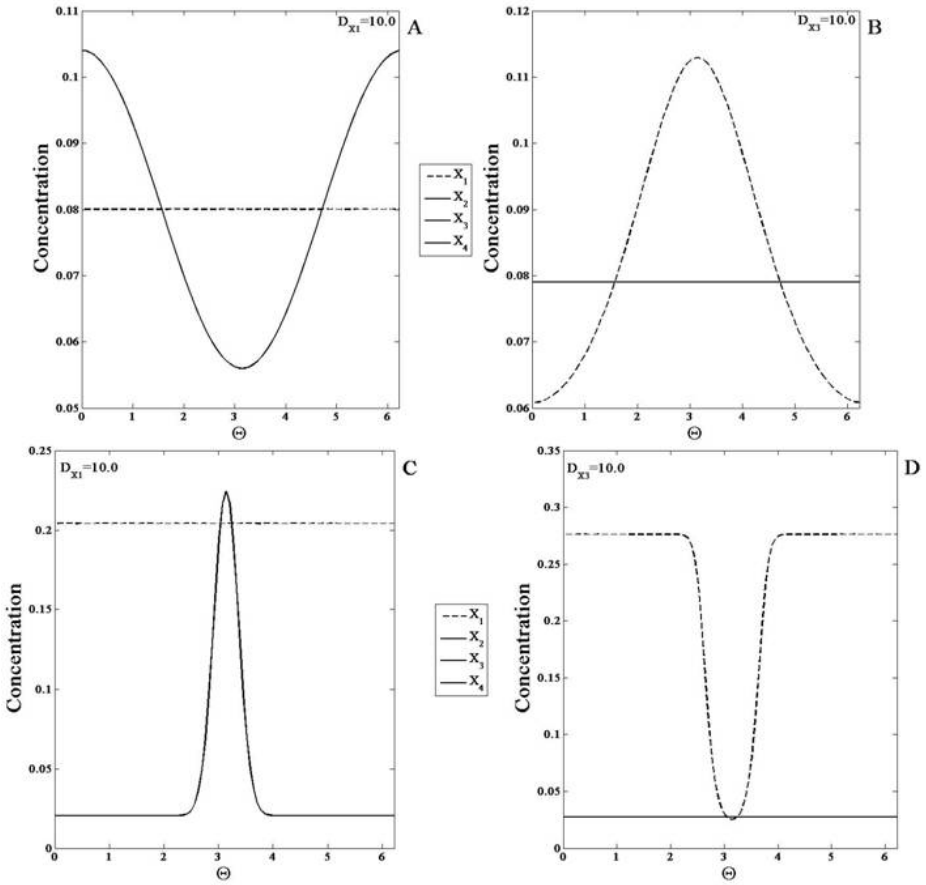


Figure 3.7: **The Cyclic Reaction network module with highly diffusible elements.** The response of the module to a (A,B) gradient signal and a (C,D) localized signal is shown when $X_1$ is highly diffusible and when $X_3$ is highly diffusible. Note that the profiles of $X_2$, $X_3$ and $X_4$ are coincident for the parameters chosen. (A,C) If only $X_1$ is highly diffusible, then $X_1$ (dashed line) is spatially homogenous and the remaining species (solid line) have a stronger spatial variation (than the corresponding non-diffusible case). (B,D) If only $X_3$ is highly diffusible then $X_2$, $X_3$ and $X_4$ (solid line) are spatially homogenous and $X_1$ (dashed line) assumes a profile qualitatively opposite to that of the signal with stronger spatial variation than the non-diffusible case.

ous examples of purely temporal cyclic networks such as the phosphotransferase system in E. Coli and metabolic cycles have been observed (Marks et al., 2009). An example of such a network with a global element(s) is seen in the extracellular signal regulated endocytosis process (Alberts et al., 2002). In endocytosis, activated GPCRs on the plasma membrane are phosphorylated and form complexes. These GPCR complexes are transported (in vesicles pinched off from the plasma membrane) to compartments in the cytosol. From these compartments they are transferred to different compartments called recycling endosomes so that they can be transported back to the plasma membrane. Thus in this cycle, certain components of the network such as the GPCR are bound to the membrane and localized

and other components such as the complexes being transported via endosomes form a part of a global pool in this network.

### 3.3.6 Monostable Switch Module

Monostable switches may be realized in different ways, for instance through co-operative effects of regulating enzymes and combination of stage-wise effects such as in MAP Kinase cascades. Here we consider a commonly used model for monostable switches, namely the Goldbeter-Koshland model. The Goldbeter Koshland module contains two enzymes S and U which act close to saturation. In the module the signal regulates the enzyme catalyzing the forward reaction, and for simplicity, the signal is identified with this enzyme. We note that the steady state output of this module as a function of signal exhibits a switch-like response.

This can be understood intuitively in a straightforward manner. Both forward and backward reactions function essentially as zeroth order reactions, and are dependent on enzyme concentrations only. If the signal is weak enough so that the backward reaction is the stronger of the two, then the response is essentially zero at steady state. On the other hand when the signal exceeds a threshold, whereby the forward reaction is now stronger than the backward reaction, the output of the module is one corresponding to essentially complete conversion of reactant $X$ into response $X^*$.

We first examine the case where none of the elements are diffusible. When a gradient signal input is applied to the module, the response exhibits this switch-like property in the spatial profile. This follows simply from the fact that in certain spatial regions, the signal is above the switch threshold and in others it is below the threshold. Thus such a binary computation is reflected in the spatial profile (Fig. 3.8). An analogous result is seen in the case of a localized input for the same reasons.

Now we consider the case where one of the elements is highly diffusible. If $X^*$ is highly diffusible, then clearly at steady state it attains a uniform profile. It should be noted that this uniform level implicitly accounts for the region where the switch is on. We now consider the case where it is X which is highly diffusible. When a gradient signal is applied to the module, the steady state profile of $X^*$ appears to be very sharp in the region of the maximum (of the signal) and flattens out in the region of the minimum (Fig. 3.8). In the case where a localized signal is applied to the module, the steady state concentration profile of $X^*$ becomes sharply localized and it is sharper than the profile observed for $X^*$ when

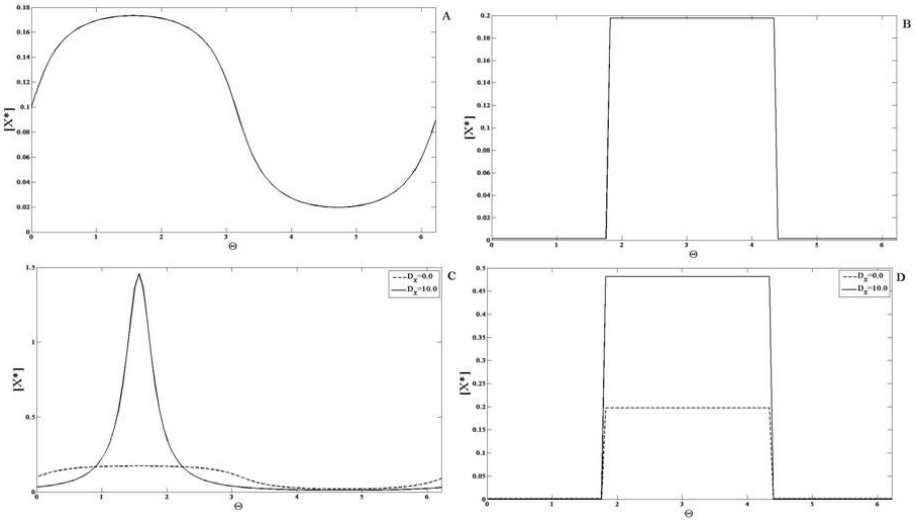


Figure 3.8: **Response of the Monostable Switch Module.** $X^*$ is shown in response to a smooth gradient signal (of the form $a+bsin\theta$, with a maximum at $\theta = \pi/2$ ) for a (A) non-diffusible and (C) highly diffusible case and a localized signal input (of the form of a square pulse) for a (B) non-diffusible and (D) highly diffusible case. (A) The concentration profile of $X^*$ is broader near the maxima and minima of the signal and it exhibits a spatial switch-like behaviour. (B) The spatial profile of $X^*$ is qualitatively similar to the signal. (C,D) $X^*$ is shown here for when $X$ is highly diffusible (solid line) and non-diffusible (dashed line). (C) In response to the gradient signal, the spatial profile of $X^*$ increases sharply in the region where the signal crosses a threshold value. Thus the diffusion of $X$ leads to an enhancement of the spatial switch response. (D) For the localized signal, the spatial profile of $X^*$ shows greater contrast when $X$ is highly diffusible.

all species are non-diffusible. Thus the fact that $X$ is diffusible in some respects enhances the effect of the switch.

These effects are examined in more detail in the analysis in (Alam-Nazki and Krishnan, 2012). A comparison to other monostable switches is also outlined in (Alam-Nazki and Krishnan, 2012). The essential conclusion in all these cases is that by having the inactive form of the network element being highly diffusible accentuates the switching effect in spatial signalling, while having no effect in temporal steady state response.

**Biological relevance** Having a global element relieves the constraint on the amplitude of the switch in spatial signalling. Monostable switches may be embedded in more complex networks where immobilization or sequestration of certain components works in conjunction with global elements to accentuate a switching response. A similar accentuation in signalling has been modellled in multiple contexts including Rho GTPase dynamics (Dawes and Edelstein-Keshet, 2007; Mori et al., 2008).

### 3.3.7 Bistable Module

#### Bistable module with weakling diffusing or non-diffusible entities

The bistable module has two elements X and Y that inhibit one another. This double negative feedback gives rise to the property of bistability. First we examine the case when none of the elements are diffusible. This module exhibits bistability for a range of input values ranging from $S_1$ to $S_2$ (Tyson et al., 2003). Simulations are performed starting from a steady state corresponding to the "lower branch" in the bifurcation diagram (depicting X as a function of signal) for some basal value (Fig. 3.9). Now if a gradient signal is applied where the local value of the signal never exceeds $S_2$, then the steady state reflects a heterogeneity broadly mirroring the input (i.e. no switching effect). On the other hand if a gradient is chosen so that the local level exceeds $S_2$, then a steady state is observed which reflects a spatial switch (Fig. 3.9). Essentially, the part of the domain where the signal is below $S_2$ ends up at a steady state on the lower branch of the bifurcation diagram, while that part of the domain which is subject to a signal above the threshold evolves to the elevated, unique steady state. Thus the temporal steady state threshold behaviour is reflected directly in the spatial profile. It is also worth pointing out that this switching behaviour is observed whether the remaining part of the domain faces a signal completely in the bistable regime (i.e. $S_1 < S < S_2$) or even if some part of the domain is in the other monostable regime (i.e. $S < S_1$).

It should be noted that here the dynamics and steady state is purely local and completely spatially decoupled (Incidentally it is worth pointing out that such a completely uncoupled bistable system possesses other steady states due to complete decoupling and locality, some of which are physically unreasonable). In such bistable systems, it is very important to check if the results in the strictly non-diffusible case carry through when species are weakly diffusible, and are not artifacts of a special situation.

Keeping this in mind, we performed simulations of the system, incorporating a weak diffusion of the element Y (similar results are obtained if X is weakly diffusing as well). What is observed may be summarized as follows. The results for the case where the input signal is such that part of the domain is above the threshold $S_2$ mirrors the non-diffusible case. A spatial switching behaviour is indeed seen here too. Again this is the case for gradient signals whether or not their lower limit falls below $S_1$ (note that the initial conditions correspond to a steady state in the lower branch at a uniform signal value). This

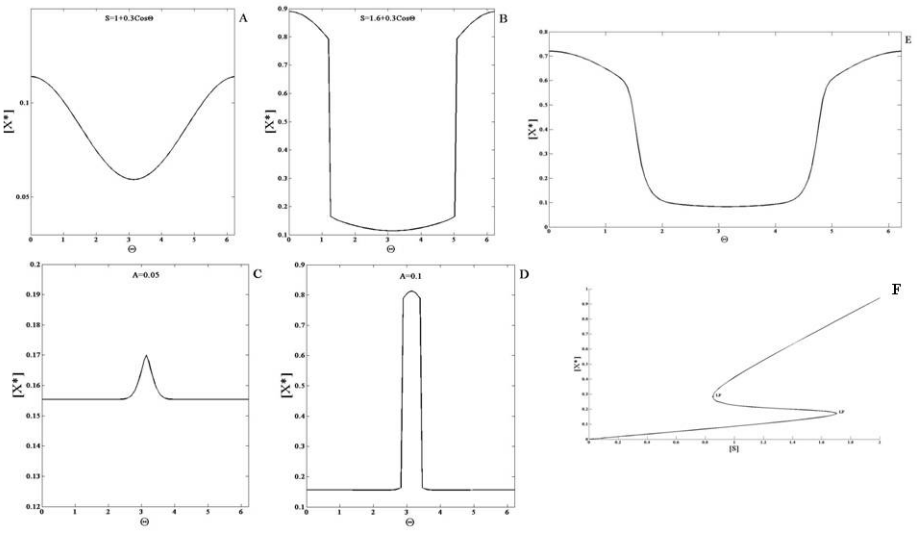


Figure 3.9: **Response of the Mutual Inhibition Bistable Switch module.** $X^*$ (solid line) is shown when the module is subjected to (A,B) gradient signals and (C,D) localized signal inputs. (A,C) When the value of the signal in the entire domain is either above or below the critical value S2 (see text), the response is qualitatively similar to the signal. (B,D) A spatial switching effect is observed when the signal crosses the critical value in some part of the domain. (E) The above switching effects are seen even if some of the elements are weakly diffusible. Furthermore, even if the signal is entirely in the bistable regime, a spatial switching effect can be seen in the profile of $X^*$ (with different initial conditions, see text and supplementary material). (F) A bifurcation diagram for this module is shown. The module has two stable steady states and one unstable steady state (between the two 'LP' markers) in a signal range (S1 to S2, see text).

confirms the fact that this spatial switching behaviour is not an artifact of species being strictly non-diffusible.

Before discussing the diffusible case, we examine some additional cases. First we examine cases where the signal lies entirely in the bistable region ($S_1 < S < S_2$). While for the initial conditions used above, a gradient signal results in heterogeneity but no switching, this is no longer true if initial conditions are changed (different initial conditions reflect the prior signalling history in network components). Here if an initial condition is chosen such that part of the domain is at (or close to ) the lower steady state branch, and the other part of the domain is at (or close to) the upper steady state branch, then it is possible for the system to exhibit spatial switching and a pulse like response (Fig. 3.9). Thus the switching does not need part of the signal to be in a monostable regime. However, it should be noted that if the signal is spatially uniform, then the above simulation results in a spatially uniform steady state. This situation can be understood easily in terms of the Maxwell condition of uniform bistable systems (Murray, 2008): generically one of the two steady states will "engulf" the other through travelling fronts which sweep across the domain. When the signal applied is a gradient, the situation is more subtle. If the heterogeneity is very weak, then the behaviour is similar to the homogeneous case, and a weakly heterogeneous steady state is obtained. On the other hand as the level of heterogeneity is systematically increased (and simulations performed with the same initial condition), one can observe the system evolve to a steady state which exhibits spatial switching. This effect is due to the fact that the fronts which tend to sweep across the domain (as they would in homogeneous bistable media) get trapped in sites of heterogeneity–this is an effect called wave pinning and has been the focus of many studies (for eg. see (Mori et al., 2008)). Overall we see that the response of a bistable module with weakly diffusing elements to gradient signals is actually very subtle. In contrast to the temporal bistable case, we see a subtle interplay between the bistability, diffusion and signal heterogeneity as well as the previous history of the system.

## Bistable module with strongly diffusing or global entities

We now turn to the case where one of the elements (Y) is highly diffusible (Fig. 3.10). We note at the outset that the high diffusivity of Y does not affect the bistability feature of the module. Indeed in spatially homogeneous signals, the module can exhibit multiple steady states. When the module is subject to a gradient, what is observed is as follows. For a gradient signal where part of the signal crosses the threshold $S_2$, we find that in contrast to

the earlier case, no spatial switching is observed. In fact a heterogeneous profile roughly reflecting the heterogeneity of the input is seen. The bistable character of the network is reflected in the fact that (depending on initial conditions), the system can evolve to the heterogeneous "equivalent" of the multiple stable temporal steady states. These results are explained analytically in (Alam-Nazki and Krishnan, 2012).

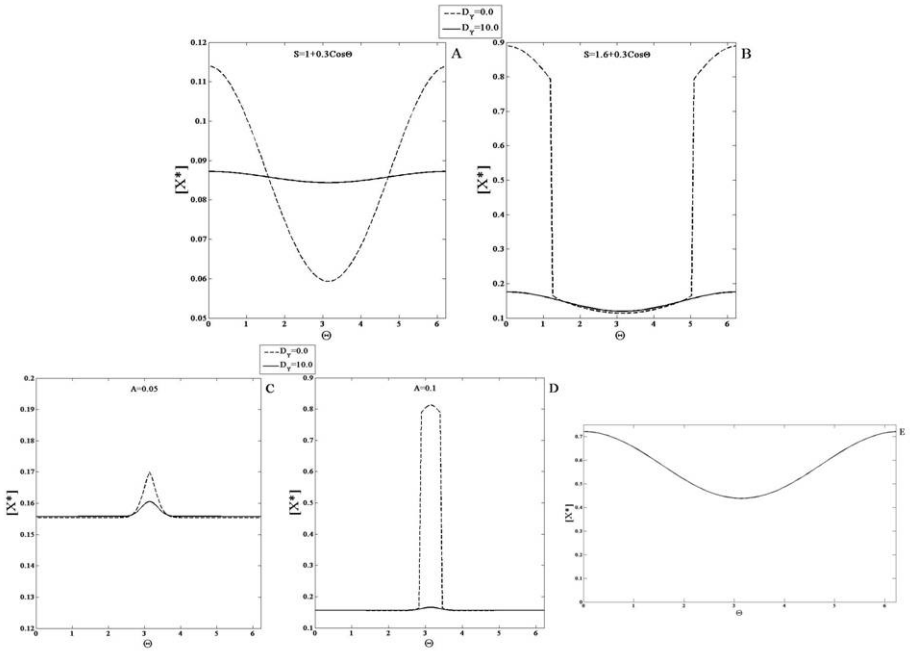


Figure 3.10: **The response of the Mutual Inhibition Bistable Switch Module with highly diffusible elements.** The spatial profile of $X^*$ is shown when $Y$ is highly diffusible (solid line) and non-diffusible (dashed line) for (A,B) gradient signals and (C,D) localized signal inputs. When $Y$ is highly diffusible, the switch-like behaviour observed in the non-diffusible case is no longer present. (E) This plot illustrates that the system can achieve a higher steady state value (with suitable initial conditions) without exhibiting spatial switching behaviour when the signal is in the bistable regime.

In summary, in the highly diffusible case, the response of the module results in multiple heterogeneous steady states but without any spatial switching.

In this subsection we have examined a type of positive feedback network which arises from a mutual inhibition network which exhibits the property of bistability. A spatial switch response is exhibited by a purely temporal network– this response appears in certain domains. Furthermore the spatial switching response has a dependence on the prior state of the system or its history. When one of the interacting elements is highly diffusible the spatial switch is no longer realized by the network. In other words having a global element in the feedback acts as a constraint as far as realizing spatial switching. Thus whether or

not a spatial switch could be realized through the bistability feature is more complex than a monostable or simple temporal bistable switch.

### Biological relevance

These results have interesting implications for the organization of networks where spatial switches are observed. Firstly bistable circuits may be able to act as spatial switches if all elements are weakly diffusible (or non-diffusible). If a global element is present in the feedback circuit giving rise to bistability, then this circuit by itself cannot give rise to spatial switching. In this case it may be that some upstream signalling actually provides the spatial switching, which is partly accentuated by the bistable circuit. The other possibility is that some sequestration mechanism or additional pathway (non-global) is responsible for realizing the spatial switch through bistability. Finally, our analysis above is based on elements where the active and inactive forms are both highly diffusible. If only the inactive form of such an element is highly diffusible, then this can play a role in accentuating the switching effect similar to the analysis in the previous section.

While bistability has been observed and studied in detail in temporal signalling, it has also been postulated to be the basis of spatial organization of Rho-GTPases in polarization (Mori et al., 2008) and give rise to phosphoprotein waves in protein kinase cascades (Markevich et al., 2006).

## 3.3.8 Negative Feedback Oscillator Module

We now examine a module where the asymptotic state may not be steady, and instead result in sustained oscillations. This is an oscillator module, and for specificity, we consider a negative feedback oscillator module. The negative feedback oscillator module consists of three species $X, Y$ and $R$, where Y is the intermediate negative feedback element and $R^*$ is the response. In this module, there is a critical value of the signal where a supercritical Hopf bifurcation occurs, leading to sustained oscillations.

We first assess the case when none of the elements are capable of diffusion. When a gradient signal is applied- with some region of the signal above the critical value for oscillations and some below it, the spatial concentration profile of $R^*$ shows irregular spatial oscillations for regions in space where the signal is in the region past the Hopf bifurcation and a smooth static profile when the signal is below it (Fig. 3.11).

When the gradient signal is completely above the bifurcation threshold (but within the oscillatory regime), then the entire profile of $R^*$ oscillates irregularly with respect to space. The spatial concentration profiles of $R^*$ are shown for a snapshot in time in Fig. 3.11. For both these gradient inputs, the concentration of $R^*$ shows irregular spatial oscillations (in the appropriate regions) as well as regular oscillations in time for these spatial regions. To obtain a clearer picture of the behaviour of the module, we created a phase plot of the concentration of the response at adjacent spatial locations. The phase plot shows a region which is essentially densely filled. This indicates the source of the irregular spatial oscillations: at any spatial location, the behaviour is one of regular temporal oscillations (in the regions which lie in the oscillatory regime). However, owing to the spatially varying signal, and complete spatial decoupling, different regions experiencing different signal values exhibit oscillations whose frequencies are not rationally commensurate with one another and this results in quasiperiodic behaviour of the distributed dynamical system. Similar insights hold good for localized inputs. This indicates that a simple spatial biasing of an oscillator circuit does not lead to regular spatial oscillations.

Now in the above case, if the elements are made diffusible, but relatively weakly so, this can cause an effective coupling between different regions. The case where some part of the domain is in the oscillatory regime is shown in Fig. 3.11. We now find a smoother spatial profile is observed, in this part of the domain. Typically as the diffusion is made stronger (but still relatively weak) , we find stronger spatial coupling and spatial (and temporal) oscillations, which lie outside the part of the domain in the oscillatory regime.

Finally we analyze the case when $Y$ is highly diffusible (Fig. 3.12). When a gradient signal is applied to the module and even if it is above the Hopf bifurcation value (i.e. oscillation threshold) the profile of $R^*$ is smooth. A phase plot of the concentration of the response at two adjacent spatial points no longer shows a filled region but a closed curve indicating that the oscillations at different points in space are now synchronized with one another. Similarly when a localized signal is applied, the profile of $R^*$ becomes smooth and amplitude of the response increases. It is worth pointing out that when the element Y is highly diffusible, this plays a role in effectively coupling different regions. Thus in this situation, we find that if the spatial average of the signal is essentially in the oscillatory regime then the entire domain oscillates in time, with spatial heterogeneity being reflected in the non-diffusible elements. On the other if the spatial average of the signal is below the threshold for oscillation, the system attains a heterogeneous steady state, even though there are regions which are locally in the oscillatory regime.

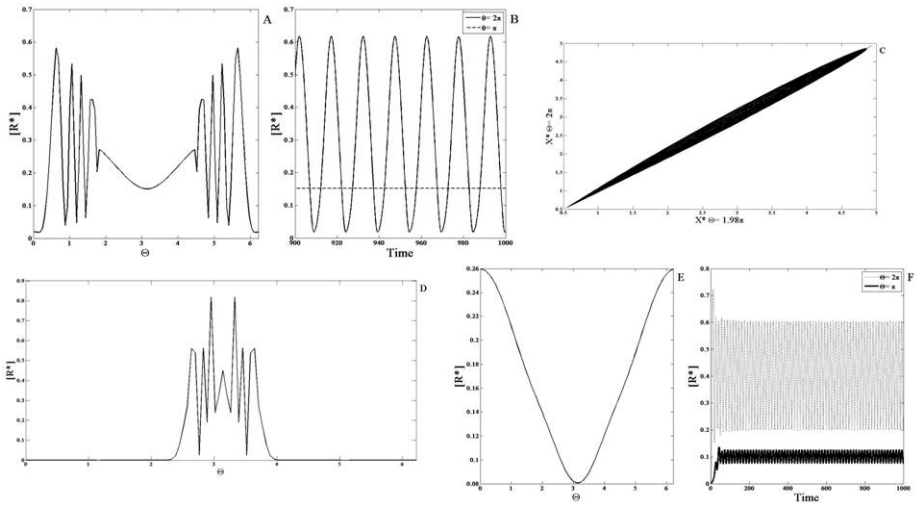


Figure 3.11: **Response of the Negative Feedback Oscillator module.** The response $R^*$ (solid line) is shown for a (A, B, E and F) gradient signal and a (D) localized signal input. (A,D) The profiles are shown at a snapshot in time. $R^*$ exhibits irregular spatial oscillations when the signal is in the oscillatory regime and the profile is smooth in regions where the signal is outside of this critical range. (B) This plot illustrates the variation of concentration of the response with respect to time at two spatial locations: the middle of the domain (dashed line) and at the boundary (solid line). The response only exhibits temporal oscillations in the regions where the signal is in the critical oscillatory range. (C) The phase plot is shown for $X^*$ at two adjacent points in the domain. It depicts a densely filled region highlighting the quasi-periodic nature of oscillations. (E) When $Y$ is weakly diffusible, the spatial profile of the response becomes smooth and (F) periodic oscillations in time are observed in the middle of the domain (solid line) whereas in the non-diffusible case they are absent in that region.

In summary, spatial biasing of an oscillator circuit can lead to oscillatory responses in different spatial regions which are regular, provided some elements are diffusible (not necessarily strongly). Having a diffusible element strongly couples different elements and results in either the entire domain oscillating or the entire domain being static.

## Biological relevance

The above results have implications for the organization of spatial oscillators (inhomogeneous regions in space which exhibit temporal oscillations) in cells. While spatial oscillators can be generated by biasing of an oscillator circuit with (not too strongly) diffusible elements, having highly diffusible elements in the circuit generating oscillations result in complete global coupling. It follows that a way in which cellular signalling networks may be organized for this purpose is to have parallel pathways/modules to provide spatial variation/localization, and an oscillator module with diffusible/global elements to

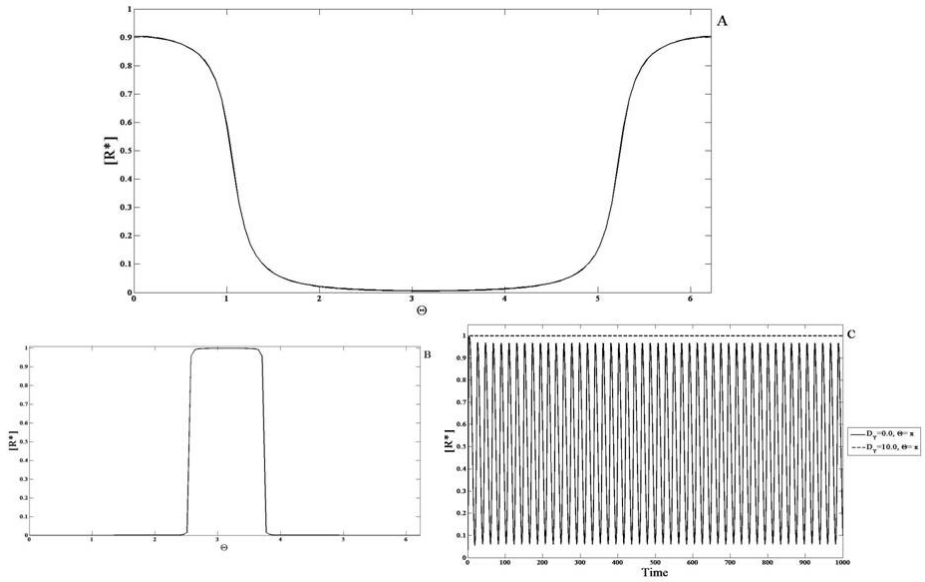


Figure 3.12: **The effect of diffusible species in the response of the Negative Feedback Oscillator.** The response is shown when the feedback element is highly diffusible (solid line) for a (A) gradient signal and (B,C) localized signal input. (A,B) A smooth concentration profile qualitatively similar to the signal is observed. This is because the diffusion of the feedback element acts to couple the different regions of the domain resulting in such a profile. (C) The temporal profile of the response is shown when $Y$ is highly diffusible (dashed line) and non-diffusible (solid line), corresponding to the signal in (B). For the non-diffusible case oscillations are observed in the middle of the domain. However when $Y$ is highly diffusible periodic oscillations are not observed in this region because the spatial average of the signal is not in the oscillatory regime. Thus, an heterogeneous, static profile emerges in the diffusible case.

provide global oscillation, which are then combined. Such a combination could give rise to co-ordinated/synchronized oscillations in different regions of the cell (for instance two poles of a migrating cell). Another way to have co-ordinated oscillations in different spatial regions is by having a circuit which generates oscillations in a relatively localized region, which is then communicated to other regions by diffusible/global intermediates. It is worth pointing out that fully self-organized spatial oscillations may also occur, and it remains to be seen how spatial oscillations in different cell types may be organized and generated.

Finally the analysis of another kind of switch module which involves positive feedback and exhibits a transcritical bifurcation is discussed in Appendix B and the related analytical results are in (Alam-Nazki and Krishnan, 2012). The essential conclusion from this analysis is also that if the feedback element is highly diffusible, then the particular switching behaviour in spatial gradients may be abolished, even though this switching continues to be observed in temporal signalling.

## 3.4 Conclusions

The past decade has seen a significant amount of work in understanding temporal aspects of cellular signal processing, both in specific contexts, and also conceptually. However in many of these studies spatial aspects of signal processing are often ignored, typically on the grounds that any key aspects of signalling can be captured in appropriate temporal models. However, even here, it is increasingly being recognized that the spatial dimension to signalling contains highly non-trivial, and in some cases vital information which provides key insights into the signal processing (for example, it has been suggested that spatial gradient information of particular entities in fission yeast is a key link which couples growth and the cell cycle (Moseley et al., 2009)). In cellular processes such as cytokinesis, eukaryotic chemotaxis, wave-propagation in the cell, spatial aspects of signalling cannot be bypassed. The spatial aspect presents extra challenges for both modelling as well as experimental elucidation of the system. It is being increasingly recognized that spatial aspects of signalling need to be seriously addressed, and that in this regard frameworks which provide conceptual understanding of relevant issues are necessary.

At the outset, we note that spatially non-trivial behaviour in signalling networks could arise, either because some external or "upstream" signals in a network are heterogeneous, or because some of the elements in the network are themselves heterogeneously distributed, or if there is some spontaneous pattern-forming process. We focus on the first case here, and will address other issues separately. We note that spatial variation in a number of signalling entities may be generically expected in cellular environments.

Our focus was on spatial aspects of signal processing, in particular with a view towards determining whether qualitatively new features emerge when one includes spatial considerations. This dictated our approach in this study: rather than focus on mechanistic modelling, we focussed on representative network modules of signalling and considered these in a spatially extended domain, with spatially inhomogeneous signals, both gradual and sharp, of the kind which may be generically expected. While our modelling was performed in 1-D in a periodic domain for specificity, most of the results carry through for other boundary conditions, and more complicated domains. Since signal processing in these networks could be significantly affected by diffusion, we considered the effect of diffusional transport in these modules, by making different elements highly diffusible. Having elements being highly diffusible can fundamentally affect the signal transduction in a network, and indeed the classic work of Turing (and others) shows how diffusible elements can

even drive spatial pattern formation, in essentially homogeneous backgrounds. By studying spatial signalling in representative modules with and without diffusion, we provide a basis for understanding how different types of typical signal transduction behaviour is realized spatially. We also believe that by considering a variety of modules together, we are able to compare these effects between different modules.

While we adopt a more general approach, we mention that many of the effects and networks we study are seen in different signalling contexts. Spatial variation of signalling entities/inputs can be generically expected in many situations, and the signalling network behaviour we investigate is repeatedly observed. Key second messengers like cAMP and cGMP are highly diffusible, and these (along with appropriate compartmentalization) regulate a number of effectors and this allows for chemical circuits to naturally include global effects (Bastein D. Gomperts, 2009). This is also true when the driving signal (say on the cell membrane), leads to signal transduction, involving cytosolic elements, which are not directly (locally) regulated by spatially inhomogeneous signals. The presence of cytosolic pools can provide the kind of the global effect studied here. Signal transduction through phosphoinositides and other species on the membrane, leads to the recruitment of cytosolic elements such as PKA (regulated by cAMP) and PKC (Rosse et al., 2010), which interacts with these networks, providing examples of global regulators in signalling networks. Other examples include the role of $IP_3$ and calcium signalling providing global regulation and feedback effects (Krauss, 2008). The role of spatial effects and diffusion has been receiving attention and is a relevant to G-protein cycles, spatial switches, polarity circuits, spatially organized oscillating elements (eg. regulation of actin in chemotaxing cells), and wave propagation (Berridge et al., 2000; Dawes and Edelstein-Keshet, 2007; Eisenbach et al., 2004; Lipshtat et al., 2010; Nelson, 2003; Othmer and Schaap, 1998; Saini et al., 2009). Highly diffusible entities and global effects have thus been incorporated in a wide range of modelling efforts (for eg. see (Gierer and Meinhardt, 1972; Narang, 2006)). Thus we expect that the analysis performed here can provide valuable insights into the potential complexities of spatial signalling in multiple contexts and the role of global regulators therein. We consolidate our findings and end with a discussion on the insights gained from our results and implications for intracellular spatial signal processing.

### 3.4.1 Spatial signalling with non-diffusible elements

The work presented here focussed on the behaviour of the modules (Table 3.1) which have a natural input and output. When we examine the response of the modules (with all elements non-diffusible) to spatial gradient inputs, the output is typically a spatial signal which reflects the steady state temporal signal processing. Indeed the signal processing here is purely local, spatially, with no coupling. This is examined firstly because it is the most basic way in which spatial signal processing can occur, and also because it is the basis for understanding spatiotemporal signal transduction (addressed subsequently). The coherent/incoherent feedforward modules, simple negative and positive feedback modules and cyclic modules all reflect their temporal signalling features in steady state spatial signalling. Likewise different monostable switches as well as switches with a transcritical bifurcation structure, reveal their switch like behaviour in spatial signal processing. This behaviour continues to hold good when any of the elements are weakly diffusible.

In the case of bistable switches if the signal range straddles the location(s) where switching occurs, then it is possible to observe spatial switching behaviour, and this continues to hold good even if different elements are weakly diffusible. On the other hand if the signal range lies entirely within the bistable regime, then it may or may not be possible to observe a spatial switching behaviour at steady state. From the perspective of spatial signalling this involves a subtle interplay between the bistability and the heterogeneity (such switching would not be observed in the absence of heterogeneity, even with bistability, if any of the elements were diffusible), and further depends in a subtle way on the history of how the gradient signal was imposed. This underscores various subtleties in understanding spatial switching in such a module, when compared to temporal signalling. In the case of an oscillator module, when subject to a gradient, we find that if the elements are non-diffusible, then temporal oscillations are observed in appropriate spatial regions, which are however spatially irregular. This is because different locations respond to local signal values which are different and not generally rationally commensurate. This leads to quasiperiodic behaviour in the spatiotemporal response. However in the case of quite weak diffusion, the coupling due to diffusion leads to a regular spatiotemporal oscillatory behaviour in appropriate regions.

| Module | Without diffusion | With diffusible element |
|---|---|---|
| *Coherent Feedforward* | Qualitatively similar to input signal | Qualitatively similar to the input signal with weaker spatial variation. |
| *Incoherent Feedforward* | If inhibitor is stronger, qualitatively opposite response; if weaker qualitatively similar response to input. | Gradient information conveyed through the non-diffusible pathway regardless of stronger pathway. |
| | Switch in qualitative nature of spatial response as mean of value of gradient signal increased. | No switch in nature of spatial response. |
| *Positive Feedback* | Increasing the feedback constant increases the concentration of the response everywhere in space. | Diffusion of feedback element weakens spatial variation. |
| *Negative Feedback* | Increasing the feedback strength causes a decrease in response at all spatial locations. | Diffusion of feedback element strengthens spatial contrast. |
| *Cyclic* | All species exhibit gradient profiles | If the directly regulated species is highly diffusible all other species show graded response with greater spatial variation. If any one of the other species is highly diffusible then the directly regulated species exhibits a graded profile while all others exhibit flat spatial profile. |
| *Monostable Switch* | Spatial switch-like property observed | May 'enhance' the spatial switching effect |
| *Bistable Switch* | Spatial switch-like property exhibited if signal value crosses threshold in some parts of the domain. Effects mirrored with weak diffusion (if signal is completely in the bistable regime in the domain then switching exhibited only for certain initial conditions and sufficiently strong heterogeniety). | System does not exhibit spatial switching behaviour. |
| *Negative Feedback Oscillator* | Irregular spatial,and regular temporal oscillations observed where signal is in the oscillatory range. If weak diffusion, smooth spatial profile observed in part of the domain in the oscillatory region. | If average value of signal is sufficiently high, temporal oscillations observed in entire domain along with a heterogenous spatial profile. |
| *Transcritical Birfurcation* | Switch-like behaviour is observed in the spatial profile. | Spatial switch-like behaviour is absent. |

Table 3.1: **Results from the analysis of the models.** A summary of results is presented in the above table, for steady state signal transduction (except for oscillator module).

### 3.4.2 Effect of highly diffusible elements

In general, we find significant differences when highly diffusible elements are present in various modules. Thus, in the case of the incoherent feedforward module, we see that whatever the relative balance of the two competing pathways, the net spatial response is determined by the non-diffusible pathway, even if it is the weaker pathway kinetically. Thus the feature of having one pathway diffusible, allows for exact, or imperfect adaptation in homogeneous stimuli, along with a robust spatial response. Similarly, analysis of a different incoherent feedforward module indicates how having one pathway diffusible prevents a reversal in gradient response, as the mean value of the signal is changed. In the positive feedback module, if the feedback element was diffusible, then this resulted in the elevation of the response everywhere in the domain, including locations which were not subject to signals. In the negative feedback module, the high diffusivity of the feedback element results in a greater spatial contrast of the response. This, along with the fact that the feedback module can result in partial adaptation to homogeneous stimuli means that this module could be viewed as a feedback equivalent of a feedforward Local Excitation Global Inhibition module (Levchenko and Iglesias, 2002). In an irreversible cyclic module, having a highly diffusible element results in spatially homogeneous profiles for all elements except that being directly regulated by the gradient signal: thus interestingly even elements "upstream" of the diffusible element attain spatially homogeneous profiles. The case of a reversible reaction with one element diffusible is a special case of this cyclic module.

Examining simple switches we find that if the inactive form of the response element is highly diffusible, then this accentuates the switching effect and leads to a larger amplitude switch, when compared to the non-diffusible case. In the case of a monostable switch realized through positive feedback (without cooperativity) resulting in a transcritical bifurcation, we find that having feedback mediated by a diffusible species abolishes the possibility of a spatial switch. It should be noted that the essential bifurcation behaviour of the signalling network continues to be reflected in its response to homogeneous signals of different strengths. Thus the switching effect of the signalling is present in a gradient, not through the manifestation of a switch in the spatial profile, but rather through a switch in the nature of the response (whether completely switched off or not) which in turn depends on the average of the signal. A very similar effect is seen in bistable switches. When the feedback element is highly diffusible, a steady state response possessing a switching effect in the spatial profile is not seen. Instead the bistability is reflected in the fact that (de-

pending on signal ranges) it is possible to have multiple stable spatially graded responses, which may be seen as spatial analogues of the temporal behaviour of the module. The effect of highly diffusible elements in oscillatory modules serves to effectively couple different regions of the domain to produce spatiotemporally oscillatory behaviour. Thus strong diffusion allows regions which are faced with signals not strong enough to excite oscillations, to oscillate robustly, and in other cases have the opposite effect.

### 3.4.3 Spatial and temporal signal processing

Our analysis of these modules provides insights into the signal processing capabilities of these modules and the constraints with regard to spatial signalling imposed by diffusion. Taken together, we can say that having highly diffusible or global elements, either completely blocks propagation of spatially varying signals and communicates only the average effects of the upstream signal, or leads to significant distortions in signal propagation. Typically having key elements being highly diffusible causes fundamental differences in steady state spatial responses: switch effects are not realized, adaptation does not occur in spatial signals, oscillations are promoted or obstructed in particular regions, redundancies in signalling are removed. Whether this is a fundamental advantage or a constraint depends on the context. The temporal dynamics and bifurcation structure of the model continues to be present and is reflected in the module response to homogeneous signals, and also in gradients (especially weak gradients). In other cases, high diffusivity can promote effects in signal processing like an increased amplification of switching, by essentially making available a larger pool for an elevated response. This also suggests how cells may employ appropriate mechanisms of localizing proteins (for eg. through scaffolds) to effectively combine with diffusible entities to result in spatial switching effects. More generally our analysis provides insights into the extent to which particular temporal signalling characteristics in networks could be translated into spatial signalling characteristics, the constraints involved, and suggests some ways in which the networks may be organized to realize particular spatial signal transduction patterns by conforming to these constraints or bypassing them using the natural machinery and elements of signal transduction available.

Our studies have focussed on a series of modules which act as representative elements for particular behaviour. For the most part, for the kind of analysis performed here, the main insights also carry through to other representative models. Thus a model of mutual activation with positive feedback (Tyson et al., 2003), leading to bistability, exhibits similar

behaviour to the mutual inhibition module for the kind of analysis performed here. A similar conclusion can be drawn for different classes of monostable modules. In this study the spatial signals considered have been relatively simple but typical. We have not considered any spatiotemporal signal inputs, and will examine these issues in detail subsequently. We will also examine more complex network structures in detail later. Likewise, for all the network modules we have considered, inspite of the strong non-linearity the resulting spatial pattern was driven by the input signal to the module. Thus, we have not dealt with genuine symmetry breaking and pattern-formation in the spatial signal processing. This again will be dealt with subsequently.

Overall we have taken the first step towards a network-based exploration of spatial signalling (whose insights extend beyond intracellular signalling), and a systematic study of the role of global elements therein. The analysis indicates various surprising effects which arise in spatial signalling arising from a complex combination of non-linearity, diffusion and heterogeneity and how they may be underlying signalling patterns in basic modules. These results provide a basis for both understanding particular patterns of chemical signal propagation where spatial effects are important, and also a way for starting to build synthetic circuits in the cell which harness spatial signal transduction in a substantial and non-trivial way (Good et al., 2011; Levskaya et al., 2009; Liu and Fletcher, 2009).

# Chapter 4

# Covalent modification cycles through the spatial prism

## 4.1 Introduction

Cells employ complex chemical networks to regulate and control intracellular processes, robustly maintain different aspects of cellular life and respond appropriately to a variety of environmental cues. Understanding the functioning of these networks and information transfer and "decision making" through them is a major theme in systems biology involving inputs from mathematical modelling, experiments and theoretical work.

In order to understand the functioning of these networks different simplifications are introduced. The signal transduction through these networks is studied largely in temporal/lumped and deterministic terms. In the last decade there has been significant progress in understanding the role of noise and stochasticity in gene regulation and signal transduction. In most studies spatial aspects are ignored, even if acknowledged, either because they are assumed *a priori* to be of secondary importance or because available data is not spatially resolved.

However, biochemical information transfer occurs through various molecules which move to different locations of the cell and interact with one another, and it is clear that spatial considerations are an integral part of information transfer and intracellular functioning. In certain processes (e.g. eukaryotic chemotaxis, polarity generation, cytokinesis, pheromone sensing), spatial aspects of signal transduction are clearly important and hence directly accounted for (Dawes and Edelstein-Keshet, 2007; Drubin, 2000; Moore et al.,

2008; Moseley et al., 2009; Rappaport, 1971; Schwarz-Romond and Gorski, 2010; Swaney et al., 2010). However there are a huge number of other pathways and processes in which the effect of space on signal transduction could be important. At the outset, a number of questions arise: what exactly is the role of space in signalling: is it just a modulatory effect or something more substantial? When can these processes be studied in temporal terms? Can spatial considerations be accounted for in an *ad hoc* way? How does the consideration of space change our understanding of signal transduction?

In order to get insights into these questions, we will focus on the spatial dimension to signal transduction in a basic building block of post-translational modification: a covalent modification cycle (Marks et al., 2009). We do this because this is a ubiquitously-occurring unit in cell signalling and understanding these issues here serves as a platform for understanding similar issues in more complex networks, complementing Alam-Nazki and Krishnan (2012).

We will systematically examine spatial aspects of signal transduction in this module, by considering in turn, the effects of graded signals, the effects of diffusion of individual entities, the effect of localization of individual species, and the combination of these factors. Taken together this provides a basis for 1) understanding the role of space in information processing in this basic module and 2) understanding spatial aspects of covalent modification in a wide range of cellular contexts.

The chapter is organized as follows. We first detail the basic model employed, briefly discussing temporal signal transduction. We then present a series of results exploring the roles of species diffusion, localization and their combination. We conclude with a synthesis and discussion.

## 4.2 Models and Methods

### 4.2.1 Model Setting

We employ a standard model which describes the modification of a protein X to $X^*$ by the enzyme K and the reverse reaction catalyzed by the enzyme P. The enzyme and its target substrate first form an enzyme-substrate complex (XK or $X^*P$) before being converted to the respective product (Fig. 4.1). For uniformity we refer to X as the substrate and $X^*$ as the product. K and P could represent kinases and phosphatases (or other enzyme pairs), respectively, catalyzing the activation and deactivation steps in reversible modification cy-

cles. The model equations are:

$$\begin{aligned}
\frac{\partial[X]}{\partial t} &= -k_1[X][K] + k_{-1}[XK] + k_4[X^*P] + D_X\frac{\partial^2 X}{\partial\theta^2} \\
\frac{\partial[X^*]}{\partial t} &= -k_3[X^*][P] + k_{-3}[X^*P] + k_2[XK] + D_{X^*}\frac{\partial^2 X^*}{\partial\theta^2} \\
\frac{\partial[K]}{\partial t} &= -k_1[X][K] + k_{-1}[XK] + k_2[XK] + D_K\frac{\partial^2 K}{\partial\theta^2} \\
\frac{\partial[P]}{\partial t} &= -k_3[X^*][P] + k_{-3}[X^*P] + k_4[X^*P] + D_P\frac{\partial^2 P}{\partial\theta^2} \\
\frac{\partial[XK]}{\partial t} &= k_1[X][K] - k_{-1}[XK] - k_2[XK] + D_{XK}\frac{\partial^2 XK}{\partial\theta^2} \\
\frac{\partial[X^*P]}{\partial t} &= k_3[X^*][P] - k_{-3}[X^*P] - k_4[X^*P] + D_{X^*P}\frac{\partial^2 X^*P}{\partial\theta^2}
\end{aligned} \tag{4.1}$$

where $k_1$ and $k_3$ are the forward rate constants for the binding of the enzymes and their substrate, $k_{-1}$ and $k_{-3}$ are the rate constants for the dissociation of the enzyme substrate complex and $k_2$ and $k_4$ are the rate constants for product formation. $\theta$ represents the spatial coordinate and $D_j$ is the diffusion coefficient for any species "j" in the cycle.

Since our primary focus is on basic aspects of spatial signal processing, we cast the model in a spatial domain in 1-D, and use periodic boundary conditions for simplicity (analogous results to the ones presented here have been obtained for no-flux boundary conditions). It is worth pointing out that for the inputs considered here, the results are exactly equivalent to those with no-flux boundary conditions in a domain half the size. Thus all essential results are equally valid for both cases and could be relevant to situation involving modification and diffusion of species in the membrane or the cytosol (see Appendix C for further discussion).

### 4.2.2 Role of space

In order to systematically understand spatial effects in steady state and dynamic signal processing in post-translational modification networks, a useful starting point is to understand the effects at play in the basic covalent modification cycle. Two ways that space may play a part in intracellular signalling are by the transport and localization (or heterogeneous distribution) of signalling species. For example, the enzymes K and P and both proteins X and $X^*$ may be spatially distributed in the membrane, the cytoplasm or organelles; they may

also be clustered in one or several locations such as at cell poles. Furthermore it is possible that any of these species may be transported from one intracellular location to another. In this investigation we focus on diffusion as the main transport mechanism because of its widespread presence (Soh et al., 2010).

### 4.2.3 Inputs

In this study we regard enzymes K and P to be the spatial inputs which have either graded or localized (or uniform) spatial concentration profiles. An issue that naturally arises when considering spatial inputs is which is the most realistic way in which a spatial signal is introduced into the system or presented to an intracellular network. In our analysis we considered two different scenarios, each of which may be plausible in cell signalling. In one scenario, the signal appears at some "initial" time point. By modelling the spatial inputs as initial values (assigned to the enzymes) we allow the dynamics of the system to run its course and cannot control the input. This corresponds to considering the cycle as a "closed" system. A second scenario is one where an imposed spatial signal is always maintained in the system. This could occur via (for instance) the continuous production and degradation of the free enzyme (which acts as the signal), or in more complex variations thereof. This is modelled by explicitly adding production and degradation terms into the enzyme kinetic description. Analysing the differences (if any) between the results in the two cases enables us to comment on the use of either description in concrete contexts. The differences in signal imposition are especially pertinent in spatial signal transduction, because unlike in the temporal case, the system is not locally closed.

In our modelling framework we examined the first scenario by assigning appropriate initial conditions to enzymes K and P. The second scenario is modelled by explicitly adding production and degradation terms into the enzyme rate equation.

$$\begin{aligned}\frac{\partial[K]}{\partial t} &= -k_1[X][K] + k_{-1}[XK] + k_2[XK] + k_{f1}S(\theta) - k_{b1}[K] + D_K\frac{\partial^2 K}{\partial\theta^2}\\ \frac{\partial[P]}{\partial t} &= -k_3[X^*][P] + k_{-3}[X^*P] + k_4[X^*P] + k_{f2}I(\theta) - k_{b2}[P] + D_P\frac{\partial^2 P}{\partial\theta^2}\end{aligned} \tag{4.2}$$

where $k_{f1}$ and $k_{f2}$ are the "production" constants and $k_{b1}$ and $k_{b2}$ are the "degradation" rate constants for the free enzymes K and P, respectively. $S(\theta)$ and $I(\theta)$ are parameters

associated with the spatial distribution of the enzymes and can be either graded or localized. These "spatial inputs" are specified as graded ($S = a + bcos\theta$ with $a > b$) or localized signals, in the form of a square pulse or gaussian curve (exact signal values are shown in Appendix C). There are many ways of representing graded and localized inputs and we chose these for convenience. In our study we have chosen the mean value of $S(\theta)$ to be greater than that of $I(\theta)$ so that the effect of K "dominates" that of P, for the choice of parameters (without loss of generality). For certain cases we also make P homogeneous and only K is spatially distributed. Spatial input signals are discussed in further detail in Appendix C.

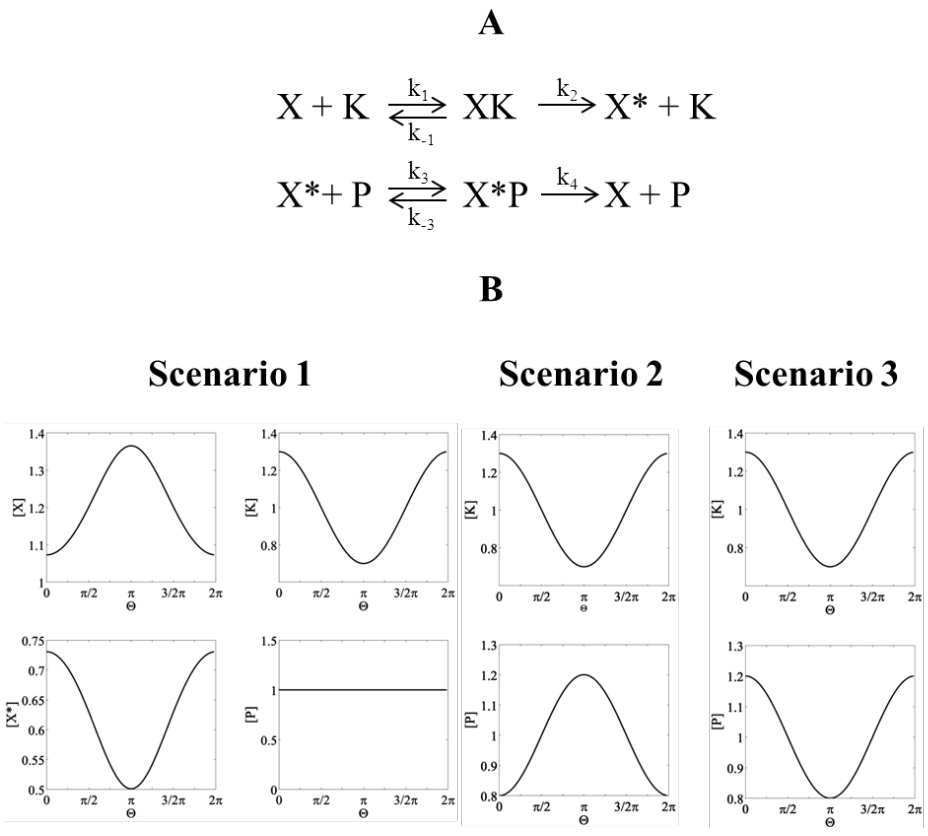


Figure 4.1: **Schematic of the cycle and the temporal reference cases.** (A) A schematic of the covalent modification cycle is shown. This is cast in a 1-D spatial domain. (B) The reference cases (where all species are essentially non-diffusible) are shown for scenarios S1, S2 and S3 (here and for other figures $\theta$ refers to the spatial coordinate). The concentration profile of K is spatially varying and that of P is homogenous in S1 while they are counter-aligned in S2 and co-aligned in S3. The choice of kinetic parameters reflects the dominance of K over P. Thus the concentration profile of $X^*$ mirrors K and that of X is qualitatively opposite to K in all scenarios (shown here for S1 only). See Appendix C for values of kinetic rate constants used in this and other figures.

### 4.2.4 Parameters

Describing the reversible modification cycle explicitly by including the kinetics for all species including the enzyme-substrate complexes in the model allows for the systematic exploration of spatial effects in this cycle. Since kinetic parameter specification in such cycles can substantially influence their behaviour, we analysed the system in different parameter regimes. The regimes we considered were 1) Mass Action: where rate of product formation is much greater than formation and dissociation of the enzyme-substrate complex 2) "Ultrasensitive": where a small change in signal input leads to a significantly larger change in output (Goldbeter and Koshland, 1981) and 3) a regime which we call "generic": where the output of the cycle is a graded function of the input and where concentrations of the complexes cannot be neglected. The first two regimes are encountered or invoked routinely in many cell signalling contexts. The generic regime allows us to investigate the issues at hand without making special assumptions or looking at limiting cases. Analysing the module in three different representative kinetic parameter regimes enables us to understand the role of space in information processing in this module under a wide range of conditions.

These representative kinetic parameters used in this work are employed in the literature to model covalent modification in the mass action, "ultrasensitive" and "generic" regimes (Ferrell, 1996; Huang and Ferrell, 1996). The essential difference between parameter regimes is reflected in the rate at which the enzyme-substrate complex is converted into the product. If this rate is small, the enzyme is sequestered in the complex and the production of product occurs slowly or comparably relative to the formation of the complex. If this rate of complex catalytic conversion to product is high, virtually no enzyme is held up in the complex. This corresponds to the mass action scenario.

Next, we introduce spatial aspects to this module by incorporating diffusion of species. This is done by examining a range of diffusion coefficients for each species- representing low, moderate and high diffusivities (appropriate to the domain size and time scales). The diffusion coefficients were based on estimates in Postma and Van Haastert (2001) and the effect of varying diffusion strength is directly examined. The non-dimensionalization of space and time is done by appropriate representative length and time scales for signalling. Additional aspects of the issues discussed above and parameter values are discussed in the Appendix C. We focus primarily on qualitative aspects and trends in signal transduction, and in many cases explain the observed behaviour analytically, directly revealing the

influence of parameters.

### Numerical Method

The partial differential equations were discretized using finite difference equations and the results were checked by doubling the discretization. All simulations were performed in MATLAB using ode15s.

## 4.3 Results

Examining different combinations of the aforementioned parameter regimes and input scenarios as well as perturbing the cycle by a range of diffusion coefficients led to a large number of results. We therefore present a selection of results in this section as follows: we first present a series of results from the "generic" parameter regime as the insights obtained here are generally representative and in fact for the most part carry through to the mass action parameter regime (qualitatively). We subsequently examine the "ultrasensitive" parameter regime. Spatial signal transduction and the effect of diffusion is examined when enzymes have spatially graded profiles, corresponding to the scenarios, **S1:** When only K is graded **S2:** When both K and P are graded and counter-aligned (for example see (Janetopoulos et al., 2004)) and **S3:** When both K and P are graded and co-aligned. We conclude by examining the effects of localization of the enzymes. The computational results presented here are complemented by analytical work, which is presented in (Alam-Nazki and Krishnan, 2013) and reproduced in the Appendix C.

We primarily present results for the case where the signal is imposed via production and degradation of the enzyme. Note that this type of imposition allows for the continuous control of the input. We will comment on this point later on in this section.

We start our presentation of the results by discussing the reference case where all species are non-diffusible (or weakly, but equally, diffusible), with the kinetics of the cycle being in the "generic" regime. We then show the effects of increasing the diffusivity of individual species. Following this, we present the effects of diffusion of combinations of species, particularly focussing on the effects of diffusion of the complex(es) (results summarized in Table 4.1).

| Diffusing Species | **Effect on spatial variation (amplitude) of concentration profile of $X^*$ (relative to the reference case)** | **Salient Features** |
|---|---|---|
| **X*** | Weaker | S2: Complexes flip (Fig. 4.2) |
| **X** | Stronger (Fig. 4.2) | |
| **K** | S1 & S2: Weaker<br>S3: Stronger | S2: Complexes flip (Fig. 4.3),<br>S3: $X^*$ andX flip (Fig. 4.3) |
| **P** | S1: Negligible effect<br>S2: Weaker<br>S3: Stronger | |
| **X and XK** | S1 and S2: Stronger at low D, Weaker at high D<br>S3: Stronger | S1 & S2: Spatial variation is non-monotonically dependent on diffusion coefficient<br>S3: X*,flips as diffusion increases (Fig. 4.3) |
| **$X^*$ and $X^*$P** | Weaker | S2: Complexes flip as diffusion increases<br>S3: X*flips (Fig. 4.3) |
| **K and XK** | S1 and S2: Weaker<br>S3: Stronger | All Scenarios: Complexes flatten<br>S3: X*flips (Fig. 4.3) |
| **P & $X^*$ P** | S1 & S2: Weaker<br>S3: Stronger at low D, Weaker at high D | All Scenarios: Complexes flatten<br>S3: X* flips as diffusion increases |

Table 4.1: **Summary of results from the cases analyzed in the "generic" parameter regime.** The effect of diffusion of one or two species on the spatial concentration profile of $X^*$ is summarized. Stronger (or weaker) refers to the amplitude of the profile of $X^*$ increasing (or decreasing) with respect to the reference case (where all the species are essentially non-diffusible). S1: K graded and P uniform, S2: K and P graded and counter-aligned and S3: K and P graded and co-aligned. If the profile of a species (for e.g. $X^*$) undergoes a qualitative reversal we simply state that it flips.

### 4.3.1 Reference case

In S1, S2 and S3, the spatial concentration profiles of species XK, $X^*$ and $X^*P$ mirror K and that of X are qualitatively opposite to K. It should be noted that the basal kinetic parameters are chosen to reflect the dominance of K over P (without loss of generality). The spatial concentration profiles of cycle components are shown in Fig. 4.1. The reference case represents an unbiased platform relative to which the effects of transport and localization can be examined.

It should be emphasized that while our reference case involves species which are essentially non-diffusible we do not require the species to be strictly non-diffusible. In fact having a reference case where all species are (equally) weakly diffusible leads to essentially the same conclusions. Reducing the diffusion coefficient in this case results in profiles which approach the non-diffusible case (see Appendix C). This in turn is because the total substrate is constant spatially, exactly like the non-diffusible case. For a reference case where all species are weakly (but unequally) diffusible, reducing the diffusion coefficients, keeping their ratio fixed, will not in general approach the non-diffusible case. However, even here, the effects of increasing diffusion of one or more species results in the same trends as those of the reference case where all species are equally weakly diffusible. We thus use the non-diffusible case as a suitable reference which also represents the (equally) weakly diffusible case, for both simulations and analysis.

Next we examine how diffusion perturbs the steady state response of the cycle in the reference case in different parameter regimes. We observed the degree of change in spatial variation of the concentration profile- whether it increases (profiles become sharper) or decreases (profiles become weaker or more spread out) along with any changes in qualitative behaviour.

It should be noted that when the input signal is imposed via the production and degradation of the free enzyme, the spatial concentration profile of the free enzyme remains fixed even when the substrate modification cycle contains diffusible components, as long as the enzyme-substrate complex is non-diffusible. This and the implications of how a signal is imposed are discussed in further detail in the Appendix C.

### 4.3.2 Perturbation by diffusion of a single species

#### Diffusion can qualitatively alter steady state spatial profiles of cycle components

We examine the effect of diffusion of one species when other species in the cycle are non-diffusible/weakly diffusible.

**Diffusion of X$^*$:** As the diffusion coefficient of X$^*$ increases, as expected, it becomes uniform while the spatial variation of X becomes stronger in all scenarios. In addition, we find the following features: in S1 as $D_{X^*}$ increases, all species (except X) become homogeneous. In S2, interestingly, the complex profiles "flip" and become qualitatively opposite to K in contrast to the reference case (shown in Fig. 4.2). This is explained in the Appendix C. In S3 the spatial variation of both complexes decreases.

**Diffusion of X:** If X diffuses then the spatial concentration profiles of the rest of the components of the cycle have greater spatial variation (as compared to the non-diffusible case) in S1-3 (S3 is shown in Fig. 4.2). X itself flattens out losing all spatial variation. This result may be interpreted as follows: in the cycle if there is only one species which is not weakly diffusible, and all other species are weakly diffusible or non-diffusible (or immobilized), then this species at steady state will exhibit an essentially homogeneous profile.

#### Diffusion of Enzymes

**Diffusion of K:** As the diffusion coefficient of K increases, the spatial variation of all species in the cycle decreases in S1. In S2 both $X^*$ and X have weaker spatial variation. The profiles of both complexes, on the other hand, undergo a qualitative change- as $D_K$ increases the profiles change from having a variation similar to that of K to a variation similar to that of P. In S3, as $D_K$ increases the profiles of X$^*$ and X change qualitatively. X$^*$ "flips" and becomes qualitatively opposite to K and X becomes qualitatively similar to K. The complete change in the nature of the response here can be understood by noting that the two enzymes are in competition, and the diffusion of one of the enzymes can alter the balance of competition in spatial signalling, even though the kinetics favours the kinase, similar to Krishnan (2009). S2 and S3 are shown in Fig. 4.3.

**Diffusion of P:** The effects of diffusion of P presents contrasting results to those above. In S1 the (moderate) diffusion of P has a negligible effect on the spatial variation of the

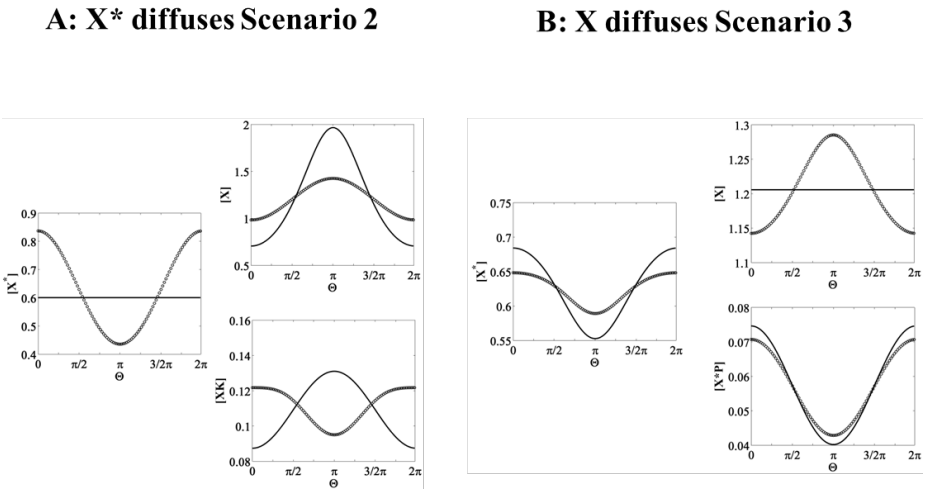


Figure 4.2: **The effects of a single species diffusing.** (A) The effect of diffusion of $X^*$ in Scenario 2: X, $X^*$ and XK are shown (Reference case: circles; $X^*$ diffuses: solid line). $X^*$ itself becomes homogenous and X becomes sharper. Diffusion of $X^*$ qualitatively changes the profiles of the complexes. (B) The effect of diffusion of X in Scenario 3: X, $X^*$ and $X^*P$ are shown (Reference case: circles; X diffuses: solid line). As the diffusion of X increases, the spatial profiles of $X^*$ and the complexes becomes sharper (similar results are seen in Scenarios 1 and 2). The range of diffusion coefficients utilized in this and the subsequent figures are in the Appendix C. Note that the diffusing entity attains the same homogenous spatial profille at steady state.

species. In S2, the profiles of $X^*$ and X have weaker spatial variation and that of the complexes has greater variation. In S3, the spatial concentration profiles of $X^*$ and X have increased spatial variation (due to decreased competition from P) and that of the complexes have less spatial variation.

Until now we have examined the effect of making only one species diffusible on the network response. Analysis of perturbation by diffusion of one species forms a basis for examining the diffusion of multiple species. It is biophysically plausible to assume that if either substrate and/or enzyme diffuse then the resulting complex can also diffuse (see (Yudushkin et al., 2007)) for an example of spatial tracking of enzyme-substrate complex). In considering the effects of the diffusion of the complex, we will next examine two situations: one where the complex diffuses as much as the substrate, and the other case where it diffuses as much as the enzyme. The combined effect of diffusion of X and $X^*$ is discussed in the Appendix C.

### 4.3.3 Perturbation by diffusion of two species

#### Diffusion of complexes can play an important and determining role

We will now examine the effect of diffusion of complexes on the cycle.

#### Both Complex and Substrate are diffusible:

**X and XK are equally diffusible:** In S1 and S2, for weak diffusion the response of the system is similar to the case when X alone diffuses. The degree of spatial variation of $X^*$ increases relative to when diffusion is absent. We note, however, that the degree of spatial variation of $X^*$ is non-monotonically dependent on the diffusion coefficient- the variation is greatest when diffusion is weak and reduces, becoming lower than the reference case, when the diffusion is high.

Along with the non-monotonic dependence of spatial amplitude on diffusion, this result also shows that in direct contrast to the effect of X alone diffusing, the combined diffusion of X and XK leads to the weakening of the $X^*$ profile. This effect is due to XK diluting the influence of K (through its own spreading). Further differences from the single species diffusion case are seen in S3 where increasing the diffusion coefficient leads to the "flipping" of $X^*$ followed by increased spatial variation (S3 is shown in Fig. 4.3).

**$X^*$ and $X^*P$ are equally diffusible:** We see surprising results here as well. In S1, all species (except X) become homogenous. This can be explained analytically (Alam-Nazki and Krishnan, 2013) (Appendix C). Only the profile of X becomes sharper. In S2, the profile of $X^*$ becomes weaker and X becomes sharper. The profiles of the complexes "flip" as the diffusivity increases. In S3, for weak diffusion $X^*$ qualitatively "flips" and its profile becomes opposite to that of K and its spatial variation decreases as the diffusivity increases (shown in Fig. 4.3 ).

For all scenarios, if the complex is weakly diffusible and the substrate is highly diffusible then the effect of the combined diffusion is essentially the same as when the substrate was alone diffusing.

#### Both Complex and Enzyme are diffusible

**Both K and XK are diffusible:** For all scenarios, diffusion results in the flattening of both complexes (explained analytically in (Alam-Nazki and Krishnan, 2013), shown in

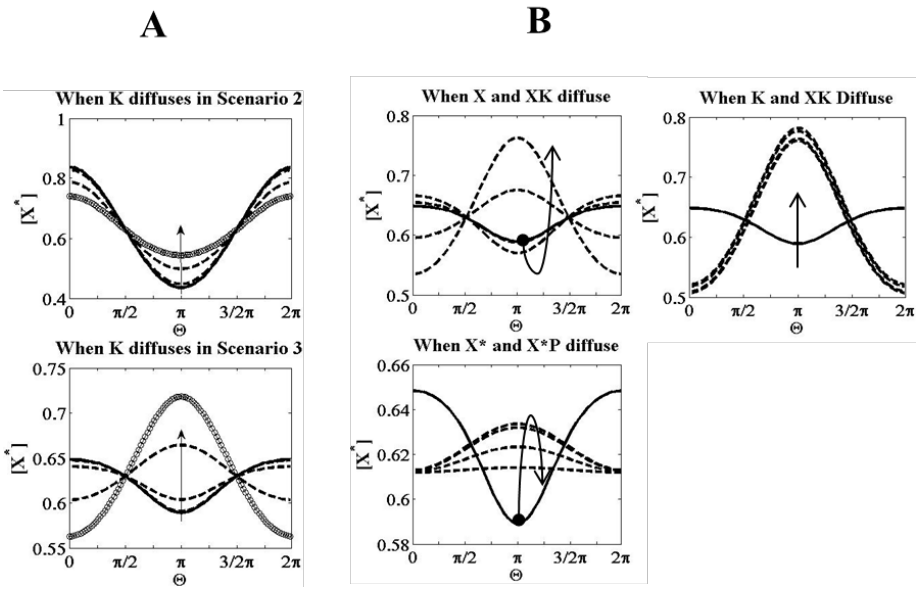


Figure 4.3: **The effect of enzyme diffusion and that of complex diffusion.** (A) The effect of enzyme diffusion: $X^*$ profiles are shown for the case when K diffuses in Scenarios 2 and 3 (Reference Case: solid line; K diffuses at low and intermediate levels: dashed lines; and at high level: solid line with circles). In S2, the spatial variation of the $X^*$ profile becomes weaker, as the diffusion of K increases. On the other hand, the complexes completely change orientation (not shown, similar to Fig. 4.2). In S3, the spatial profile of $X^*$ "flips" and becomes qualitatively opposite to K, as the diffusion of K increases. Next, we have show the effect of two species diffusion. (B) The spatial profile of $X^*$ is shown for cases when the pairs X and XK, $X^*$ and $X^*$P and K and XK diffuse in Scenario 3 (Reference Case: solid line; species diffusing: dashed lines). In all three cases $X^*$ shows a qualitative change- the profile "flips" as the diffusivity increases. When K and XK diffuse we also find that the complex $X^*$P becomes homogenous (not shown). This shows how diffusion of complexes can qualitatively alter the spatial profile of different species. The arrow points to the direction in which the profiles change as the diffusion coefficient increases.

Appendix C). In S1 and S2 as the diffusion increases, the spatial variation of $X^*$ becomes weaker (flat in S1). In S3, for weak diffusion the profile of $X^*$ qualitatively "flips" (becoming opposite to K and P) and as the diffusion becomes stronger, its spatial variation increases (S3 is shown in Fig. 4.3 ).

**Both P and $X^*$P are diffusible:** For all scenarios, diffusion again results in the flattening of both complexes (explained analytically in (Alam-Nazki and Krishnan, 2013), also shown in Appendix C). In S1 and S2, as the diffusion coefficient increases, the $X^*$ profile weakens (in S1 it becomes homogenous). In S3, increasing the diffusion leads to a "flipping" of the $X^*$ profile whose amplitude increases and then eventually decreases. Here we see a very different trend to the scenario when P alone is diffusible.

These results clearly demonstrate that diffusion of a complex can play important and unexpected roles in spatial signal transduction. It also shows that the explicit description

of complex formation could be important in understanding spatial signal transduction in different contexts.

### 4.3.4 Spatial Signalling in the "Ultrasensitive" Parameter Regime

#### Spatial signal transduction and switch-like behaviour

So far we have shown the results for the generic parameter regime. Next we outline the effects of perturbing the cycle by diffusion when it lies in the "ultrasensitive" parameter regime. In this regime $X^*$ displays a switch-like response as a function of input. The study of switch-like behaviour in signal transduction has been the focus of a number of temporal studies with some discussion of spatial aspects (Lipshtat et al., 2010). In making a transition from the purely temporal to the spatial model of the cycle, we see that in the "closed" model (spatial distribution of enzymes is imposed via initial conditions), the effect of a switch-like behaviour continues to be seen, if the enzymes (and complexes) are non-diffusible. In this case, the spatial signal transduction can be understood from the temporal signalling characteristic of the cycle. However a steady state switch-like response is not seen when the enzymes (and possibly complexes) are diffusible, because a gradient of enzymes cannot be sustained at steady state. Put another way, the enzymes need to be immobilized to elicit a switch-like response in this case. Otherwise any possible switch-like effect will be transient.

Since we wish to examine possible switch-like behaviour to externally imposed spatial signals, we consider the "open" model. Note that we used this model where production and degradation of the free enzyme were used to determine the spatial distribution of the enzymes. An analysis of this model shows that such a description of signal imposition keeps the free enzyme concentration essentially fixed (this is true even in the purely temporal case). An examination of such a model shows that this will not be able to exhibit the switch-like behaviour desired because no strong sequestration effect of enzyme is possible (see the Appendix C).

Based on the discussion above, we see that for a steady state switch-like behaviour to be present when species are diffusible, some local sequestration effect must be present. We therefore examine a modification of the basic model incorporating this effect, to examine whether spatial switch-like behaviour may be seen at steady state. The minor modifications to the model (shown in the Appendix C) incorporate degradation of all X species (X, XK,

$X^*$ and $X^*P$) and a small generation of X (without loss of generality). In this modified model we have a conservation of total X species locally (under homogenous conditions). Further, the total enzyme concentration is determined as the ratio of the enzyme production and the degradation rate (of enzyme and complex assumed equal). Thus, in contrast to the model employed earlier, the total enzyme concentration (as opposed to free enzyme concentration) is essentially fixed, locally. This (open) model formulation therefore allows the free enzyme to be taken up substantially into the complex and serves as a platform for examining the effects of diffusion. Note that in temporal closed models of cycles, the total enzyme and substrate are fixed, and the appropriate kinetic parameter regime allows for switch-like behaviour. The above model may be seen as a spatial analogue of this, imposing essentially fixed local pools of enzyme and substrate.

An analysis of the modified model shows that it is indeed able to exhibit switch-like behaviour in response to spatially graded inputs (when all species are essentially non-diffusible). This is seen in the profile of $X^*$ (shown in Fig. 4.4). This shows how maintaining essentially fixed enzyme/substrate pools locally can lead to spatial switch-like behaviour in this open model.

Here we consider only one scenario where input spatial information to the module occurs only through K. We discuss the effect on the output $X^*$ when diffusing species are present in the cycle.

## Effect of diffusion of a single species:

If X diffuses, the spatial variation (and "switch amplitude") of the concentration profile of $X^*$ is enhanced even further (shown in Fig. 4.4). If $X^*$ itself diffuses, the spatial variation of X becomes enhanced while the $X^*$ spatial profile becomes graded and weaker. Thus, the spatial switch is weakened. If the enzyme K diffuses (Fig. 4.4), the spatial switch dampens even for moderate values of diffusivity and finally is lost. Even if enzyme P diffuses, the spatial switch becomes dampened. This last conclusion highlights new aspects of the interplay between transport and signal processing in the cycle, since the diffusion of initially uniform enzyme plays a significant role in the outcome. It shows how diffusion can cause "replenishment" of the phosphatase enzyme, diminishing the spatial switching effect.

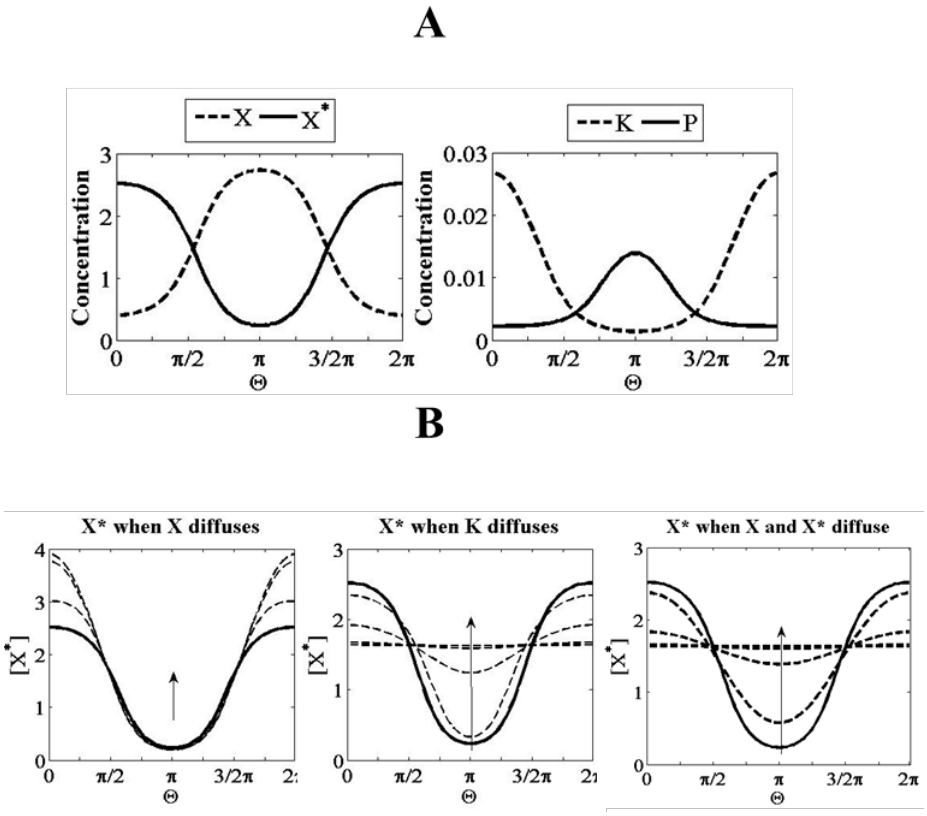


Figure 4.4: **Effect of diffusion on the cycle when it is in the ultrasensitive kinetic parameter regime.** (A) The spatial profiles of X (dashed lines) and $X^*$ (solid line) and K (dashed lines) and P (solid line) are shown when no diffusion is present: a spatial switch is seen in the profile of $X^*$. (B) When X diffuses the spatial switch in $X^*$ is enhanced. On the other hand, when K diffuses, the spatial switch in the profile of $X^*$ is increasingly dampened as $D_K$ increases until it is finally lost. When both X and $X^*$ equally diffuse, as their diffusivity increases, the spatial switch in $X^*$ disappears. (In (B) Reference Case: solid line; species diffusing: dashed lines; the arrow points to the direction in which the profiles change as the diffusion coefficient increases.)

## Effect of diffusion of two species:

We now consider what happens if two entities diffuse, as above. If XK and X diffuse then the spatial switching effect in $X^*$ is lost. This is in contrast to when X alone diffuses. Similarly if one considers moderate diffusion of the pairs (K and XK, $X^*$ and $X^*P$) the spatial variation of $X^*$ becomes weaker in all these cases and the spatial switch is again lost. If P and $X^*P$ diffuse the switch is dampened.

Finally, if both X and $X^*$ equally diffuse then the switch is dampened before eventually being lost (shown in Fig. 4.4). If $X^*$ is weakly diffusible and X highly diffusible the switch is dampened but maintained. In this situation the diffusion of X counteracts the diffusion

of $X^*$.

Overall, we find that the cycle is capable of exhibiting a steady state spatial switch-like profile (even if species are weakly diffusible), in situations where an essentially fixed pool of enzyme/substrate is maintained locally, and significant sequestration in complex occurs. We observe that in this case the spatial switch can either be enhanced, dampened or completely destroyed by diffusing species and that even moderate diffusion can play a strong role in dampening switching effects.

### 4.3.5 Interplay between Diffusion and Localization

We now examine the effects of localization of the enzymes (where enzymes are present in certain locations and not free to move). Examples of localization of kinase/phosphatase pairs are observed in bacteria (Shapiro et al., 2009), PI3K/PTEN in *D. discoideum* (Janetopoulos et al., 2004) and also Par proteins in *C. elegans* (Griffin et al., 2011). While localization could be thought of as another spatial enzyme profile (as considered previously) it also brings up new aspects which we examine here. In this section, we examine the effects of localizing K and P in separate regions as well as in the same region. We will particularly focus on the spatial average of the concentration of $X^*$, as this represents the average response over the spatial domain. If we compare the spatial average of $X^*$ in both the aforementioned scenarios (when no diffusion is present), we find that the average is higher when the enzymes are separated than when they are in the same domain. The absence of substantial local competition between the enzymes allows for a greater average $X^*$. Next we studied the effect of both X and $X^*$ diffusing together in each of these cases (if the enzymes are localized in separate regions, the diffusion of substrates is necessary to complete the cycle).

While increasing the diffusion has the expected effect of reducing spatial variation (as seen in Fig. 4.5), the effect on the spatial average of $X^*$ was more interesting. When the enzymes were located in separate domains, the spatial average of the concentration of $X^*$ exhibited both monotonic and non-monotonic trends as the diffusion coefficient was increased. We found that for certain parameter regimes, the spatial average of $X^*$ was an increasing function of diffusion coefficient while in other cases it reached a maximum at some intermediate diffusion coefficient before gradually reducing to its asymptotic value (shown in Fig. 4.5). The diffusion coefficient at which the spatial average reaches its peak can be shifted (either increased or decreased) by modulating the parameter values (for

e.g. total concentration of the enzymes). This result shows that in this case there is an "optimal" diffusion coefficient at which the maximum average conversion of X to $X^*$ can be achieved; there is a subtle balance between the diffusion of species and the conversion of the substrate. It is worth pointing out that the origins of this biphasic effect are independent of any enzyme sequestration: we readily observe the same behaviour in mass action models of the covalent modification module.

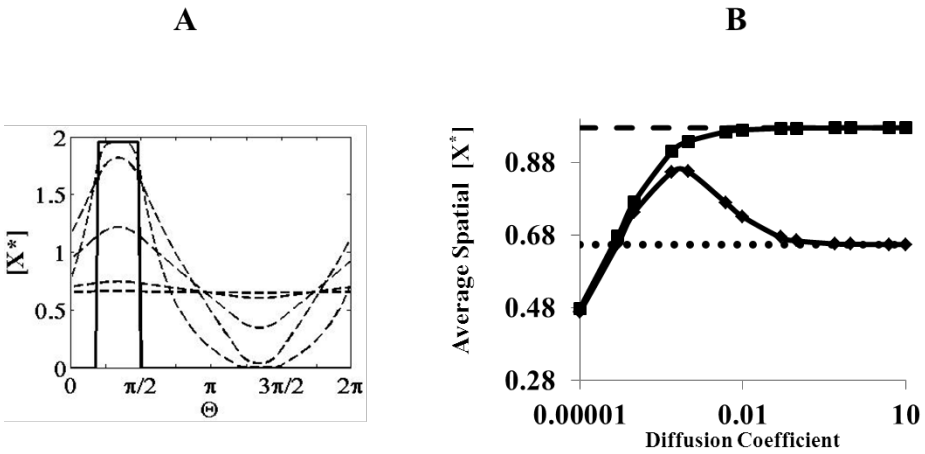


Figure 4.5: **The interplay between diffusion and localization.** (A) The profile of $X^*$ is shown for the case when enzymes are spatially segregated (Reference case: solid line). The effect of X and $X^*$ equally diffusing (dashed lines) is shown. As the diffusivity increases (shown by direction of arrow), the profile becomes more spread out. (B) We examine the effect of diffusion of X and $X^*$ on the spatial average of $X^*$. Two cases are shown here where the average of the spatial concentration of $X^*$ both non-monotonically (solid line with diamonds) and monotonically (solid line with squares) varies with respect to the diffusion coefficient of X and $X^*$. We have also shown the asymptotic limit for the spatial concentrations of $X^*$ when the diffusion becomes very large (pertaining to the non-monotonic case: dotted lines; monotonic case: dashed lines).

Taken together our analysis reveals different facets and surprising aspects of the interaction of diffusion with the modification cycle kinetics.

## 4.4 Conclusion

Temporal signal transduction in covalent modification cycles has been the focus of many studies. Spatial signal transduction in covalent modification cycles and cascades have been the focus of a few studies, from specific perspectives. The effects of separated enzymes in generating large activity gradients is studied in Brown and Kholodenko (1999). The generation of phosphoprotein waves arising from bistability in protein kinase cascades, as a potential mechanism for long range signalling is considered in Markevich et al. (2006).

The ability of signalling cascades to transmit information from the membrane to the nucleus is studied in Muñoz-García et al. (2009). Effects of enzyme localization in affecting amplification is studied in Van Albada and Ten Wolde (2007). The review Kholodenko (2006) discusses the role and relevance of temporal control and spatial distribution of signalling species in decision making. It also discusses spatial signalling mechanisms including the recruitment of entities to the membrane or subcellular locations, gradients and phosphoprotein waves.

In contrast, we start with a standard model of a covalent modification cycle (with all kinetic steps explicitly described), extended to incorporate spatial signalling. We focus on different facets of spatial signal transduction as revealed by a systematic analysis of this model, with a focus on qualitative trends. The model contains a number of scenarios (e.g. immobilized substrates or enzymes) as special cases or limiting regimes. We considered different basal parameter regimes for the module and also different ways in which this module could be subjected to signals: imposing enzyme profiles either as initial conditions (closed system scenario) or with active upstream regulation (open system scenario). Our consideration of multiple scenarios allows us to systematically elucidate common aspects of signal transduction and also identify important differences where they exist. This is also useful when one considers the many extensions and variations of such modules encountered in cellular contexts.

**Signal Imposition:** While in some cases, spatial signal transduction could be largely understood in terms of temporal signalling features, in other cases spatial aspects played an important and even determining role. To start with, while the temporal steady state behaviour of such cycles could be studied by considering the total amounts of kinase and phosphatase as parameters, the steady state spatial behaviour depended on how a signal was imposed (corresponding either to an "open" or "closed" system), when entities were diffusible. For instance when substrates and complexes were (moderately) diffusible, in a closed system, an enzyme spatial signal could not necessarily be sustained (due to the "redistribution" of enzymes via diffusion of complexes), unless some extra mechanism of localization (e.g. scaffold) was present. This is one example where a specifically spatial aspect (transport of substrate and complexes) plays a substantial role in distorting an "upstream" entity which does not have a direct temporal analogue. In general we can say that when enzymes and complexes are non-diffusible, the spatial behaviour of the cycle could be understood more easily and predictably from the temporal behaviour of the cycle (though substrate diffusion may play a non-trivial role), and in this case, both open and

closed system scenarios for signal imposition give similar results. When enzymes and/or complexes may diffuse even moderately, the steady state behaviour in both scenarios is different (and hence so is the transient behaviour).

We can summarize the effects of species diffusion and localization as follows.

### 4.4.1 Diffusion

The role of diffusion in signal transduction in the cycle could be substantial. Diffusion (even moderate) of individual or multiple species could lead to the abolishment or considerable weakening of spatial gradients of individual entities. It could play a substantial role even when both enzyme profiles were counter-aligned (both enzymes "co-operating" in spatial signal transduction); it could alter the balance of power when enzymes were co-aligned ("competing" in spatial signalling, see (Krishnan, 2009) for a similar effect). The diffusion of complexes could play an additional complicating and important role, which may be unintuitive. This demonstrates the need for carefully and explicitly accounting for the dynamics of complexes and their diffusion. Diffusion of species at moderate levels could alter, or even substantially diminish the capacity of the cycle to exhibit a switch-like behaviour to spatial signals. Our analysis provides a framework for understanding the effects of diffusion of species both individually and in multiple combinations.

It is worth pointing out that while differences in diffusion of enzymes may be expected, substantial differences in diffusion due to post-translational modification of proteins have also been observed experimentally both on the membrane (Conchonaud et al., 2007) as well as in the cytoplasm. For example, in the cases of proteins such as MEX-5 and PIE-1 (Daniels et al., 2009; Griffin et al., 2011), modification leads to differences in diffusion between the unmodified and modified forms of these species. It has been argued there and elsewhere (Lipkow and Odde, 2008) that this is likely to be because of substantial differences in affinity for proteins or lipid rafts on the membrane or proteins and other entities (for e.g. vesicles) in the cytoplasm.

### 4.4.2 Localization and transport

It was found that the spatial localization of kinase and phosphatase could strongly affect the total modification of substrate in the domain. A spatial co-localization of both enzymes generally led to less overall modification than localized and separated enzymes. In the

latter case, the effect of diffusion of the substrate(s) was interesting: while in some cases, an increase of the diffusivity led to an increased overall modification, in other cases overall modification was a non-monotonic function of diffusivity: here an intermediate diffusion coefficient resulted in the maximal overall conversion suggesting an optimal combination of separation and transport.

Overall our analysis reveals many subtle and new competing effects at play when the spatial dimension to signal transduction and the "interweaving" of spatial factors and enzyme kinetics is studied in detail. We can expect combinations of such competing factors at play in concrete instances (the effects of some of which may be wrongly attributed to extraneous factors). This analysis is important both for understanding the intrinsic signal processing capabilities of this module, and also for appropriately and systematically employing it (or simplifying it) in specific modelling contexts. Our study also suggests that examining limited data may in fact mask a subtle combination of factors.

More generally, our studies indicate that the effect of space may not be correctly understood by including spatial aspects in an *ad hoc* way in signal transduction, even in this basic module. The role of space in covalent modification and signal transduction may arise in multiple ways. In some cases the spatial aspects are central and necessary (such as cells imposing internal gradients for various purposes), while in other cases they are incidental (spatial variation of protein concentrations occur due to transport to particular localized targets). By noting the abundance of covalent modifications of proteins in cells, and the multiplicity of contexts in which they occur, we see that various different scenarios (and parameter regimes) examined, as well as extensions (such as signalling in cascades) may be encountered. It is clear that an understanding of these contexts can utilize and build upon the insights obtained here, to reveal the role of space in information processing. This is relevant even for modification cycles and extensions which have been studied hitherto in purely lumped terms.

### 4.4.3 Transient effects

Our study here has focussed on steady state analysis only. We recognize that transient effects may be important and in some specific contexts, even be the dominant effect. However, given the nature of the analysis, it is both easier and necessary to start with steady state analysis. Indeed, a systematic analysis of the model demonstrates many competing effects and subtle behaviour at steady state. Since transient responses have to evolve to this

steady state in principle, the relevant effects observed here will kick in at some time point. In order to thoroughly study transient dynamics in a systematic manner, it is important to be aware of the steady state behaviour and also examine in detail effects of how the signal is imposed temporally and spatially. Such analysis of necessity builds on the results presented here, and we will examine this in detail in the future.

### 4.4.4 Implications

We discuss some further implications of our analysis below. To start with, even in the basic modelling of covalent modifications, while various assumptions are used (mass action kinetics and Michaelis Menten kinetics), other implicit assumptions are made about spatial aspects (spatial homogeneity), which may or may not be true. An understanding of signal transduction requires both the explicit description of enzyme-substrate complexes and spatial aspects as well their interplay. Our studies above show firstly that spatial variation and diffusion may combine in unintuitive ways, and secondly, by accounting for transport of complexes, important changes can occur. Thus this serves as a platform to re-evaluate the validity of different assumptions in multiple contexts.

Our results suggest that while certain circuits may function to give rise to certain behaviour (such as switches) in an ODE setting, and even in a stochastic setting, while including spatial aspects things may be different. Firstly the circuit may not necessarily be able to demonstrate the same behaviour to spatial signals and be quite sensitive to the diffusion of species involved. The mechanism for generating an ultrasensitive switch temporally relies on an essentially fixed pool of enzyme. This may or may not be possible to realize locally, spatially, not least because of enzyme and complex diffusion. Our analysis shows that when an essentially fixed (total) local pool of enzyme is maintained, the cycle may be able to act as a switch to spatial signals. This has implications for the construction of spatial switches (Lipshtat et al., 2010) and also for the extent to which temporal circuits could act as temporal switches when spatial heterogeneity and/or transport is present. Our analysis also suggests ways in which some of the limitations due to diffusion on switch-like behaviour may be bypassed. One possibility is the use of scaffolds which may limit the effects of transport of enzyme/substrate relative to one another. Another possibility is the employment of some molecular titration mechanism of enzymes to generate threshold-like behaviour (Buchler and Louis, 2008; Seaton and Krishnan, 2011).

We can build on our analysis to examine how multistep cascades may function as spatial

switches. It suggests (and analytical results confirm) that transport of enzymes (and complexes) would significantly affect spatial switching behaviour from such pathways as well, unless an essentially fixed input enzyme pool was maintained locally. It suggests that either the use of mechanisms mentioned above, or some degree of upstream "pre-processing" which allows an essentially fixed pool of enzyme to be maintained locally would facilitate conditions for spatial switch-like behaviour from such cascades.

While considering the total (or spatial average) modification of substrate, we find that this depends on the localization of individual enzymes. Since the spatial average of protein concentrations is the usual experimental measure of protein concentration, we see that this not only masks important internal variation and dynamic interplay between species, but can also be the basis of mistaken estimates of kinetic parameters from experiments. More generally the effect of such internal variation can also result in incorrect causal inferences made from experiments.

### 4.4.5 Examples

An example of spatial aspects of covalent modification cycles and extensions thereof is the modification cycle involving MEX-5 (Griffin et al., 2011). Experiments and modelling have postulated that the enzyme substrate complex may combine with other entities and may have different diffusion rates depending on its location in the cell (and interacting with other complexes accordingly), thus profoundly affecting many aspects of covalent modification. We thus see an example of a complex spatial version of a covalent modification cycle which not only possesses the basic features examined above, but highlights a more complex interplay between transport, complex formation and heterogeneity. Other examples of parallels we have studied, include G-protein spatial cycles (Rocks et al., 2010) and separated phosphorylation/dephosphorylation at the membrane and endoplasmic reticulum in eukaryotic cells (Yudushkin et al., 2007) where enzyme substrate complexes are tracked spatially. The RanGEF/GAP example (Vartak and Bastiaens, 2010) is yet another example of localization of enzymes in different spatial locations. An even more striking example of such behaviour is seen in bacteria where phosphorylation/dephosphorylation cycles have localized and separated modification at poles of the bacteria, which are, in some cases, mediated by a bifunctional kinase (Chen et al., 2011). This shows how basic elementary spatial variations in the modification cycle are seen in bacteria and include bifunctional kinases as well. This undoubtedly removes certain constraints associated with co-localizing

bifunctional kinases.

Covalent modification cycles are basic building blocks in protein signalling networks and it is to be expected that spatial effects will be present in multiple forms and guises in cell signalling. Our results provide a basis for starting to elucidate a number of related themes in signal transduction. This includes the role of localization and its interplay with transport, and also the ways in which cells may use machinery available to them, such as scaffolds (Good et al., 2011), to harness (Agapakis et al., 2012), accentuate or insulate signalling from spatial effects. We expect that elucidating the spatial dimension to signal transduction will provide an important window into understanding cellular information processing.

# Chapter 5

# Spatial control of biochemical modification cascades and pathways

## 5.1 Introduction

Cells respond to their environment and regulate their internal functioning through complex and sophisticated networks of proteins and genes. Chemical information is transmitted in these networks via various sequences of chemical modifications. The nature of chemical information transmission in signalling cascades is the focus of a large body of work, which has revealed the effects of modifications, the enzymatic regimes, as well as the effects of enzyme and substrate sequestration.

However sequences of chemical modifications often involve relevant species moving to different locations where other species may be localized (Hurtley, 2009). Thus, while modelling and understanding information transmission in signalling cascades through ordinary differential equations provides many useful insights, it completely ignores the spatial dimension to signal transduction. In most studies spatial aspects are ignored, even if acknowledged, either because they are assumed *a priori* to be of secondary importance or because available data is not spatially resolved. At the outset, an implicit assumption often made is that spatial effects may be easily subsumed within a kinetic description through the alteration of relevant kinetic constants, or that it plays a minor role in signal transduction. However it is not at all clear if that is indeed the case, or if spatial factors may introduce important changes in information processing.

In this chapter, we dissect and examine the effects of space and localization in different

signal transduction cascades. Spatial control through localization/ compartmentalization is a recurrent theme in cellular biology, observed in many signalling pathways; additionally localization/ compartmentalization through the creation of micro-compartments is emerging as an experimental tool in synthetic biology (Chen and Silver, 2012; Hurtley, 2009; Kam et al., 2013; Shapiro et al., 2009). We systematically disentangle the interplay of localization, diffusion and the nature of the modification cascades, in a controlled in-silico setting. By employing fairly general models and representative scenarios, we aim to tease out the effects of space in signal transduction cascades. This is contrasted with ODE models of the cascades highlighting exactly when and how spatial factors may significantly affect and shape signal transduction.

## 5.2 Models and Methods

Our goal in this work is to dissect the effects of space in signal transduction through modification cascades. One of the most widespread ways in which spatial effects come into play in cells is through localization of entities and reactions/modifications. Thus we will largely focus on the effects of space and localization/ compartmentalization on the behaviour of modification cascades.

Modification cascades (i.e. sequences of modifications) can arise through different ways in cell signalling. One common way is when a modified substrate acts as an enzyme for a subsequent step. A second way is when a modified substrate acts as a substrate for a subsequent modification. Another distinct way in which sequences of modifications can occur is through phosphotransfer. The typical way in which these modification sequences is studied and understood is through ODEs. Stochastic descriptions are invoked to study the effects of small numbers of molecules. Usually however the effects of space are ignored. In this work we systematically dissect and examine the effects of space and spatial control on these modification sequences. This is done by constructing explicit spatial models of the localization and transport of species and comparing them with the default ODE models of these processes.

### 5.2.1 Model Setting

We employ multiple models, each describing different sequences of modifications, as mentioned above. The basic enzymatic reaction is described in a standard way by incorporating

enzyme binding to substrate (reversibly) to give rise to the complex which irreversibly gets converted to the modified substrate. For instance, a single covalent modification cycle mediating the conversion of a protein $X$ to its modified version $X^*$, involving the modifying enzyme K and the "demodifying" enzyme P is described by the following widely used model:

$$\begin{aligned}
\frac{\partial[X]}{\partial t} &= -k_1[X][K] + k_{-1}[XK] + k_4[X^*P] + D_X\frac{\partial^2 X}{\partial\theta^2} \\
\frac{\partial[X^*]}{\partial t} &= -k_3[X^*][P] + k_{-3}[X^*P] + k_2[XK] + D_{X^*}\frac{\partial^2 X^*}{\partial\theta^2} \\
\frac{\partial[K]}{\partial t} &= -k_1[X][K] + k_{-1}[XK] + k_2[XK] + D_K\frac{\partial^2 K}{\partial\theta^2} \\
\frac{\partial[P]}{\partial t} &= -k_3[X^*][P] + k_{-3}[X^*P] + k_4[X^*P] + D_P\frac{\partial^2 P}{\partial\theta^2} \\
\frac{\partial[XK]}{\partial t} &= k_1[X][K] - k_{-1}[XK] - k_2[XK] + D_{XK}\frac{\partial^2 XK}{\partial\theta^2} \\
\frac{\partial[X^*P]}{\partial t} &= k_3[X^*][P] - k_{-3}[X^*P] - k_4[X^*P] + D_{X^*P}\frac{\partial^2 X^*P}{\partial\theta^2}
\end{aligned} \tag{5.1}$$

where $k_1$ and $k_3$ are the forward rate constants for the binding of the enzymes and their substrate, $k_{-1}$ and $k_{-3}$ are the rate constants for the dissociation of the enzyme substrate complex and $k_2$ and $k_4$ are the rate constants for product formation. $\theta$ represents the spatial coordinate and $D_j$ is the diffusion coefficient for any species "j" in the cycle. K and P could represent kinases and phosphatases respectively. The above model includes the diffusion of multiple species. The species which are localized in a given region are regarded as non-diffusible. Thus the above model confined to a spatial subdomain of (or a "localized patch" in) the full domain would involve all species not diffusing (variants to the above model involving species diffusing but being prevented to exit the subdomain by imposing no-flux boundary conditions are also possible, but these distinctions are not needed here).

### 5.2.2 Enzymatic cascades

Our goal is to examine the effects of localization in sequences of chemical modifications. Thus when the modified substrate $X^*$ serves as an enzyme for a second modification cycle, the second modification cycle is described in an analogous way with $X^*$ playing the role of a kinase. $X^*$ mediates the conversion of $Y$ to $Y^*$, and the reverse conversion is mediated

by a phosphatase $P_2$. The equations for this modification are exactly analogous to those of the first step and are presented in the Appendix D. Having both modification cycles (and all relevant enzymes) in the same domain, and having all species non-diffusible would correspond to having a localized sequence of modifications in a single compartment. This essentially corresponds to an ODE description of the modification cascade. A schematic of such enzymatic cascades is shown in Fig. 5.1.

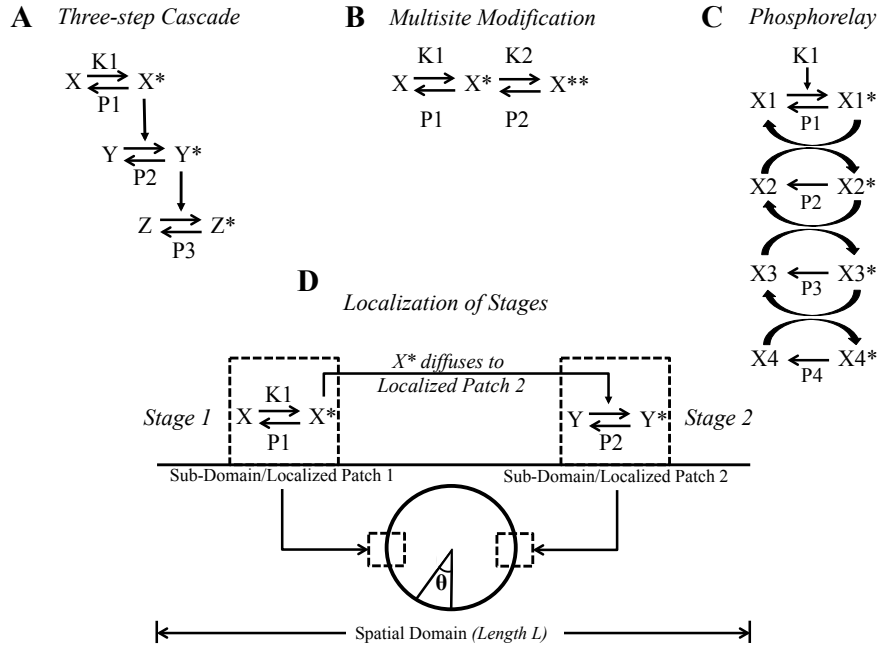


Figure 5.1: **Schematic of different kinds of cascades and their localization.** (A) Three step cascade- the modified substrate in the preceding step acts as the enzyme in the next step. (B) Multi-site modification- steps leading to the modification of a substrate at two sites is shown. The relevant enzymes (kinases/phosphatases) for different sites can either be different (as shown here) or the same. (C) Phosphorelay- shown here is a series of phosphotransfer reactions where the modified substrate transfers its phosphoryl group to the subsequent substrate species. Additionally, phosphatases that remove the phosphoryl group may also be present. (D) Shown here is a schematic of the spatial domain. The square pulses (dashed lines) represent the localized patches with corresponding reactions, $X^*$ is the communicating species and diffusing in the spatial domain.

### 5.2.3 Modification sequence with multiple enzymes

An alternative way in which a sequence of modifications occurs is when a modified substrate is modified by other enzymes subsequently. The modification status of a substrate is sometimes referred to as a molecular bar-code. If all enzymes and the relevant substrate

are present in the same location, assuming a specific ordering to the modification, a basic ODE model describes the modification of $X$ to $X^*$ mediated by the enzyme pair $K_1, P_1$ and the conversion of $X^*$ to $X^{**}$ mediated by the pair $K_2, P_2$. Each elementary modification cycle is described by unpacking the covalent modification cycle as described above. The combination of the description of the two modification cycles, provides the ODE model for the sequence of modifications (see Fig 5.1. for a schematic).

### 5.2.4 Phosphotransfer mechanism

Another basic mechanism of chemical information transmission is via a phosphotransfer. A two-step phosphorelay is considered. The substrate in the first step, $X_1$, is phosphorylated by an enzyme (K). The phosphorylated form, $X_1^*$, transfers its phosphate group to the substrate of the second step, $X_2$, producing $X_2^*$ resulting in $X_1^*$ converting back to $X_1$. A phosphatase P catalyzes the dephosphorylation of $X_2^*$ to $X_2$. Different variants of phosphotransfer models exist which vary depending on whether phosphatases exist for individual steps in the cascade (Knudsen et al., 2012). For specificity we consider a scenario where individual steps have phosphatases, and so $X_1^*$ can be dephosphorylated by a phosphatase $P_1$. Other variants of phosphotransfer models were also examined, and we comment on this subsequently. We also briefly discuss multistep phosphotransfer mechanisms in the Appendix D (see Fig. 5.1 for a schematic).

### 5.2.5 Spatial model

In order to systematically understand spatial and localization/ compartmentalization effects in steady state and dynamic signal processing in cascades, we examine spatial models of the above modification sequences. This is done as follows. The first reaction/modification (and relevant species) is localized in one patch/subdomain, and the second reaction/modification (and relevant species) is localized in a second patch (of equal size to the first). If none of the species diffuses, then the two patches are isolated and the sequence of modifications is broken. This is true for all the modification sequences considered. We examine the most natural spatial versions of the above models, by allowing the common agent of the multiple steps to diffuse in the spatial domain, reach the second region where the next step in the modification sequence is effected. Thus in the case of a two-step cascade $X^*$ diffuses and reaches the second location catalyzing the second reaction. In the case of

multiple enzymatic modifications, the modified substrate diffuses into the domain, reaching the location where the second pair of enzymes is localized. Likewise, we also consider a spatial version of the phosphotransfer model where $X_1^*$ diffuses and reaches the second domain and transfers a phosphate group to $X_2$ which is localized there. Fig 5.1. depicts a 2 step cascade with localization.

In this manner, we examine how localization/ compartmentalization can affect and control a modification cascade. The results are contrasted with ODE models of these modification cascades which corresponds to all steps localized in the same location.

It is worth pointing out that individual steps are localized in different locations and we have one species which diffuses to effect a communication between the two locations. Naturally it is possible to consider more complex scenarios where multiple species may be diffusing, and these can easily be analyzed by simply making other species diffuse in our modelling framework. For the purposes of this work, we restrict ourselves to the scenario above, as a description of the simplest non-trivial spatial perturbation of the modification sequence. We discuss some aspects of multiple species diffusing, in the Appendix D.

Since our primary focus is on basic aspects of spatial and localization control of modification cascades, we cast the model in a spatial domain in 1-D, and use periodic boundary conditions for simplicity (analogous results to the ones presented here have been obtained for no-flux boundary conditions). Note that the two patches are of equal size and are symmetrically located at diametrically opposite points on the circle. It is worth pointing out that for the scenarios considered here, the results are exactly equivalent to those with no-flux boundary conditions in a domain half the size. Thus all essential results are equally valid for both cases and could be relevant to situation involving modification and diffusion of species in the membrane or the cytosol.

### 5.2.6 Inputs

The modification sequences are initiated by the presence of enzymes for the first stage. These enzymes are assumed to be localized in the first domain and their concentration is varied as part of our analysis

### 5.2.7 Parameters

Describing the various modification sequences explicitly, involves a number of kinetic parameters, even in simple two step cascades. Naturally the parameters also affect the enzymatic regime and resulting information processing. Our approach regarding choice of parameters is dictated by the questions of interest. Since the main focus here is on the role of space, and our analysis will contrast the spatial and ODE models, we approach this as follows. We will choose a basal set of kinetic parameters (in both enzymatic mechanisms and phosphotransfer), which represents enzymatic modification in a "generic" parameter regime. We separately examine special parameter regimes such as the mass-action or ultrasensitive parameter regime to check that similar trends (where applicable) apply here as well. The remaining parameters are the diffusivity of relevant species and the relative sizes of the patch and the overall domain. Again, we choose representative basal parameter values for these parameters. We then directly study the effect of these parameters in our analysis. Since we contrast the PDE models with ODE models, we are able to directly assess the effects of these parameters. In some cases we are also able to assess the effects of specific parameters analytically, to explicitly reveal their influence. Parameter values are presented in Appendix D.

### 5.2.8 Numerical Method

The partial differential equations were discretized using finite difference equations and the results were checked by doubling the discretization. All simulations were performed in MATLAB using ode15s. In addition, we were able to compare the kinetic parts of our models in MATLAB with corresponding models in COPASI (which are automatically generated) for checking our computational models.

## 5.3 Results

We will systematically examine the effects of space, and in particular, localization/ compartmentalization in modification cascades. We will discuss our results by starting with enzymatic modification cascades, and subsequently discuss multisite enzymatic and phosphotransfer mechanisms, exploring some biologically motivated variations of each of these along the way. The computational results presented here are complemented by analytical

work, which is presented in (Alam-Nazki and Krishnan, 2014, *manuscript under revision*) and is reproduced in the Appendix D.

We begin by discussing a two step signalling cascade.

First, we examine the effect of localization of the two different steps of the cascade at different locations, contrasting this with the situation where all elements are localized in the same location (Fig. 5.2).

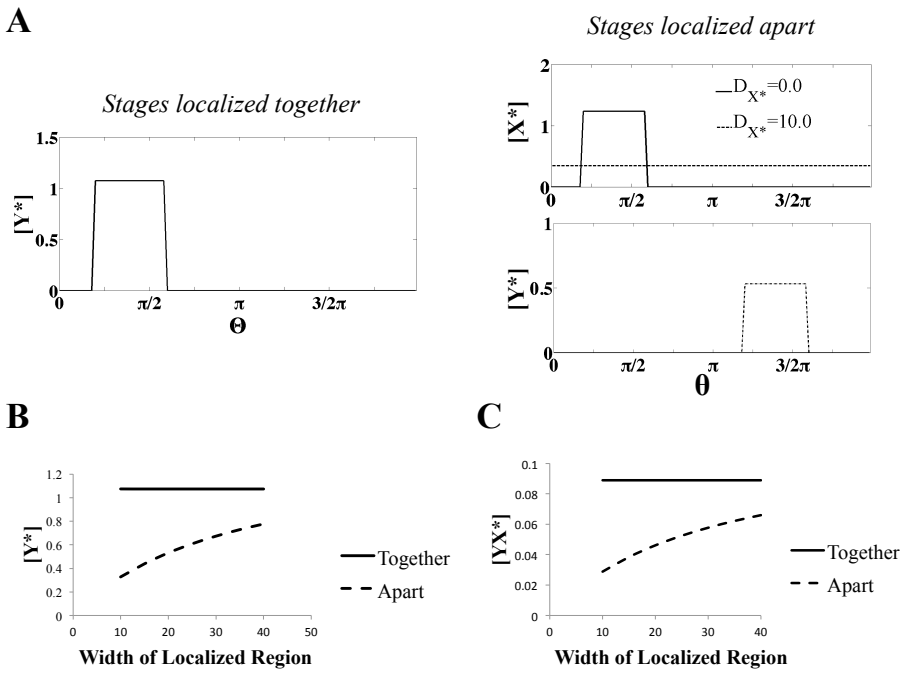


Figure 5.2: **Localization in the two step cascade.** Spatial concentration profiles of species when all localized together (solid line) and when separated (dashed line) are shown. (A) When X and Y are in different regions of the domain, the concentration of $Y^*$ is reduced as a result of separation of the steps of the cascade, while $X^*$ attains a uniform profile. (B) $[Y^*]$ is compared between the together (solid line) and apart (dashed line) cases for a range of widths of the localized patches in the domain. When apart, as the width of the localized region is increased, $[Y^*]$ increases, but is still less than $[Y^*]$ when all reactions are co-localized. (C) The concentration of the complex $[YX^*]$ in these two cases is shown. A reduction of $[YX^*]$ concentration when the steps are separated is seen, implying a reduction in retroactivity.

### 5.3.1 Less enzyme is available locally when the modifications occur in different locations

By contrasting the two situations, we find that the concentration of the final product is less when the modifications occur in different locations. This is understood by noting that

that when the modification steps are separated, the modified species at the first step $X^*$ must diffuse in order to complete the second modification- as a result its concentration is spread over the domain- leading to a "dilution effect." The concentration of $X^*$ available to the second step will be less compared to the scenario where all modifications occur in the same region. This result remains the same even when the width of the localized regions is increased. Although the total concentration available when the width increases is higher, the concentration of the final product will always be lower for the scenario where the modifications are apart (Fig. 5.2). Furthermore, if the domain size is increased (for a fixed width of localized patches), the concentration of the final product will further decrease, as the concentration of $X^*$ will be spread over a longer domain effectively lowering the concentration available locally to the second step, thus accentuating the dilution effect.

A second related point worth mentioning in this context is related to the dilution effect. We find that when the components of the cascade are separated, the retroactivity is weakened. This is seen by examining the effect of the total concentration of species in the second layer of the cascade, on variables in the first layer of the cascade. We find that the retroactivity effect is significantly weakened when compared to the scenario when all species are together (Fig 5.2). This can be understood by noting the dilution effect significantly reduces the amount of $X^*$ in the second domain, and hence also reduces the amount of $X^*$ sequestered in the second step of the cascade. The above aspects are further analyzed in (Alam-Nazki and Krishnan, 2014, *manuscript under revision*) and reproduced in the Appendix D.

## The dilution effect can be mitigated under different conditions

It is clear that if a pool of a species is initially localized and one of the species (say a modified form of this species) diffuses in the entire domain, then the local concentration of this species will be reduced. However, this dilution effect can be reduced under certain conditions. One obvious way to do this is to increase the width of the first domain. A second way is maintaining conditions where $X^*$ is low. This can be achieved, for instance, by having a high amount of phosphatase in the first domain. The reason why this reduces the dilution effect is as follows. It is clear that at steady state $X^*$ attains a uniform profile. This is seen by adding all the equations for the species in the first cycle. The kinetic terms cancel out leaving the diffusion term for $X^*$, and so at steady state $X^*$ is spatially uniform. If conditions are such that $X^*$ is low, then this means that the amount of species $X^*$ which

has leaked out of the first compartment is small. The leaking out of $X^*$ results in a modified total X in the first domain. Now if there is negligible retroactivity, the steady states of all X species can be determined from the steady state enzyme kinetics in the first step of the cascade, along with the modified total X, accounting for the leakage. We therefore see that when the total X in domain 1 is modified to a small degree, then the steady state of all X species (including $X^*$) is in fact close to the situation where no $X^*$ exits. Therefore the dilution effect on $X^*$ is negligible, both in absolute and relative terms. Table D.1 in the Appendix D shows how increasing the phosphatase concentration in domain 1 results in attenuation of the dilution effect.

### 5.3.2 Spatial effects on a Goldbeter Koshland type switch

If we examine a two step cascade, where the first step is in the ultrasensitive parameter regime (Goldbeter and Koshland, 1981) and (for simplicity) the second step operates in the mass action kinetic regime, we find that when all components are in the same location, the output of the cascade $Y^*$ exhibits a switch-like response to the input, as expected. Now if the second layer of the cascade is separated, then this switch like effect is typically severely attenuated (Fig. D.2.). This is because the enzymatic cascade at the first layer is now an open system, and the leaking out of $X^*$ and dilution effects works against switch like behaviour, in effect making more phosphatase available. It is then of interest to see under what conditions a switch like behaviour is maintained even when the steps in the cascade are separated. One way in which this can happen is to ensure that the diffusing species is not directly involved in producing the switch. Thus if we have an intermediate layer with species $I$ which is modified to $I^*$ by $X^*$ and $I^*$ diffuses to the new domain, then the switch like effect can indeed be seen. In fact if a high amount of $I$ is maintained, then the switch like characteristic is preserved without much attenuation. This illustrates an aspect relevant to the propagation of switch-like effects in spatially separated enzymatic cascades: keeping the factors responsible for a switch localized (negligible leaking out), and propagating the effect via downstream pathways close to mass-action kinetics works to maintain the integrity of the switch.

### 5.3.3 Analysis of three step cascades

Having analyzed two step cascades, we examine some aspects of three step cascades from the perspective of spatial control. As a starting point, we will use a model of the MAPK cascade developed by Huang and Ferrell (1996): this describes the three tier modification cascade of MAPK signalling. It is worth pointing out that some aspects of the MAPK signalling are not included here, including the distributive multisite modification at each stage. From the perspective of our study, we examine this three step cascade as an example of switch-like behaviour generation, and aim to elucidate aspects of spatial control therein. We use the model of Huang and Ferrell, also studied elsewhere (Ventura et al., 2008). These studies show that it is possible for such a cascade to exhibit switch-like behaviour. We describe each modification step in the standard way (with explicit description of complexes) and our reference model employs parameters used in (Ventura et al., 2008). The basal scenario corresponds to all species localized in the same domain, and this is described by the ODE models employed. We now discuss the effects of spatial localization in this cascade.

#### Input-Output Relationships are distorted differently with different spatial partitioning of the cascade.

The three tier cascade has three modifications occurring in a series of consecutive steps. It is immediately obvious that with different locations to localize three modifications- a number of combinations or spatial "designs" are possible for the cascade. For example the first modification, that of X to $X^*$, may occur in one location and those of Y and Z to $Y^*$ and $Z^*$, respectively, could occur in another location. Another possibility may be that X and Y are modified in one location and Z in another. In the former case $X^*$ would have to diffuse to catalyze the modification of Y and in the latter $Y^*$ would have to diffuse to the second location to complete the modification cascade. Fig.5.3 shows four different spatial designs and are denoted I, II, III and IV. With an increased possibility of spatial designs, a cell may have more room to exert spatial control over the interactions and hence achieve a variety of distinct responses. The steady state input-output relationships for spatial designs I-IV in Fig. 5.3 are examined. This comparison was made for two different sizes of the overall domain. When the modifications occur in one place, for both domain sizes, (and when none of the species diffuse) the input-output relationship at steady state is sigmoidal.

**A**

| Spatial Design | Position in Spatial Domain: Localized Patch | | |
|---|---|---|---|
| | X | Y | Z |
| I | 1 | 1 | 1 |
| II | 1 | 1 | 2 |
| III | 1 | 2 | 2 |
| IV | 1 | 2 | 1 |

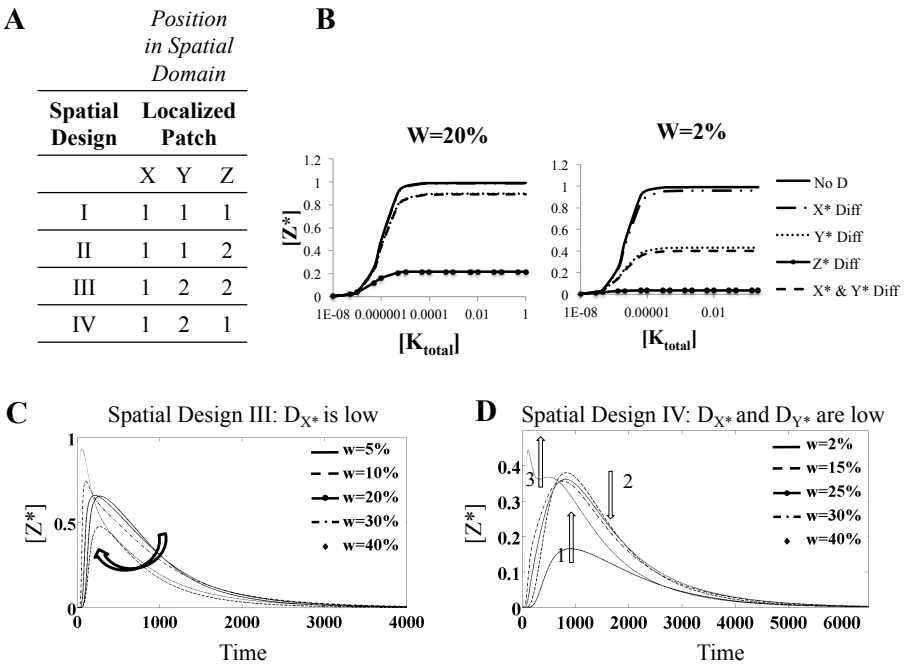


Figure 5.3: **Three step cascade.** (A) Four examples of 'spatial' designs are shown. Each design consists of a distinct combination of where each modification step is localized- I) when X, Y and Z are modified in localization patch 1, II) modification of X and Y in localization patch 1 and of Z in localization patch 2, III) modification of X in localization patch 1 and of Y and Z in localization patch 2 IV) modification of X and Z in localization patch 1 and of Y in localized patch 2. (B) Two sets of steady state Input -Output curves for the cascade are shown: one when the width of the localized patch is 1/5th of the domain size (left) and the other when the width is 1/50th of the domain size (right). In both plots, the case where all modifications are co-localized ("No D" case; solid line) corresponds to spatial design I. The cases when species in the cascade are diffusing corresponds to spatial designs III ($X^*$ diffuses, dashed-dotted line), II ($Y^*$ diffuses; dots or both $X^*$ and $Y^*$; dashed line), I ($Z^*$ diffuses; solid line with circles). These plots show that when patch size is smaller (RHS), the diffusion of $Y^*$ (dots) (and both $X^*$ and $Y^*$ (dashed line)) has a significant effect on the input-output curve- the sensitivity of the response to the input decreases. In the LHS plot, the curve for $X^*$ diffusing is practically indistinguishable from the non-diffusing case, and the curves for $Y^*$ diffusing and $X^*$ and $Y^*$ diffusing are practically indistinguishable. For both domain sizes when $X^*$ diffuses (dashed-dotted line), the input-output curve largely maintains its characteristics. (C, D) Transient signal input to a 3 step cascade: (C) Spatial design III and (D) Spatial Design IV. The duration of the pulse is kept constant and diffusion coefficient of the communicating species: $X^*$ (in case of design III) or both $X^*$ and $Y^*$ (in case of design IV) are fixed. The spatial width of the patches is varied. (C) As the width increases, a non-monotonic response is seen for design III, the amplitude of $Z^*$ initially decreases and then increases. (D) For design IV, a non-monotonic response similar to design III is seen- the amplitude of $Z^*$ increases, decreases and then again increases. The arrows indicate the direction of increasing patch width.

Now if the modifications are separated, then diffusion of the communicating species was considered (the communicating species in each design can be inferred from Fig. 5.3(A)). Each spatial design had different effects on the sensitivity of the input-output relationship. Furthermore, different patch sizes distorted the sigmoidal curve to different degrees.

For the case of larger size of patches, when $X^*$ or $Y^*$ is the communicating species, the input-output relationship is largely maintained and still appears sigmoidal. The input-output relationship is distorted significantly when the patch size is smaller and if $Y^*$ is the communicating species the curve becomes much less sigmoidal. However, if $X^*$ is the communicating species, the input-output curve is less distorted and still sigmoidal. For both cases, when $Z^*$ only diffuses (corresponding to a localized cascade with downstream species leaking out), the relationship becomes significantly less sigmoidal (Fig. 5.3). This shows how the localization of species at different spatial locations can have both subtle and strong effects on the cascade behaviour. It also demonstrates that it is possible to design a spatially separated cascade which may be able to largely retain the basic input output characteristics. The fact that having X localized in one location and $X^*$ being the communicating species leads to a small distortion of the switch can be understood from our analysis of 2-step cascades. In this cascade, the concentration of $X^*$ is typically low (this is true in the ODEs as well). Having it diffuse in the medium actually leads to negligible dilution and distortion of steady state characteristics.

### 5.3.4 Varied responses are obtained with transient inputs

We examine the behaviour of different spatial designs of cascades to transient inputs. We focus, in particular on the concentration profile of $Z^*$ for different diffusion coefficients of the diffusing species. We subject the module to a square pulse input.

#### The effect of diffusion coefficient of communicating species for fixed duration of the pulse:

When $X^*$ is the diffusing species, the steady state of the module when subject to a step input is very close to that when all species are localized together. We therefore examine transient aspects of signal transduction in this situation, with a square pulse as input, focussing on the effect of diffusivity of $X^*$. As the value of the diffusion coefficient increases, the transient peak concentration attained is higher and the time taken to reach steady state also decreases. There is less difference between the transient peak concentrations for intermediate and high diffusion coefficient values. For example, for width of each patch being about 1/5th of the domain, peak concentrations of $Z^*$ for both intermediate, and high diffusion coefficients are very close to one another. However the difference between peak concentrations for

low and intermediate diffusion coefficients is appreciable. This indicates how key transient characteristics of the module output may be shaped by the diffusivity of the communicating species.

### The effect of the duration of the pulse

As the duration of the pulse is increased, the transient peak concentration also increases. As before, at higher diffusion coefficients the variation in the peak concentration is smaller than when the diffusion coefficient values are low.

### The effect of the size of the patches for fixed pulse duration and diffusion coefficient of communicating species

Here we examine the effect of variation of the size of the patches. Note that patch size has no effect when all elements are localized in the same location. As the spatial width of the patches is increased, the transient peak concentration of $Z^*$ increases and the time taken to reach steady state decreases. Non-monotonic behaviour is observed in the spatial designs III and IV . In spatial design III only, when the diffusion coefficient is low, as the width increases, transient peak concentration of $Z^*$ first decreases and then increases and the time taken to reach steady state first increases and then decreases (Fig. 5.3). In spatial design IV, the transient peak concentration of $Z^*$ first increases, decreases and then increases again (Fig. 5.3). This shows how the interplay between transient inputs, domain size, the diffusion of communicating species and its location in the cascade can be subtle.

It is worth pointing out that while we have considered the effect of different species localized in different domains, with a communicating species, one can also study a scenario where all species are localized in the same domain, but one species leaks out of the domain. This leaking out has an effect on both steady state and transient responses (e.g. the case of $Z^*$ diffusing shown in Fig 5.3), but this is not discussed further here.

## 5.3.5 Multisite Modification

In this module, unlike the cascade module, the product of the first step acts as the substrate for the next modification step. The modifications may occur in the same location or in different locations. In the latter scenario, the product, $X^*$, has to diffuse to the second

location, where the enzymes that catalyze the second modification are present, to complete the circuit of modifications (to become $X^{**}$). Having multiple modifications (similar to the cascade module) also increases the number of spatial designs for the modification locations. The focus of this analysis is the two site modification module.

First, the concentration of the final modified product ($X^{**}$) when the modifications are together was compared to when they were apart or in different locations. The enzymes for the first modification are K1 and P1 and the second modification are K2 and P2. When the modifications occur in one place, the localized concentration of $X^{**}$ is greater than when the modifications are apart. Similar to the two step module, the dilution effect of the diffusing species $X^*$ plays a role. The local concentration of $X^*$, when it diffuses, is lower everywhere in the spatial domain and hence less is available for its conversion to $X^{**}$. If the width of the localized region of species is increased, the concentration of $X^{**}$ also increases; however it is still lower than when compared to when the modifications are together (Fig. 5.4). In the above situation if we examine the spatial average concentration of the intermediate phosphoform $X^*$, we find that when the modification occurs in two different locations, the average concentration of this phosphoform is higher than in the scenario where all modifications are together (Fig. 5.4). In fact the average yield of $X^*$ increases with spatial separation (this is discussed in (Alam-Nazki and Krishnan, 2014, *manuscript under revision*) and reproduced in the Appendix D).

We now consider two variants of the above scenario. In the first, we have both modifications occurring in the same compartment, but $X^{**}$ diffuses (leaks) out of the patch. Again here, similar to the situation above, a higher average conversion rate to $X^{**}$ can be obtained if it is allowed to leak out of the localized compartment because less of it is accessible to its phosphatase. Thus this shows that diffusion does not necessarily decrease the mean yield of the product, but is context dependent.

The second scenario corresponds to one where the first and second modification steps were catalyzed by two kinases K1 and K2, respectively and the reverse reactions of both steps were catalyzed by a single phosphatase P1. When the modifications are in separate locations, the steady state concentration of $X^{**}$ (and $X^*$) is zero. This is due to the presence of the shared enzyme P1. P1 converts $X^{**}$ to $X^*$ and $X^*$ to X and thus a localized concentration of X is present in the second location as well (Fig. 5.4). However when the modifications are together, the modifying enzymes K1 and K2 are present together with P1 to compensate for the reverse reaction. Thus non-zero steady states are observed for $X^*$ and $X^{**}$. The modifications being apart poses a locational constraint for obtaining a non-

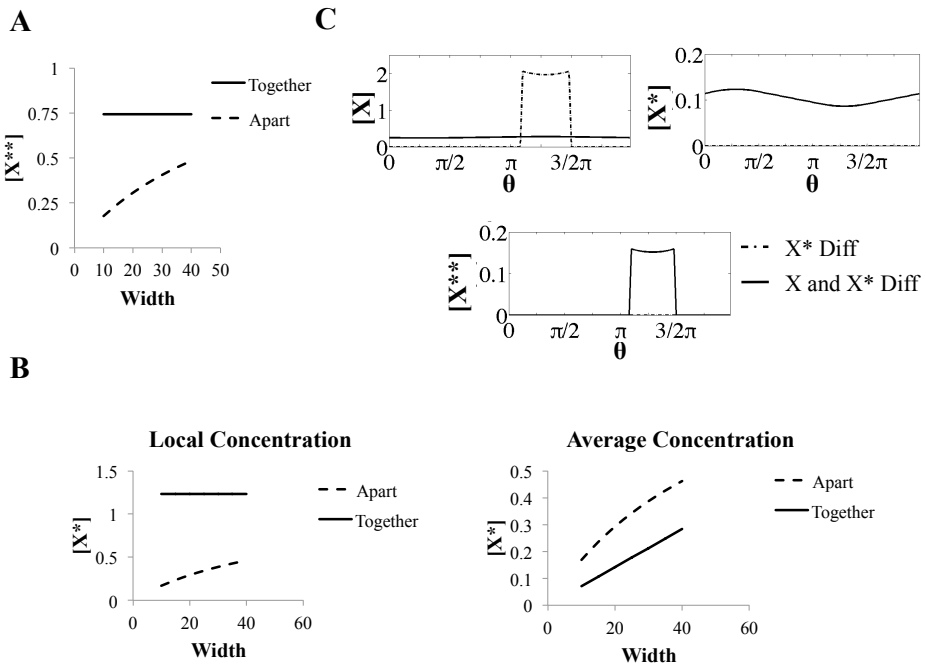


Figure 5.4: **Multisite modification.** In (A) and (B), the kinases and phosphatase pairs are different for both modification steps (K1, P1 and K2, P2). (A) [$X^{**}$] is plotted against the width of the localized patch (expressed as a fraction of total domain length): [$X^{**}$] is always higher when the modifications occur in the same location. The $X^{**}$ concentration increases with the width of the patch. (B) The average and local concentrations of $X^*$ are compared in these cases. The average concentration of $X^*$ is greater when modifications are in different locations. (C) When the kinases for both modification steps are different but the phosphatases are shared (and the modifications take place in separate compartments), at steady state the concentration of $X^{**}$ will be zero if $X^*$ is the only communicating species (dashed dotted line). A way to overcome this locational constraint is by having both X and $X^*$ diffuse in the domain (solid line).

zero steady state response at the second location in this case. Alternatively it may also be a capability for the module- a way to achieve a purely transient/adaptive response (a transient increase in $X^{**}$ in the second location before it falls back down to zero). If viewed as a constraint, a way in which this constraint could be bypassed is by having both X and $X^*$ diffuse (Fig. 5.4). This ensures that a continuous cycling of $X$ and $X^*$ between the two patches occurs, resulting in non-zero concentrations of $X^{**}$ at the second location.

Incidentally, in this context, it is worth pointing out that even in a single step modification cycle, if the kinase is present where the substrate is located, and a modified form of the substrate diffuses to a second location where the phosphatase is present, then this will necessarily result in a purely transient increase in the concentration of modified species at the second location before decreasing to zero. This is in contrast to having substrate and both enzymes co-localized in one location.

A couple of related aspects of spatial control of multisite modification are worth mentioning. In the above we have assumed a specific order for multisite modification. If we now examine a random multisite modification mechanism (i.e. either modification can occur first), then we notice immediately that the spatial separation of kinase phosphatase pairs automatically imposes an order for modification, if the unmodified substrate is initially present in one of the compartments. Thus in the case above, multisite modification via a random mechanism would still proceed in a specific order. If the substrate modified by the second kinase remains localized in the second compartment, this order is maintained and reflected in both transient and steady state behaviour.

### 5.3.6 Phosphorelay Model

In the phosphorelay model, an enzyme catalyzes the first phosphorylation step. The product of the first step transfers its phosphoryl group to the substrate of the second step and so on. A typical phosphorelay has four steps. The product of each step before the last, loses its phosphoryl group to the next step. Phosphatases may also be present at every stage. The product of the last step is typically dephosphorylated by a phosphatase. First a simpler variant of the relay- a two-step relay, is considered and then a four step relay is also briefly analyzed.

To begin with, the concentration of the final product of the two step relay, $X2^*$, is compared in the scenario when the relay occurs in one location to when the transfer of the phosphoryl group occurs in a different location. A similar result to the shared phosphatase case in the multisite phosphorylation module is seen here. When the transfer of the group occurs in a different place, $X1^*$ (product of the first step) diffuses to a different location and transfers its P group to $X2$ (getting converted back to $X1$). The phosphatase at that location dephosphorylates $X2^*$ back to $X2$; at steady state both $X1^*$ and $X2^*$ attain a steady state value of zero at the second location. Both X1 and X2 are present at steady state at the second location. This is because, $X1^*$ is diffusing out of the first location and essentially being converted back to $X1$ at the second location. Thus it is eventually entirely leaves its original location and since it is converted back to X1 at the first location, $X1^*$ reaches a zero steady state and the relay stalls (Fig. 5.5).

Here again a locational constraint is present- when the transfer occurs in one place $X2^*$ attains a non-zero steady state. However when it takes place in different locations then the concentration of $X2^*$ only transiently increases at the second location. This holds true for

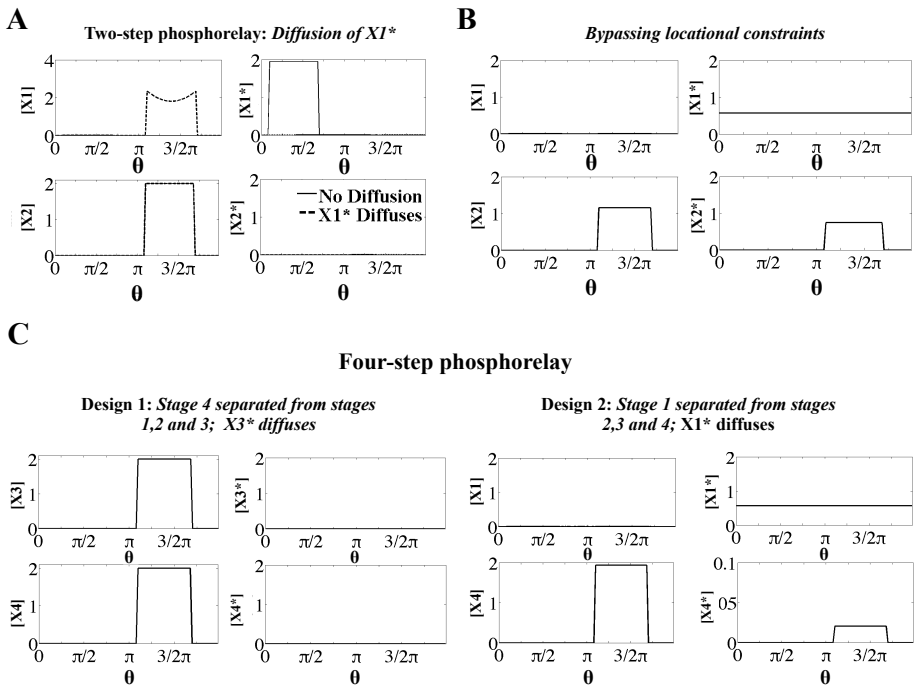


Figure 5.5: **Phosphorelay.** A 2-step phosphorelay is considered in (A) and (B). (A) When the relay steps occur in separate locations (dashed line), [X2$^*$] only transiently increases; its steady state concentration is zero. (B) A possible way to sustain a non-zero level of X2$^*$ and bypass this locational constraint is by having a uniform input signal/input at both locations. Shown is the case of uniform input signal.(C) A case where the phosphorelay has four steps and the input kinase is a bifunctional enzyme that acts as the kinase (in the first step) and phosphatase (for the last step) as well is shown. Two spatial designs are shown: X1, X2, X3: domain 1 and X4 domain 2 (LHS Design 1). X3$^*$ is the communicating/diffusing species and [X4*] is zero at steady state. In the second design (RHS Design 2), X1 is in domain 1 and X2, X3 and X4 in domain 2. Here, X1$^*$ is the diffusing species and the steady state of X4* is non-zero. This is because the bifunctional enzyme is present in both locations and will ensure that an equilibrium between X1$^*$ and X1 exists at the second location preventing the relay from stalling.

a three and a four step relay as well. There are two ways to bypass this constraint, first by removing the phosphatase of the second step and second by having X1 diffuse (in addition to $X1^*$): this ensures a continuous cycling of $X1$ and $X1^*$ between the locations. A third possibility is having the input signal itself be present everywhere in the spatial domain, or at least at the second location also (Fig 5.5): this is able to convert $X1$ to $X1^*$ in the second domain.

An interesting variation of the above result occurs when the input enzyme of the phosphorelay is also the phosphatase of the last step. Such scenarios have been observed in nature (Chen et al., 2009). If we consider a 4-step relay and examine, for instance, the situation where $X3^*$ diffuses from the first compartment to the second, we find exactly as

before that $X4^*$ at steady state is zero. The one point of difference with a two step cascade here is that for a two step cascade with a bifunctional kinase of this kind, the output $X2^*$ can be non zero because the bifunctional enzyme at the second location can activate the relay mechanism at the second location. However in the case of a 4 step relay, depending on the position of the communicating species in the phosphorelay cascade, this may or may not be possible. In particular, if the communicating species is either $X2^*$ or $X3^*$, then the presence of a bifunctional enzyme at the second location, cannot be used for the purposes of activation. This can however happen if the communicating species is $X1^*$ (see Fig 5.5). This again reveals another facet of the interplay between localization, modification cascades and their mechanisms.

### 5.3.7 Open Cascades

All the examples considered about involved fixed total amounts of substrates in the spatial domain, whether or not species entered or exited compartments. As a final example, we consider a modification sequence which involves a steady supply of substrate which enters and leaves the domain. We examine the irreversible conversion of $X_1$ to $X_2$ to $X_3$ with "inflow" of $X_1$ and "outflow" of $X_3$. Such modification sequences have been studied via ordinary differential equations. In particular if a signal causes the conversion of either $X_1$ or $X_2$, the output of the system $X_3$ at steady state is independent of the signal, and this is thus an example of adaptation. This happens irrespective of the position in the cascade where the signal acts. We revisit this situation with an explicit spatial model. We first consider the case where the signal modifies $X_2$ to $X_3$ (in the second location).We consider the situation that $X_1$ is in one compartment and $X_3$ in the other. $X_2$ which is produced in one compartment diffuses to the other, causing a modification to $X_3$ (Fig D.4). An analysis of this scenario shows that in this case $X_3$ does not exhibit (exact) adaptive behaviour locally in the second compartment. In fact $X_3$ exhibits spatial variation in the second compartment whose amplitude is dependent on the signal and the diffusion coefficient of $X_2$. A simple analysis shown in (Alam-Nazki and Krishnan, 2014, *manuscript under revision*) (reproduced in Appendix D) shows however that the spatial average of $X_3$ is in fact independent of the signal. This example shows how localization and spatial separation can change (local)adaptive behaviour into non-adaptive behaviour, even though adaptation of the average amount of $X_3$ occurs. It is worth pointing out that if the diffusion coefficient of $X_2$ becomes high then this effect is reduced. The diffusion coefficient also affects transient

signalling characteristics. On the other hand, when the signal acts to convert $X1$ to $X2$ (in compartment 1), we find that the steady state $X3$ reaches a steady state independent of the signal value, irrespective of the diffusivity of $X2$, demonstrating that such a spatially distributed open cascade can in fact adapt to signals at certain positions in the cascade.

## 5.4 Conclusion

Information processing in cells occurs largely through chemical means, and involves the movement of molecules to appropriate locations for this purpose (Brown and Kholodenko, 1999; Hurtley, 2009; Kholodenko, 2006; Marks et al., 2009; Vartak and Bastiaens, 2010). Nevertheless, the default method of understanding information processing in cellular systems is through ordinary differential equations, with additional studies in a few cases, aimed at elucidating the role of stochasticity. The effect of spatial factors in information processing has not been investigated in depth, even though it is clear that spatial control is an important aspect of cellular information processing networks.

One of the most common ways in which spatial control mechanisms function in cells is through localization and compartmentalization of components (Cyert, 2001; Laloux and Jacobs-Wagner, 2014; Rudner et al., 2002; Shapiro et al., 2009). There are multiple biological examples of this, including in MAPK signalling and Fox-O signalling, where certain entities in the cascade translocate to a new location (e.g. nucleus) to complete the cascade (Cyert, 2001; Eijkelenboom and Burgering, 2013; Kondoh et al., 2005). In general, the phosphorylation/modification status of a protein is a natural chemical mechanism to control its transport, especially out of/into compartments, and there are multiple examples of this both in single site and multi-site phosphorylation (Blenis and Resh, 1993; Walsh, 2006). In this chapter, we focussed on understanding the effect of localization/ compartmentalization on modification cascades in cells. We examined different scenarios of modification cascades: one in which the modified form at one stage acts as the enzyme for the next, another where the modified form acts as a substrate in the next stage, and the third was a phosphotransfer mechanism. All these mechanisms have been studied and analyzed through ODEs. We aimed to tease out the effects of spatial localization and spatial control in these modification cascades. This led us to analyze explicit spatial models of these cascades, where different species are localized in different locations. This controlled setting allowed us to dissect the role of spatial localization in these cascades. Analyzing these different modification cascades together provides a global view of the effect of spatial control on different

kinds of modification cascades, revealing similarities and essential differences.

Our analysis of enzymatic cascades reveals that localization of different steps at different spatial locations itself introduces new effects, when contrasted with the situation where all steps are localized in the same location (a scenario which corresponds to the ODE description). Firstly we find that the movement of the communicating species in the medium can result in a significant dilution effect, and hence result in a strongly attenuated response. Secondly, we find that by tuning kinetic parameters or phosphatase concentrations in the cascade it is possible to buffer against this dilution effect to a large extent. Thirdly, we find that localization and separation of steps in a cascade can reduce retroactivity. It is likely that this may be a basic mechanism by which retroactivity is reduced/suppressed in multiple cellular contexts. Incidentally, it is worth pointing out that these effects are revealed by an explicit spatial model, and that some of these effects may not be seen in compartmental models. By examining three step cascades, we find that spatial separation can strongly reduce switch like behaviour resulting from cascades, also in agreement with Takahashi et al. (2010). We find here, however that depending on the location in the cascade where the spatial separation happens, it is possible that the switch like characteristic is largely preserved, pointing to the subtle interplay between modification cascades and spatial localization. On the other hand, we find that in cases where modification steps where the switch like behaviour largely occurs in one step through a Goldbeter-Koshland mechanism, the localization of species involved in this stage is necessary for maintaining a switch.

Our analysis of multisite modification mechanisms reveals that spatial separation can significantly alter information processing through such mechanisms, and that they may not be adequately described by ODEs. In fact we find that through compartmentalization, a random enzymatic modification mechanism (with multiple enzymes) can be converted into an ordered mechanism. Additionally, spatially averaging the results across the domain (in effect done when measurements are taken at the cellular level), masks and distorts important aspects of the actual behaviour of the multisite modification. It is worth pointing out that if different modifications share a common phosphatase, then the spatially separated modification scheme results in the reversal of all modified forms at steady state, completely in contrast to the ODE models. This can be traced to the fact that at the "downstream" location the phosphatase is able to reverse both the full as well as partial phosphorylated form. This separated scheme thus results in a single shot adaptive mechanism for the phosphoforms. It is worth pointing out that in a single step covalent modification scheme, a separated phosphatase at a downstream location also leads to such a behaviour. This again

is due to the fact that at the downstream location, there is no kinase enzyme which can directly compete with the phosphatase. In such cases, an additional cellular mechanism is then needed to synthesize/transfer relevant substrate to the original location to replenish it. Phosphotransfer mechanisms again reveal echoes of the same behaviour, if different steps of the chain are separated. Interestingly, a phosphorelay cascade with the phosphatase of the last step acting as a bifunctional kinase (a design observed in nature) can allow the phosphorelay to function (in certain cases) even with compartmentalization, relieving the above constraint.

Space, and in particular, spatial localization/ compartmentalization is a basic recurrent theme in cellular systems. Its importance has been acknowledged in the biological literature, and yet the consequences of localization have not been examined systematically across different kinds of cascades. Spatial localization and its control of signal transduction is therefore relevant from multiple viewpoints: as a basic ingredient in the evolution of information processing networks, as a source of complexity in elucidating information processing and decision making in cells, and as a new mode of control for synthetic biology. We discuss the consequences of our results in relation to these themes.

The evolution of biological networks has resulted in a marked increase in complexity of signal transduction pathways as one progresses from bacteria to eukaryotes. The complexity is due to an increased number of components, new modes of interaction, increased feedback regulation and new entities which are parts of the signal transduction pathways. Even though localization is present in bacteria as well, it is clear that there are many additional ways of compartmentalization and localization in eukaryotes, with the increased number of compartments possible. This indicates that with all the additional complexity of signal transduction components in eukaryotes, spatial localization may provide important capabilities for realizing different modes of information processing, while also bypassing existing constraints. Of course, depending on the context, localization may itself provide important constraints in information processing.

At the outset, it is not easy to guess the "rules" by which evolution works: the general belief is that evolution works by tinkering with existing networks and circuits, refining, adding and perhaps deleting elements. Naturally with a substantially increased number of components and possibility of interactions, the complexity of a signal transduction network greatly increases, also increasing the possibility of undesirable interactions. One basic capability which is provided by localization of components in different places is the insulation of parts of a pathway from the other, minimizing extraneous interactions and un-

wanted crosstalk. Thus even for a desired mode of information processing (e.g. a switch) the spatially distributed solution may provide a new more robust alternative. For such a spatially distributed design, our analysis provides insights into how a spatially distributed cascade (with the same kinetic properties) may be organized or "optimally" partitioned to give rise to a switch. Correspondingly, if the spatially distributed nature of a pathway is given, it may be possible to make local kinetic refinements and arrive at a robust switch-like behaviour of the cascade which works around the spatial constraints. In addition, as we have discussed, it is possible to use localization as a mechanism to generate new modes of signal transduction as well, without extraneous kinetic interactions. It is then possible to employ additional refinements to such mechanisms to generate new, more robust circuits exhibiting this behaviour.

A default method for studying information processing in signalling pathways is through ODEs. ODEs make an assumption about well mixed systems, with sufficient numbers of molecules, so as to justify the kinetic descriptions. Even in some cases where these assumptions may not strictly be met, the ODE description may provide an adequate initial description of the system, essentially because the ODE encodes a form of causal interaction which is the dominant factor in the information processing. The ODEs may be modelled and the results compared with data which implicitly makes similar assumptions. Similarly tools of reverse engineering of networks also make similar assumptions. While a widespread, and generally sensible approach is to develop a model (and employ an appropriate framework) based on the available data, it is also important to examine the actual combination of factors which give rise to the relevant behaviour. As our study indicates, spatial localization results in both modulatory and drastic changes in signal transduction characteristics. While in some cases, spatial distribution may be essentially subsumed within a kinetic description, in other cases as we have seen, this is simply not the case. Modelling such processes with ODEs may then involve invoking additional pathways/feedback effects which may simply be incorrect. Likewise, making measurements using spatial averages (as is done by lysing cells) may simply distort the actual picture.

These aspects come to the fore especially in the presence of strongly nonlinearity, which is, of course, a basic and widespread element in signalling pathways. Likewise other tools for analyzing circuits, including robustness of circuits, usually employ ODE models. It is very possible that spatial localization and compartmentalization may in fact be a key aspect relevant to the robustness of the circuit. It is also interesting to note that one of the recurrent themes in signal transduction has been the effects of sequestration (Buchler and Louis,

2008; Del Vecchio et al., 2008; Feliu and Wiuf, 2012; Seaton and Krishnan, 2011) and how this can result in monostable switches (through molecular titration), retroactivity and even bistability (through enzyme sharing for instance). When we examine spatially distributed signalling pathways, we find that some of these effects may in fact be reduced simply due to the spatial compartmentalization and separation, which results in open systems. On the other hand, it may also happen that spatial separation can actually work to accentuate some of this behaviour. For instance, spatial separation and the dilution effect discussed above can result in altering the availability of enzymes in one compartment allowing for a regime of bistability, if this is an intrinsic capability of the enzymatic mechanism (as in multisite phosphorylation on multiple sites by a single kinase/phosphatase pair).

Another tool being used to understand different aspects of cellular decision making is information theory (Shannon, 1948). Information theory itself relies on some basic abstractions and assumptions, describing the communication process in unidirectional terms, incorporating information encoding, transmission and decoding. The spatially localized and separate steps we have studied in some respects comes close to the scenario depicted by such a picture. Our studies demonstrate that specific physiochemical aspects such as the nature of the chemical modification, the spatial location of auxilliary chemical entities and the size of the domain play a vital role in how chemical information is actually transmitted and processed.

The spatial regulation of information is also directly relevant to spatial control of pathways through synthetic and other means. Indeed, in the recent past, experimental approaches in synthetic biology have employed scaffolds to manipulate and shape signal transduction (Good et al., 2011). More recently, the development of microcompartments is another step in this direction (Agapakis et al., 2012; Chen and Silver, 2012; Peters et al., 2014; Sachdeva et al., 2014). The development of a theoretical framework allows for a systematic exploration of capabilities and constraints associated with the spatial manipulation of information processing, using the building blocks available to cells along with additional engineered components. It also brings to light hidden tradeoffs involved in this process, and could suggest ways to design synthetic circuits which are engineered with an explicit spatial organization. Overall, in combination with new and emerging experimental capabilities, it provides a systematic platform for employing tools which harness or manipulate spatial aspects to shape signal transduction and pathway behaviour in general. Finally, this is also relevant in related emerging areas such as molecular communication and chemical information processing/computing (Katz, 2012; Nakano et al., 2013), each of which

deals with the transmission of information, through molecular transport and interaction.

# Chapter 6

# From building blocks to elucidating signal transduction in signalling networks in *Caulobacter crescentus*

## 6.1 Introduction

Organisms are products of evolution and signatures of evolution may be seen when the subcellular organization of cells is examined. The sophistication of the inner spatial architecture increases as one moves from studying bacterial systems to observing eukaryotes. At the same time, there are common spatial features or mechanisms present in both types of systems- an example is the spatial compartmentalization/localization of signalling entities (reviewed in (Rudner and Losick, 2010; Shapiro et al., 2009)). The exact nature of the mechanism may be more complex in eukaryotes, for instance due having a larger number of compartments and components. This, combined with other factors such as smaller genomes (and well-developed genomic tools) (Goley, 2013), makes bacterial systems relatively more tractable systems for studying spatial organization in signalling networks and gaining insight into fundamental cellular phenomena such as cell division and morphology. It also makes these systems more amenable to synthetic manipulation.

In this respect, a model bacterial organism known as *Caulobacter crescentus* has been the subject of extensive investigation. There is a considerable amount of focus on the spatial control mechanisms and structures regulating fundamental processes such as the cell cycle, cellular differentiation and polarity (Ausmees and Jacobs-Wagner, 2003) in this or-

ganism. *Caulobacter* cells utilize a number of different spatial control mechanisms (Collier and Shapiro, 2007), for example the dynamic localization of proteins at its poles and the spatial distribution of signaling proteins have been shown to play an important role during its asymmetric development. Positional/spatial cues are utilized to determine the timing and positioning in cell division (Goley et al., 2009). The cytoskeleton and the geometry of the membrane also play an important role in establishing cell polarity (Collier and Shapiro, 2007). Furthermore, these spatial regulatory control mechanisms are integrated with multiple feedback interactions as well. The spatial and temporal interactions in the cell cycle are depicted in Fig. 6.1. This figure has been taken from (Thanbichler, 2009) and reproduced here.

A closer look at the spatiotemporal signalling networks regulating the *Caulobacter* cell cycle reveals echoes of representative building blocks and modules that we have studied previously. These include the covalent modification cycle in 4 and phosphorelays in 5. Also present are modules, which we have not yet explored, such as modification cycles catalyzed by bifunctional enzymes (enzymes capable of driving both, the modification and reverse modification of substrates) and phospho-signalling network motifs. The polar localization of the bifunctional and other enzymes has been shown to be an important control mechanism integrated in the function of these networks. A brief synopsis of bifunctional enzymes and related modeling and experimental studies is presented in the Appendix E.

Surveying the *Caulobacter* literature reveals that while there is an intensive experimental effort to understand spatial dynamics and mechanisms in the regulatory processes of the cell cycle, there are very few modeling studies that have taken spatial aspects into account. The complex web of interactions that give rise to the cell cycle make it challenging to understand even in solely temporal terms and spatiotemporal aspects add another layer of complexity. Elucidating the role of spatial regulation and control in the underlying signalling networks is vital to our fundamental understanding of this cell cycle. Motivated by this, we utilize a multipronged systems and *in silico* synthetic design approach to develop a mathematical modeling framework to examine the spatial organization and control in the *Caulobacter* cell cycle signaling networks.

We carry out this study in two parts, starting with the systematic dissection of spatial control in building blocks centered on the bifunctional enzyme modification cycle (which in itself is an unexplored feature of modification cycles). We use the study of building blocks to reduce the gap between understanding the complexities of the cell cycle and it spatiotemporal regulatory mechanisms. Also, using building block models allows us to by-

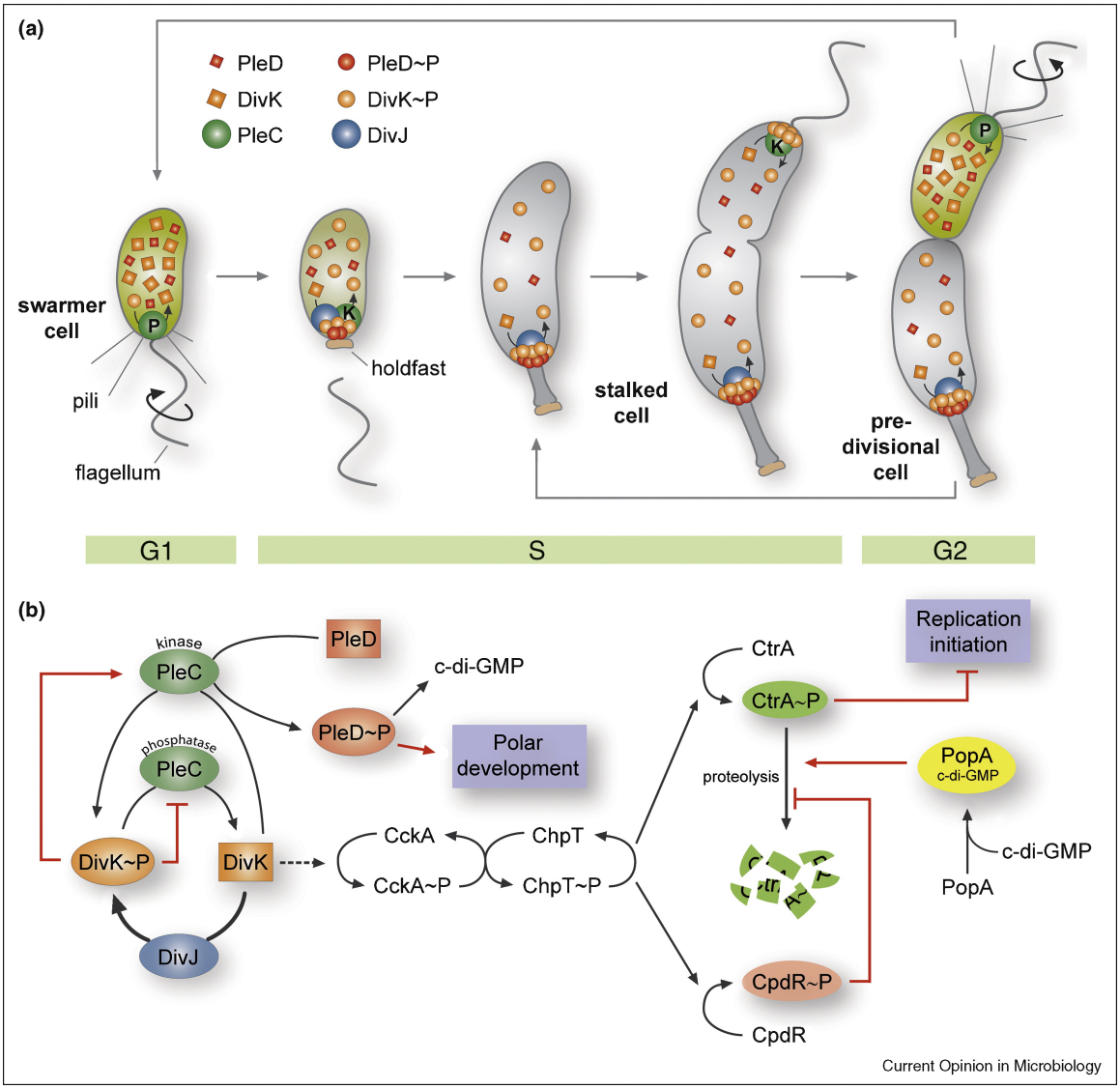


Figure 6.1: **The spatial and temporal mechanisms that control the cell cycle signalling networks in *Caulobacter* (Thanbichler, 2009).** The spatial coordination of the phospho-signalling interactions in different phases of the cell cycle is shown here. The enzymes are localized at different poles during each phase and the spatial distribution of the signalling species is modulated accordingly. This figure has been reproduced from the paper (Thanbichler, 2009).

pass missing details and incorporate and examine the essential signaling interactions in this system. This in turn allows us to gain transparent insights into the role of spatial regulation in these building blocks. Furthermore it gives us the flexibility to examine different aspects of spatial signaling beyond the context of *Caulobacter* and apply our insights in the broader context of bacterial cells.

In the second part of the study, we extend the analysis to examine the role of space in the context of the *Caulobacter* cell cycle. We focus on investigating how the temporal interaction between different building blocks may be affected by the introduction of spatial effects in the form of localization or compartmentalization of species. We aim to answer the following questions (1) what role does localization play in the temporal interaction of the networks, (2) what is the consequence of disrupting or changing the localization?

With a broader context in mind, we use an *in silico* synthetic design approach to explore related and alternative spatial distributions or designs of these networks. This approach is akin to an experimental synthetic design approach, here we computationally manipulate the localization of the individual species or the network modules with an aim to shed light on the different types of spatial designs cells may employ and the limitations and advantages associated with each design in different contexts. Going further, we also address the role of the dynamic nature of the spatiotemporal networks controlling the cell cycle. To achieve this, we study the role of differential localization of enzymes as the cell cycle progresses in time from one phase to another. Hence the dynamic localization of enzymes and its effects on the spatial distributions of signalling species comes under scrutiny here.

Overall, the goal of the entire study is to bring to the fore the role of spatial control and regulation in the *Caulobacter* cell cycle signalling networks by applying and building on the insights gained from examining spatial organization of representative building blocks.

This chapter is organized as follows- the models used in the analysis are discussed next followed by a discussion of the results and finally the chapter is closed with the concluding remarks.

## 6.2 Models and methods

In this study our goal is to shed light on the spatiotemporal organisation and control mechanisms underlying the cell cycle signalling networks in *Caulobacter crescents*. This investigation is carried out in two sequential parts. First, we examine the spatial regulation in building block models that are centred on the modification cycle with a bifunctional enzyme. These building blocks reflect signalling interactions and control features seen in the *Caulobacter* cell cycle networks. Armed with the insights obtained from this part of the study, our goal in the second part is to build on these and apply them towards understanding the spatio-temporal interactions within the *Caulobacter* signalling networks. As part of this, we utilise combinations of building block models to study different types of *in silico* spatial designs of these networks. In this part of the study we also examine existing spatial models of *Caulobacter* networks as well as make the first step towards examining spatiotemporal control mechanisms in the entire cell cycle.

We begin by discussing the building block models. The core of the building block comprises of the modification and reverse modification of two forms of a species X and $X^*$. The enzyme catalyzing the reaction is bifunctional, i.e. it is capable of acting as either a kinase or a phosphatase.

We begin by examining the simplest building block, and in a systematic fashion, we build in different types of feedforward and feedback interactions into this model (one at a time). This not only gives us the opportunity to systematically examine the effects of spatial control with distinct signalling interactions but also gives rise to a suite of models that mirror the control mechanisms in the concrete *Caulobacter* signalling networks. Even though these models might not be exactly similar to the networks observed, they encompass the essential signalling interactions seen within these and enable us to clearly delineate the role of spatial regulation in each setting. These models are described next.

### 6.2.1 Part 1: Building Block Models

#### Model I

Model I (Fig. 6.2) consists of an enzyme "E" catalysing the forward and reverse modification reactions of two forms of a species- X and $X^*$. The equations governing this model are:

$$
\begin{aligned}
\frac{\partial[X]}{\partial t} &= -k_1[X][E] + k_{-1}[XE] + k_4[X^*E] + D_X\frac{\partial^2 X}{\partial\theta^2} \\
\frac{\partial[X^*]}{\partial t} &= -k_3[X^*][E] + k_{-3}[X^*E] + k_2[XE] + D_{X^*}\frac{\partial^2 X^*}{\partial\theta^2} \\
\frac{\partial[E]}{\partial t} &= -k_1[X][E] + k_{-1}[XE] + k_2[XE] - k_3[X^*][E] + k_{-3}[X^*E] + k_4[X^*E] \\
&\quad +k_{f1}S(\theta) - k_{b1}[K] + D_E\frac{\partial^2 E}{\partial\theta^2} \\
\frac{\partial[XE]}{\partial t} &= k_1[X][E] - k_{-1}[XE] - k_2[XE] \\
&\quad +D_{XE}\frac{\partial^2 XE}{\partial\theta^2} \\
\frac{\partial[X^*E]}{\partial t} &= k_3[X^*][E] - k_{-3}[X^*E] - k_4[X^*E] + D_{X^*E}\frac{\partial^2 X^*E}{\partial\theta^2}
\end{aligned}
\tag{6.1}
$$

where $k_1$ and $k_3$ are the forward rate constants for the binding of the enzyme to X and X*, respectively, $k_{-1}$ and $k_{-3}$ are the rate constants for the dissociation of the enzyme substrate complexes X and X*E, respectively. $k_2$ and $k_4$ are the rate constants for product formation. $k_{f1}$ and $k_{b1}$ are the "production" and "degradation" rate constants for the free enzyme E, respectively; $S(\theta)$ is the parameter associated with the spatial distribution of the enzyme and can be homogenous or graded. $\theta$ represents the spatial coordinate and $D_j$ is the diffusion coefficient for any species "j" in the cycle. This is a description of a simple covalent modification cycle where the same enzyme does the both modifications (Fig. 6.2).

## Model II: Feedforward control by an external signal

Next, an additional feedforward interaction was built into Model I. In Model II (Fig. 6.2), the two activities or forms of the enzyme, E and E*, are regulated by an external signal S. S may regulate either the conversion of E to E* or E* to E. These reactions were assumed to be in the mass action regime. The model equations are:

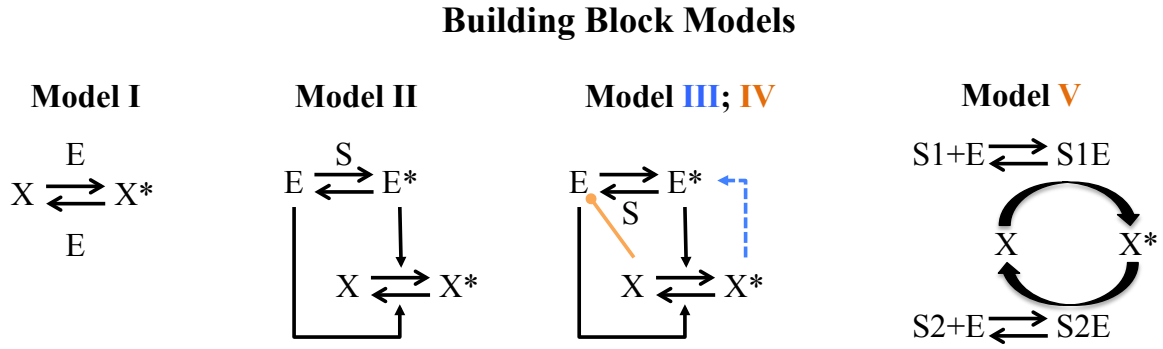


Figure 6.2: **Building block models analysed in the first phase of the study** The models become progressively more complex as additional feedforward and feedback interactions are introduced into the basic mechanism. Model I is the simplest model. It consists of a bifunctional enzyme E catalyzing the inter-conversion between the two forms of a species- $X^*$ and X. Model II: Feedforward regulation by an external signal S is added to regulate the conversion between the two forms of the bifunctional enzyme. S catalyzing E to $E^*$ case is depicted (cases where S catalyzes $E^*$ to E were also considered). $E^*$ in turn catalyzes the conversion of X to $X^*$ and E catalyzes the reverse reaction. Models III and IV: these are depicted here in a compact manner. Model III: the signal S regulates the conversion of $E^*$ to E (or the reverse reaction, not shown) and a positive feedback interaction is present between the product $X^*$ and $E^*$ (blue dashed arrow). Model IV: In addition to the positive feedback interaction another interaction is present where X inhibits the E form of the enzyme (orange arrow with a round end). Model V: This model contains feedforward regulation by two external signals S1 and S2, which bind to the enzyme to give the complexes S1E and S2E, respectively. S1E mediates the conversion of X to $X^*$ and S2E catalyzes the reverse reaction.

$$
\begin{aligned}
\frac{\partial[X]}{\partial t} &= -k_1[X][E^*] + k_{-1}[XE^*] + k_4[X^*E] + D_X\frac{\partial^2 X}{\partial\theta^2} \\
\frac{\partial[X^*]}{\partial t} &= -k_3[X^*][E] + k_{-3}[X^*E] + k_2[XE^*] + D_{X^*}\frac{\partial^2 X^*}{\partial\theta^2} \\
\frac{\partial[E^*]}{\partial t} &= k_s[S][E] + k_{fb}[E] - k_{bb}[E^*] - k_1[X][E^*] + k_{-1}[XE^*] + k_2[XE^*] \\
&\quad + D_{E^*}\frac{\partial^2 E^*}{\partial\theta^2} \\
\frac{\partial[E]}{\partial t} &= -k_s[S][E] - k_{fb}[E] + k_{bb}[E^*] - k_3[X^*][E] + k_{-3}[X^*E] + k_4[X^*E] \\
&\quad + D_E\frac{\partial^2 E}{\partial\theta^2} \\
\frac{\partial[XE^*]}{\partial t} &= k_1[X][E^*] - k_{-1}[XE^*] - k_2[XE^*] + D_{XE^*}\frac{\partial^2 XE^*}{\partial\theta^2} \\
\frac{\partial[X^*E]}{\partial t} &= k_3[X^*][E] - k_{-3}[X^*E] - k_4[X^*E] + D_{X^*E}\frac{\partial^2 X^*E}{\partial\theta^2}
\end{aligned}
\tag{6.2}
$$

where $k_s$ is the rate constant associated with binding of signal to one form of the enzyme and $k_{fb}$ and $k_{bb}$ are the basal forward and backward rate constants for the interconversion between the two forms of the enzyme E and $E^*$, respectively. The remaining parameter denotations are the same as in Model I. In the case where the signal regulates the conversion of $E^*$ to E, the equations for both species would be:

$$\begin{aligned}\frac{\partial[E^*]}{\partial t} &= -k_s[S][E^*] + k_{fb}[E] - k_{bb}[E^*] - k_1[X][E^*] + k_{-1}[XE^*] + k_2[XE^*] \\ &\quad + D_{E^*}\frac{\partial^2 E^*}{\partial\theta^2} \\ \frac{\partial[E]}{\partial t} &= k_s[S][E^*] - k_{fb}[E] + k_{bb}[E^*] - k_3[X^*][E] + k_{-3}[X^*E] + k_4[X^*E] \\ &\quad + D_E\frac{\partial^2 E}{\partial\theta^2}\end{aligned} \tag{6.3}$$

**Ultrasensitive Response:** In a parameter regime where the two activities of the enzyme are operating at saturation and if the signal binds with high affinity, Model II is capable of exhibiting an "ultrasensitive" response (the underlying analytical reasoning is shown in (Straube, 2014)). The ultrasensitive response is discussed and analysed in detail in Chapter 3. Very briefly, for a very small change in the concentration of the input, the change in the concentration of the output is relatively large- thus the response concentration curve is sigmoidal with respect to the output. The ultrasensitive response was perturbed by different spatial effects as part of the analysis of Model II.

## Model III: Feedforward and feedback control

Model III was obtained by incorporating a positive feedback interaction between $X^*$ and $E^*$ into Model II (Fig. 6.2). This may be achieved in two ways- by increasing the production of $E^*$ or inhibiting its degradation. We chose the former (the interaction is assumed to be in the mass action regime) and the relevant modified equations of the enzyme forms are:

$$\begin{aligned}
\frac{\partial[E^*]}{\partial t} &= -k_s[S][E^*] + k_{fb}[E] - k_{bb}[E^*] - k_1[X][E^*] + k_{-1}[XE^*] + k_2[XE^*] \\
&\quad +k_{pf}[X^*][E] + D_{E^*}\frac{\partial^2 E^*}{\partial\theta^2} \\
\frac{\partial[E]}{\partial t} &= k_s[S][E^*] - k_{fb}[E] + k_{bb}[E^*] - k_3[X^*][E] + k_{-3}[X^*E] + k_4[X^*E] \\
&\quad -k_{pf}[X^*][E] + D_E\frac{\partial^2 E}{\partial\theta^2}
\end{aligned} \tag{6.4}$$

where $k_{pf}$ is the positive feedback rate constant. The remaining equations and associated parameters are the same as in Model II. Note that here the signal regulates the increase of E. The feedback rate constant $k_{pf}$ is varied in the analysis of the model.

**Transcritical Bifurcation:** In a certain parameter regime (where the basal rate constants $k_{fb}$ and $k_{bb}$ are zero), this model shows a particular kind of thresholding effect which arises through a transcritical bifurcation. This type of behaviour is discussed in detail in Chapter 3. The model has two steady states- one is non-zero and if the signal exceeds a threshold (or transcritical bifurcation point) the other is zero. The spatial perturbation of this effect is the focus of the analysis in Model III.

## Model IV: Feedforward inhibition and feedback control

Model IV was obtained by adding another interaction into Model III- the inhibition of E activity/form of the enzyme by substrate X (Fig. 6.2). This was done by sequestering E in a complex XE. The resulting set of equations for Model IV are (note that the positive feedback between $E^*$ and X is also present):

$$\begin{aligned}
\frac{\partial[X]}{\partial t} &= -k_1[X][E^*] + k_{-1}[XE^*] + k_4[X^*E] - k_5[X][E] + k_6[XE] \\
&\quad + D_X\frac{\partial^2 X}{\partial\theta^2} \\
\frac{\partial[E]}{\partial t} &= k_s[S][E^*] - k_{fb}[E] + k_{bb}[E^*] - k_3[X^*][E] + k_{-3}[X^*E] + k_4[X^*E] \\
&\quad - k_{pf}[X^*][E]] - k_5[X][E] + k_6[XE] + D_E\frac{\partial^2 E}{\partial\theta^2} \\
\frac{\partial[XE]}{\partial t} &= k_5[X][E] - k_6[XE] + D_{XE}\frac{\partial^2 XE}{\partial\theta^2}
\end{aligned} \tag{6.5}$$

where $k_5$ and $k_6$ are forward and backward rate constants associated with inhibition of E by X to form XE.

**Bistable Response:** This model contains multiple feedforward and feedback interactions. Besides the substrate-enzyme interactions, there may be other possible interactions in the covalent modification cycle, for example, between the product and enzyme (Seaton and Krishnan, 2012). In this model, we incorporate the inhibition of the enzyme form E by its product X. This single change allows this model to exhibit a bistable response (in a particular parameter regime). Thus we see here that with this one modification, the model changes from having a transcritical bifurcation to exhibiting a bistable response. This particular temporal behaviour was the focus the investigation in Model IV.

The bistable response arising from a mutual inhibition model has been discussed in detail in Chapter 3. In a certain range of a parameters, the model has three steady states, two of which are stable. This model comes under a class of models, where the bistable switching response arises due sequestration. Another class of models that also exhibits this response is one where a Hill type cooperativity is present. We have also considered a model of this type with a cooperative positive feedback interaction is present between $X^*$ and $E^*$ and subjected it to similar analysis to Model IV. This is shown in Appendix E. The essential qualitative results were similar for both types of models with respect to perturbation by spatial effects.

## Model V: Feedforward control by two separate signals

In Model V we explore the regulation of the bifunctional enzyme activities via feedforward interactions by two external signals, S1 and S2 (Fig. 6.2). S1 and S2 separately bind to E resulting in the formation of the complexes S1E and S2E, respectively. S1E catalyzes the conversion of X to X$^*$ and S2E catalyzes the reverse reaction (to form the complexes XS1E and X$^*$S2E, respectively). The equations of the model are:

$$\begin{aligned}
\frac{\partial[X]}{\partial t} &= -k_1[X][S1E] + k_{-1}[XS1E] + k_4[X^*S2E] + D_X\frac{\partial^2 X}{\partial\theta^2} \\
\frac{\partial[X^*]}{\partial t} &= -k_3[X^*][S2E] + k_{-3}[X^*S2E] + k_2[XS1E] + D_{X^*}\frac{\partial^2 X^*}{\partial\theta^2} \\
\frac{\partial[S1E]}{\partial t} &= k_{s1}[S1][E] - k_{b1}[S1E] - k_1[X][S1E] + k_{-1}[XS1E] + k_2[XS1E] \\
&\quad + D_{S1E}\frac{\partial^2 S1E}{\partial\theta^2} \\
\frac{\partial[S2E]}{\partial t} &= k_{s2}[S2][E] - k_{b2}[S2E] - k_3[X^*][S2E] + k_{-3}[X^*S2E] + k_4[X^*S2E] \\
&\quad + D_{S2E}\frac{\partial^2 S2E}{\partial\theta^2} \\
\frac{\partial[XS1E]}{\partial t} &= k_1[X][S1E] - k_{-1}[XS1E] - k_2[XS1E] + D_{XS1E}\frac{\partial^2 XS1E}{\partial\theta^2} \\
\frac{\partial[X^*S2E]}{\partial t} &= k_3[X^*][S2E] - k_{-3}[X^*S2E] - k_4[X^*S2E] + D_{X^*S2E}\frac{\partial^2 X^*S2E}{\partial\theta^2}
\end{aligned} \tag{6.6}$$

where $k_{s1}$ and $k_{s2}$ are the binding rate constants for S1 and S2 respectively and the backward basal rate constants for the respective reverse reactions are $k_{b1}$ and $k_{b2}$. The remaining parameters are the same as before.

## Spatial effects in the building block models

Our aim is to understand the role of spatial regulation in each of these building block modules. To achieve this we systematically examine different kinds of spatial effects (which are observed in *Caulobacter* signalling networks). The models are subjected to two types of spatial perturbations (separately)- graded signals and localization or compartmentalization of signalling entities. Each of these are combined with diffusion of species in the cycle.

**Graded signals:** In this case, the signal (or the enzyme in case of Model I) has a graded profile (of the form a+bCos($\theta$)). The response of the cycle is examined and used as a reference case for when (either one or two) species in the cycle are also diffusing (other species maybe non-diffusible/weakly diffusing). The basic methodology used in this analysis is described in detail in Chapter 4.

**Localization:** In the second type of perturbation, the species of the cycle are localized in a patch/sub-domain in the spatial domain. X or $X^*$ (or both) may be allowed to diffuse into the spatial domain. The basic methodology used here is similar to the one in Chapter 5.

The distortion of the unique temporal characteristics: the ultrasensitive response, thresholding effect due to transcritical bifurcation and the bistable switch in Models II, III and IV, respectively, are probed using these methods. Since our primary focus is on basic aspects of spatial and localization control of modification cascades, we cast the models in a spatial domain in 1-D, and use periodic boundary conditions (where the domain is $\theta\epsilon[0, 2\pi]$) for simplicity. It is worth pointing out that for the scenarios considered here, the results are exactly equivalent to those with no-flux boundary conditions in a domain half the size. Thus all essential results are equally valid for both cases and could be relevant to the situation involving diffusion of species in the membrane or the cytosol.

### 6.2.2 Part 2: *Caulobacter crescentus* networks

#### Biochemical signalling networks

In this part of the study, the insights from the building blocks are applied towards the study of signalling networks implicated in the cell cycle of *Caulobacter crescentus* (Fig. 6.4). Numerous interrelated and interconnected networks are present in this cell cycle. In this work we focus on two sub-networks that are the subject of spatially motivated experimental investigation. These are the DivK-DivJ-PleC and the CckA-CtrA networks (labelled A and B, respectively, in Fig. 6.3). We refer to these as DivK and CtrA networks in the text, respectively.

The interactions in the DivK network are: DivK is phosphorylated by DivJ to give DivKP which in turn is dephosphorylated by PleC. In the CckA-CtrA network, the phosphorylation and dephosphorylation of CtrA and CtrAP, respectively, is regulated by the bifunctional enzyme CckA. An enzyme species DivL acts as an intermediate between the two networks. It has been suggested that DivKP, which is upstream of DivL, downreg-

ulates DivL by binding and sequestering it in a complex [DivKP-DivL] (Tsokos et al., 2011). DivL in turn mediates the conversion of the phosphatase form of CckA to the kinase form (Chen et al., 2011; Iniesta et al., 2010b; Reisinger et al., 2007; Tsokos et al., 2011). We probe the interactions between these two networks when different spatial effects are present.

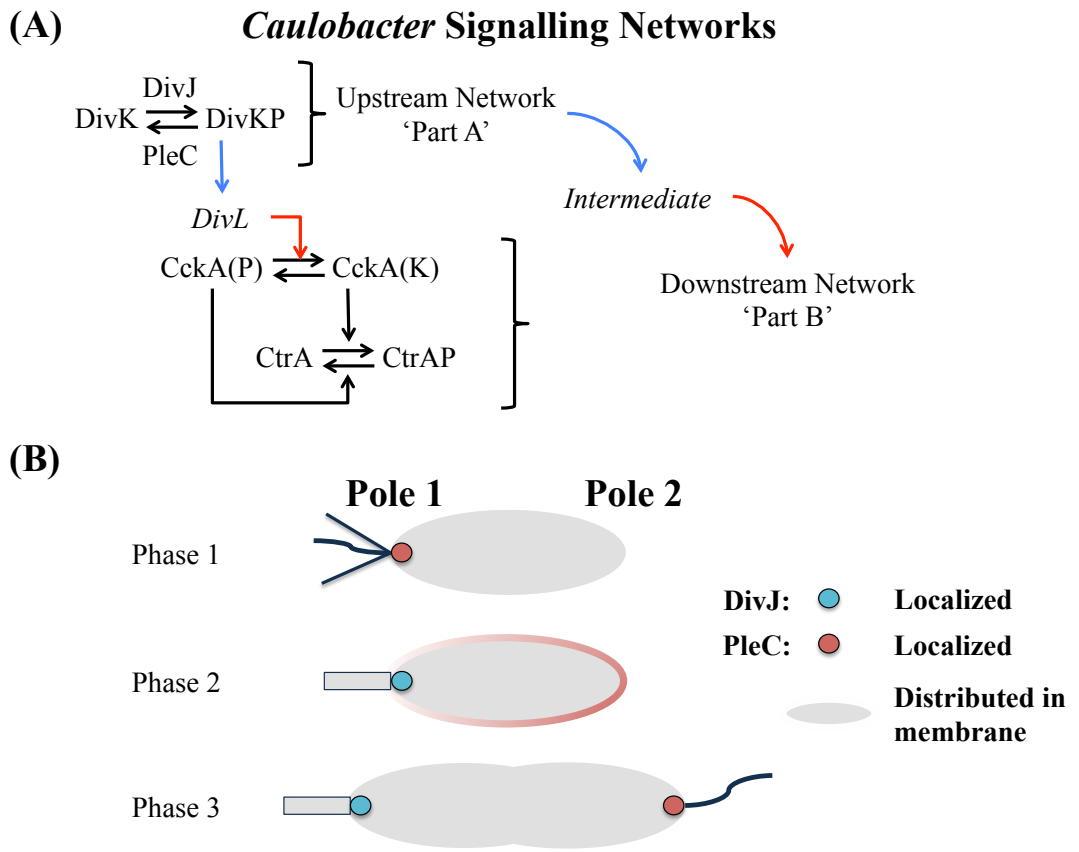


Figure 6.3: **The *Caulobacter crescentus* cell cycle signalling networks considered in the analysis** (A) Network Part A/Module MI: involves the interactions between the kinase DivJ, phosphatase PleC and the substrate DivK. This is the upstream network. Network Part B//Module MII a bifunctional enzyme CckA catalyzes the phosphorylation and dephosphorylation of CtrA. This is the downstream network. The two network modules interact via the intermediate DivL. (B) A simple depiction of the *Caulobacter)* cell is shown. The poles of the cell are labelled as pole 1 and pole 2. The distribution of enzymes PleC (orange) and DivJ (blue) of the upstream network are shown for each phase of the cell cycle (García Véscovi et al., 2010). PleC is localized in pole 1 in phase 1, distributed in the membrane in phase 2 and localised in pole 2 in phase 3. DivJ is mainly localized in pole 1.

**Localization of species:** This cell has two poles (that are morphologically dissimilar). In each phase of the cell cycle, the poles are known by slightly different names. We generally refer to the pole where old flagellum is shed and the new stalk grows as the "stalked"

pole or localised region 1 or pole 1 and where the location of the new flagellum develops (the opposite pole) as the "swarmer" pole or localised region 2 or pole 2.

In each phase of the cell cycle, the localisation of the enzymes in both the above mentioned networks has been observed to change. These enzymes may alternate between being localized at one or both of these poles and being distributed in the membrane (Ausmees and Jacobs-Wagner, 2003; García Véscovi et al., 2010). A simple depiction of the localization of enzymes PleC and DivJ is shown in Fig. 6.3. The differential or dynamic localization of these enzymes is suggested to play the role of positional cues that are linked to the progression of the cell cycle. Thus this is an important mechanism which spatially regulates the interactions within the signalling networks of the cell cycle (Ausmees and Jacobs-Wagner, 2003).

In this part of the study our goal was to understand the role of localization in the above signalling networks and how this spatial control mechanism affects the interactions between these networks as well. We split this part of the study in two halves- in one half we utilised a combination of building block models to study the effect of localization. In the second half we utilised existing spatial models of the above signalling networks to analyse the effect of localization. The first half, where combinations of building blocks were employed, is discussed first.

## From individual building blocks to analysis of interactions between building block models

In this part of the study, we utilise two different combinations of building block models. The building blocks chosen for this analysis contain interactions that reflect the ones in the DivK and CtrA networks. The concrete signalling networks are phospho-signalling networks- i.e. the enzymes carry out the modifications of the substrates via phosphotransferase reactions (the phosphotransfer mechanism is discussed in Appendix E). In this part of the study we assume that the phosphotransfer mechanism underlies the modification in these building block models. Each combinations of the building block models consists of two modules that interact through an intermediate species. The two different combination are termed BBC1 and BBC2 and are discussed next (see Table 6.1).

## Building Block Combination BBC1

In this model the interactions of the upstream module are akin to those in the DivJ-PleC-DivK network and those in the downstream module are similar to those in the CckA-CtrA network. In generic terms, the upstream module consists of two separate enzymes 'K' and 'P' catalysing the modification of the species 'X' and downstream module consists of a bifunctional enzyme with two forms 'E' and 'E$^*$' catalyzing the modification of a species 'Y.' The modules interact through a species 'I' (DivL) (see Table 6.1). X$^*$ inhibits I and I regulates the conversion between the E and E$^*$ forms of the bifunctional enzyme in the downstream module. The equations governing these modules and their interactions are:

**Upstream Module:**

$$\begin{aligned}
\frac{\partial[DivK]}{\partial t} &= -k_1[DivK][DivJ] + k_{-1}[DivK - DivJ] + k_4[DivKP - PleC] \\
&\quad + D_{DivK}\frac{\partial^2 DivK}{\partial \theta^2} \\
\frac{\partial[DivKP]}{\partial t} &= -k_3[DivKP][PleC] + k_{-3}[DivKP - PleC] + k_2[DivK - DivJ] \\
&\quad + D_{DivKP}\frac{\partial^2 DivKP}{\partial \theta^2} \\
\frac{d[DivJ]}{dt} &= -k_1[DivK][DivJ] + k_{-1}[DivK - DivJ] + k_j[DivJ_i] - k_{fj}[DivJ] \\
\frac{d[PleC]}{dt} &= -k_3[DivKP][PleC] + k_{-3}[DivKP - PleC] + k_4[DivKP - PleC] \\
\frac{d[DivK - DivJ]}{dt} &= k_1[DivK][DivJ] - (k_{-1} + k_2)[DivK - DivJ] \\
\frac{d[DivKP - PleC]}{dt} &= k_3[DivKP][PleC] - k_{-3}[DivKP - PleC] - k_4[DivKP - PleC] \\
\frac{d[DivJ_i]}{dt} &= k_2[DivK - DivJ] - k_j[DivJ_i] + k_{fj}[DivJ]
\end{aligned} \tag{6.7}$$

**Downstream Module:**

$$
\begin{aligned}
\frac{\partial[CtrA]}{\partial t} &= -k_a[CtrA][CckAK] + k_{-a}[CtrA - CckAK] \\
&\quad +k_d[CtrAP - CckAP] + D_{CtrA}\frac{\partial^2 CtrA}{\partial\theta^2} \\
\frac{\partial[CtrAP]}{\partial t} &= -k_c[CtrAP][CckAP] + k_{-c}[CtrAP - CckAP] \\
&\quad +k_b[CtrA - CckAK] + D_{CtrAP}\frac{\partial^2 CtrAP}{\partial\theta^2} \\
\frac{d[CckAK]}{dt} &= -k_a[CtrA][CckAK] + k_{-a}[CtrA - CckAK] \\
&\quad -k_{ff}[CckAK] + k_{bb}[CckAP] + k_i[DivL][CckAP] \\
\frac{d[CckAP]}{dt} &= -k_c[CtrAP][CckAP] + k_{-c}[CtrAP - CckAP] \\
&\quad +k_d[CtrAP - CckAP] + k_b[CtrA - CckAK] \\
&\quad +k_{ff}[CckAK] - k_{bb}[CckAP] - k_i[DivL][CckAP] \\
\frac{d[CtrA - CckAK]}{dt} &= k_a[CtrA][CckAK] - (k_{-a} + k_b)[CtrA - CckAK] \\
\frac{d[CtrAP - CckAP]}{dt} &= k_c[CtrAP][CckAP] - (k_{-c} + k_d)[CtrAP - CckAP]
\end{aligned}
\tag{6.8}
$$

where $k_1$, $k_3$, $k_a$ and $k_c$ are the forward rate constants for the binding of the enzyme to the unmodified form and phosphorylated form of the substrates, respectively. $k_{-1}$, $k_{-3}$, $k_{-a}$ and $k_{-b}$ are the rate constants for the dissociation of the enzyme substrate complexes and $k_2$, $k_4$, $k_b$ and $k_d$ are the rate constants for product formation. Note that DivJ and the CckAK carry out the phosphotransferase reactions. DivJ is assumed to undergo an autophosphorylation reaction, where the inactive form ($DivJ_i$) is converted to the active form, DivJ, which is then assumed to be catalytically active. $k_j$ and $k_{-j}$ are the associated rate constants. The two forms of the enzyme CckA are also assumed to have basal rate of interconversion ($k_{ff}$ and $k_{bb}$ are the associated rate constants) and DivL regulates the conversion of CckAP to CckAK (assumed to be in the mass action regime). $\theta$ represents the spatial coordinate and $D_j$ is the diffusion coefficient for any species "j" in the cycle. It should be noted that we only consider the enzymes and enzyme substrate complexes to be localized and the substrate species are free to diffuse. Thus the diffusion term present is only in the equations for the substrate and product species (and not in the enzyme and

enzyme-substrate complex) descriptions.

**Interaction between the upstream module and the intermediate species:** We account for two types of possibilities for the interactions between the upstream module and the intermediate. This gave rise to two model variants: In the first model variant, the inhibition of DivL by DivKP was assumed to be in the mass action regime, i.e. there is no uptake of DivKP in the reaction. In the second model variant, the binding of DivKP and DivL was explicitly modelled to understand the effect of sequestration of both species in the DivKP-DivL complex. As previously mentioned, the latter interaction is suggested based on experimental evidence (Tsokos et al., 2011). The intermediate is assumed to exist as a fixed pool containing an active and inactive form DivL and $\mathrm{DivL}_i$, respectively.

*First variant where interaction in mass action regime:* The first variant is described by the following set of equations:

$$\begin{aligned} \frac{\partial[DivL_i]}{\partial t} &= k_{bi}[DivL] - k_{fi}[DivL_i] - k_5[DivKP][DivL_i] + D_D\frac{\partial^2 DivL_i}{\partial\theta^2} \\ \frac{\partial[DivL]}{\partial t} &= -k_{bi}[DivL] + k_{fi}[DivL_i] + k_5[DivKP][DivL_i] + D_D\frac{\partial^2 DivL}{\partial\theta^2} \end{aligned} \tag{6.9}$$

where $\mathrm{k}_{bi}$ and $\mathrm{k}_{fi}$ are the basal interconversion rate constants between the inactive and active forms and $\mathrm{k}_5$ is the rate constant associated with the inhibition of DivL by DivKP. $\mathrm{D}_D$ is the diffusion coefficient for DivL (assumed to be equal for both forms).

*Second variant where interaction occurs via binding:*In the second variant, DivKP reacts with DivL to form a complex DivKP-DivL, this is governed by the following equations:

$$\begin{aligned}
\frac{\partial[DivKP]}{\partial t} &= -k_3[DivKP][PleC] + k_{-3}[DivKP - PleC] \\
&\quad +k_2[DivK - DivJ] - k_5[DivKP][DivL] + k_6[DivKP - DivL] \\
&\quad +D_{DivKP}\frac{\partial^2 DivKP}{\partial\theta^2} \\
\frac{\partial[DivL]}{\partial t} &= -k_{bi}[DivL] + k_{fi}[DivL_i] - k_5[DivKP][DivL] \\
&\quad +k_6[DivKP - DivL] + D_D\frac{\partial^2 DivL}{\partial\theta^2} \\
\frac{\partial[DivL_i]}{\partial t} &= k_{bi}[DivL] - k_{fi}[DivL_i] + D_D\frac{\partial^2 DivL_i}{\partial\theta^2} \\
\frac{\partial[DivKP - DivL]}{\partial t} &= k_5[DivKP][DivL] - k_6[DivKP - DivL] \\
&\quad +D_{DivKP-DivL}\frac{\partial^2 DivKP - DivL}{\partial\theta^2}
\end{aligned} \tag{6.10}$$

where $k_5$ and $k_6$ are the forward and backward rate constants for the formation and dissociation of the complex DivKP-DivL, respectively and $D_{DivKP-DivL}$ is the diffusion coefficient for the complex (the remaining parameters are the same as before). Note that the equation for DivKP has changed and now contains the terms related to the formation of the complex DivKP-DivL and the change in concentration of this complex is also explicitly considered in the model.

## Building Block Combination BBC2: Upstream module is bistable

The second combination of building block models we consider is one where the upstream module exhibits a bistable response. We consider this in our analysis because it has been suggested in (Subramanian et al., 2013) that the transition between the first and second phases of the cell cycle occurs due to the bistable nature of the PleC and DivJ network (on which the upstream module is based). In (Subramanian et al., 2013) PleC is explicitly modelled as a bifunctional enzyme. It is hypothesised that there is a positive feedback present between the modified substrate, DivKP and the kinase form of PleC: DivKP mediates the conversion of the phosphatase form of PleC to its kinase form which in turn catalyses the phosphorylation of DivK. That such positive feedback loops may potentially function as

bistable "toggle switches" (Tyson et al., 2003) and these switches have been suggested to play a role in transitions in the eukaryotic cell cycle. Based on this reasoning, Subramanian et al. (2013) suggest that the PleC bistable switch is a plausible mechanism underlying the transition between the first and second phases in the *Caulobacter* cell cycle (in the appropriate parameter regime, this model exhibits bistability). We do not employ the same model as in (Subramanian et al., 2013) as it contains detailed enzyme-substrate interactions (descriptions are based on the Monod-Wyman-Changeux model) which are tangential to our analysis.

In order to incorporate bistability, we base the interactions in the upstream module on those in Model IV (from the building blocks study, refer to Fig. 6.2). Model IV exhibits bistability (arising through the combination of a positive feedback interaction and inhibition via sequestration) and is more appropriate for our purpose. The equations in Model IV were adjusted to reflect the phosphotransferase mechanism and this forms the upstream module in BBC2. The intermediate and downstream module is the same as in BBC1 (see Table 6.1). It is known that if a part of the model exhibits bistability, the entire model will as well. Thus BBC2 exhibits the bistable response and this was confirmed by checking the model in MATCONT.

| **Building Block Combination** | **Upstream Module** | **Intermediate** | **Downstream Module** |
|---|---|---|---|
| **Model BBC1** | Modification cycle with separate enzymes (PleC and DivJ) regulating modification of the substrate (DivK) | DivL Inhibited by DivK | Modification cycle with a bifunctional enzyme (CckA) regulated by DivL |
| **Model BBC2** | Modification cycle based on the above network with a bifunctional enzyme. Exhibits bistability | Same as above | Same as above |

Table 6.1: A summary of the upstream and downstream modules in the Spatial Design Models 1 and 2.

## Analysis of *in silico* Spatial Designs in BBC1 and BBC2

As previously mentioned, our aim is to understand the effect of localization on the interactions between the two concrete signalling networks DivK and CtrA. In order to do this we analyse the effect of different "*in silico* Spatial Designs" on the interactions in each of the building block combination models.

**Spatial Design:** A "spatial design" is a set of spatial configurations of localization of enzymes in both networks. Each configuration is known as a spatial design. Each network has multiple species and each of these may be localized in two different locations or distributed in the membrane. Hence, in theory, numerous spatial designs are possible. The spatial designs we have analysed are based on the different localization pattern of enzymes of the above mentioned networks in *Caulobacter* (Fig. 6.3). We also consider possible alternative localization/distribution patterns of these enzymes (which may been in other bacteria). An example of of a spatial design is- the enzymes PleC and DivJ are localised together in pole 1 and the enzyme CckA is localized in pole 2. The spatial designs we consider are listed in detail in Table 6.2 in the Results section.

## Existing Spatial Models of *Caulobacter* networks

In this part of the investigation, we analyse the interactions between the DivK and CtrA networks using the existing models of the signalling networks in the *Caulobacter* cell cycle. In the current literature, the three most recent models of these networks are by Chen et al. (2011), Tropini and Huang (2012) and Subramanian et al. (2013). The first two models are spatially distributed and each is based on the individual networks (DivK (Tropini and Huang, 2012) and CtrA (Chen et al., 2011)). The aforementioned model in (Subramanian et al., 2013) as well as those in (Li et al., 2008, 2009) describe the temporal dynamics of the interactions within the *Caulobacter* cell cycle in detail. The most current model (Subramanian et al., 2013) takes into account interactions between the aforementioned networks, however it is a purely temporal model. The authors state that the interactions in the model are based on a phase of the cell cycle where all the interacting species are localized in one region of the cell, i.e. at one pole. Thus the model may be described by ODEs (although the authors do note the need for designing models that take into account the complex spatio-temporal control mechanisms present in the cell cycle).

Each of these models has missing ingredients and as a result there is no model in the

literature governing the spatiotemporal interactions between the DivK and CtrA networks. Thus we explore the interactions between the DivK and CtrA networks in light of different spatial designs and in order to do this we utilise the two models in (Tropini and Huang, 2012). These are simple reaction diffusion models and the effects of spatial localisation of enzymes may be more transparently investigated in these models (as compared to the model in (Subramanian et al., 2013) which contains detailed enzyme-substrate interactions).

The analysis is carried out in the following order: each model is first examined individually. Next, we "connect" these two models via an intermediate (to achieve a model describing the full network as shown in Fig. 6.3) and explore the interactions between the network models. Here we dissect the role of localization of enzymes on these interactions by considering the localization and distribution of enzymes in different phases of the *Caulobacter* cell cycle. These are discussed in the Results section.

We describe the individual models in (Tropini and Huang, 2012) next. The first model (Model A) describes the interactions between the DivK-DivJ-PleC network and the second model (Model B) is based on the interactions in the CckA-CtrA network.

**Model A- DivK-DivJ-PleC model:** In this model Tropini and Huang (2012), DivK is phosphorylated by DivJ to give DivKP which in turn is dephosphorylated by PleC. Different forms of DivK and DivKP are modelled; two freely diffusing species $\text{DivK}_f$ and $\text{DivKP}_f$ and three non-diffusing species that are bound to the membrane: 1) $\text{DivK}_b$- DivK bound to DivJ prior to phosphorylation, 2) $\text{DivKP}_b$- DivKP bound to PleC before dephosphorylation, and 3) $\text{DivKP}_p$- DivKP bound to the swarmer pole (independent of PleC). We use periodic boundary conditions to represent the membrane of the cell (whereas in (Tropini and Huang, 2012) the concentrations of species are modelled along the length of a 1-D cell). In our representation of the model, the oppositely localized regions are the stalked pole/pole 1 (where DivJ is present; sub-domain on the "left") and the swarmer pole/pole 2 (where PleC is present) (Fig. 6.3).

The equations governing this model are:

$$\begin{aligned}
\frac{\partial[DivK_f]}{\partial t} &= -k_j(\theta)[DivK_f] + k_p[DivKP_b] + k_{po}([DivKP_f] + [DivKP_b]) \\
&\quad + D\frac{\partial^2 DivK_f}{\partial \theta^2} \\
\frac{\partial[DivKP_f]}{\partial t} &= k_k[DivK_b] + sw(\theta)(-k_b[DivKP_f] + k_u[DivKP_b]) - k_c(\theta)[DivKP_f] \\
&\quad - k_{po}[DivKP_f] + D\frac{\partial^2 DivKP_f}{\partial \theta^2} \\
\frac{\partial[DivK_b]}{\partial t} &= k_j(\theta)[DivK_f] - k_k[DivK_b] \\
\frac{\partial[DivKP_b]}{\partial t} &= k_c(\theta)[DivKP_f] - k_p[DivKP_b] - k_{po}[DivKP_b] \\
\frac{\partial[DivKP_p]}{\partial t} &= sw(\theta)(k_b[DivKP_f] - k_u[DivKP_b])
\end{aligned} \tag{6.11}$$

where $k_j(\theta)$ and $k_k$ are the rates for binding and phosphorylation by DivJ, respectively, and $k_c(\theta)$ and $k_p$ are the rates for binding and dephosphorylation by PleC, respectively. The binding rates were "localised", i.e. only active in the pole where the associated enzyme was present and zero in the remaining spatial domain. The swarmer pole was explicitly considered to incorporate the binding of DivKP observed (experimentally) in the absence of PleC at the swarmer pole and is denoted by $sw(\theta)$. The binding and unbinding rate constants are given by $k_b$ and $k_u$. $sw(\theta)$ is only non-zero in the swarmer pole localisation and zero everywhere else. D is the diffusion coefficient for the free forms of the species (considered equal for both forms). The authors also assume that a "background phosphatase" is present in the cell and the parameter $k_{po}$ represents the rate at which this species dephosphorylates the DivKP species.

In (Tropini and Huang, 2012), different spatial localisations of the enzymes have been analysed. The localization of enzymes in the "wild type" case was used as a reference and compared to different spatial localisations reflecting "spatial mutants" of these enzymes (mislocalized enzymes for examples). The aim of the analysis was to ascertain how a certain development process during the cell cycle would be affected by the mutant localization designs.

**Model B- CckA-CtrA model:** In the CckA-CtrA network, Chen et al. (2011) have investigated the phosphorylation and dephosphorylation of CtrA and CtrAP, respectively,

by the bifunctional enzyme CckA. The model consists of two equations describing both substrate species:

$$\begin{aligned}\frac{\partial[CtrA]}{\partial t} &= -(k_{ph}Sw(\theta)+k_{pho})[CtrA]+(k_{dp}St(\theta)+k_{do})[CtrAP] \\ &\quad +D_C\frac{\partial^2 CtrA}{\partial\theta^2} \\ \frac{\partial[CtrAP]}{\partial t} &= (k_{ph}Sw(\theta)+k_{pho})[CtrA]-(k_{dp}St(\theta)+k_{do})[CtrAP] \\ &\quad +D_C\frac{\partial^2 CtrAP}{\partial\theta^2}\end{aligned} \tag{6.12}$$

where $k_{ph}$ and $k_{dp}$ are the phosphorylation and dephosphorylation rate constants, respectively. $k_{pho}$ and $k_{do}$ are also (background) phosphorylation and dephosphorylation rate constants, respectively, due to other enzymes present in the cell. $k_{pho}$ and $k_{do}$ are relatively low compared to $k_{ph}$ and $k_{dp}$. The $Sw(\theta)$ and $St(\theta)$ denote the locations of the swarmer and stalked poles (CtrAP is thus dephosphorylated at the stalked pole where the phosphatase form of CckA is predominantly assumed to be present). $Sw(\theta)$ and $St(\theta)$ are zero everywhere else except at their respective poles. $D_C$ is the diffusion coefficient for CtrA (assumed equal to be for both forms).

This model was used to understand how the graded spatial distribution of CtrA and CtrAP species may exist and lead to the chemical compartmentalisation of the cell before the process of cell division begins. Chen et al. (2011) have only analysed one type of spatial configuration in their model- when the two forms of CckA are localised at different poles. Next we outline how Model A and Model B are "connected."

## Interaction between Network Models

In order to examine the different ways in which the networks parts may interact, Models A and B were combined using an intermediate species and these interactions were studied in the "combined" model. Similar to the study of BBC1 and BBC2 models described previously, here as well we considered two types of interactions between DivKP and DivL, each is studied in a separate variant of the combined model. In the first model variant, the inhibition of DivL by DivKP was assumed to be in the mass action regime, i.e. there is no uptake of DivKP in the reaction. In the second model variant, the binding of DivKP

and DivL was explicitly modelled to understand the effect of sequestration of both species in the DivKP-DivL complex. In both model variants, DivL is assumed to exist as a fixed pool containing an active and inactive form DivL and DivL$_i$, respectively. We describe how these interactions were incorporated next.

**Upstream interaction between DivL and DivK:** When the interaction between DivKP$_b$ and DivL is in the mass action regime (first model variant), the equations for DivL are:

$$\begin{aligned}\frac{\partial[DivL]}{\partial t} &= -k_{bi}[DivL] + k_{fi}[DivL_i] - k_5[DivKP_b][DivL_i] + D_D\frac{\partial^2 DivL}{\partial\theta^2}\\ \frac{\partial[DivL_i]}{\partial t} &= k_{bi}[DivL] - k_{fi}[DivL_i] + k_5[DivKP_b][DivL_i] + D_D\frac{\partial^2 DivL_i}{\partial\theta^2}\end{aligned} \tag{6.13}$$

where k$_{bi}$ and k$_{fi}$ are the basal interconversion rate constants between the inactive and active forms and k$_5$ is the rate constant associated with the inhibition of DivL by DivKP$_b$ (it must be noted that the interaction is hypothesised to occur only at the swarmer pole and we assume that is the case here as well, thus the bound form of DivKP is involved in the interaction) . D$_D$ is the diffusion coefficient for DivL (assumed to be equal for both forms).

In the second model variant, the interaction between DivK$P_b$ and DivL leads to sequestration in the complex [DivKP$_b$-DivL].

$$\begin{aligned}\frac{d[DivKP_b]}{dt} &= k_c(\theta)[DivKP_f] - k_p[DivKP_b] - k_{po}[DivKP_b]\\ &\quad -k_5[DivKP_b][DivL] + k_6[DivKP_b - DivL]\\ \frac{\partial[DivL]}{\partial t} &= -k_{bi}[DivL] + k_{fi}[DivL_i] - k_5[DivKP_b][DivL]\\ &\quad +k_6[DivKP_b - DivL] + D_D\frac{\partial^2 DivL}{\partial\theta^2}\\ \frac{\partial[DivL_i]}{\partial t} &= k_{bi}[DivL] - k_{fi}[DivL_i] + D_D\frac{\partial^2 DivL_i}{\partial\theta^2}\\ \frac{\partial[DivKP_b - DivL]}{\partial t} &= k_5[DivKP_b][DivL] - k_6[DivKP_b - DivL]\\ &\quad +D_{DivKP_b-DivL}\frac{\partial^2 DivKP_b - DivL}{\partial\theta^2}\end{aligned} \tag{6.14}$$

where $k_5$ and $k_6$ are the forward and backward rate constants for the formation and dissociation of the complex DivKP$_b$-DivL, respectively and $D_{DivKP_b-DivL}$ is the diffusion coefficient for the complex (the remaining parameters are the same as above).

**Downstream interaction between DivL and CtrA:** As previously mentioned, DivL is implicated in regulating the conversion of the phosphatase form of the enzyme CckA to its kinase form. Thus the concentration of CtrAP is an increasing function of DivL concentration. This interaction is incorporated into the downstream interaction of the combined model (in both variants) as follows: the "$k_{ph}$" term in the ODEs of CtrA species in the original Model B encompasses the total concentration of the kinase K (which represents the kinase from of CckA). In the combined model, we make a modification where K is now assumed to be a variable and modelled as a part of a fixed pool. This pool consists of two forms $K_o$ and K, interconverting between one another. Thus the total K species, $K_t$, is the sum of [$K_o$] and [K]. The conversion of $K_o$ to K is regulated by DivL. Thus the rate equation for K is given by the following ODE:

$$\frac{d[K]}{dt} = k_f[K_{total} - K][DivL] - k_r[K] \tag{6.15}$$

where $k_f$ and $k_r$ are forward and backward rate constants for the conversion of $K_o$ to K. (An equivalent way to modify the equations of CtrA and CtrAP would be to replace the K parameter with DivL/(c+DivL), where c is a constant). This modification reflects the regulation of "K" as an increasing function of the intermediate DivL. Thus PDEs governing the CtrA species would change to:

$$\begin{aligned}
\frac{\partial[CtrA]}{\partial t} &= -(Sw(\theta)(k_1[K]) + k_{pho})[CtrA] + (k_{dp}St(\theta) + k_{do})[CtrAP] \\
&\quad + D\frac{\partial^2 CtrA}{\partial\theta^2} \\
\frac{\partial[CtrAP]}{\partial t} &= (Sw(\theta)(k_1[K]) + k_{pho})[CtrA] - (k_{dp}St(\theta) + k_{do})[CtrAP] \\
&\quad + D\frac{\partial^2 CtrA}{\partial\theta^2}
\end{aligned} \tag{6.16}$$

where $k_1$ rate constant associated with phosphorylation of CtrAP by K. A preliminary sensitivity analysis was performed with the newly introduced parameters in the combined modified model.

Thus, the two variants of the combined model consist of the following equations:
1) Variant 1 (upstream interaction is in the mass action regime): (9), (11), (13) and (14)
2) Variant 2 (upstream interaction is via sequestration): Equations for all DivK species (except DivKP$_b$) in (9), (12), (13) and (14)

In both variants, the downstream and upstream interactions are examined in detail by tuning the appropriate interaction parameters. We examined the effects of the different localization patterns of enzymes in different phases of the cell cycle on the interaction between these network models.

## Dynamic Localization Model

In this part of the investigation, our goal was to understand the consequences of dynamic localisation of the enzymes on the interactions of the network, in the different phases of the cell cycle. In order to achieve this we employ the individual Model A and mainly focus on the dynamic localization of one enzyme in the network it describes- PleC. Evidence in the literature suggests that the spatial distribution and localization of PleC changes as the cell cycle progresses (García Véscovi et al., 2010). In the first phase, it is present at pole1; in the second phase it is distributed everywhere in the domain and in the third and subsequent phases it is localized at the opposite end or at pole 2. The enzyme DivJ is present at the stalked pole/pole 1 in all these phases (these localisation are depicted in Fig. 6.3). Therefore, we mainly vary the spatial distribution and localization of PleC. This was done as follows. Three additional entities were introduced into Model A: F, P and FP. F and P react to form the complex FP. The equations for these reactions are given by:

$$\begin{aligned}
\frac{\partial[F]}{\partial t} &= -k_f(\theta)[F][P] + k_{-f}[FP] + D_F\frac{\partial^2 F}{\partial\theta^2} \\
\frac{\partial[P]}{\partial t} &= -k_f(\theta)[F][P] + k_{-f}[FP] + D_P\frac{\partial^2 P}{\partial\theta^2} \\
\frac{\partial[FP]}{\partial t} &= k_f(\theta)[F][P] - k_{-f}[FP] + D_{FP}\frac{\partial^2 FP}{\partial\theta^2}
\end{aligned} \tag{6.17}$$

where k$_{f(\theta)}$ and k$_{-f}$ are forward and backward rate constants for the formation and dissociation of the complex FP, respectively and D$_j$ are the diffusion coefficients for each species "j". We assume that initially, the reaction between F and P is localised at pole 1. This

represents the first phase or phase 1. After a time period $t_a$, P is allowed to diffuse into the domain and the forward reaction constant $k_f$ is reduced (using an exponential function $e^{((ta-t)/c)}$) till it becomes zero. Thus the concentration of [FP] eventually becomes zero as well and only F and P are present at steady state. Time $t_a$ to $t_b$ represents phase 2 of the cycle. After time $t_b$, $k_f$ is turned "on" and the reaction between F and P is localised to the opposite region or the pole 2. This represents phase 3 of the cell cycle ($t_b$ to $t_f$). The freely diffusible form of DivKP binds to both P and FP. The bound DivKP is dephosphorylated which results in the release of $DivK_f$. The time period of each phase of the cycle is chosen to be long enough to allow all species concentration to reach steady state during each phase before proceeding to the next.

Equations of Model A were modified to incorporate these interactions:

$$\begin{aligned}
\frac{\partial[DivK_f]}{\partial t} &= -k_j(\theta)[DivK_f] + k_{p2}(\theta)[DivKP_b] + k_{po}([DivKP_f] + [DivKP_b]) \\
&\quad +k_d[CtrAP - CckAP] + k_b[CtrA - CckAK] \\
&\quad +D\frac{\partial^2 DivK_f}{\partial\theta^2} \\
\frac{\partial[DivKP_f]}{\partial t} &= k_k[DivK_b] + sw(\theta)(-k_b[DivKP_f] + k_u[DivKP_b]) \\
&\quad -k_p[DivKP_f][FP] - k_e[DivKP_f][P] - k_{po}[DivKP_f] + D\frac{\partial^2 DivKP_f}{\partial\theta^2} \\
\frac{d[DivK_b]}{dt} &= k_j(\theta)[DivK_f] - k_k[DivK_b] \\
\frac{d[DivKP_b]}{dt} &= k_p[DivKP_f][FP] + k_e[DivKP_f][P] - k_{p2}(\theta)[DivKP_b] - k_{po}[DivKP_b] \\
\frac{d[DivKP_p]}{dt} &= sw(\theta)(k_b[DivKP_f] - k_u[DivKP_b])
\end{aligned} \tag{6.18}$$

where $k_e$ and $k_{po}$ are binding constants for $DivK_f$ for P and FP, respectively, and $k_{p2}$ is the rate constant for the dephosphorylation of $DivK_b$. The remaining parameters are the same as before. In this analysis we focus on how the spatial distribution of the concentration of total [DivK] changes from one phase to the next.

### 6.2.3 Parameters

Different parameter sets are used in this study. We have employed both, generic parameter sets, in the cases where building blocks are examined, as well as specific parameters which are based on estimations from experimental data, in the cases where the concrete networks are studied.

**Building block Models:** In the first part of the study, we have analysed building block models which involve a number of kinetic and transport parameters. We have either used a "generic" parameter regime or a special parameter regime so that a a particular temporal behaviour could be examined. The aim of our investigations is to ascertain the qualitative differences in behaviour due to introduction of spatial effects and thus a range of parameters is chosen to reflect the behaviour we are trying to study. In the case of gradient spatial effects, a range of values are tested as inputs. When the models are localised, basal representative values are chosen to represent the diffusivity of the species, the relative width of the patch/subdomain and the length of the entire domain. Since we are comparing ODE models to PDE models, we directly study the effect of all these parameters on the behaviours of the models.

**Combination of building block models BBC1 and BBC2:** In model BBC1 a "generic" set of parameter values are employed. In the model BBC2, the upstream module is based on Model IV (the building block model) and hence a set of parameters that allows this model to exhibit bistability are chosen. Here again, the goal of our study dictates the choice of parameters. We are interested in studying the role of space- how localisation and diffusion affects the response of the system. Thus, the kinetic parameters reflect the qualitative behaviours we wish to investigate. The spatial parameters (patch width, diffusion coefficients) are varied in the investigation to ascertain their effects on the system.

***Caulobacter crescentus* network Models A and B:** The parameters chosen were based on those given in (Chen et al., 2011; Tropini and Huang, 2012). These parameters were estimated through experiments (which included fluorescence recovery after photobleaching) (Chen et al., 2011) or from experimental data obtained by studying the effect of enzymes with mutations affecting both their catalytic activities and their abilities to correctly localise spatially (Tropini and Huang, 2012). The parameters were non-dimensionalized based on the length and time scale of the cell and reactions. Since we utilise periodic boundary conditions in our model setting, the diffusion coefficients were scaled to reflect the equivalent value for a different length.

**Dynamic Localization Model:** We have utilised Model A for this study and again used the parameters in (Tropini and Huang, 2012). The parameters in the modified part of the model are based on this work as well. In the dynamic localisation study of enzymes, it is known that during the course of the cell cycle the length of the cell increases thus this would have an effect on the transport parameters. However, we do not considered a change in diffusion coefficient for the species from phase to phase- incorporating this effect could be in the scope of a future study. All parameter values are shown in the Appendix E.

**Numerical Method:** The partial differential equations were discretized using finite difference equations and the results were checked by doubling the discretization. All simulations were performed in MATLAB using ode15s. The bifurcation analysis was performed using MATCONT.

## 6.3 Results and Discussion

The aim of this investigation is to build a bridge towards understanding the spatial organization and control of signalling networks regulating the cell cycle in *Caulobacter crescentus*. To achieve this we divided the investigation in two parts- in the first part we dissected the spatial regulation and control of signalling in a suite of building blocks models. In the second part, the insights obtained from investigating the building block models are extended to the study of the concrete *Caulobacter* signalling networks (Fig. 6.4).

The building blocks models are centered on the modification cycle with a bifunctional enzyme, which is a basic enzymatic building block found in the cell cycle networks. In our analysis, we start with the simplest description of this module and in a step-wise fashion incorporate different signalling interactions- adding one layer of complexity at a time. This gives rise to a suite of distinct models (Fig. 6.2). Each model is examined in light of different spatial effects; these are gradients, localization or compartmentalization of signalling entities and diffusion. The interactions that were incorporated into the models along with the spatial effects examined reflect the temporal and spatial control mechanisms observed in the cell cycle networks.

Thus, by investigating spatial control of signalling in a hierarchy of models, we were able to i) systematically analyze the consequence of different types of signalling interactions in each model temporally, ii) in a transparent way attribute the role of different spatial effects in each model and iii) develop a platform to investigate the temporal and spatial control mechanisms in the concrete cell cycle networks. We start by discussing the analysis of the building block models.

### 6.3.1 Analysis of building block models

The effects of space, specifically gradient signals and localization control, were examined in each of the building block models I, II, III, IV and V. First, the temporal response of each model was examined, i.e. when diffusion was not present in the cycle. The signal transduction is local in this case and may be described by the ODE model. The temporal response acted as the reference case. Next, diffusion of species in the cycle is introduced and the response is contrasted against the reference case. The discussion of model analysis is presented in a sequential order.

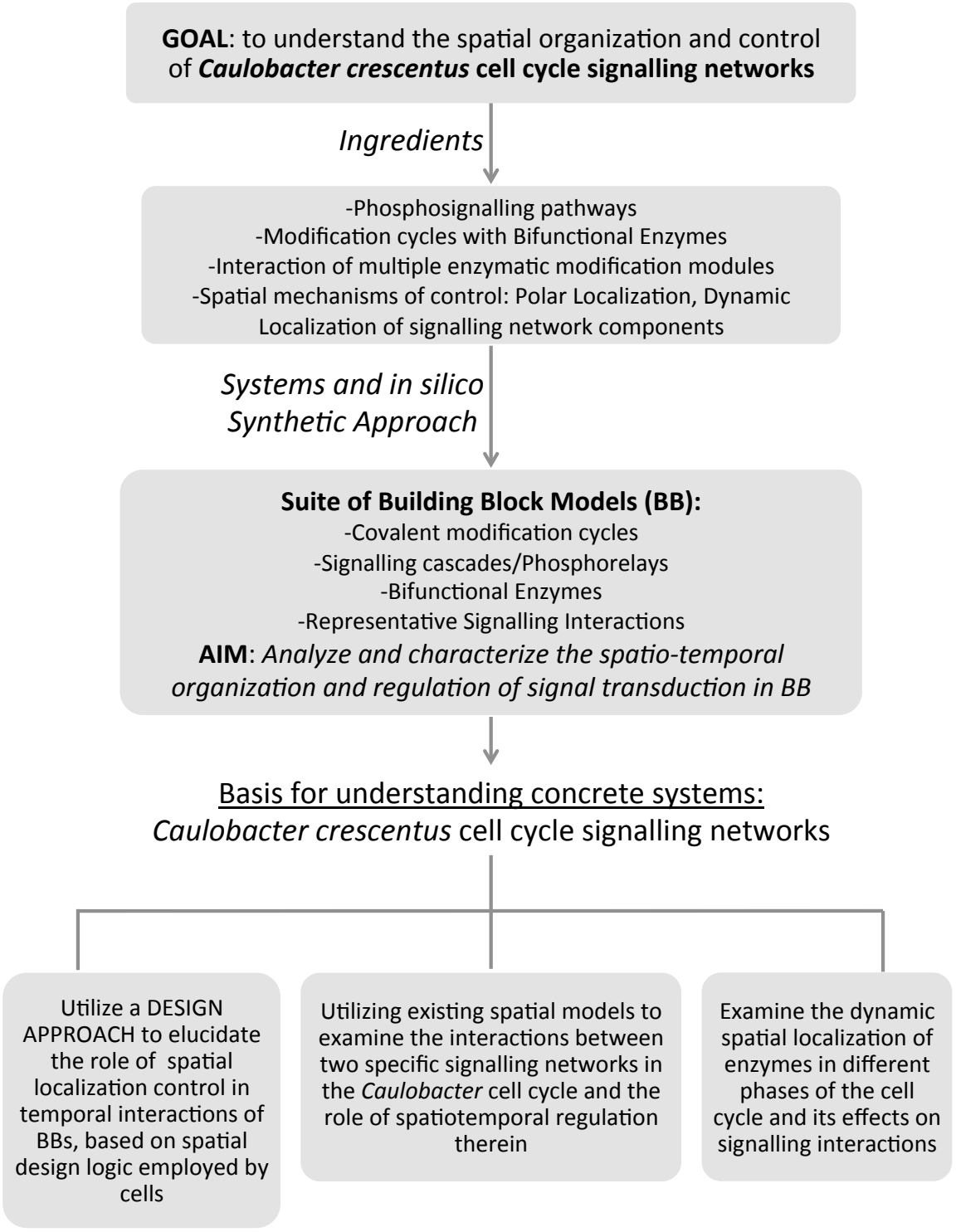


Figure 6.4: **From building block modules to signalling networks in the *Caulobacter* cell cycle.** A schematic outlining the aim of this study and the approaches employed

## Model I

We start with the most basic description of the bifunctional enzyme modification cycle. The description of the cycle is similar to the covalent modification cycle module except that here, one enzyme E catalyzes both the forward and reverse modifications of X and $X^*$. Hence, we may expect some differences in the response when we examine the bifunctional cycle.

First, we examine the case where the enzyme has a spatially graded distribution. Here and in the analysis of the rest of the models, we examine the degree of change in the spatial variation of the species steady state concentration profiles (relative to the reference case) when diffusion is introduced. In particular, we observed whether the degree of spatial variation increases ("sharpens") or decreases (becomes "weaker") as well as if any accompanying qualitative changes are also present.

**Graded Signals**

***Temporal/Reference Case*:** The temporal response of the model was first examined, i.e. when no diffusing species were present. For a spatially graded enzyme, the spatial concentration profiles of X and $X^*$ are also graded (Fig. 6.5). Here we note that the direction of the spatial gradient of the substrate species profiles is determined by the spatial distribution of one enzyme only. Furthermore the profiles are distributed in the same direction (co-aligned with one another) and counter-aligned with that of the enzyme. This is in contrast to the cycle with two separate enzymes, where different combinations of the spatial distributions of the two enzymes are possible. For example, the enzymes may be co-aligned or counter-aligned with one another. Thus, this would result in a number of possible combinations of the spatial distribution of the substrate species profiles as well. This possibility is constrained in the bifunctional cycle due to the presence of a single enzyme.

Next, each species in the cycle is allowed to diffuse and the consequences are examined.

***Diffusion of substrate species*:** When either X or $X^*$ are allowed to diffuse, the resulting spatial concentration profiles of both X and $X^*$ lose spatial variation and become flat (Fig. 6.5). Here again, this result is in contrast to the case when two separate enzymes are driving the catalysis of the cycle, where diffusion of X results in a sharper $X^*$ spatial profile. When both X and $X^*$ are allowed to diffuse, the spatial concentration profiles of both species become weaker.

***Diffusion of enzyme*:** Next we examined the case when the enzyme is diffusible. As the diffusion coefficient value of the enzyme is increased, the spatial variation of the concen-

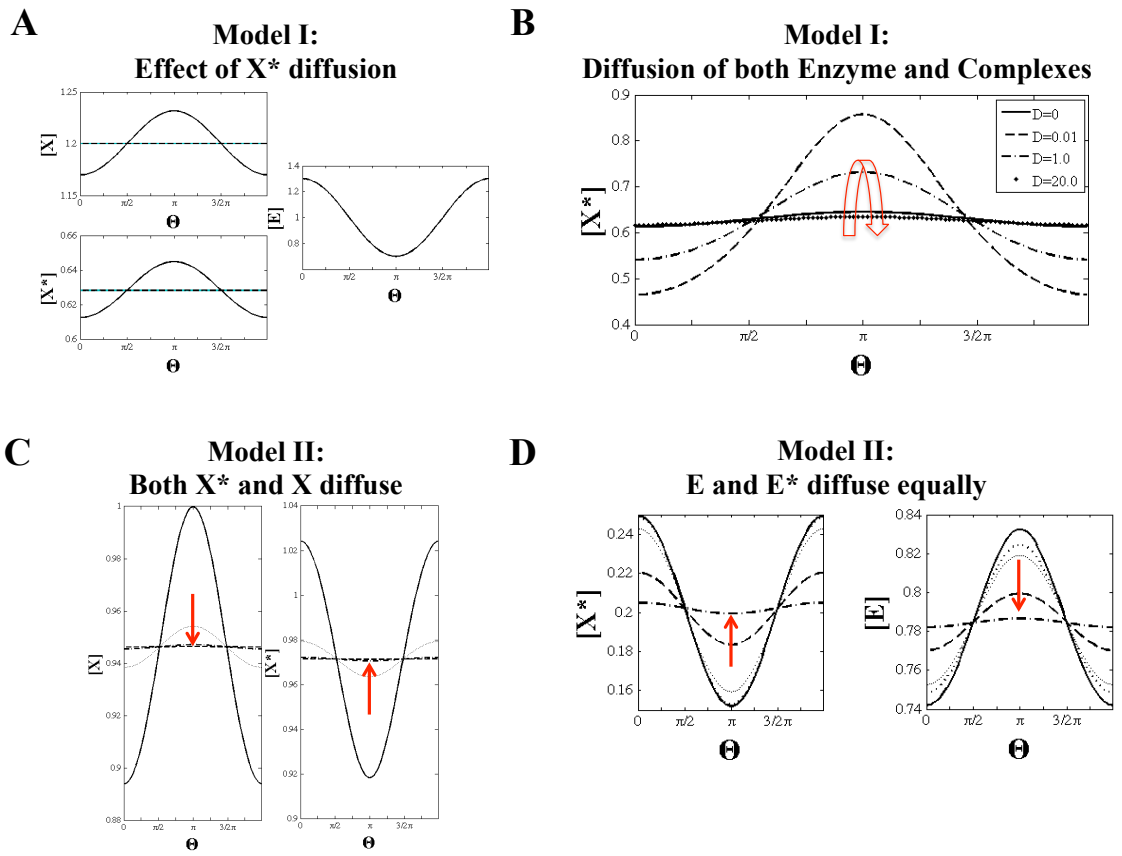


Figure 6.5: **The effect of graded signals and diffusion of species on Models I and II.** Models I and II are subjected to a graded enzyme/signal (in the form of a+bcos$\theta$). The concentration profiles with respect to $\theta$ are shown. (A,B) Model I: No diffusion case (solid line): Both X and X$^*$ are counter-aligned with E. (A) If X$^*$ diffuses (dashed line) the spatial concentration profiles of both X and X$^*$ lose spatial variation and become flat. (B) If both the enzyme-substrate complexes and the enzyme diffuse (equally), the spatial profile of X$^*$ shows non-monotonic behaviour: it has sharper spatial variation for low diffusion coefficient values and relatively less sharp spatial variation for high diffusion coefficients. The arrow denotes the direction of increasing diffusion coefficient values. (C,D) Model II, No diffusion case (solid line): X and X$^*$ follow the heterogeneity of the spatial profiles of E and E*, respectively. (C) When both X (left) and X$^*$ (right) diffuse, as the diffusion coefficients increase, their spatial concentration profiles become weaker. (D) When E and E$^*$ forms of the enzyme equally diffuse, the concentration profiles of both X and X$^*$ become spatially weaker. The direction of increase of diffusion coefficients is denoted by the arrow.

tration profiles of all the species becomes weaker. This is expected because the enzyme is the only source of spatial information in the model. Thus the weakening of spatial variation of its own spatial profile would consequently weaken those of other species in the cycle. Next we examine cases where the complex is diffusing along with either the substrate or the enzyme. Our analysis of the covalent modification cycle in the Chapter 4 revealed that examining diffusion of complexes could have important consequences for the cycle response.

We expect this to be the case here as well.

***Both substrate and complex diffuse*:** If X and the complex EX equally diffuse, then as the diffusion coefficient values are increased, the spatial concentration profile of $X^*$ becomes sharper. The profiles of X and both complexes become weaker. If $X^*$ and the complex [$EX^*$] both equally diffuse, then spatial concentration profiles of $X^*$ and both the complexes become weaker and the profile of X becomes sharper, as the diffusion coefficient values increase. In both these cases, the result is different from when the single substrate species is diffusing.

***Both enzyme and complex diffuse*:** Here we consider the cases where the enzymes and either or both complexes [EX] and [$EX^*$] diffuse equally. In both cases, as the diffusion coefficient values are increased, the spatial concentration profile of the enzyme becomes weaker and those of both complexes become homogenous. The effect on the profiles of X and $X^*$ is non-monotonic- for low diffusion coefficients the profile is sharper than when there is no diffusion. As the diffusion coefficients are increased both the profiles become weaker (Fig. 6.5).

These results illustrate that the diffusion of the complexes plays a non-trivial role. It has different consequences for the spatial profiles of the species than when only substrate or enzyme is alone diffusing. Taken together, our results show the different ways in which diffusion of species may alter the spatial profiles of the cycle component. Furthermore the findings reveal differences in responses between a cycle with two separate enzymes and a single bifunctional enzyme (modelled in this way) when spatial effects are present.

**Localization/compartmentalization of signalling entities:** We briefly discuss the effects of localization/compartmentalization of signalling entities here. The scenario we examine here (and in the rest of the cases) is that the modification cycle is localized in a single sub-domain. The response of the cycle is then compared to the case when substrate species are allowed to diffuse out of the localized patch. These scenarios are akin to cases in the cell where an entire signalling pathway may be localized in a single compartment and species may be transported out of the compartment (to carry out downstream interactions for example).

In Model I, in the scenario where all cycle species are present in a single sub-domain, the results are similar to the ODE case. Next we considered the case where X and $X^*$ diffuse. As expected, $X^*$ concentration in the overall spatial domain is diluted due to its spreading, resulting in the local concentration of $X^*$ in the sub-domain to also be lower.

So far, the results discussed are for when the model is in the "generic" parameter

regime. The next step was to examine this model in a special parameter regime- the Goldbeter Koshland parameter regime which would allow the model to exhibit an "ultrasensitive" response (Goldbeter and Koshland, 1981). However, it has been shown in (Straube, 2012) and (Ortega et al., 2002) that a simple extension of the Goldbeter Koshland model to the case of bifunctional enzymes (specifically modelled in this manner) would not result in an ultrasensitive response. Very briefly, the reason for this is that there is a single conservation relationship for the total amount of the bifunctional enzyme. As a result, the steady state concentration of the modified substrate does not depend on the total enzyme concentration. Thus, this implies that additional factors must be present in the model in order for it to exhibit an ultrasensitive response. This is discussed in the latter part of the next subsection.

## Model II: Examining feedforward control

Having gained a preliminary understanding of how graded enzyme distributions combined with diffusion affect the basic bifunctional modification model, we move on to examining Model II. In contrast to Model I, in Model II an external signal (S) controls the kinase ($E^*$) and phosphatase (E) activities of the bifunctional enzyme. Thus, this feedforward regulation creates an additional avenue for tuning the activities of the two different forms of the enzyme as well as controlling the spatial distribution of the substrate species concentration profiles (making this cycle more similar to the case where separate enzymes are present). We first consider the case when the external signal is graded.

**Effect of Graded Signals**

We begin by analyzing Model II in the "generic" parameter regime. First, the case where there is no diffusion is discussed. The spatial concentration profiles of $E^*$ and $X^*$ are co-aligned with the spatial distribution of the signal and that of E and X are counter-aligned (Fig. 6.5). Next, the diffusion of species is examined.

***Substrate species diffuse*:** When X diffuses, the spatial concentration profile of $X^*$ becomes stronger and those of the complexes change direction or "flip" (they change from being counter-aligned to being co-aligned with the signal). The profile of X itself become homogenous (the reason for this is explained in Appendix C).

When $X^*$ diffuses, it itself becomes homogenous and the spatial profiles of X and the complexes have increased spatial variation. Finally, when both X and $X^*$ diffuse (Fig. 6.5), the profiles of X and $X^*$ become weaker and eventually flat as the diffusion coefficients

increase. On the other hand the profiles of both complexes become stronger. These results have many parallels to those in the cycle with separate enzymes that are counter-aligned.

***Diffusion of Enzymes*:** The effects of diffusion of E and $E^*$ are examined next. Two cases are considered- 1) equal diffusion of both forms and 2) one form of the enzyme may be more diffusible than the other. In the latter case, one form of the enzyme is made to diffuse weakly while the other form has a higher diffusion coefficient value. The differences in diffusivity of enzyme forms is a hypothetical possibility. When both enzyme forms are equally diffusible, as we would expect, the spatial profiles all species become weaker (Fig. 6.5). If the diffusion is unequal, then the spatial profiles of X and $X^*$ change very slightly (similar qualitative results are obtained in the limiting case where only one of enzyme form is diffusing). Thus there is a difference in the consequence for the alteration of the spatial profiles of cycle components when unequal and equal diffusivities of enzyme forms are explicitly considered.

Taken together, these findings again highlight how the presence of diffusing species alters the spatial profiles in different ways.

In the cases examined so far, the responses of Model I and II are different. Thus, these findings also reveal the consequences of incorporating a feedforward control by an external signal into the cycle, when diffusion is both, absent and present. Furthermore, the effect on spatial variation in Model II has more parallels (than Model I) with the case when separate enzymes are present (however in certain regimes, where there limitations due to having one enzyme pool only, differences between the two cases are revealed).

So far, Model II has been examined for a generic parameter regime. The regulation of the enzyme forms by an external signal in Model II enables it to exhibit an ultrasensitive response in a particular parameter regime. This is in contrast to Model I where this kind of behaviour is absent. Next, we focus our analysis on this temporal behaviour and examine it in light of different spatial perturbations. Based on our findings in Chapters 4 and 5 we expect that this behaviour will be significantly distorted. The analysis was carried out as follows: the temporal behaviour is analyzed for a graded input signal (when none of the species diffuse). Next, the diffusion of one or two species is introduced and the effect on the temporal behaviour is investigated. We separately examine another type of spatial effect- the species of the cycle are localized in a patch/subdomain of the entire spatial domain. Either X or $X^*$ is allowed to diffuse and the affect on the ultrasensitive response was examined.

## Model II: Diffusion affects the Ultrasensitive response

Before the results are discussed, a note is made about a slight modification in Model II. Straube (2014) has investigated how ultrasensitive behaviour may be achieved by the modification of the basic bifunctional enzyme covalent modification model. Based on the model proposed in that paper, Model II was adjusted to achieve a sharper ultrasensitive response (by taking into account the conservation condition for the signal; the relevant equation is shown in Appendix E). Both the original and modified models exhibit an ultrasensitive response. Since the response is more sensitive in the case of the modified model, it is utilized for the rest of the analysis. The results obtained hold true for both versions of the model.

**Graded Signals**

***Temporal response*:** First, the temporal response of the model is examined. The model is subjected to a graded external signal and we examine the case when none of the species are diffusing. We find that $X^*$ exhibits a spatial switch-like profile. Thus, the temporal switch properties of the module are present in the spatial context as well. Next, the effect of diffusion of species in the cycle is analysed.

***Diffusion of cycle species*:** When X diffuses, the spatial switch-like profile of $X^*$ is enhanced (Fig. 6.6). When $X^*$ itself is diffusing, the spatial switch-like profile is lost and the profile of $X^*$ becomes graded. When both forms of the enzyme were equally diffusible the spatial switch-like profile is again lost- as the diffusion coefficient is increased, the $X^*$ spatial concentration profile becomes graded and eventually flat for high diffusion coefficients (Fig. 6.6). A similar result is seen for the case when X and $X^*$ both diffuse. Thus diffusion of species in the cycle, results in the distortion of the spatial switch profile of $X^*$. Diffusion (even moderate) may either enhance or abolish this response.

**Localization of cycle components:**

Next, the effects of localization and diffusion on the ultrasensitive response are examined. The cycle components are initially localized together in a sub-domain (of width w) in the spatial domain. Different widths of the localized patches are examined: width w of the localized module is 1) 2%, 2) 20% and 3) 90% of the length of the spatial domain. First the case where none of the species are diffusing is examined. For all three widths, the resulting sensitivity or input-output curve ($[X^*]$ vs [S]) is sharp (and the same as that of the ODE case when the cycle species are uniform everywhere in the spatial domain) (Fig. 6.6). Next the case when species are diffusing into the spatial domain is examined.

***Diffusion of species*:** We analyse the effect of X or $X^*$ or both diffusing on the input-

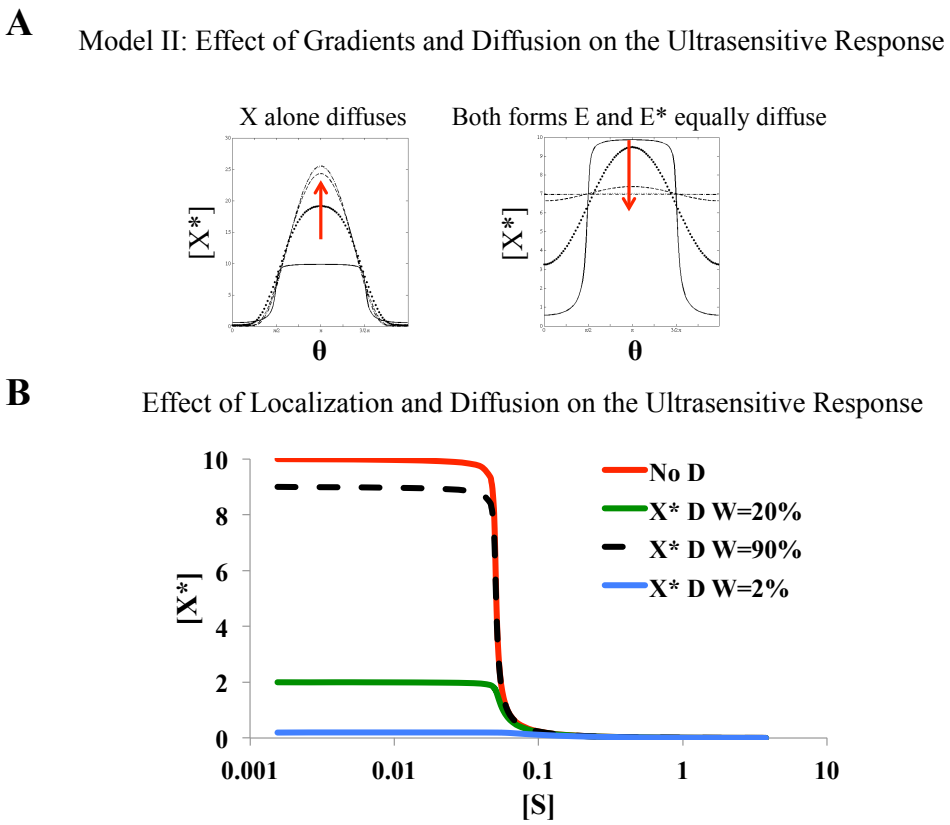


Figure 6.6: **Spatial perturbation of the Ultrasensitive Response in Model II.** (A) Perturbation by an external graded signal and diffusion of species: When there is no diffusion $X^*$ displays a switch-like spatial concentration profile (solid line). When X diffuses (left hand side plot) the spatial switch-like profile is enhanced. When E and $E^*$ both diffuse equally, the switch-like profile is destroyed. The arrow denotes the direction of increasing diffusion coefficient values. (B) Perturbation by localization and diffusion on the input-output (I/O) relationship between $[X^*]$ and external signal [S] is shown. Both enzyme forms and X and $X^*$ are localized together in one patch of the spatial domain. I/O curves are shown here for when none of the species diffuse (red line) as well as when species were allowed to diffuse. Three separate cases are shown for when $X^*$ diffuses out of the localized patch: when the width, W, of the localized patch is 20% of the length of the domain (green), W=90% (dashed black) and when W=2% (blue). The sensitivity of the switch drastically reduces as the width of the localized patch becomes smaller.

output curve. If these species diffuse, we find that the sensitivity of the curve is affected- the $X^*$ concentration becomes less sensitive to small concentration changes in the input. Furthermore, we observe that the degree to which the sensitivity of the response is reduced is dependent on w. We find that smaller the width of the localized patch, greater is the decrease in the sensitivity of the input-output curve (Fig. 6.6).

The decrease in sensitivity of the curve maybe explained as follows- one of the factors instrumental in achieving an ultrasensitive response (as predicted by a Goldbeter-Koshland

type model (Goldbeter and Koshland, 1981)) is that the enzymes mediating the reactions must be acting at saturation. Now, when species are diffusing, the spreading of X or $X^*$ or both in the spatial domain results in the lowering of the total X species in the localized patch (this is termed the "dilution effect" studied in detail in Chapter 5). This in turn would affect whether the enzymes would act at saturation. Furthermore as the width (of the localized patch) decreases, the dilution effect becomes stronger. If the localized patch is large enough (i.e. as illustrated by the w=90% case), the dilution effect may be countered enough so that there is a smaller decrease in the sensitivity of the response to the input (Fig. 6.6).

Taken together, our findings reveal the different ways in which diffusion combines with two different spatial effects and distorts the ultrasensitive behaviour in this model of the bifunctional cycle.

## Model III: Examining feedback control

In Model III, in addition to an external signal regulating the opposing activities of the enzyme, a positive feedback interaction from $X^*$ to $E^*$ is also present. In this part of the analysis, we examine the effect of this feedback mechanism in light of different spatial effects. The presence of the feedback interaction results in a thresholding effect, which arises through a transcritical bifurcation in a particular parameter regime (Fig. 6.7). The transcritical bifurcation has been analysed in detail in Chapter 3. In this type of bifurcation, for a particular range of signal values, the steady state concentration of $X^*$ is non-zero and when the signal crosses a particular threshold value (i.e. $S > S_{critical}$), the steady state concentration of $X^*$ becomes zero. In a manner similar to the analysis in Model II, this thresholding effect is examined in light of different spatial perturbations.

**Thresholding response is affected by graded signals and diffusion:** The spatial perturbations were introduced in the same order as before. First the model was subjected to a graded signal input when the model was in the transcritical parameter regime. The case where none of the species are diffusing is discussed next.

***Temporal response*:** We started by examining three different types of signal ranges which either straddle the threshold or critical value or do not include it.

*Case 1*: The input gradient is such that $S < S_{critical}$ in all parts of the domain. When none of the species diffuse the profile of $X^*$ is graded and non-zero at steady state (Fig. 6.7).

*Case 2*: If S exceeds $S_{critical}$ everywhere in the domain then the entire spatial profile of $X^*$

is at zero steady state.

*Case 3*: The signal input gradient is such that $S > S_{critical}$ in certain parts of the domain and $S < S_{critical}$ in others. If none of the species diffuse, a thresholding effect in spatial profile of $X^*$ is present- in some regions of the domain the spatial concentration profile of $X^*$ is zero and in others it is graded and non-zero at steady state (Fig. 6.7). This illustrates that the thresholding effect is also present for a gradient as expected.

***Diffusing species are present*:** Next the diffusion of species is examined in each of these cases. As expected, in Case 1 when species in the cycle are diffusing, while the spatial profile of $X^*$ is modulated, it remains at a non-zero steady state (Fig. 6.7). In Case 2, the entire spatial profile of $X^*$ remains at zero steady state value if any of the species in the cycle are made to diffuse.

*Case 3*: Now we consider the case where the signal values straddle the threshold point. If X is diffusing, the thresholding effect is lost from the $X^*$ spatial profile and it becomes sharply graded.

If $X^*$ diffuses, the profile of $X^*$ itself becomes flat and the concentration of $X^*$ reduces to a very low value but remains non-zero. Similarly, if both X and $X^*$ are diffusing equally, the profile of $X^*$ becomes weaker and eventually flat (but is non-zero) as the diffusion coefficient values are increased (Fig. 6.7). As would be expected, equal diffusion of both enzyme forms also results in the loss of the thresholding effect in the spatial profile of $X^*$.

Thus we see in all these cases, that the thresholding effect is manifested in the spatial profile in the present of gradient signals and when diffusing entities are present in the cycle, this effect is lost. Next, we will examine the effect of localization on this switching response.

***Effect of localization and diffusion*:** We first examine the case where the input and cycle components are localized in one patch (of width w) in the spatial domain. Naturally, the profile of $X^*$ is also localized and at a non-zero steady state in the localized region. Next, we examine the effect of diffusion of species (Fig. 6.7). We start by considering the case in which the width of the sub-domain is small. If X alone or both X and $X^*$ are diffusing, the steady state concentration of $X^*$ becomes zero everywhere in the domain. Here again the dilution effect plays a role. As a result of the decrease in the availability of substrate in the localized patch, the cycle is pushed beyond the transcritical threshold. When $X^*$ itself diffuses, its concentration becomes relatively small but its steady state concentration is non-zero. Thus, the transcritical threshold is not crossed in this case.

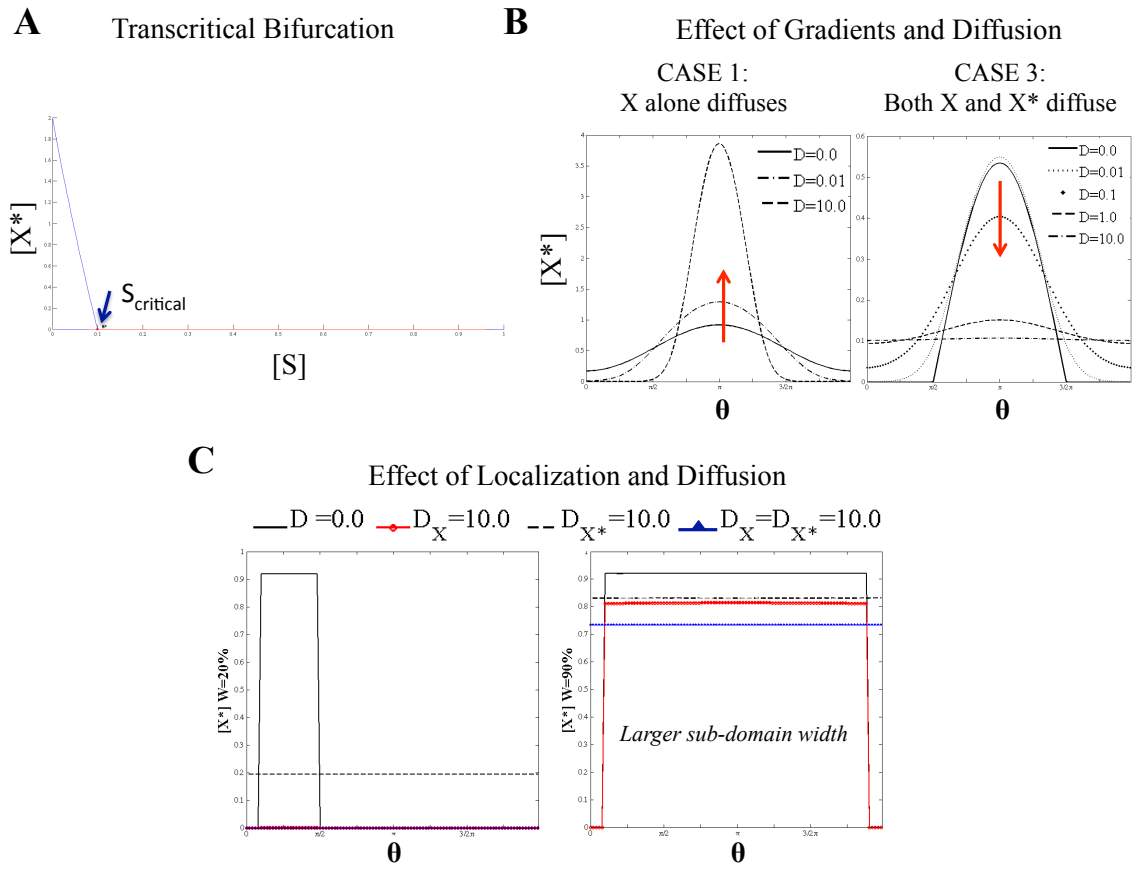


Figure 6.7: **Spatial effects and the transcritical bifurcation in Model III.** (A) A transcritical bifurcation curve is shown here; X* concentration is plotted against the bifurcation parameter- [S]. The concentration of X* is zero when $[S] > [S_{critical}]$. (B) For a graded input signal: (LHS plot) Case 1: If $[S] < [S_{critical}]$ (and none of the species diffuse (solid line)) the spatial concentration profile of X* is graded . When X diffuses, the spatial profile of X* becomes sharper (RHS plot) Case 3: $[S] > [S_{critical}]$ in some region of the domain and $[S] < [S_{critical}]$ in other regions: When there is no diffusion (solid line), a "thresholding" effect is seen in the spatial concentration profile of X*- in some part of the domain concentration the profile is zero and in other parts it has non-zero steady state values. When species are allowed to diffuse, this thresholding effect is lost from the spatial profile. The case of X and X* diffusing is shown. The arrow indicates the direction in which the diffusion coefficient increases. (C) The transcritical behaviour is perturbed by localization and diffusion. The species in the model are localized together in one sub-domain. (LHS plot) The width of localized patch is 20% of the domain length. When none of the species diffuse, the profile of X* has a non-zero amplitude at steady state. When either X or both X and X* diffuse (red and blue lines, respectively) the concentration of X* is zero at steady state. When X* alone diffuses (dashed lines) the profile of X* is homogenous in the spatial domain and at a non-zero steady state. (RHS) The width of localized patch is 90% of the domain length. When X* or X or both X and X* diffuse the profile of X* maintains a non-zero steady state. This case illustrates how a localized region with large enough width can counter the dilution effect (see main text) and prevent the response from being pushed into the transcritical regime.

When a larger width of the localized patch is examined, we find that if X or X* or both diffuse, the amplitude of X* decreases but remains at the non-zero steady state. Hence, a

larger width may counter the dilution effect enough so that the cycle is not pushed beyond the transcritical threshold. Overall, we find that the interplay of localization and diffusion has varying effects on the thresholding effect arising through a transcritical bifurcation in this model.

## Model IV: Examining the bistable response

Model IV is distinct from the previous models; in addition to the feedback and feedforward interactions it contains an additional interaction between X and E (which carries out the phosphatase activity). X inhibits the E form of the enzyme by sequestering it in a complex. When examined in a particular parameter regime, this model is found to exhibit a bistable response (the bistable switch has been discussed in detail in Chapter 3). For a particular range of signal values, S1<S<S2, the model has three steady states, two of which are stable (the bifurcation diagram is shown in Fig. 6.8). Next, we discuss how the bistable behaviour may be perturbed by the introduction of spatial effects.

**Bistable switch is distorted by gradients and diffusion**

***Temporal response*:** We start by examining the temporal case; the model is subjected to different graded signal inputs and all species are non-diffusible. The initial conditions for all substrate species are chosen such that they are on the higher branch steady state (i.e. corresponding to S<S1 values). We examine this response for various ranges of signal values.

*Case 1*: If the signal S is graded and the local values of the signal in the spatial domain never exceed S2, then the resultant spatial concentration profile of $X^*$ is also graded, and mirrors the signal (Fig. 6.8).

*Case 2*: However if the signal values exceeded S2, then a spatial switch-type profile is seen for $X^*$. In one part of the domain, the concentration profile is on the lower branch and in another part of the domain $X^*$ concentration profile is on the higher branch steady state.

*Case 3*: A switch-like profile is also seen when S1<S<S2 (i.e. S is completely in the bistable region). However this depends on the initial conditions chosen. If the initial conditions are chosen such that in one part of domain the profile of $X^*$ is on the lower branch and in the other its concentrations are on the higher branch- then a spatial switch-like profile is seen for the given signal (Fig. 6.8). Otherwise, if the initial conditions are spatially uniform then the result is a profile reflecting the heterogeneity of the signal.

***Diffusing species are present*:** Next diffusion of both species X and $X^*$ is considered.

In Case 1, the profile of $X^*$ becomes weakly graded (Fig. 6.8). In Case 2, $X^*$ spatial profiles become flat and the spatial switch like profile is lost. For Case 3, when the initial conditions are heterogenous, the switch-like profile is again lost and the profile is weakly graded (Fig. 6.8). In summary, diffusion of substrate species results in the loss of the switch-like spatial profile.

**Examining the effects of localization and diffusion**

Now we examine the effect of localization and diffusion on the bistable switch. First, the signal and cycle components are localized together in a patch in the spatial domain and the case where none of the species are diffusing is analysed. We consider a case in which the width is W=20% for the localized region. If the range of S values is in either of the monostable regions ($S < S1$ or $S > S2$), then, the steady state of $X^*$ also corresponds to the higher or lower branch values, respectively. If S is such that $S1 < S < S2$, then depending on the initial conditions, $X^*$ would reach a steady state concentration corresponding to either the higher branch or the lower branch (Fig. 6.8).

***Diffusing species are present*:** Next, either or both X and $X^*$ are allowed to diffuse out of the localized patch. For the above signal values, when $X^*$ diffuses or when both X and $X^*$ are diffusing, $X^*$ profile becomes flat and homogenous in the domain. The concentration of $X^*$ reduces to a very low concentration (closer to the lower branch $X^*$ concentration). When X alone diffuses, $X^*$ concentration becomes very low in the localized region. In all these cases, $X^*$ and hence the total amount of X species, $[X_{total}]$, is reduced in the localized patch.

It was shown through mathematical reasoning (in Chapter 5), that when substrate species are allowed to diffuse, the conservation condition for $X_{total}$ is perturbed by a factor which is equivalent to the length of the domain outside the localized patch ($L_{outside}$) multiplied by the concentration of $X^*$. If the term $L_{outside}$ is very large, mathematical reasoning of this kind suggests that this would result in the loss of the bistable response. However if the term were small enough, for example if the width W of the localized patch were 90% of the domain length, the cycle would still be able to exhibit the bistable response (Alam-Nazki and Krishnan, *in preparation*).

Different classes of models may exhibit a bistable response. So far only one type of model has been discussed (Model IV)- in this class of models, sequestration plays an instrumental role in bringing about the bistable response. Another class of model that also exhibits the bistable response (and which is well known) is the model with a strong enough non-linear positive feedback. This type of model was also analyzed by us. The model was

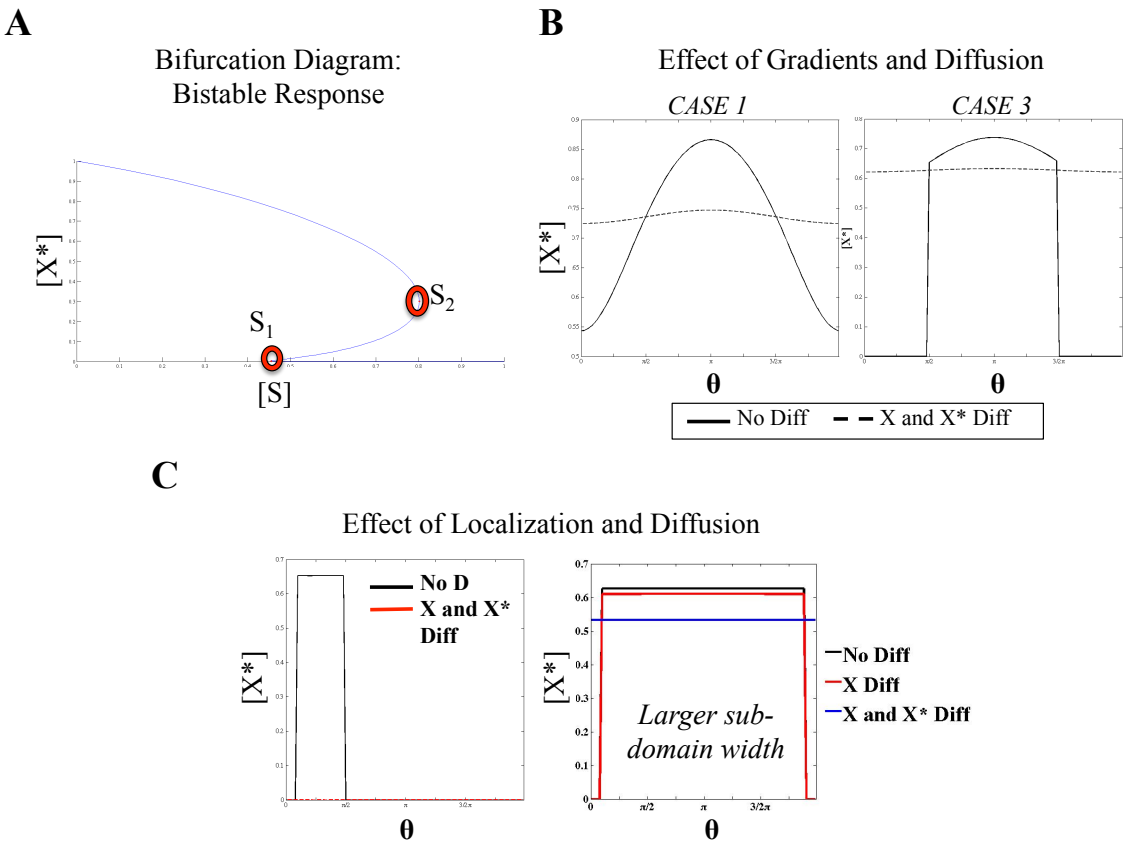


Figure 6.8: **Spatial effects in Model IV: distortion of the bistable response.** (A) A bifurcation curve is shown for $X^*$ with respect to the parameter [S]. Critical values S1 and S2 are labeled. (B) The bistable response is perturbed by a graded external signal. (LHS plot) In*Case 1* S<S2. When none of the species diffuse (solid line), the profile of $X^*$ mirrors that of the graded signal. When both X and $X^*$ diffuse, the profile of $X^*$ becomes weaker (dashed line). (RHS plot) In Case 3 S1<S<S2 (for heterogenous initial conditions): The concentration profile of $X^*$ shows a spatial switch-like characteristic when none of the species diffuse (solid line). When both X and $X^*$ diffuse (dashed line) this switch-like character is lost and the profile is weakly graded. (C) Perturbation by localization and diffusion: All species are localized together in one patch of the spatial domain. When none of the species diffuse (black line) the profile of $X^*$ has an amplitude commensurate with the higher steady state branch. (LHS plot) If both X and X* diffuse, the concentration of $X^*$ reduces to a very low value (near the lower steady state branch). (RHS plot) In the case where the width of the localized patch is larger, diffusion of species (X (red line), X and $X^*$ (blue line)) does not result in loss of bistability (the second steady state is not shown in the diagram). The underlying reasoning is related to mitigating the dilution effect (discussed in main text).

perturbed in a similar way: by introduction of spatial effects (gradients, localization and diffusion) and the effect on the bistable response was examined. The results obtained for this class of model qualitatively mirrored the ones obtained for the model discussed in this section. A snapshot of the results is shown in Appendix E.

## Model V: Feedforward regulation by two external signals

The last model that was analysed, Model V, differs from the previous models. In this model, two separate external signals, S1 and S2, regulate the bifunctional enzyme. S1 binds to E and the resulting complex S1E catalyzes the conversion of X to $X^*$. S2 binds to E and the complex S2E catalyzes the conversion of $X^*$ to X. The presence of two different signals (as opposed to one) allows for greater control over the different activities of the enzyme. Furthermore, if the signals are present in different locations, it allows the enzyme to exhibit distinct activities, one in each separate spatial location. We now discuss the effect of different spatial perturbations on the response of the model.

**Examining the effect of gradients and diffusion**

***Temporal response*:** First, the temporal response of the model is analysed when it is subjected to graded external signals. The model is in the generic parameter regime. Different spatial distributions of the signals are examined. The signals, S1 and S2, may be co-aligned or counter-aligned with one another or one may be graded and the other may be homogenous (this is similar to analysis done for the covalent modification cycle module in Chapter 4.

***Diffusing species are present*:** The response of the model when species were allowed to diffuse is discussed next. For all three scenarios of spatial distributions of S1 and S2, diffusion of X results in the sharpening of the $X^*$ spatial concentration profile (Fig. 6.9). If $X^*$ is diffusible, then its spatial profile becomes homogenous. These results are parallel to the ones in Model II. However, for different scenarios of spatial distribution of signals, diffusion of enzyme has varying effects. If the signals are counter-aligned or (only S1 is graded), then there is a negligible change in the spatial profile of $X^*$. However, we find that if the signals are co-aligned then the spatial profile of $X^*$ may be weaker or stronger and this depends on the balance of the relative gradients of the two signals. If the relative gradient of S1>S2 then diffusion of E results in the slight weakening of the spatial profile of $X^*$. For the opposite case S1<S2, when E diffuses the concentration profile of $X^*$ becomes spatially stronger.

Thus, here we see that different spatial distributions of the resultant substrate species are possible. Here again, the presence of diffusion can alter the spatial profiles of the species in the cycle.

***Examining the effect of localization and diffusion*:** As previously mentioned, in Model V, the presence of two different signals enables greater control over the activities of the en-

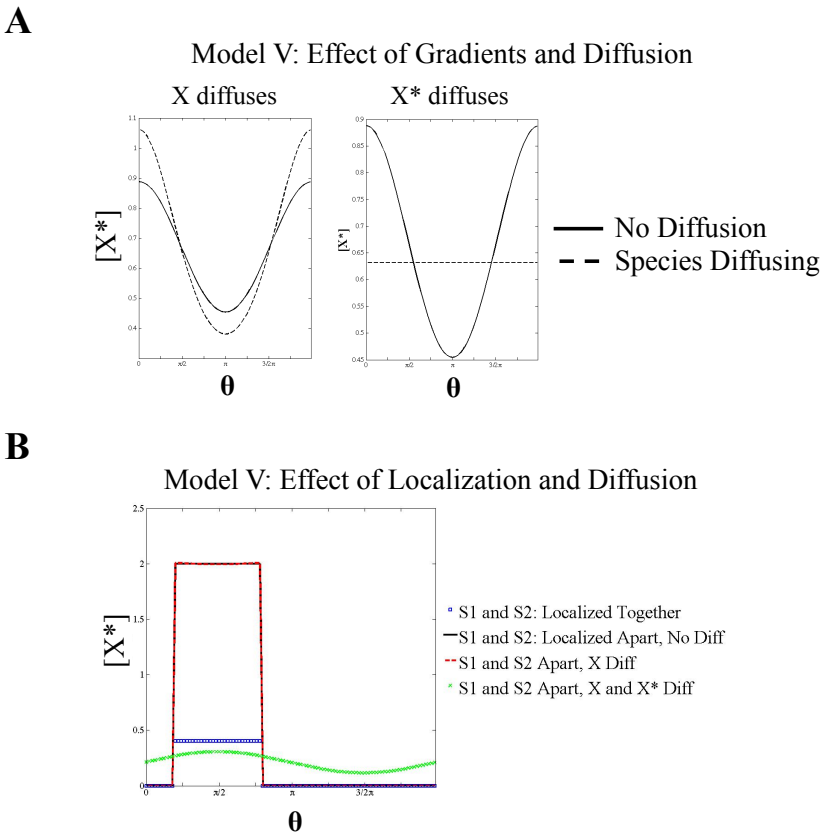


Figure 6.9: **Analysis of Model V.** (A) External Signals S1 and S2 are graded and counter-aligned. When species do not diffuse (solid line), the spatial concentration profile of $X^*$ mirrors S1. (LHS plot) When X diffuses, the spatial profile of $X^*$ weakens. (RHS plot) If $X^*$ diffuses, the concentration profile of $X^*$ becomes homogenous at steady state. (B) Two scenarios were compared: 1) the signals S1 and S2 are localized together (blue squares) and 2) S1 and S2 are apart. When S1 and S2 are apart in opposite locations, at steady state, all of X is converted to $X^*$ in the region where S1 is localized (solid black line *coincides with the red dashed line*). If X diffuses (red dashed line), at steady its concentration becomes zero and only $X^*$ which is present where S1 is localized. If both X and X* diffuse, the spatial profiles of each species are graded in the entire domain.

zyme. This is especially the case if the activities of the enzymes need to be distinct at separate locations. Localizing the signals in different locations may achieve this. Keeping this in mind, in this section we will explore two scenarios (Fig. 6.9)- first both the signals are localized together and second the signals are localized separately in different regions of the domain. We examine the response for both of these scenarios and contrast them.

***Together case*:** In the first scenario, both signals and the species of the model are localized together in the spatial domain and this results in a localized profile for both X and $X^*$. Now if either or both of the substrates diffuse, the local concentration of substrate

species decreases.

***S1 and S2 are apart*:** In the second scenario, S2 is apart from the rest of the species of the cycle. If none of the species are diffusing, then in the location where S1 and the cycle species are initially present, all of X is naturally converted to $X^*$. Thus at steady state only $X^*$ is present at that location. Next we consider the case when species diffuse. If $X^*$ alone diffuses, then in the second location where S2 is present, all of $X^*$ is converted to X. Thus at steady state, only X is present at the second location. When the signals are localised separately, the enzymatic reaction at each location cannot be reversed. This is because, as a result of separate localization of signals, enzyme activities are also separated in space. Separating the activates of the enzymes may either be a constraint or an advantage. It could be the latter (depending on the context) if a transient increase is required of the substrate species in one location, which is akin to a spatial analog of an adaptive response (where the response transiently increases/decreases before returning to its pre-stimulus value). If localization introduces a constraint, then allowing both X and $X^*$ to diffuse will ensure that both species are present at steady state in both locations. However, the trade-off here is that the profiles of X and $X^*$ will have a heterogeneous spatial distribution in the spatial domain and will no longer be localized.

This concludes the first part of the analysis of the suite of building blocks models. In summary, we used a systematic approach to examine five different building block models based on the basic bifunctional enzyme modification cycle and its extensions. The temporal information processing capabilities resulting from building in distinct signalling interactions into the basic modification cycle were examined. Having elucidated the temporal aspects of the building blocks, different spatial effects (gradients, localization and diffusion) were introduced and analysed in each building block. By utilizing such an approach, we were able to shed light on the different ways in which spatial signalling distorts existing signal processing capabilities as well as introduces new behaviours. Thus, we have gained insight into the effects of different types of spatial control and regulation on the different temporal signalling interactions within each building block. Going further, we build on the insights gained from this analysis in the study of the concrete *Caulobacter* signalling networks (see Fig. 6.4).

### 6.3.2 From building blocks to signalling networks in the *Caulobacter crescentus* cell cycle

The *Caulobacter* life cycle is characterized by a sequence of developmental events and (morphologically) asymmetric cell division. Numerous signalling and regulatory interactions drive the progression of the cell cycle- choreographing the events in each developmental phase and the transition to the next. Probing the cell cycle in *Caulobacter* has revealed striking examples of spatial control and regulatory mechanisms. These act in tandem with temporal regulation to organize the signalling interactions in the cell cycle regulatory networks (Goley et al., 2009).

Phospho-signalling pathways, many of which contain bifunctional enzymes, are a part of the core of regulatory processes driving the cell cycle. Spatial localization of signalling entities is one of the key mechanisms by which the phosphorylation/dephosphorylation events are controlled and coordinated. The cell makes use of its polar regions to differentially localize enzymes throughout the cell cycle. In any given phase of the cell cycle, enzymes catalyzing the phosphorylation/dephosphorylation reactions maybe localized together at the same pole or apart at different poles. Furthermore, the localization of certain enzymes is dynamic and changes from one phase to another. Thus in one phase the enzyme maybe located one pole and in the next it may dynamically localize to the opposite pole.

What are the different ways in which localization is enforced and when are localization events timed into the cell cycle are questions that arise time and again in investigations. Charting the sequences of interactions between the signalling species and uncovering the role of spatial cues provided by localization in orchestrating these sequences is one of the main focal points of experimental investigations. Modelling efforts are useful especially where spatiotemporal resolution of experimental tools is limited. However, there are only a handful of modelling studies that address the role of spatial control in this cell cycle. These address the role of localization control, gradients and diffusion in specific individual signalling networks in a particular phase of the cell cycle (Chen et al., 2011; Tropini and Huang, 2012). Others have mainly focused on modelling temporal aspects of interactions of key regulatory proteins throughout the progression of the cell cycle (Li et al., 2008, 2009; Subramanian et al., 2013).

The multiple levels at which the signalling networks are organized- phospho-signalling pathways, enzymatic mechanisms driven by bifunctional enzymes and the role of spatial control via localization and diffusion therein, have been systematically examined by us

earlier in the study of the building block models. We now use this study as a platform and take it to the next level to address some of the questions and gaps in elucidating spatial control and regulation in the *Caulobacter* cell cycle signalling networks.

We mainly focus on two individual signalling networks observed to be involved throughout the cell cycle. These are the PleC-DivJ-DivK and CtrA-CckA phospho-signalling pathways. These pathways consist of bifunctional enzymes (in combination with mono-functional enzymes) regulating the modification reaction pathways. These networks are suggested to interact with one another through signalling intermediates (Tsokos et al., 2011). Furthermore, the constituent enzymes and the intermediates maybe localized at different poles during each phase in the cell cycle and also dynamically through the different phases.

Viewed from a systems perspective, the ingredients of the problem are as follows: there are mainly two signalling modules- these come under the class of enzymatic building blocks where the catalysis is driven by bifunctional as well as mono-functional enzymes. Extensions or variants of these may exist- for example relating to the underlying mechanism of modification (phosphotransfer or covalent modification) or relating to their dynamics (mono-stable or bistable). Thus these building blocks and their extensions may be individually examined to gain insight into their organization and signalling processing capabilities. This informed our approach in the first part of the study where we examined different building block models.

The next sets of ingredients are the interactions between these modules in the spatio-temporal context (Fig. 6.4). An *in silico* synthetic design framework provides an avenue to scrutinise these interactions in light of different "spatial designs." A "spatial design" corresponds to one set of possibilities of spatial localization/distributions of all module components in the spatial domain.

There are a finite number of components in each module and various possibilities for the localization of each- the components of each module may all be at one location (akin to a pole), distributed between two locations. Alternatively certain components may be present everywhere in the spatial domain (there are other possibilities present, for example localization in a different part of the cell membrane). These three scenarios themselves yield a large number of possibilities of spatial designs. Choosing designs based on those the cells themselves utilize narrows down these possibilities. Furthermore, certain designs may also be redundant. The concept of "synthetic spatial control" is inspired by synthetic engineering applications involving the manipulation and control of spatial localization of

components of signalling networks to achieve specific outputs and functions (Sachdeva et al., 2014).

Such a combination of systems and synthetic design views informs our approach and we structure our analysis accordingly. To start with our goals are: i) To investigate both the aforementioned network modules individually ii) To examine the temporal interactions between them and iii) To shed light on the role of spatial localization in combination with diffusion therein.

We structure our analysis in the following way (Fig. 6.4): i) First, we will utilize building block models from our earlier framework to study these networks. The building blocks we choose to examine encompass signalling interactions similar to the ones within these networks.

a. In order to examine temporal interactions between these networks, we will examine the interactions between different combinations of the chosen building block models. This will be done by tuning the relevant kinetic parameters.

b. We will dissect the role of spatial localization control and its interplay with diffusion on the individual networks and their temporal interactions. We will achieve this by utilizing an *in silico* synthetic design approach, and examining the effect of having different spatial localization designs. There are two main spatial configurations that these designs will stem from- when all the components of the networks are together and when they are apart/distributed between two regions. We will study a number of spatial designs based on these, especially in light of the reason that the cell itself utilizes this spatial design logic to control the signalling events in the cell cycle. We also consider possible alternative localization/distribution patterns (which may been in other bacterial cells).

ii) Next, we will examine existing spatial models of these networks (Chen et al., 2011; Tropini and Huang, 2012).

a. We will individually examine these models and then "connect" them using intermediate species and examine the interactions between them.

b. Next we will dissect the consequences of localization of enzymes on the interactions within the combined model.

c. Going further, we will take the first steps towards incorporating spatial control mechanisms in the study of the progression of the cell cycle. To achieve this we will employ the existing spatial model, which is based on the PleC-DivJ network (Tropini and Huang, 2012). We will aim to elucidate, in the sequence suggested in the literature, the dynamic localization of one enzyme in particular, PleC and its consequences on the response of the

network. We will analyze the mechanism by which dynamic localization may be incorporated into this network. Also, we will study the consequences of having different "localization mutants" or "incorrectly" localized species (relative to the wild type localization trends) present.

By examining the signalling networks along these two axes, we will shed light on both broad and specific questions and issues : i) How does spatial control affect different phospho-signalling pathways?
ii) What are the constraints and capabilities that naturally arise from having locational control of bifunctional enzymes in these cycles?
iii) A specific mechanism is suggested (in the experimental literature) to underlie the interaction between the two networks- what are the consequences of incorporating this in a combined spatio-temporal setting?
iv) The transition between two phases in the cell cycle is hypothesized to be the result of a bistable switch exhibited by a bifunctional enzyme in the PleC-DivJ network. We utilize our building block models to ascertain how this switching behaviour would be affected when additional interactions are present, especially in the spatiotemporal context.
v) How do the different spatial localization designs affect the interactions in individual networks and in between the networks? How does the interplay of localization and diffusion affect this interaction? Furthermore, in light of the fact that the cell utilizes these spatial designs, what kind of constraints or capabilities does each spatial configuration introduce, in light of the signalling interactions present?
vi) By studying the dynamic localization of enzymes at different poles during different phases of the cell cycle we aim to gain insight into the dynamic feedforward control mechanism utilized by the cell.

We will begin with presenting the analysis of the building blocks with respect to different *in silico* synthetic spatial designs.

### 6.3.3 Exploring *in silico* synthetic spatial designs in the combination of building block models BBC1 and BBC2

In this phase of the study, we employ two different combinations of building block models (termed BBC1 and BBC2, see Models and Methods). Each model consists of an upstream module and a downstream module. For simplicity we term the upstream module "MU" and

the downstream model "MD."

**BBC1:** In BBC1, the upstream module (Table 6.1) consists of two separate enzymes K and P (analogous to DivJ and PleC, respectively) that catalyze the conversion between X and $X^*$ (analogous to DivK and DivKP, respectively). This module is similar to the covalent modification cycle module with separate enzymes (studied in Chapter 4) but in the current module, the catalysis is driven by a phosphotransfer mechanism. This module lies upstream in the series of interactions. DivKP interacts with the downstream building block module via an intermediate I (analogous to DivL).

The downstream module consists of a bifunctional enzyme (analogous to CckA) driving the conversion between Y and $Y^*$ (analogous to CtrA and CtrAP). DivL mediates the conversion of the phosphatase form of the bifunctional enzyme (CckAP) to the kinase form (CckAK). The interactions are illustrated in Fig. 6.3. The species will be referred to by their biological analogues for the remaining sections. This constitutes the interaction in the so-called Model BBC1 (analysis of Model BBC2 is discussed later).

## Model BBC 1

Before we examine the interaction between the modules in light of the spatial designs, we first analyse and discuss the spatial designs that are possible in this model.

**Contending with the large array of possibilities for the spatial designs**

It is possible to have numerous spatial designs with two modules and two spatial locations (pole 1 and pole 2). To reduce this number of possibilities, we consider spatial designs that stem from the two basic spatial designs seen in *Caulobacter*. These designs are- species are localized together and species are localized apart at different poles/subdomains. Thus 1) components of the upstream and downstream modules, may be localized in one region of the spatial domain. Incidentally this also corresponds to the temporal case because all interactions are local (ODE case). 2) Components of both modules are apart from one another i.e. localized in different parts of the spatial domain. The spatial designs that stem from the second category may require that diffusing species be present in order to complete the circuit of reactions.

Controlling the localization of the enzymes DivJ and PleC in the upstream module and CckA in the downstream module along with the intermediate DivL, gives rise to the different spatial designs. In our analysis, the effect of diffusion of the substrates and modified species in both modules, as well as the intermediate DivL is examined (enzymes are

assumed to be non-diffusible; however a special case is also considered later where the enzymes diffuse). Table 6.2 lists the different spatial designs. An example of a spatial design we consider is- the enzymes DivJ and PleC in the upstream module are localized in region 1, the bifunctional enzyme CckA in the downstream module is localized in regions 1 and 2 and DivL is localized in region 1 only (spatial design IIIa in Table 6.2).

**Separately localizing activities of bifunctional enzymes**

The number of spatial designs possible when a module contains a bifunctional enzyme maybe limited. In general, if the two different activities of the bifunctional enzyme need to be separately localized, then the signalling interactions present within the module may or may not allow this. Through the examination of the building block models in the first part of the study we were directly able to ascertain which signalling interactions would allow this possibility. In general, if external regulation of the enzyme activity is absent, one form of the enzyme cannot be exclusively present at any given location. Thus, the enzyme forms/activities cannot be separated unless there are species present at each location, mediating the activities of the enzyme such that at each location it is dominantly present as one form. We examined this type of feedforward regulation in detail in Model V in the first part of the study, where two external signals were modulating the opposing enzyme activities. If "locational control" of the activity were implemented then this case would be similar to having separate enzymes catalyzing the reactions.

In the downstream module considered here, DivL regulates the two activities of CckA by mediating the conversion of CckAP to CckAK. It is possible to adjust the relevant kinetic rate constants such that one form of the enzyme may be dominant in the absence of DivL and the other form dominant in its presence. For example, by having the basal forward reaction kinetic rate constant smaller than the backward rate constant. Now if DivL was localized in one region and CckA was allowed to localize in this same region as well as a separate region, then this type of parameter setup would result in a greater proportion of CckAK where DivL is localized. CckAP would mainly be present in the opposite region where DivL is absent. This would effectively separate the two enzyme activities spatially. We will examine this kind of possibility in the subsequent analysis.

**Certain spatial designs require the presence of global/diffusing entities**

The location of DivKP must coincide with that of DivL in order to complete the interaction between the models. The location of DivL, in turn, must coincide with the enzyme in the downstream model. Thus, in this type of spatial design, the transport of species is not required to complete the circuit of reactions between the modules. However, in spatial

| *Spatial Designs* | **Localized Region I/Pole 1** | **Localized Region II/Pole 2** |
|---|---|---|
| *Ia* | Upstream Module (MU)<br>-Enzymes: PleC and DivJ<br>Intermediate DivL<br>Downstream Module (MD)<br>-Bifunctional Enzyme: CckA | |
| *IIa* | MU | DivL<br>MD |
| *IIIa* | MU<br>DivL uniform<br>MD | DivL uniform<br>MD |
| *IVa* | MU<br>DivL<br>MD | MD |
| *Va* | MU<br>MD | DivL<br>MD |
| *Ib* | DivJ<br>DivL<br>MD | PleC |
| *IIb* | DivJ | PleC<br>DivL<br>MD |
| *IIIb* | DivJ<br>DivL uniform<br>MD | PleC<br>DivL uniform<br>MD |
| *IVb* | DivJ<br>DivL<br>MD | PleC<br>MD |
| *Vb* | DivJ<br>MD | PleC<br>DivL<br>MD |

Table 6.2: **Summary of the Spatial Designs.** In the spatial designs, the components of the upstream and downstream modules may be localized at either Pole 1 or Pole 2. Components of modules may also be separated from one another and present at both poles. DivL, the intermediate species, may also be uniform and present everywhere in the spatial domain. In Spatial designs I-V*a* the enzymes of the upstream module (MU) are in region I only and the enzyme in the downstream module (MD) is localized at either one pole or both poles. In Spatial designs I-V*b* the enzymes in MU (DivJ and PleC) are apart in different poles and the localization of the enzyme in MD is again varied as before.

designs where DivKP and DivL are separated, either DivL or DivKP must diffuse in order for the interaction to occur. Also, if DivL and the downstream enzyme it regulates, CckA, are separated, either DivL or CckA must diffuse in order to effect the changes downstream.

We emphasize this point for the following reason. In the cell, the locations of enzymes act as spatial cues for signalling interactions and also sites for recruiting downstream signalling species. For example, in *Caulobacter*, the localization of DivL at one pole is suggested to be necessary for recruiting and activating CckA (Iniesta et al., 2010a). Thus we highlight in which spatial designs transport is necessary to achieve interactions between modules.

**Various spatial distributions of modified substrates arise as a result of different spatial designs**

Different spatial configurations of the components in the upstream and downstream modules lead to various spatial distributions of the modified substrates, DivKP and CtrAP. In the concrete context, substrate levels and their spatial distributions have consequences for the processes in which they are involved. For example, the gradient of CtrAP is suggested to be involved in establishing the asymmetry in a pre-divisional *Caulobacter* cell even before the cytokinesis occurs (Chen et al., 2011). Hence, we closely examine these spatial distributions. Also with the improvement of localization and visualization experimental tools, the spatial distribution of substrates may be observed and measured experimentally as well as directly manipulated (Lasker and Shapiro, 2014). Thus, examining the spatial distributions in different spatial designs is relevant at multiple levels.

Different spatial designs result in :1) **A graded profile**: this is seen designs where the enzymes are localized separately and substrate diffusion is slow or moderate. For example spatial designs IIIa, IVa, Va and all designs with a "b" allow this type of profile (Table 6.2). 2) **A localized profile**: As expected, a localized profile is achieved in spatial designs where the modifying enzymes are present together in the same compartment (and the substrates are non-diffusible). Spatial designs with an "a" and also Ib and IIb may result in this distribution. 3) **A uniform/homogenous profile**: In a spatial design, if the enzymes are apart, and if the substrates species are highly diffusible, the resulting profiles will be uniform. If the enzymes are localized together and the substrate species diffuse out of the localized region then this would also result in an essentially uniform spatial concentration profiles of the substrates at steady state.

Having analysed different aspects of the spatial designs we now move on to analyzing the temporal interactions between the modules in light of these designs.

**Different spatial designs perturb the temporal interactions between modules**

We now examine the effect of different spatial designs (Table 6.2) on both, the upstream interaction and the downstream interaction of DivL. We start by discussing the upstream interaction, which involves DivKP inhibiting DivL.

The interaction between DivKP and DivL is modelled in two different ways- 1) the inhibition of DivL by DivKP is in the mass action regime and 2) DivKP binds to DivL and both are sequestered in a complex [DivKP-DivL]. The latter is suggested to underlie the interaction between the species in the concrete network (Tsokos et al., 2011). Based on our analysis in Chapter 4, we expect that in the latter case, the effect of diffusion of DivL would propagate into the upstream module and perturb the spatial concentration profiles of its components. This "back propagation" effect would result from DivKP being sequestered in a complex with DivL (whereas if the interaction is modelled in the mass action regime this effect would be absent). This effect is analysed in light of different spatial designs and discussed later.

***Consequences of different spatial designs on the DivK-DivL upstream interaction*:** We discuss the simplest case first- if the modules are together (for example in Spatial Design Ia), the interactions are also localized in one place. In the spatial designs in which DivKP and DivL are localized in different locations, the diffusion of at least one of these species is necessary for the upstream interaction to occur. As a result, diffusion or spreading of the species leads to it being present at a lower local concentration in the domain, relative to the case when the species are localized together and non-diffusible. This is the aforementioned "dilution effect" (and has been studied in detail in Chapter 5). Fig. 6.10 illustrates these effects in the two types of spatial designs. We discuss the consequences of different of each species.

***DivKP alone diffuses*:** The consequence of this is that the amount of DivKP available to inhibit or bind to DivL is lowered and hence less DivL is inhibited. The effect of DivKP diffusing in the domain is shown in Fig. 6.10.

***DivL alone diffuses*:** Similarly if DivL diffuses, it's local concentration is lowered (as compared to when the modules are together and it is non-diffusible). In the case where the DivKP-DivL interaction is modelled to explicitly account for the binding and sequestration of both species in a complex; as we expect, the "back-propagation" effect is present here. DivL diffusion results in the decrease of the steady state concentration of DivKP Fig. 6.10 as well as the rest of the species upstream.

In the *Caulobacter* cell, the concentration levels of signalling species are suggested to

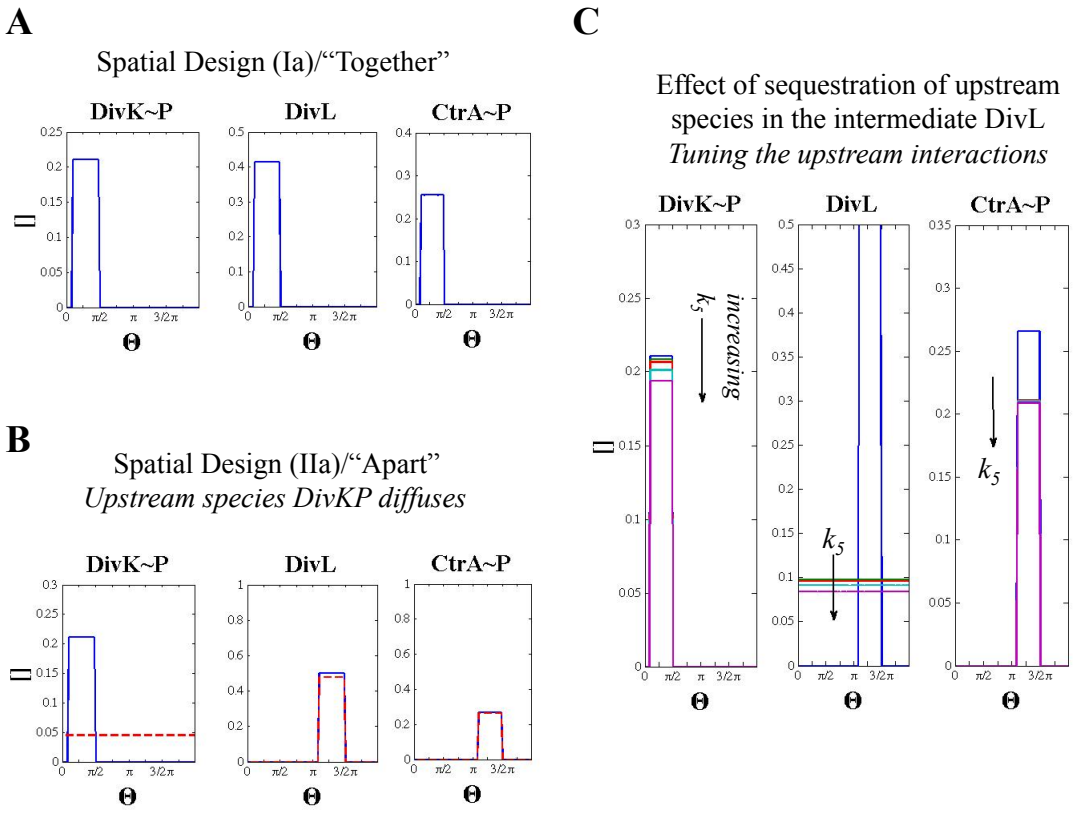


Figure 6.10: **An illustration of the different types of spatial designs and tuning the interactions between modules.** (A) The upstream and downstream modules are together (Spatial Design Ia). (B) The modules are apart (Spatial Design IIa). The cases where none of the species diffuse (blue) and when DivK and DivKP diffuse (dashed red line) are shown. The profile of DivKP becomes flat and its concentration reduces everywhere in the spatial domain. DivL and CtrAP concentrations slightly decrease. (C) The effect of diffusion in the model variant where DivKP and DivL are sequestered in a complex in Spatial Design IIa. None of the species diffuse (blue line). When DivL diffuses, its concentration is reduced at the pole and everywhere else in the domain. This results in a decrease in the concentration of the downstream substrate CtrAP. The concentration of DivKP, the upstream species, is reduced as well. This is due to the effect of DivKP being sequestered in a complex with DivL ("back propagation" effect). Modulating the upstream interaction parameter $k_5$ between DivKP and DivL leads to modulation of the levels of species both upstream and downstream. Arrows denote the direction of increasing value of $k_5$.

play an important role for the initiation of development events during the cell cycle. For example the level of DivK is suggested to modulate flagellar pole development. In light of this, there are two different implications of the dilution effect: first, the cell may use this effect to its advantage to achieve a lower concentration of a particular signalling species below a certain value to affect a response. Alternatively if the dilution effect poses as a possible disadvantage then the cell may employ different ways to mitigate/bypass it.

As the analysis in Chapter 5 suggests- the effect of dilution may be mitigated if, for example, in the case of the substrate DivKP diffusing, the concentration of DivKP is low to begin with. Then, if it spreads in the domain, there would not be a large difference in its local concentration. Or if the total amount of phosphatase acting on DivKP were high- this would also result in countering the dilution effect- for the similar reason that DivKP concentration is kept low.

Next we analyse the downstream interaction in light of different spatial designs.

***Consequences of different spatial designs on the DivL-CckA downstream interaction*:** DivL mediates the conversion of the phosphatase form of CckA to its kinase form. Hence, this interaction results in an increase in the kinase form of CckA, which in turn results in an increase in the modified form of CtrA (CtrAP). We expect locational constraints arising from different spatial designs to have consequences for this interaction as well. If the modules are localized together, and none of the species diffuse, a larger concentration of DivL is available to mediate the downstream reaction when compared to the scenario where species are apart and DivL is diffusing. Thus the dilution effect plays a role here as well.

***Tuning the temporal interactions between modules*:** Next, we examine the consequence of varying the parameters relevant to the interactions between the modules (and we discuss this for the model where DivK and DivL are sequestered in the complex). We first modulated the upstream interaction by varying the forward rate constant associated with the binding of DivKP and DivL ($k_5$). When this parameter is varied, both upstream and downstream concentrations are affected. This is shown in Fig. 6.10 for spatial design IIa for the case in which DivL is diffusing (a similar trend is also seen when the modules are localized together).

***Tuning the interactions to modulate spatial distributions*:** Next we modulated the kinetic parameter in the downstream interaction ($k_i$ which is associated with the regulation of CckA by DivL). When the components of the downstream module and DivL are localized together, increasing this parameter leads to an increase in the kinase form of CckA, which in turn results in an increase in CtrAP concentration levels. Tuning this parameter has no effect on the upstream components.

In a spatial design where the CckA forms are localized separately, at steady state, the spatial profile of CtrAP will be graded (CtrA and CtrAP must be diffusing in the spatial domain). When $k_i$ is varied in this case, we found that the steepness of this graded profile is modulated. Here it must be noted that if the enzyme is bifunctional then a steep gradient may be possible if in one (or both) locations, one form of the enzyme is dominant. This

is effectively what happens when DivL is localized only in one region and $k_i$ is increased. Fig. 6.11 shows a graded profile of CtrAP for Design Vb that is modulated by tuning the interaction parameter $k_i$ between DivL and CckA in Location 2.

**Effect of Modulating the Downstream Interaction** (Spatial Design Vb)

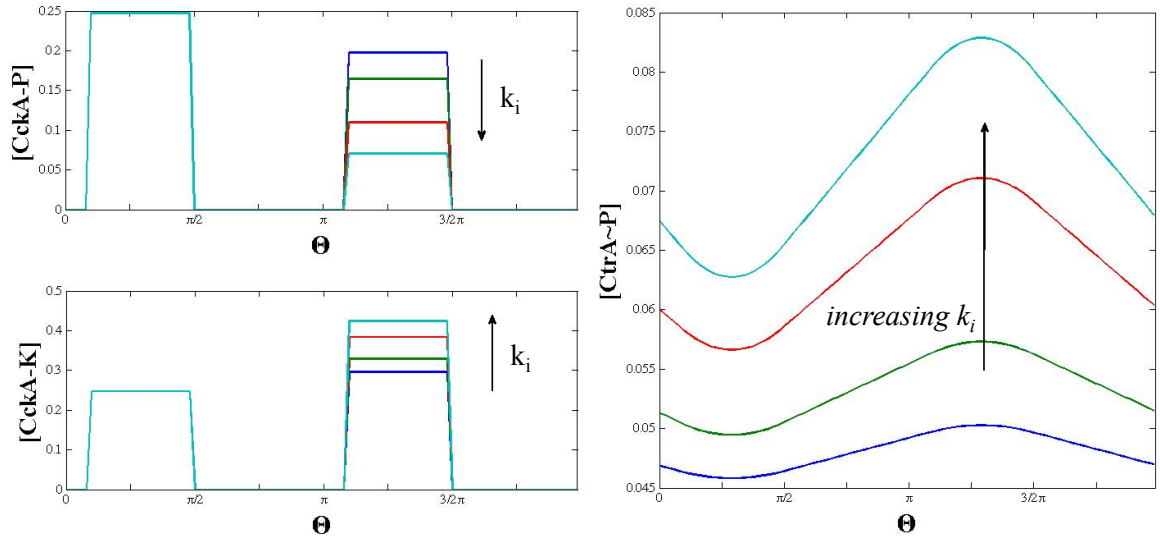


Figure 6.11: **Effect of modulating the downstream interaction.** (LHS plots) The spatial concentration profiles of the phosphatase (P) (top) and kinase (K) (bottom) forms of CckA in Spatial Design Vb are shown. In this design DivL is at pole 2 (localised region 2 on the left) and both forms of the CckA enzyme at present at both poles. The RHS plot shows the resulting spatial concentration profile of CtrAP and the arrow denotes the direction of increasing the parameter $k_i$ (the forward rate constant for the reaction between DivL and CckA(P)). As the parameter is increased, the gradient becomes steeper and the overall concentration increases.

Another way to modulate the steepness would be to change the total concentration of enzyme present at the different locations (for example greater concentration of CckAP is present in region 2 than CckAK in region 1). Naturally, tuning the diffusion coefficient values of CtrA and CtrAP also affects the graded profile (lower diffusion leads to steeper gradient). Next we analyze how different spatial distribution of DivL affects the downstream species.

If DivL is localized in one region (and non-diffusible), it will affect the steady state concentration of CckA and thus CtrAP in that location only. Now if DivL forms a graded profile in the spatial domain (if it diffuses across the domain), then the positions of the downstream species in the spatial domain (with respect to DivL spatial distribution- upgradient or downgradient) will determine their steady state concentrations. Thus having

a global intermediate provides several avenues for spatially controlling the levels of the downstream species.

## Model BBC2: Examining the bistability hypothesis

From our investigation of the building blocks in the first part of the study and Model BBC1, we expect that different spatial designs will affect the interaction between the modules as well as any special temporal behaviour the modules exhibit. Keeping this in mind, next we analysed the second building block combination model BBC2 where the upstream module exhibits bistability. Here again, the DivKP interaction with DivL was studied using two model variants (via mass action or binding). We only discuss the second variant here, reason being diffusion of downstream species does not affect the upstream species in the first variant. The interactions downstream of DivL are the same as in Model BBC1 (see Table 6.1).

**Different spatial designs distort the bistable response**

First we examine the spatial design where all the components are localized together and none of the species are diffusing. This corresponds to the ODE case. Next, we examined the affect of tuning the kinetic parameter $k_5$, the interaction parameter between DivL and DivKP, for this spatial design. If $k_5$ is increased, the system is pushed out of the bistable regime. This is expected as the bistable response occurs for a particular range of parameters only.

Next we consider spatial designs where DivKP and DivL are apart and DivKP is diffusing. Our study of the individual building blocks (Model IV) suggests that if the substrates diffuse, then the bistable response would be lost. We find this is the case here as well; when DivKP diffuses the bistable response is lost (Fig. 6.12). We also consider the case where DivL is diffusing. In this case, we find that while the DivKP concentration level is reduced, the bistable response is maintained (Fig. 6.12).

It has been suggested in (Subramanian et al., 2013) that a bistable switch underlies the transition between the first two phases of the cell cycle. However, the analysis in that paper has been performed in a purely temporal model. Since the networks are spatially distributed in all phases, this effect merits examination in a spatial setting. Our analysis reveals the conditions and spatial designs in which the bistability may be preserved or distorted. Having a diffusible intermediate communicate between two interacting networks that are separately localized, ensures the preservation of the bistable response.

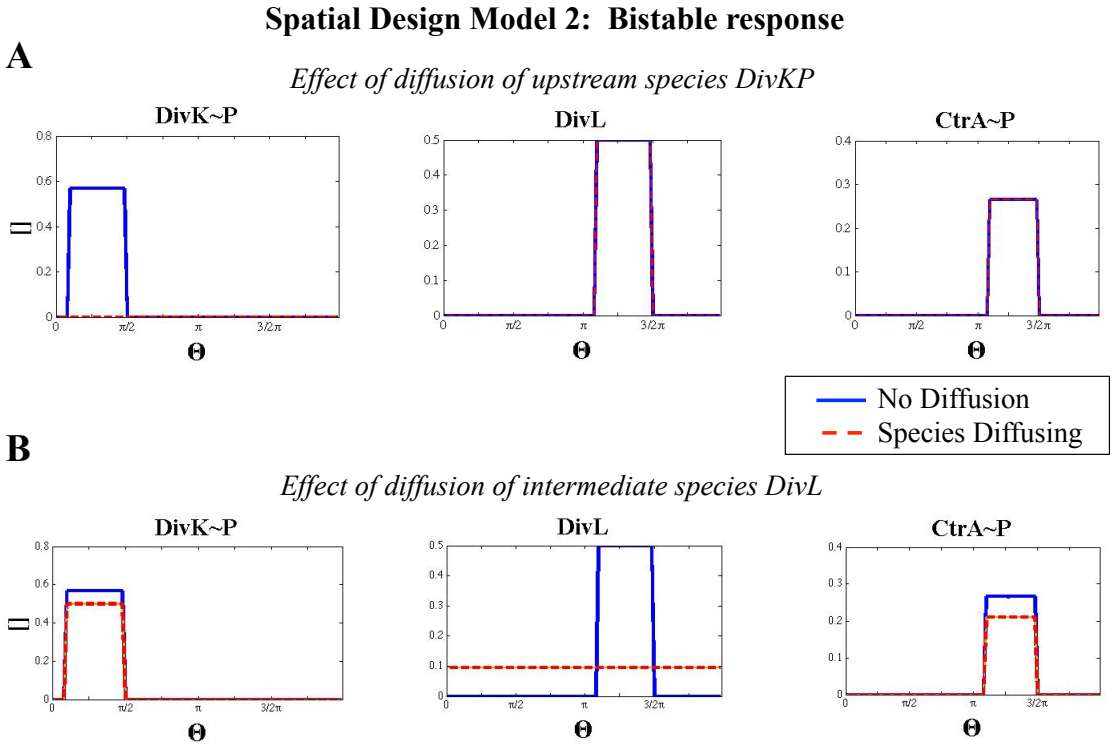


Figure 6.12: **The effect of localization and diffusion on the bistable response.** (A) In Spatial Design IIa: DivKP diffuses (red line, close to the zero axis in the DivKP plot); (no diffusion- blue line). In this case when DivKP diffuses the bistable response is lost. (B) DivL diffuses (red line); no diffusion (blue line). When DivL diffuses, the bistability is preserved (the other steady state corresponding to the lower branch is not shown).

In summary, we have systematically explored the temporal interaction in various spatial settings. Our findings reveal the constraints and capabilities that come with multiple types of spatial designs and their implications for the interactions between the network modules. Next, we explore existing spatial models of the *Caulobacter* network and utilize them to examine the temporal interactions between the networks and the effect of localization of enzymes (Fig. 6.4).

### 6.3.4 Exploring spatio-temporal interactions in existing spatial models

In this phase of the study the spatial models in (Chen et al., 2011; Tropini and Huang, 2012) are analysed. The models are individually examined briefly and then they are "connected" via downstream intermediate and analysed in light of different spatial designs.

#### Analysis of the individual models

The models described in (Chen et al., 2011; Tropini and Huang, 2012) are based on the PleC-DivJ-DivK network (Network A, Model A) and on the CckA-CtrA network (Network B, Model B), respectively (Fig. 6.3). In the analysis of each model, we examined different localizations of the constituent enzyme species. The effect on the steady state spatial concentration profiles of the response- *total* DivK (Model A) (see Models and Methods section) and the two forms of CtrA (CtrA and CtrAP, Model B) was analyzed. (Note that for all cases that were examined, the "free" forms of DivK and the two forms of CtrA were allowed to diffuse in the spatial domain).

The oppositely localized regions are the "stalked pole/pole 1" and the "swarmer pole/pole 2" (labeled in Fig. 6.13). We have used periodic boundary conditions to represent the membrane of the cell. In Fig. 6.13), the region between the vertical lines shown (where the poles have been marked), would represent one half of the cell membrane.

***Analysis of Model A*:** In Model A, when the enzymes are co-localized in one region of the domain, the spatial concentration profile of total DivK mirrors the profiles of the enzymes and is localized in the same region as well (the diffusion of the free forms of DivK results in a non-zero concentration of total DivK in the rest of the domain). When the enzymes are localized at opposite poles, the spatial concentration profile of total DivK is mainly localized in both poles as well. Both free forms of DivK must diffuse in order for total DivK to accumulate in both localized regions (Fig. 6.13).

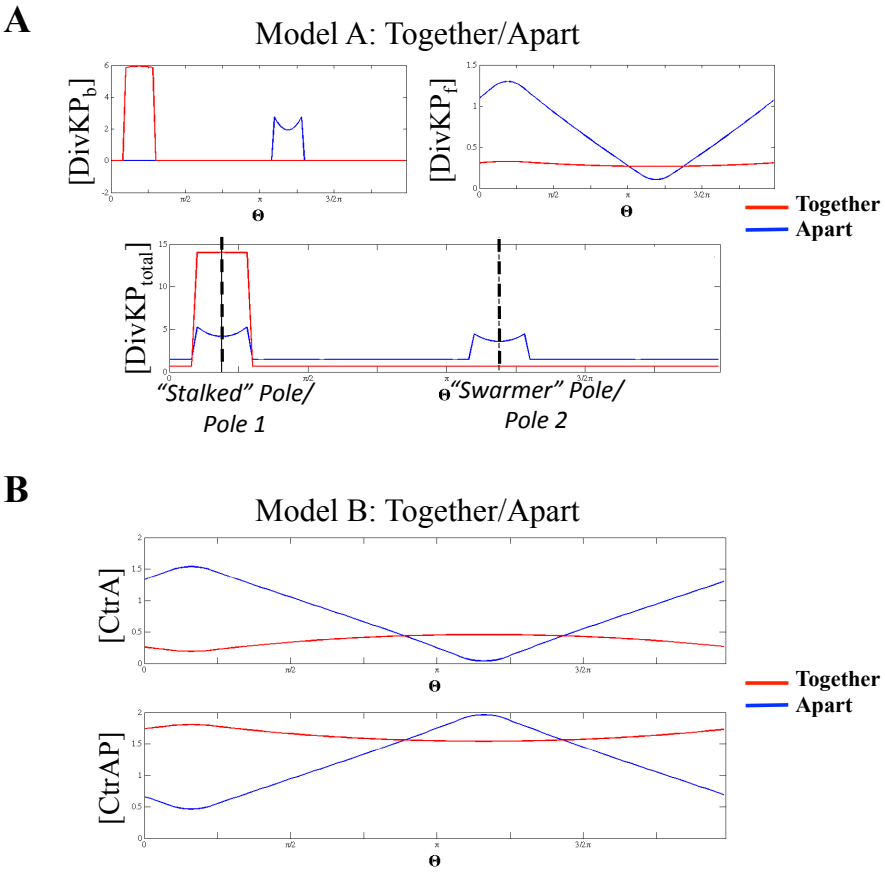


Figure 6.13: **Examining Networks A and B individually.** (A) The two localized regions are labeled "stalked" pole/Pole 1 and "swarmer" pole/Pole 2. The region in between the dashed vertical lines represents one half of the boundary/membrane of the cell. (A) Network A: the bound and free DivKP species (top right and left) and total concentration of all DivK species (bottom) are shown. When all enzyme species are together (red line), the bound DivKP species is present at the stalked pole, the free DivKP is weakly graded in the spatial domain and the total DivK concentration mainly accumulates at the stalked pole. When the enzymes are apart (blue line), the bound DivKP species is at the swarmer pole, the free DivKP is graded in the spatial domain and the total DivK species concentration accumulates at both poles as well as is present in the regions between the poles. (B) Network B: The spatial concentration profiles of CtrA and CtrA P are shown. When all enzyme species are together (red line), both species are weakly graded in the spatial domain and when apart (blue line), the graded profiles are steeper.

***Analysis of Model B*:** In Model B, when the enzymes are localized together in one region of the domain, the spatial concentration profiles of CtrA are spread in the spatial domain and weakly graded (Fig. 6.13). The diffusion of the CtrA forms results in the weak gradation (if the diffusion were turned off, the profiles would be localized in one region only). When the enzymes are localized apart, the spatial concentration profiles of CtrA have steeper graded profiles. The preliminary analysis presented here led to the basic understanding of the each model with respect to different spatial distribution of enzymes.

Next the interactions between Models A and B were investigated. This was achieved by modifying both models and having them interact through an intermediate.

## Analysing interactions between network modules A and B

The next part of the study involved examining different types of temporal/kinetic interactions between the networks and analyzing how spatial perturbation by localization may affect these interactions. The analysis of the combined model (Model A and Model B interacting via the intermediate DivL) is presented next.

**Localizing enzymes at separate poles requires transport of intermediate species**

In this part of the study, the interactions between network parts A and B, in a combined model (representing the entire network) were investigated (Fig. 6.3). The analysis was performed in a systematic manner: the spatial distributions of the enzymes upstream and downstream of DivL were varied (by localizing them at the same or different poles) and for each spatial configuration the interaction parameters associated with DivL and DivKP were tuned.

The spatial configurations were based on the distributions of enzymes found in the experimental literature (García Véscovi et al., 2010). The consequences of having different spatial configurations combined with tuning the kinetic parameters were examined on the *total* DivK as well as CtrA (both forms) spatial concentration profiles. For simplicity (to reduce the number of configurations) we assume that the intermediate DivL is always localized with the CtrAP species.

The two main types of spatial configurations are first discussed. The first configuration to naturally examine is when all the species (upstream and downstream of DivL) are co-localized at one pole (for example the stalked pole). As expected, the total DivK concentration is mainly localized in one region of the domain and both forms of CtrA are weakly graded across the length of the spatial domain. As such there are no spatial constraints present here, i.e. the network interactions are localized.

The next configuration we examine is when the enzymes upstream of DivL are localized at the stalked pole and those downstream (and DivL itself) are localized at the swarmer pole. As previously mentioned, the upstream interaction occurs between DivL and the bound form of DivKP (which is non-diffusible) (equations 6.13 and 6.14). As a result of this configuration, these two species are apart and DivL must diffuse to the other pole (or be present everywhere/globally in the spatial domain) to complete the circuit of

interactions. Thus, additional spatial effects must be present, in the form of DivL being a global intermediate, in order for separately localized networks to interact.

If spatial tracking of DivL reveals that it is tethered to the pole/unable to diffuse, then we propose that an additional global intermediate must be present in order to enable the interaction between bound DivKP and DivL (if they are localized at opposite poles). If the upstream interaction with DivL was via freely diffusing form of DivKP, then DivL would not be required to diffuse. The spatial constraints associated with the second configuration-apply to any other configuration where DivKP (bound form) is situated away from DivL.

**Tuning the temporal interactions between the networks**

Next, the effect of modulating the interaction between DivL and DivK was analysed. To start with, two spatial configurations were considered (all spatial configurations are listed in Table 6.3). In configuration 1, all enzyme species are localized together at one pole and in configuration 2, the opposite enzymes (upstream and downstream of DivL) are localized in opposite poles. In both these configurations, the resultant DivL and DivKP (bound form) concentrations are localized at the same pole, thus DivL is not required to diffuse in the domain. The effect of tuning the parameter $k_5$ (associated with the inhibition of DivL by DivKP) is discussed next.

| | **Upstream** | | **Downstream** | | |
|---|---|---|---|---|---|
| **SC** | *DivJ* | *PleC* | *CcKA* | *CcKA* | *DivL* |
| | (K) | (P) | (K) | (P) | (I) |
| **1** | St | St | St | St | St |
| **2** | St | Sw | St | Sw | Sw |
| **3** | St | St | Sw | Sw | Global |
| **4** | St | Sw | St | Sw | Global |

Table 6.3: **Different spatial configurations are listed.** The localization of each enzyme in the network is explicitly listed. SC- Spatial Configuration, K- Kinase, P- Phosphatase, St- Stalked pole, Sw- Swarmer pole

***The direction of the graded profiles of the downstream substrate CtrA may be modulated when enzymes are co-localized*:** In configuration 1, both CtrA species are diffusing and are found to be weakly graded in the domain. The effect of varying $k_5$ is examined in this configuration. The overall concentration of DivL and CtrAP decreases as $k_5$ is increased. We found that when $k_5$ exceeds a certain value, the graded spatial profiles of both CtrA species change direction or "flip" (Fig. 6.14). The reason for this is as follows. First,

it must be noted that the phosphorylation and the dephosphorylation reaction of CtrA occur in the same localized region in this configuration. Now, at a certain value of $k_5$, the phosphorylation rate constant is greater than the dephosphorylation rate constant, $k_{k2} > k_{p2}$. However, when $k_5$ exceeds a certain value the inequality changes and now $k_{k2} < k_{p2}$. Thus the spatial profiles of CtrAP and CtrA flip and are now distributed in the opposite direction in the spatial domain.

***Steepness of the graded profiles of CtrA may be modulated when enzymes are localized in different poles*:** In configuration 2, the profiles of both CtrA species are steeply graded in the domain (Fig. 6.14). This is because in this case the phosphorylation and the dephosphorylation of CtrA occurs in separately localized regions (swarmer and stalked poles, respectively). Hence, the two modification steps do not directly compete with one another at the same location (unlike in spatial configuration 1). As a result, steeply graded spatial concentration profiles of both forms of CtrA are present in the spatial domain.

If the rate constant $k_5$ is increased, the steepness of the gradient of both profiles decreases. This is because as $k_5$ increases, the concentration of DivL decreases, but as it is localized and non-diffusible, only in the localized region of the swarmer pole. Consequently, in that region, the rate of phosphorylation of CtrA also decreases. This leads to a decrease in CtrAP concentration in that localized region and thus the steepness of graded profiles of CtrAP (and CtrA) also decreases.

The direction of the gradient of CtrAP is suggested to establish the asymmetry in a predivisional *Caulobacter* cell. Our findings indicate which spatial designs results in steep or shallow graded profiles for CtrA and suggest how, by tuning the interaction parameters, the steepness and direction of the profiles may be modulated by the cell.

In these configurations 1 and 2, DivL is not required to diffuse in the spatial domain in order for the interactions between the upstream and downstream modules to take place. Next, configurations where diffusion of DivL is necessary in order to complete the circuit of interactions is considered. Two more spatial configurations are examined next (Table 6.3).

***Effect of diffusion of DivL*:** In configuration 3, all the upstream species are present at the stalked pole and all downstream components are present at the swarmer pole. In this case, the profiles of both CtrA species are weakly graded (for the same reason as in configuration 1). The effect of varying $k_5$ is examined next; as this parameter is increased, the overall concentration of CtrA increases and that of CtrAP decreases. However, unlike in configuration 1, a "flip" in the spatial profiles is not seen (Fig. 6.14).

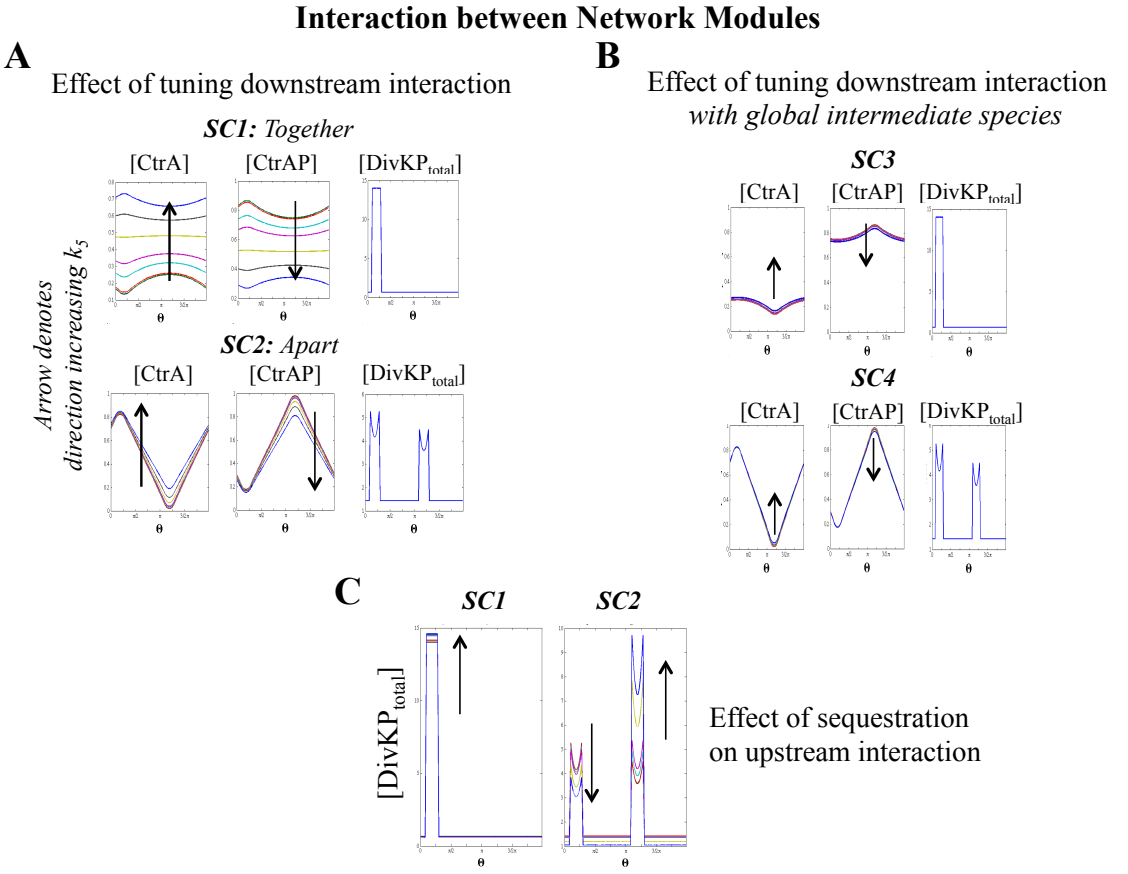


Figure 6.14: **Effect of localization of enzymes on the temporal interaction between the network modules.** (A,B,C) The arrows denote the direction of increase of $k_5$ (the upstream interaction parameter between DivKP and DivL). (A,B) The effect of tuning $k_5$ for spatial configurations SC1 and SC2 on the spatial profiles of both CtrA species and total DivK concentrations are shown. The different types of spatial configurations are listed in Table 6.3. (A) (Top) For Spatial configuration 1 (SC1), the overall concentrations of CtrA increases and that of CtrAP increases. Also the direction of the spatial profile "flips" when $k_5$ crosses a certain value. (Bottom) In Spatial configuration 2 (SC2), as $k_5$ is increased, the spatial profile of both CtrA species becomes weaker. (B) Spatial concentration profiles for (Top) Spatial configurations SC3 and (bottom) SC4 are shown when the interaction parameter $k_5$ is varied. The effect parameter variation is relatively less than (A). (C) The effect of varying the localization/diffusion of DivL is shown for when DivL and DivKP are sequestered in a complex. In SC1 (LHS), the total DivK concentration at the stalked pole increases and in SC2 (RHS) the concentration varies in opposite directions at both poles as the parameter $k_5$ is increased.

Configuration 4, is similar to configuration 2 but in this case DivL is diffusing and present everywhere in the spatial domain. As expected, the spatial profiles of CtrA are steeply graded across the domain here as well. We examine the effect of varying the rate constant $k_5$. We found that as it increases, the steepness of the concentration gradients of CtrA spatial profiles decreased, but only slightly (Fig. 6.14).

In both these configurations, upstream of DivL is the localized DivKP species and thus

the spatial information DivL receives is from a localized source. However, DivL itself is globally distributed or its own concentration is spread in the spatial domain. Thus, the upstream localized spatial information received is averaged out in the spatial domain. Now, in the downstream module, the enzyme receiving information from DivL is localized. Thus, it only "reads" the information present in that localized region. Since the information received is an average of the localized information from the upstream network, the effect on the downstream network when $k_5$ is tuned is less compared to when the information received is purely localized (as in configuration 2).

***Distribution of DivKP is affected when DivL diffuses*:** We have previously mentioned that two model variants that differ in the manner in which DivKP and DivL interact are considered in the analysis. In the first variant the inhibition of DivL is considered to be in the mass action regime and in the second variant DivL and DivKP are sequestered in a complex. Our analysis shows that when different spatial configurations are considered, the difference in the responses of two variants lies in the way the concentrations of the profiles of the upstream species are affected. This was seen in the earlier spatial designs study with building blocks as well.

In the first variant, the concentration profiles of the upstream species are unaffected by the tuning of the interaction parameter ($k_5$) and/or the diffusion of species downstream (this can be seen in Fig. 6.14). However, in the second variant where DivL and DivK are sequestered in a complex, varying the interaction parameter $k_5$ or varying the spatial distribution and diffusion of DivL (or both) has an effect on the concentration profile of DivKP and hence the remaining upstream species as well.

*Spatial distribution of DivL has an effect that back propagates upstream*: If DivL is localized in the same region as all the upstream species (configuration 1), when the parameter $k_5$ is modulated, the concentration of DivKP will increase in that localized region as $k_5$ increases (Fig. 6.14). In configuration 2, DivL is localized at the same pole as DivKP (bound form), the concentration of DivK total will increase in this pole (swarmer), however in the opposite pole (stalked) the concentration will decrease (Fig. 6.14). This would also be the case if DivL is a global entity present everywhere in the spatial domain (configuration 4). The reason the total increases is that DivL-DivKP complex is now being formed in that localized region and therefore contributing to the increased total DivKP in that particular region. However the other forms of DivK species are decreasing. Thus in the location where the complex is absent, the total DivK decreases.

In summary, we have examined two spatial models of the networks in the Caulobacter

cell cycle in order to explore the spatiotemporal interactions within. We have analyzed the effects of different spatial configurations on the temporal interactions and discussed the implications of each in the concrete networks.

### 6.3.5 Exploring dynamic feedforward spatial control in the cell cycle

The cell cycle is a continuous transition between different phases and a medley of spatiotemporal interactions takes place within each phase. Of particular interest is the dynamic localization of enzymes from one phase to another. Experiments show that the localization of species plays an instrumental role in orchestrating key developmental events during the cell cycle. What is not clear however is how. Answering this question is a major challenge- not least because it needs to be answered in a setting where are a multitude of interacting species and many details are yet to be uncovered. However, it is an important goal to move towards, especially in light of the fact that spatial organization is an important aspect of the cell cycle, across different organisms- from eukaryotes to prokaryotes. Without understanding this key mode of control, our understanding of the cell cycle is very far from complete and has important qualitative gaps.

In recognizing the challenging nature of this task but at the same time its importance, we take steps towards creating a platform to understand how spatial control mechanisms act in tandem with temporal signalling events to coordinate the cell cycle. We create this platform by systematically examining the role dynamic spatial control in enzymatic building blocks and thus provide a basis for conceptualizing and understanding how such dynamic spatiotemporal control mechanisms are integrated into the cell cycle.

The enzymatic pathway we focus on is the PleC-DivK-DivJ pathway. Recall that DivJ and PleC regulate the phosphorylation and dephosphorylation of DivK, respectively. Several aspects of this pathway make it an ideal candidate for the purposes of this investigation. Firstly, PleC dynamically localized through out the cell cycle. In the first phase or phase 1, PleC is present at the "old" swarmer pole, in phase 2 it is present everywhere in the membrane and in phase 3 it is present at the "new" swarmer pole only. In simpler terms, in phase 1 PleC is at pole '1', in phase 2 it is everywhere and in phase 3 it is at pole '2'. Second, DivJ is also subject to locational control- it suggested to be inactive/absent in phase 1, and localized at pole 1 only in phases 2 and 3. Third- DivK is present throughout the cell cycle and its spatial distribution changes as well. In phase 1, the concentration of DivK is present everywhere, in phase 2 it is mainly localized at the stalked pole and in phase 3 it is

localized at both poles (Jacobs et al., 2001).

In light of the observed spatial distributions, we then ask the question- what effect does the dynamic localization of PleC and localization of DivJ have on the spatial distribution of DivK in light of the underlying signalling interactions? To address this question we take an existing spatial model of this network (Tropini and Huang, 2012) (Model A), and modify it to incorporate the dynamic localization of PleC (details are discussed in the Models and Methods section). We then examine how the resulting spatial distribution of total DivK concentration changes as the localization of PleC changes.

By conducting our study in this manner, we aim to shed light on the following question: are the resulting spatial distributions of DivK commensurate with the experimentally observed distributions? If not, what are the possible factors missing/needed for them to be so? After addressing this question, we extend our platform to also examine the causal links hypothesized (in the experimental literature) between the observed spatial behaviour and the underlying phospho-signalling interactions- i.e. how are the spatial and temporal mechanisms linked? We utilize our platform to ascertain if these may or may not be realized in such a setting. Furthermore, we also examine existing spatial models, which implicitly utilize these hypotheses and discuss how their conclusions fit into the overall picture. We begin by discussing our analysis.

## Effect of dynamic localization of PleC on DivK spatial distribution

The simulated spatial distributions of the total DivK concentration are shown in Fig. 6.15 for the three different phases. The majority of the total concentration is mainly present at pole 1 in phases 1 and 2. In phase 3, the DivK total concentration is localized at both poles and also distributed in the domain in between the poles and at the swarmer pole. When compared to the experimental evidence, the simulated distribution in phases 2 and 3 (but not in phase 1) reflects the experimental evidence. We further examine why this difference between predicted and experimental results exists in phase 1.

The interactions in (the original) Model A (Tropini and Huang, 2012) describe the experimentally observed accumulation of DivK at the two poles during phase 3. In this phase, recall that DivJ is localized at pole 1 and PleC at pole 2. The accumulation is modelled as a two step-process involving binding to the enzyme at the pole and catalysis of the substrate followed by immediate release. The reaction kinetics are assumed to be slow compared to the rate of binding. Furthermore, in light of experimental evidence that

suggests that DivK may bind to pole 2 even if PleC is not present, additional binding and unbinding rate constants are introduced for pole 2. This resulted in a steady state spatial distribution of total DivK that peaks at both poles and is almost flat in between the poles.

In modifying Model A, we have not changed the existing parameters. Furthermore we have assumed that DivJ, is present and localized at pole 1 during all three phases. If we take into consideration that DivJ might be inactive during phase 1, and that experimental evidence does not suggest that DivK accumulates at the poles in phase 1 then the parameters of the model must reflect this as well. We examined the effect of modulating the rate constants such that the binding is now slower than the phosphorylation/dephosphorylation kinetics. This results in a nearly uniform profile of total DivK (Fig. 6.15). If the parameters are further modulated to reflect the inactivity/absence of DivJ in phase 1 (by making the phosphorylation and binding parameters zero) then this results in a uniform profile of total DivK.

**Addressing experimental hypotheses**

Where do the existing models stand in light of the observed spatial distributions? In this model the assumptions about the binding and kinetics of the network are based on the experimentally observed distribution in phase 3. In our utilization of the model in (Tropini and Huang, 2012) we find that in order for this model to be commensurate with the observed spatial distribution in phase 1 new assumptions need to be made and subsequently incorporated into the model through adjustment of parameters. Thus implicitly we assume that the binding mechanisms are subject to change from one phase to another. Or that additional factors or interactions, which are already present at the time of localization of PleC or are triggered by its localization in different phases may modulate the signalling interactions within this network.

We also examine the hypotheses concerning the spatial localization of entities in another model in (Subramanian et al., 2013). This model is based on a set of biological hypotheses put forward to explain the transition between phases 1 and 2 (Paul et al., 2008). In this model all signalling interactions are assumed to be local and this is based on the hypothesis that all the entities involved are localized together at one pole in this transitory period. Thus justifying the use of ODEs to describe the reactions. Furthermore, based on biochemical evidence, this model takes into account that the enzyme PleC is bifunctional and that its substrate DivKP, activates its autokinase activity. The kinase form of PleC in turn drives the phosphorylation of DivK (in addition to DivJ)- resulting in a positive feedback effect. The analysis of the model shows that under a suitable parameter regime

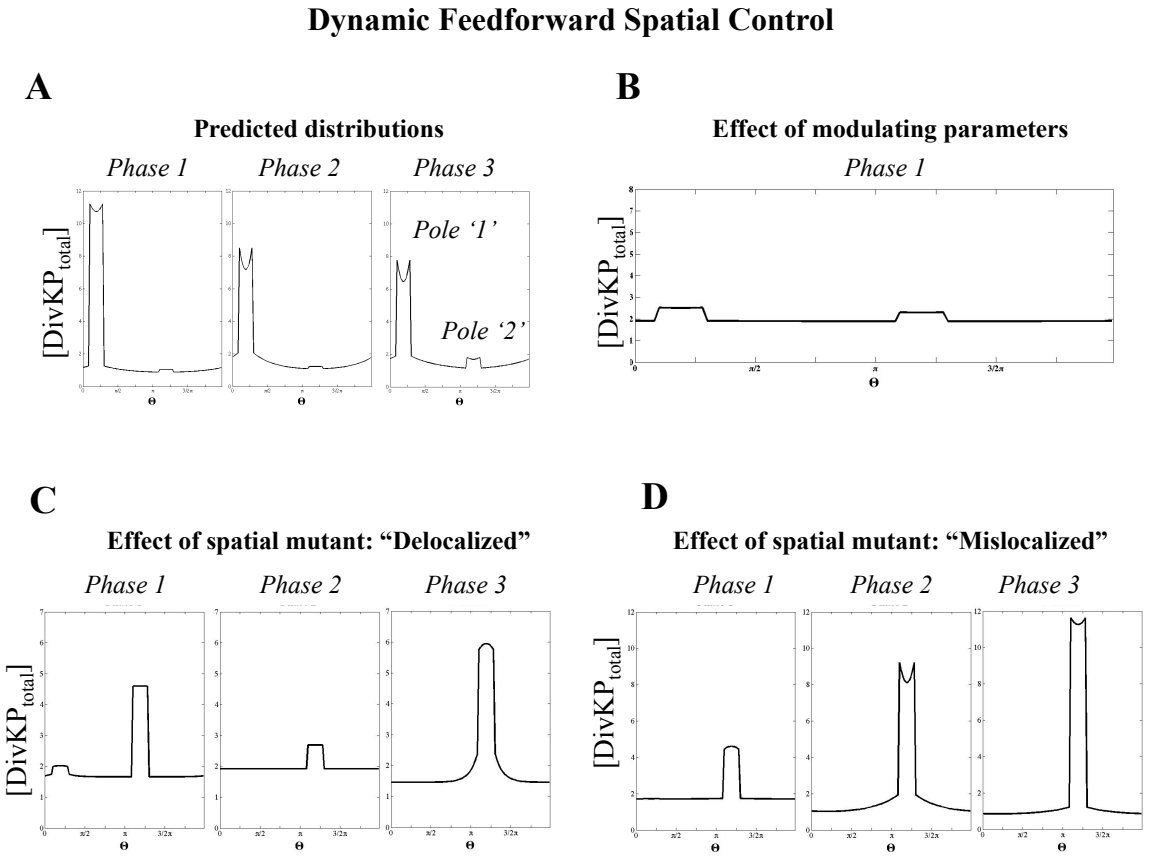


Figure 6.15: **Effect of Dynamic Feedforward Localization Control.**: The total DivK concentration is shown for three different phases of the cell cycle. (A) The total concentration was mainly present at pole 1 in phases 1 and 2. In phase 3, the DivK total concentration is distributed between both poles. (B) After the balance between the binding and phosphorylation kinetic rates are adjusted, the total DivK concentration is nearly uniform everywhere in phase 1. Network with spatial mutants: (C) DivJ is "delocalized", i.e. present everywhere in the domain, throughout the three phases (D) DivJ is mislocalized: i.e. present at pole 2, in all three phases. The total DivK concentration mainly accumulates and localizes only at pole 2 in all three phases.

a bistable switch can arise due to this positive feedback effect. This bistable switch is suggested to underlie the transition between phase 1 and phase 2.

Our study of individual building blocks and their interactions, reveals that such a bistable switch maybe distorted if certain spatial designs are present, especially if the modified substrate is diffusing. The spatial distribution of DivK is observed to be uniform in phase 1 and partially localized and spread out in phase 2. Also, in phase 2 PleC is no longer localized but distributed in the membrane. This implies that between phases 1 and 2, both DivK and PleC are diffusing. If this is found to be the case during the transition between the phases then these effects must be taken into consideration in any model describing the transition

between the two phases.

Specifically with respect to the bistable switch effect arising in the model (Subramanian et al., 2013) may or may not be preserved due to diffusion/distribution of the species in this network. There could be two reasons for this, first substrate diffusion results in a dilution effect (the consequences of which are discussed in the earlier part of the study), which leads to loss of the bistability. Second, the feedback through which the bistability arises would now be global feedback due to both enzyme and substrate diffusion and no longer localized. This may again result in the distortion of the bistable response. This implies that it may not be valid to suggest that the transition between phases arises through the bistable mechanism suggested in Subramanian et al. (2013). Thus the assumptions in that model, i.e. purely temporal interactions, merit a closer examination.

**Effects of spatial mutations on DivK spatial distribution**

Mutants of proteins and enzymes in networks are widely used in experiments to understand the organization of network interactions. Spatial mutants, signalling entities whose localization or distribution is distorted, are currently being developed and are increasingly being used to probe the effects of spatial localization on signalling interactions (Etoc et al., 2013; Lasker and Shapiro, 2014). In this part of the study, we examined two spatial mutants of DivJ. Two different types of mutants were considered- one where the enzyme DivJ was "delocalized", i.e. present everywhere in the domain, throughout the three phases (Fig. 6.15). In the second mutant, DivJ was mislocalized i.e. present only at pole 2, in all three phases (Fig. 6.15). Similar *in silico* mutants were utilized in (Tropini and Huang, 2012), but only for phase 3 of the cell cycle. While these particular mutants have not yet been created in experimental efforts, we take the opportunity to provide testable predictions for when they would be developed.

We expect that when compared to the observed wild type distribution, the total DivK concentration in the mutant network models will be different. We find that in both mutants, that the majority of the total DivK concentration in all three phases is localized only at pole 2. DivK is suggested to play a role in the polar development of the cell. In mutant cells where either PleC or DivJ (or both) are deleted, the phenotypes of the resultant daughter cell are abnormal. For example in DivJ deleted mutants, the progeny develop stalks at both ends or even in the middle of the cell. It is suggested that this may be due to the aberrant distribution of DivK as a result of the deletion (Wheeler and Shapiro, 1999). Our findings predict that due to the mutant localization of DivJ, DivK distribution is also abnormal. Thus it would have consequences for the morphology of the daughter cells. With experi-

mental tools that directly control the localization of proteins being applied to understand the *Caulobacter* cell cycle (Lasker and Shapiro, 2014), we expect that such predictions would soon be tested as well.

## 6.4 Conclusions

In previous studies, we have examined the role of spatial regulation and control in representative networks and enzymatic building block modules and signalling cascades (Alam-Nazki and Krishnan, 2012, 2013) and ((Alam-Nazki and Krishnan, 2014))/Chapter 5). Echoes of enzymatic building block modules that we have investigated are found in a wide range of eukaryotic and bacterial organisms. In particular, in the bacterium *Caulobacter*, there are striking examples of spatial control mechanisms coordinating the signalling events underlying its life and growth cycles. The spatio-temporal aspects of the cell cycle signalling networks as well as the relatively more tractable nature of bacteria is the motivation for this study: to understand the spatio-temporal organization and control of signal information processing networks in the *Caulobacter* cell cycle.

One major focus of the investigation of the cell cycle in *Caulobacter* is to understand how spatial control mechanisms work in tandem with the temporal signalling interactions and where and how do these fit into the sequence of events in the cell cycle. The complex web of interactions within the cell cycle with its myriad details makes answering these questions a major challenge. While there are extensive experimental efforts being made to address these questions, our understanding of the cell cycle still has many qualitative gaps. Furthermore, there are only a very small number of modelling studies that address the spatial organization of signalling networks in the cell cycle. Without understanding this basic aspect, our understanding of the cell cycle remains fundamentally incomplete. A platform is needed to conceptualize and achieve a basic understanding of how the spatial and temporal aspects of the cell cycle are organized and coordinated together.

From a systems engineering vantage point, the cell cycle may be seen as a collection of interacting building blocks. Individual building blocks are centered on phospho-signalling modification cycles with either mono-functional or bifunctional enzymes (or both) driving the modification reactions. Spatial control is integrated into these building blocks by way of localization or compartmentalization of different enzymes or modification steps. Two basic types of spatial localization designs that the cell employs are the localization of entities together in one region (i.e. at the same pole) or in opposite regions (at different

poles). The entities may also be distributed in the region between the poles. Furthermore, the localization of entities is dynamically controlled, i.e. the locations of entities change from one phase of the cell cycle to another. It remains to be understood how these spatial designs act in conjunction with the underlying phospho-signalling networks to give rise to the signalling behaviours and the dynamics observed. We utilized a systems approach combined with *in silico* synthetic engineering design approach to shed light on this question and other related issues pertaining to the spatio-temporal organization of the cell cycle signalling networks in *Caulobacter*.

We began our investigation by examining the spatial regulation of a range of building block models at the core of which are the modification cycles/pathways driven by bifunctional enzymes. The signalling interactions in these building blocks are representative of the kinds of interactions seen in the *Caulobacter* cell cycle signalling networks, as are the spatial effects we examine. Armed with the insights from the systematic investigation of spatial organization of building blocks, we moved towards understanding the spatiotemporal organization of the concrete networks. We focused on two networks in the *Caulobacter* in particular. This phase of the investigation was divided into two parts. First, we examined a selected combination of building blocks (that reflect the signalling interactions within these two networks) and investigated their temporal interactions. We then explored the effect of different spatial designs of localization and distribution of signalling entities on the interactions between these building block combinations. Along with providing a basis to understand how the interactions between signalling modules are spatially organized in *Caulobacter*, our study of different spatial designs also gives us insight into the spatial organization in other bacterial systems where similar questions may be relevant.

In the second part, we examined existing spatial models of the two *Caulobacter* signalling networks mentioned above. Here again, using a selection of spatial design configurations that are based on the cells own design logic, we explored the spatio-temporal regulation of the interactions between these networks. In the last part of this study we took the first step towards elucidating how dynamic feedforward control of signalling entities regulates the underlying phosho-signalling interactions in space and time. We used our platform to examine how our findings fit into the current experimental observations and hypotheses. We also utilize *in silico* spatial mutants to make testable predictions about the potential consequences of the aberrant localization of species on signalling behaviour. We summarize the results of each part of the investigation in the remaining section.

### 6.4.1 Summary of the analysis of building block models

While temporal aspects of the modification cycle with a bifunctional enzyme have been the focus of many recent experimental and modelling efforts, modelling studies examining the role of spatial effects in this basic mechanism are missing. In the first part our investigation we developed a mathematical modelling framework within which we systematically examined the spatial organization of this cycle and its extensions.

We started with the simplest description of the modification cycle with a bifunctional enzyme. Then, in a systematic way, we built in different feedback and feedforward interactions, one step at a time into this basic model. This gave rise to a suite of building blocks/modules with multiple modes of control and the signalling interactions within each model reflected the kinds seen in the cell cycle networks. Building layers of complexity into the basic mechanism in a systematic and step-wise manner allowed us to clearly delineate the effects that arise through the incorporation of each interaction. With each new addition, we examined the model in light of different spatial effects. Thus, this allowed us to transparently ascertain how introducing different spatial perturbations affected each set of signalling interactions.

Different spatial effects were introduced into the temporal bifunctional modification cycle modules to establish how the temporal information processing behaviour of each module would be modulated/distorted. The spatial effects examined were- spatially varying signals (graded signals/enzymes) and localization or compartmentalization of signalling entities. Each model was first examined in a purely temporal setting and the resulting response was then compared to the response when entities in the modification cycle were allowed to diffuse. Our results showed that when diffusion was absent, an analog of the temporal steady state response was present in the spatial signalling response. Our findings have many parallels to the ones in (Alam-Nazki and Krishnan, 2013) (Chapter 4). We found that when a combination of graded signals and diffusing species was considered present, the diffusion of species, including the complexes, played a significant role in modulating and altering the spatial profiles of species in the cycle.

#### The effect of incorporating feedforward control

We examined the effect of incorporating feedforward control of the two activities of the enzyme via an external signal (or signals). A consequence of incorporating this type of

control was that the temporal and spatial signalling behaviours of this modification cycle started to resemble those in a cycle with separate or mono-functional enzymes. Different spatial (graded) distributions of the signal allowed for different combinations of spatial distribution of cycle species (which was constrained in the simple model). Furthermore, localization of the signal and cycle components also provided a way to spatially control the activities of the enzymes. For example separately localizing the regulating signal(s) in two different locations enabled one form of the enzyme to be dominant at each location.

Reciprocal control of the enzyme activities by an external signal enabled the cycle to exhibit an "ultrasensitive" response in a special parameter regime. This behaviour has been studied in detail in the bifunctional modification cycle in (Straube, 2014). We examined this response in a spatial setting and found that for a graded signal input, the spatial profile of the modified species had a spatial switch-like characteristic. When diffusion of species was introduced into the cycle, our results showed that this spatial switching effect could either be enhanced or abolished (depending on which species was diffusing). Similar insights were obtained in the analysis in (Alam-Nazki and Krishnan, 2013).

While examining the effect of localization of the cycle components on the input-output relationship (between the concentrations of modified substrate and the external signal), we found that in the case when diffusion was absent, this relationship was identical to the temporal case. However when species were allowed to diffuse, our findings showed that a decrease in the sensitivity of the input-output relationship occurred and this resulted in the loss of the switch. Similar insights were obtained in the analysis of the Goldbeter Koshland type switch in Chapter 5.

## Effect of the positive feedback interaction

Next, the effect of introducing a positive feedback interaction (between the kinase activity of the enzyme and the modified substrate species) was examined on the cycle. This model was found to exhibit a thresholding effect arising through a transcritical bifurcation in a particular parameter regime. We examined the model in this parameter regime and our findings showed that for a graded signal input (straddling the threshold on either side), a thresholding effect was manifested in the spatial profile of the modified substrate as well. When substrates were allowed to diffuse, our findings showed that this resulted in the loss of this effect.

Our analysis showed that the interplay of diffusion and localization affected this tem-

poral response in different ways. When species were localized in a patch in the spatial domain and if both substrate species were allowed to diffuse out of the patch, the concentration of the modified species at steady state became zero/"turned off." In the case where the modified species itself was diffusing the steady state response remained non-zero.

## Effect of enzyme sequestration and the bistable switching response

Our analysis shows that when strong enough positive feedback interaction is present, this cycle is capable of exhibiting a bistable response. Alternatively, bistability also arises through the combined effect of sequestering the enzyme through inhibition by its substrate and the positive feedback (there are other possible sequestration mechanisms from which bistability may arise as well). We studied the effect of gradients and localization in both these types of models and obtained similar qualitative insights. When a graded signal was present, depending on the range of local signal values, the steady state concentration profile of the response either had a graded or a spatial switch like characteristic. If in the bistable regime, appropriate initial conditions were required for the spatial profile to have the switch-like characteristic. Diffusion of the substrate species resulted in the loss of the switch like characteristic in the spatial profile. In the cases where localization of cycle components was examined, the response was identical to that of the temporal case. However, if the substrates were allowed to diffuse out of the localized patch, then this resulted in the loss of the bistability.

**Consequences of the dilution effect:** Interestingly a common theme emerged when each of the three temporal behaviours were perturbed by spatial localization effects. When substrates were allowed to diffuse out of the localized patch, it resulted in the loss of the ultrasensitive switch or the cycle being pushed past the transcritical threshold or loss of the bistable response. The spreading of the species results in a significant dilution effect and this effect, in turn results in the distortion of each of these temporal characteristics. This effect has been studied in detail in Chapter 5 (Alam-Nazki and Krishnan, 2014).

If the dilution effect is mitigated, for example by increasing the width of the localized patch, then the resulting response is also different in each of these cases. In the case of the ultrasensitive response the decrease in the sensitivity of the input-output response may be reduced and thus the switch may be salvaged. In the case of the transcritical bifurcation, the response does not cross the threshold and thus the steady state of the response remains at a non-zero steady value. Finally in the case of the bistable response, mitigating the dilution

effect results in the preservation of bistability.

Overall, the spatial effects we have examined play a non-trivial role in each of the building block models. The impact of spatial regulation on temporal signalling behaviour is a result of a subtle combination of factors that come to light when such spatial effects are explicitly considered. Next, we used the analysis of building blocks as a platform to study concrete signalling networks in the *Caulobacter* cell cycle. This is discussed next.

In the next phase of the investigation we focused on two signalling networks of the cell cycle- the PleC-DivK-DivJ and CtrA-CckA networks. In the first part of the study we selected building block/modules that closely represent the signalling interactions within these networks and examined their interactions in light of different *in silico* synthetic spatial designs. These spatial designs arose through different configurations of spatial locations/spatial distributions of enzymes within these networks. These designs were based on the concrete configurations seen in *Caulobacter* as well as alternate designs that might be present in other bacterial systems.

### 6.4.2 Temporal interactions between building block models and the effect of spatial designs

We have incorporated an intermediate species (suggested to connect the two networks above (Tsokos et al., 2011)). We examined the temporal interaction between these networks by using two different combinations of building block models (Table 6.1) We probed how different spatial designs affected these temporal interactions. Our findings also uncovered the capabilities and constraints associated with each of these designs.

There are two basic types of designs- when the components of the modules are together or when they are localized separately. In the latter case, relevant species must diffuse in order to complete the circuit of interactions. Thus the presence of global entities is a requirement in certain spatial designs. Also, we found that the presence of bifunctional enzymes (CckA) in the modification cycle imposed restrictions on the number of possibilities of spatial designs that could be achieved (when compared to a cycle with separate enzymes). Regulation of the two activities of the bifunctional enzymes by the intermediate species through kinetic as well as localization control helped bypass these constraints.

Different types of spatial designs led to different types of spatial distributions of the modified species (graded, localized or uniform). We also uncovered the consequences of spatial control via localization of modules for the temporal interactions between the mod-

ules. Locational constraints could either mitigate or enhance the effect of an interaction-for example inhibition of the intermediate DivL by the modified substrate in the upstream network, DivKP, is reduced when DivKP diffuses as result of the dilution effect. The cell may bypass this constraint by either maintaining low levels of DivKP concentration or use this effect to its advantage to keep DivK concentrations beneath a certain level.

The level of DivK is suggested to be an important cue or threshold for the development of the flagellar pole and our findings shed light on different spatial designs that affect DivK levels. Our findings illustrate that is important to consider the effects of different spatial designs on the spatial distribution of modified species as these distributions play key roles in developmental events during the cell cycle.

In the second combination of building block models, we analysed different hypotheses that have been suggested to underlie the temporal interactions between these networks. First, it has been suggested that the PleC-DivJ network exhibits bistability (Tsokos et al., 2011; Tyson et al., 2003) and second, it has been hypothesized that DivKP inhibits the intermediate species DivL by binding to it and sequestering in a complex. We examined both these hypotheses here. In the latter case, we found that the kinetics of the interaction-whether involving mass action or sequestration will indeed have consequences. A "back propagation" effect was seen if the upstream species was sequestered in the intermediate. Due to this effect, the diffusion of the intermediate resulted in the alteration of the concentration levels of not only the downstream species but those of the upstream species as well.

Now in the case of the upstream module exhibiting a bistable response, we found that the bistability may be lost if the substrates of the upstream module were diffusing. However, if the upstream species maintained their localization and the intermediate was diffusing instead, this resulted in the preservation of the bistable response. These findings highlight the importance of explicitly accounting for the spatial regulation of these signalling networks.

With regards to the suggestion that the transition between two phases of the cell cycle arises through a bistable switch (Subramanian et al., 2013); the model in that paper in purely temporal terms. When the bistability is examined with respect to different spatial designs, our results indicate that, depending on which species in the networks are diffusing, the bistable response may be preserved or lost. Without taking into account how the effect of diffusion combines with that of localization of signalling entities (both are observed to be present in the phases under consideration) the answer to the question of whether bistability

underlies this transition is incomplete.

We recognize the fact in the concrete networks; the exact interactions through which bistability arises may be different from the one being considered in our analysis (or in (Subramanian et al., 2013)). However, bistability ultimately emerges through a strong feedback interaction or through partial sequestration and we have examined models employing both of these mechanisms. Furthermore, our goal is to gain a qualitative understanding of the effect of the interplay of spatial localization and diffusion on the bistable response. In any given system the details of the interactions may vary- but these qualitative signatures may be present in similar ways across different systems. With this final insight, our study of *in silico* synthetic spatial designs came to a close. Now we present the discussion of results in the second part of this study.

### 6.4.3 Discussion of the analysis of the existing spatial models of *Caulobacter* networks

In this part of the study we used two models in (Chen et al., 2011) (which describes the PleC-DivJ network) and (Tropini and Huang, 2012) (which describes the CckA-CtrA network). These networks were made to interact via the incorporation of an intermediate species DivL. Here as well, we examined the consequences of localizing enzymes in different spatial configurations on the temporal interactions between the networks. Some of the insights obtained in this part of the study were similar to the our results showed that if the enzymes of the upstream and downstream networks were localized separately, a diffusible global intermediate was required in order to convey information from one location to another. Otherwise, in the absence of the intermediate, the product of the upstream network would have to itself diffuse to the second location in order to complete the circuit. As we found in the case where the upstream network exhibited a bistable response, diffusion of species in the upstream network may important consequences for the temporal signalling behaviours, if any are present.

Our results indicated that different spatial configurations of enzyme localization lead to either sharp or weakly graded profiles of the phosphorylated species in the spatial domain. Properties of the spatial distributions, for example the steepness or the direction of the graded profiles, were sensitive to the modulation of relevant kinetic and/or transport parameters. Spatially graded profiles of species have been suggested to play an important role in certain processes involved in different phases of the cell cycle. For example the

graded profile of the modified substrate CtrAP is proposed to establish asymmetry in the pre-divisional cell even before cytokinesis occurs. In this context, our results indicate that the different spatial configurations of enzymes combine with the kinetic interactions to play a non-trivial role in determining the spatial distributions of signalling species. Thus the interaction of both must be explicitly accounted for in any modelling study of the signalling networks in the cell cycle.

We also took the first steps in creating a platform to examine the dynamic feedforward control of signalling species and how this control mechanism may coordinate with signalling interactions in the cell cycle. We examined the dynamic localization of enzymes in the PleC-DivJ network and focused on the resulting spatial distribution of DivK. We compared predicted distributions of DivK to the experimentally observed ones and our findings revealed which assumptions naturally led to commensurate distributions. Also when differences between predicted and observed distributions were seen, we showed which additional effects were necessary in order achieve similar distributions. We were also able to use our platform to evaluate the relevance of hypotheses in existing models of the cell cycle in a spatio-temporal setting. Finally we examined two kinds of spatial mutations of the enzyme DivJ and made testable predictions about how each could disrupt the spatial distributions of DivK. It must be noted here, that as the cell cycle progresses, the size of the cell changes and this would impact certain parameters (for example diffusion coefficients). We recognize that this would potentially affect the outcomes in each phase. While we do not address this change in our current model, we will consider these aspects in future investigations.

Basic qualitative gaps in our understanding of the cell cycle will remain if the spatiotemporal control and regulation of the signalling networks within is ignored. In this investigation we have taken a combined systems and synthetic approach to understand these fundamental aspects. Our investigation began with examining spatial organization of bifunctional modification models and building on the insights gained from these studies, moved towards elucidating the spatiotemporal organization of concrete signalling networks in the *Caulobacter* cell cycle. Utilizing such an approach allowed us to engage with the complexity of the *Caulobacter* cycle on one hand but also gain some transparent insights without being weighed down by the various details of the system.

Our *in silico* synthetic design approach reflects the kinds of experimental tools being applied to directly control the localization of proteins (Lasker and Shapiro, 2014) in *Caulobacter*. Our *in silico* investigation of spatial designs and the insights obtained may find relevance in multiple types of concrete systems and could also act a platform for de-

signing synthetic systems which utilize the advantages of spatially controlling enzymes and reaction pathways via localization (Sachdeva et al., 2014).

# Chapter 7

# Conclusions

Signal transduction networks are the focus of a large number of investigations and are typically studied in temporal terms. The study of the spatial dimension of signalling is a very important aspect that is missing from many of these investigations. Numerous examples in the biological literature illustrate that at a fundamental level, spatial organization and control are integrated into the functioning and dynamics of signalling networks. Chemotaxis, generation and maintenance of cell polarity and cycling of G-proteins are just a few examples of important processes where space plays a central role and cannot be ignored (Eisenbach et al., 2004; Nelson, 2003; Rappaport, 1971; Vartak and Bastiaens, 2010). Even bacteria- that were previously assumed to be well mixed vessels of enzymes devoid of any sub-cellular organization, contain a complex internal spatial architecture. Their subcellular spatial organization plays an integral role in driving key regulatory processes such as cell division and differentiation (Shapiro et al., 2009). For example, *E. coli* utilize the spatiotemporal oscillations of the Min proteins between poles (Min protein waves) in their strategy to establish the correct site for cell division (Loose et al., 2008).

In recent years, various experimental papers and special issues in journals have been highlighting the need to account for spatial effects in signal transduction (Hurtley, 2009; Kholodenko et al., 2010; Schwarz-Romond and Gorski, 2010). Furthermore, experimental techniques are being developed to gain better quality of spatially resolved data as well as spatial control over signalling networks. Some examples of new tools that are being developed to control signalling activity at the subcellular scale are optogenetics and magnetogenetics (Etoc et al., 2013; Levskaya et al., 2009). Recently, these have been applied to proteins known as Rho GTPases, which are important players in spatiotemporally regu-

lating cell morphology.

In synthetic biology, researchers are taking inspiration from the natural strategies utilized by cells (for example compartmentalization of reaction pathways) and implementing these in synthetic systems. For example, RNA-based scaffolds have been developed to spatially organize enzymatic metabolic reaction pathways in *E. coli* in order to achieve an increased output Sachdeva et al. (2014). Researchers are also utilizing spatially organizing tools that naturally occur in signalling networks to reshape and engineer diverse signalling behavior (Lim, 2010). For example in eukaryotes- the Ste5 protein scaffold which plays a role in yeast mating pathways, was used to demonstrate how modifying the scaffold in a modular fashion could lead to different types of mating responses (Bashor et al., 2008).

These examples highlight some important points. First, it is evident from these examples that transport and localization are integrated in the chemical circuits driving cellular processes. Second, these examples also demonstrate that accounting for the spatial dimension to signalling is important for understanding specific cellular processes, as well as for harnessing the natural strategies employed by these cells towards synthetic applications. Third, the complexity of spatial organization of cellular signalling increases as one moves from examining prokaryotes to eukaryotes. Exploring the nature of spatial control and regulation of signal transduction in different organisms may allow us to understand the way in which cell signalling has naturally evolved across organisms. Fleshing out the role of space in signal transduction in both specific contexts as well as a broad setting involves many challenges, both theoretical and experimental. A framework through which the relevant issues may be examined and understood is absent from the signalling literature.

Through this work, we developed a multipronged approach in order to understand the impact of spatial regulation and control of signalling networks at multiple levels. Our initial investigation focused on the study of different aspects of how networks are organized in chemotaxis to give rise to both, attractive and repulsive responses (Chapter 2). This study motivated the investigation of other aspects of spatial signalling in broader contexts. First, we examined the role of spatial regulation in different types of networks (Chapter 3). Next, we disentangled the role of various spatial effects in a ubiquitously occurring, basic covalent modification cycle (Chapter 4) and subsequently in enzymatic modification cascades and pathways (Chapter 5). The insights gained from these studies served as a platform and bridge for elucidating the role of spatial control and regulation in concrete systems. In Chapter 6 we dissected the spatial organization of building blocks underlying the cell cycle signalling networks in *Caulobacter crescentus*.

## Examining the combined role of spatial effects and signal processing in chemotactic networks

Chemotaxing cells may be attracted or repelled by the same of different signals and different cell types exhibit distinct behaviours while sensing and migrating. For example, some cells may employ local sensing mechanisms, others show adaptation and some are observed to spontaneously polarize. This leads to the question- how are different cells able to exhibit both attractive and repulsive responses in light of these known behaviours? In the investigation discussed in Chapter 2, we developed a design framework within which we examined how representative chemotactic signalling networks are organized to give both attractive and repulsive responses. Our aim was to uncover the design features and principles underlying how these networks are wired for a cell to exhibit both responses, given the kinds of signalling behaviours seen in concrete systems. The representative networks that we analyzed encapsulate different qualitative behaviors mentioned above.

Our findings revealed which signalling design configurations may or may not lead to the desired behaviour and what constraints are at play for different signal transduction characteristics. For example, our analysis showed that when a simple opposite upstream regulation of the networks was present (a polarity switch), opposite responses could be obtained in each network. However this design came saddled with important constraints. For example, our results showed that with the polarity switch design feature, spontaneous polarization was seen only for the attractive response but not when the response switched to a repulsive one. However, having an adaptive signalling configuration relieved this constraint. This result shows adaptation in a new light- not only is adaptation useful for cells to access a broad range of dynamic signals but also plays an interesting role with relation to the polarity switch. We also examined another design feature involving competing pathways and our results showed that it was possible to obtain both responses with this feature. When combined with the spontaneous polarization characteristic, it was possible to both polarize and de-polarize the cell. Spontaneous depolarization has been observed in experiments in T cells (Prof A. Ridley, personal communication).

Thus our design framework revealed the capabilities, constraints and tradeoffs for each design configuration. The constraints and capabilities associated with each design are implicit and only come to light when building this design framework. Based on our insights we were able to suggest focused experiments for further probing individual systems as well as for manipulating migration in different cell types- which may be carried out even if all

the details associated with that system have not been fully characterized. Thus this work acts as a platform to understand chemotactic signalling in detail in concrete networks. Our insights are also relevant for other types of signals beyond chemicals- for example electrical and mechanical signals (Li et al., 2005; Zhao et al., 2006). Also our approach could be applied to conceptualize and design synthetic tools to engineer and exploit cellular migratory behavior. Currently, there is mounting interest in such applications. Levskaya et al. (2009) have synthetically re-engineered proteins so that they can be controlled by light signals and used this technique to control upstream regulators of the RhoGTPase proteins, which play important roles in the cells polarity circuit.

Moving on from the study of chemotaxis, in the following series of studies we examined the role of spatial regulation in information processing in signalling networks at multiple levels and in a broader setting.

## Examining spatial effects in typical network modules

In Chapter 3, we analyzed a number of representative modules that encapsulate qualitatively different signalling patterns commonly seen in biological networks. These modules have been temporally well characterized. Our goal was to understand the response of different signalling circuits to spatially varying signals as well as to shed light on how diffusion of network components affects the temporal signal processing behaviour.

Our analysis revealed how the presence of diffusion can significantly distort signalling behaviour of each network. We found that in an incoherent feedforward network, the presence of global entities led to the loss of an adaptive response, when spatially varying signals were present. In the case of the negative feedback network module, the response showed a sharper spatial contrast when the feedback was global. In the case of spatial switches- the presence of diffusing species may have an enhancing effect (monostable switches) or completely abolish this characteristic (bistable switches). These findings also illustrated how diffusion plays a role in introducing capabilities or imposing constraints and shed light on how constraints maybe bypassed by the cell. For example cells may immobilize species through localization mechanisms (for example through protein scaffolds) and combine with diffusion of signalling entities to accentuate switching responses.

Using our findings as a basis, in the future, investigations could focus on understanding the role of spatial effects in more complex representative networks as well as in concrete signalling networks. In this study, we have considered the spatial variation of upstream

signals in combination with diffusion of networks elements. Since localization or compartmentalization of signalling entities/networks is a widely utilized mechanism in cellular signal transduction, another future work could focus on examining the localization or compartmentalization of network elements in combination with diffusion. Also engineering localized networks or pathways has become an important focus of synthetic biology applications in recent years. For example, there is a large focus on the synthetic design of scaffolds to improve the effectiveness of reaction pathways (Lim, 2010). The findings revealed in this work may be tested experimentally by developing synthetic circuits where global pools of entities are present or where the localization of entities maybe manipulated.

In the next study, we shifted focus from the network level of information processing to the enzymatic level.

## Examining spatial effects in a basic enzymatic building block

In Chapter 4 we discussed the investigation of a basic enzymatic building block known as the covalent modification cycle. This basic enzymatic mechanism is a commonly occurring unit of posttranslational modification in signalling networks. Even at this basic level, spatial effects play an integral role and this aspect has been largely unexplored. In this study our aim was to uncover the role of space in information processing in this basic module. In our analysis we examined two different kinds of spatial effects, gradation of enzymes and localization of entities. We studied the effect of these as well as their combination with the diffusion of substrates, enzymes and complexes.

Our findings showed that the role of diffusion is non-trivial and even unexpected in some cases. When one or more species were diffusing (even moderately), the spatial responses of multiple species in the cycle were altered. When a spatial analogue of the ultrasensitive behavior was analyzed, we found that the switch-like characteristic in the spatial response was distorted (lost or enhanced) if species in the cycle were diffusing. Other surprising insights were revealed when examining the effects of localization and diffusion. Probing the interweaving of spatial transport and enzyme kinetics and diffusion revealed the presence of subtle and new features, for example competing effects, even in this basic module.

This study also highlighted certain related aspects, such as implications related to open and closed systems. For example considering whether or not a fixed pool of enzyme exists may have consequences for realizing a spatial switch. Other insights related to modelling

this mechanism also emerged, for e.g. certain assumptions, such as the ones made in the Michaelis Menten kinetic models or about spatially homogeneity, may not be accurate. Taken together, our study illustrates how even in this basic enzymatic module, the signal processing capabilities may be significantly altered or new effects may be introduced when different aspects of spatial signalling are examined.

## Dissecting the role of space in enzymatic modification cascades and pathways

In the subsequent study (Chapter 5), we moved on to investigating of the role of spatial organization in signalling cascades. We especially focused on the effects of localization and compartmentalization of the different stages of the cascades. We examined multiple variants of these cascades- this included cases when the modified form of one species of one stage (i) acts as an enzyme for the next stage (ii) acts as a substrate for the next stage (iii) is involved in phosphotransfer (as seen in a variety of bacterial systems). By examining an array of modification cascades, we were able to gain a panoramic view of the role of spatial localization control across different variants as well as contrast and compare the effects on signalling between each type of cascade.

In our analysis, we examined the consequences of separating and localizing different stages of the cascades. We found that the transport of communicating species (between different steps) resulted in a 'dilution' effect. This significantly altered signal transduction characteristics- for example, it resulted in a decrease in retroactivity and also resulted in the distortion of input-output relationships. Our findings brought to the fore several constraints and capabilities introduced by localization in these variants. For example, in cases where multiple stages were present, certain designs of spatial separation did not allow the phosphorelay to sustain a steady state response. However a naturally occurring design associated with phosphorelays (Chen et al., 2009) may bypass such locational constraints and allow the pathway to do so. In the case of the multisite modification mechanism, our findings implied that separation of the cascade stages confers an order to an otherwise random modification mechanism.

Our study has shed light on how the complex interplay of localization and diffusion combined with the differing nature of each modification cascade can significantly affect information processing in these signalling cascades. Complex extensions of these cascades

may be examined in the future. Important effects such as feedback or feedforward control and the mechanism of crosstalk- concepts that are the focus of many biological and modelling studies could also be studied through the spatial lens in the future. In MAPK cascades, the effects of localization and diffusion are present, understanding these cascades in light of these effects would have relevance for a wide variety of signalling pathways where these are integrated. Our examination of localization in these modules may also be used as a foundation to implement these modules in synthetic biological systems. Localization is seen across different biological systems- in both eukaryotes and bacteria. Bacteria are considered to be more tractable especially in terms of the synthetic design of biological parts or building blocks. In this area researchers are looking to harness the advantages that come with applying effects such as compartmentalization, for example isolation from toxic byproducts when designing synthetic metabolic reaction pathways (Sachdeva et al., 2014). Overall, our findings may be useful and applied in a variety of contexts where localization and transport are integral to cellular information processing.

## Disentangling spatio-temporal regulation in *Caulobacter crescentus* signalling networks

Our final study (Chapter 6) was motivated by the striking examples of spatio-temporal control mechanisms regulating the developmental events in the *Caulobacter* cell cycle. We utilized a systems engineering approach in order to understand how spatial mechanisms work in conjunction with the temporal interactions of the underlying signalling networks. We started by isolating key building blocks of these networks- phospho-signalling pathways catalyzed by bifunctional enzymes and systematically examined their spatial regulation. Our findings brought into sharp light how spatial factors affect different kinds of feedback and feedforward signalling interactions in these building blocks.

Armed with these insights, we moved towards investigating concrete signalling networks in *Caulobacter* and how localization together with diffusion of signalling entities affects the interactions between these networks. First, we utilized appropriate combinations of building blocks and studied the interactions therein in light of different spatial designs. These designs were based on the localization patterns observed in the cell as well as potential alternative designs that may be seen in other bacterial systems. Each spatial design presented different capabilities and constraints for the signalling interactions and our

findings shed light on the consequences of each design for the phospho-signalling interactions in *Caulobacter* networks. Furthermore, the insights we obtained may also be relevant in different cell types, beyond *Caulobacter*, where spatial localization is a recurrent theme in the constituent signalling networks.

In order to understand how spatial control via localization regulated the signalling interactions in these networks in different phases of the cell cycle, we examined existing spatial models of these networks. Our results revealed the impact of different localization patterns on key signalling species in the network that are known to play a determining role in developmental events in the cell cycle. Finally, we also took the first steps towards exploring dynamic localization of enzymes in different phases of the cell cycle. By examining the impact of the feedforward control of the spatial localization of enzymes on the underlying phosho-signalling interactions, we were able to create a platform from which we could shed light on how well current experimental observations match with experimental and modelling hypotheses. For example it allowed us to evaluate hypotheses regarding the role of bistability in the transition between first two phases of the cell cycle. We also analyzed the effect of "spatial mutants" (enzymes with abnormal localization) and made testable predictions regarding their potential effect on developmental events during the cell cycle.

While, we did not incorporate all of the associated complexity of the cell cycle into our model, our analysis still acts are a starting point to conceptualize and execute the incorporation of spatiotemporal effects in modelling the cell cycle. This is important for closing the fundamental gaps in our understanding of the cell cycle. In a future effort, these effects may be built into the model and examined in light of the specific details of the concrete system. The network modules we have studied here- phosphorelays and bifunctional enzyme modification cycles are also seen in other bacterial systems- for example *B. subtilis* and the insights gained from this study may be applied to other bacterial systems which harbour such spatiotemporal networks as well.

In summary, through our multipronged approach we have combined the analysis of spatial regulation and control in networks modules, enzymatic modules, pathways and concrete systems. This has allowed us to systematically examine the spatial dimension to information processing in signalling at different levels. A common insight that emerges from our results is that when investigating signalling networks where the effect of space is important, care must be taken to explicitly account for spatial effects and *ad hoc* descriptions added as an afterthought may not be sufficient. Our studies have opened avenues for a number of fu-

ture efforts that could broaden the scope of our investigations by examining more complex extensions of the networks and modules we have considered. Our insights may be applied towards elucidating the role of spatial organization in signalling networks in multiple concrete systems as well as in synthetic contexts. Recently this area has generated a significant amount of interest and has been the focus of numerous experimental efforts. Our findings may also find relevance in applications related to communication in biomolecular networks where designing different ways of information processing is a fundamental feature (Nakano et al., 2013). This work mainly utilizes deterministic approaches. A few studies which take into account the role of diffusion in the regulation of intracellular networks using stochastic approaches exist (Shahrezaei and Swain, 2008; Takahashi et al., 2010; Welf and Haugh, 2012). A systematic study using stochastic approaches to study the effect of diffusion and other spatial effects in intracellular networks would not only be a useful complement to this work but would also reveal new aspects of spatial signalling. In such cases deterministic approaches serve as a useful basis from which to understand the new features introduced by stochasticity. Improvements in experimental techniques could offer a promising avenue for stochastic approaches.

We expect that a concerted series of theoretical and experimental investigations will substantially enhance our understanding of the role of space in cellular information processing. This would set the stage for an improved understanding of many cellular processes of basic and applied interest and open up new avenues for their manipulation.

# Appendix A

# An investigation of design principles underlying repulsive and attractive biasing: Discussion of temporal sensing and parameter values

## Switching response in temporal sensing

In chapter 2 we examined different potential design principles which allowed a given cell to exhibit both attractive and repulsive sensing. The analysis was based on spatial sensing mechanisms. One of the settings we focussed on was whether the opposite regulation of an upstream reaction by attractant and repellent could be the basis of the opposite nature of the response.

In this section, we examine this in the case of a purely temporal sensing chemotactic mechanism, which involves adaptation: the gradient sensing mechanism in E.coli. This is a widely studied system, which exhibits adaptive sensing over a wide range of concentrations. We focus on a simplified description of the signalling, based on a reduction of the well-known Barkai Leibler model for sensory transduction Barkai and Leibler (1997). The model has three components active methylated receptors $X_m^*$ (the output), inactive methylated receptors $X_m$ and demethylated receptors $X_0$ Alon (2006b). A chemoattractant deactivates the methylated receptors converting it into inactive methylated receptors. It is assumed that demethylation occurs only of active methylated receptors (via the enzyme

CheB) and demethylated receptors can be methylated by the enzyme CheR, a reaction assumed to follow zeroth order kinetics. An increase in the output tends to increase the probability of the bacterium to tumble (and change direction).

The equations for the model are given below.

$$\begin{aligned} dX_m^*/dt &= -k_b S X_m^* + k_f X_m - k_1 CheB X_m^*/(k_{m1} + X_m^*) \\ dX_m/dt &= k_b S X_m^* - k_f X_m + k_1 CheR X_0/(k_{m2} + X_0) \end{aligned} \tag{A.1}$$

If the enzymatic reaction involving CheR is acting as a zeroth order reaction, then the dependence on $X_0$ drops out. Adding the above two equations, and examining this at steady state immediately reveals that the steady state response $X_m^*$ is independent of the signal.

It is worth examining how a chemorepellent would work in the similar situation. If a chemorepellent mediates the opposite reaction as the chemoattractant above (the equivalent of a polarity switch), then we immediately see by repeating the analysis above that the response still exhibits exact adaptation with the opposite temporal response. This indicates that the mediation of the opposite reaction can give rise to the desired opposite response, preserving the adaptation property.

Another point to be made is that the chemorepellent may be involved in the activation of different methylated receptors (from the chemoattractant), which involve a very similar network structure and dynamics. In this case, while an adaptive opposite response may be observed, the repellent may be involved in regulating the reverse reaction for a different methylated receptor pair (active/inactive). It is of course possible that a repellent may be regulating the opposite reaction for a different methylated receptor pair, which does not have the same kind of dynamics/methylation or even show adaptation.

## Parameters

### Fig. 2.2 Parameters

(A) Local module $k_f = 2.0; k_r = 1.0; k = 1.0; k_d = 0.0$. (B) Adaptive module: attractive $k_a = 1.0; k_{-a} = 1.0; k_i = 2.0; k_{-i} = 2.0; k_f = 1.0; k_r = 1.0; k_{da} = 0.0; k_{di} = 10.0$. For the repulsive response in the adaptive module, diffusivities of activator and inhibitor are interchanged.

## Fig. 2.3 Parameters

Attractive responses (A,C): The signal is $S = 1 + 0.05cos\theta$ (A) and $S = 1 + 0.4cos\theta$ (C). Attractive responses are obtained for these set of parameter values $a_{12} = 4.0; a_{13} = 1/3; a_{21} = 3/2; a_{22} = 1/2; a_{23} = 1/2; a_{31} = 1.0; a_{32} = 2.0; a_{33} = 1.0; \rho_2 = 2.0, \rho_3 = 1.0$. Repulsive responses (B,D): Again the same signals $S = 1 + 0.05cos\theta$ (B) and $S = 1 + 0.4cos\theta$ (D) are employed. Repulsive responses are obtained for the following set of parameter values: $a_{12} = 1.0/2.0; a_{13} = 4.0; a_{21} = 1.0; a_{22} = 1.0; a_{23} = 2.0; a_{31} = 3.0/2.0; a_{32} = 1.0/2.0; a_{33} = 1.0/2.0; r_2 = 1.0; r_3 = 2.0;$

## Fig. 2.5 Parameters

(A) Parameters are $k_{f1} = 2$ (decreased to 0.1 for the repulsive response), $k_{r1} = 1, k_1 = 1$. (B) Parameters are $k_{f1} = 1.0, k_{r1} = 1, k_1 = 1$.

## Fig. 2.6 Parameters

The signal is $2 + 0.4cos\theta$. Parameters for (A) and (B) are $k_{f1} = 1, k_{r1} = 1, k_1 = 1$ For (C) $k_{f1} = 1, k_1 = 1, k_{r1} = 1, k_{da} = 10.0$.

## Fig. 2.8 Parameters

Parameter values for (A) are: $k_a = 2.0; k_{fa} = 0; k_{ba} = 1.0; k_b = 1.0; k_{fb} = 0.0; k_{bb} = 1.0$ for the parallel positive regulation and $k_a = 1.0; k_{fa} = 2.0; k_{ba} = 0.0; k_b = 1.0; k_{fb} = 1.0; k_{bb} = 0.0$ for the parallel negative regulation. In both cases $A_{tot} = 1; B_{tot} = 0.5$, $k_f = k_r = 1.0; R_{tot} = 3.0$. Parameter values for (B) are $k_a = 2.0; k_{ba} = 1.0; k_{fb} = 1.0; k_b = 1.0$ for positive regulation of *A* and negative regulation of *B* and $k_{fa} = 2.0; k_a = 1.0; k_b = 1.0; k_{bb} = 1.0$ for the positive regulation of *B* and negative regulation of *A*. $k_f = 1.0; k_r = 1.0; B_{tot} = 0.5; A_{tot} = 1.0; R_{tot} = 3.0;$. Any other constants are zero.

## Fig. 2.9 Parameters

Parameter values for (A) are $k_a = 2.0; k_{ba} = 1.0; k_{fb} = 1.0; k_b = 1.0; k_f = 1.0; k_r = 1.0;$. Parameter values for (B) are $k_{fa} = 2.0, k_a = 1.0, k_b = 1.0, k_{bb} = 1.0, k_f = 1.0, k_r = 1.0$.

## Fig. 2.10 Parameters

Parameter values are: $k_a = 2.0; k_{ba} = 1.0; k_{fb} = 1.0; k_b = 1.0;$ and (A) $A_{tot} = 0.7, B_{tot} = 0.3$ (B)$A_{tot} = 0.3, B_{tot} = 0.7$ (C)$A_{tot} = 0.5, B_{tot} = 0.5$. For (D) $A_{tot} = 0.5, B_{tot} = 0.5$,$k_a = 1.0; k_{ba} = 1.0; k_{fb} = 1.0; k_b = 2.0;$.

## Fig. 2.11 Parameters

(A,B) Parameters are the same as in Fig. 2.10A except $k_{ba} = 2, A_{tot} = B_{tot} = 0.5$. (C) The parameters are $k_a = 1.0; k_{ba} = 1.0; k_{fb} = 1.0; k_b = 1.0, R_{tot} = 10.0$. $A_{tot} = 1.0$ and $B_{tot} = 2.0$ (solid line, repulsive response) and $B_{tot} = 1.0$ and $A_{tot} = 2.0$ (solid line with circles, attractive response).

## Fig. 2.12 Parameters

(A,B) Parameters for (A) and (B) are the same as Fig. 2.10C except that $k_f = 0.01, R_{tot} = 115$.

# Appendix B

# An investigation of spatial signal transduction in cellular networks: Discussion of the transcritical switch model and Parameter values

## Transcritical Switch Model

Here, we examine a different kind of monostable switch, which arises from a positive feedback, which is distinct from the switches examined in the text. This is a positive feedback module which results in a switch with a transcritical bifurcation. We examine this module separately, as it is of interest to examine whether this distinct kind of switching behaviour yields results which are different from the other monostable switch and has been used in modelling Aguda (1999); Albeck et al. (2008). This switch involves a simple positive feedback circuit where the active form of a species activates the active form of another species Y which feeds back to enhance the production of $X^*$. In this case, we will consider the external signal to regulate the degradation of $X^*$. Here $X^*$ is regarded as the output of the module.

## The Model Equations

The equations governing the Transcritical Switch module are given by

$$\begin{aligned} \frac{\partial X^*}{\partial t} &= -k_{sx} S X^* + k_1 X Y^* + D_X \frac{\partial^2 X^*}{\partial \theta^2} \\ \frac{\partial Y^*}{\partial t} &= k_2 X^* Y - k_{-y} Y^* + D_Y \frac{\partial^2 Y^*}{\partial \theta^2} \end{aligned} \tag{B.1}$$

In the above equations, Y is the intermediate feedback element. The signal S acts to degrade $X^*$ and $k_{sx}$ denotes the associated rate constant. $k_1$ is the kinetic rate constant associated with the positive feedback between the species $X$ and $Y$. $k_2$ denotes the rate constant for the conversion of $Y$ to $Y^*$. $k_{-y}$ is the rate constant for the constitutive conversion between the active and inactive forms of Y.

Now an analysis of the temporal dynamics of this circuit (discussed in Alam-Nazki and Krishnan (2012)) clearly reveals the presence of a transcritical bifurcation. Thus, with regard to the effect of the signal $S$, the circuit behaves like a switch, which is different from both the monostable and bistable switches considered earlier. In particular, if the signal exceeds a particular threshold (the transcritical bifurcation point), the only stable response is the zero response. This is because for this range of signals, the positive feedback is not strong enough to sustain the production of a non-zero response in the face of the strong degradation (which is mediated by the external signal). We note in passing that if the signal were acting to increase the production of $X^*$ (rather than degrade it) then the transcritical bifurcation would be broken by the presence of the signal, though a switch-like effect would still be evident if the signal were at low levels. We adopt a representative circuit model where the transcritical bifurcation structure is preserved, and hence consider the signal degrading $X^*$.

## Analysis of the Transcritical Switch Model

The transcritical switch module is distinct from the monostable and bistable modules considered earlier. This is a module which also involves positive feedback, but where the switching (or more precisely thresholding) effect arises through a transcritical bifurcation. This module consists of two species X and Y, where the element Y is the intermediate element through which X catalyzes its own production. The signal (assumed non-zero) catalyzes the degradation of $X^*$. Since the signal catalyzes the backward reaction, this

system exhibits a transcritical bifurcation, which is not destroyed by the presence of the signal.

We note from a basic analysis of the module, that two steady states exist ($X^* = 0$) and a non-zero steady state value. While performing simulations for different homogeneous values of the signal, we find that above a critical value of the signal, the observed steady state is $X^* = 0$. This is easily understood in terms of the characteristic transition associated with a transcritical bifurcation: there are two steady states which exchange stabilities when the critical level of the signal is crossed. Below the critical level, the positive feedback is the dominant effect and a non-zero steady state emerges as the observed state. When the signal crosses a threshold, the positive feedback is defeated by the degradation effect associated with the signal, resulting in a zero response.

First we examine the case when none of the elements diffuse. If the input gradient signal is such that the local signal level at every location is completely below the critical value of the signal then the profile of $R^*$ follows a spatial variation that is qualitatively opposite to that of the signal (note that the signal is acting to degrade the response, so this is expected). If the signal gradient is such that locally it is everywhere above the critical threshold, then a homogeneous zero response is observed (Fig. B.1). Both these results are easily understood in terms of the dynamics of the module. However, if the gradient is above the critical value for some regions in space, then for those regions in space the concentration of $R^*$ is zero and for the regions where the signal is below the threshold, it is non-zero and follows a variation opposite to the signal. This result illustrates the switching effect in spatial gradients. Similar observations hold for a localized signal input (Fig. B.1).

Finally, we examine the case where highly diffusible elements are present in the network. If the response $X^*$ is diffusible then it naturally exhibits no spatial variation. We consider a situation where Y is highly diffusible, If the signal is everywhere below the critical value corresponding to the bifurcation, the steady state concentration profile is qualitatively opposite to that of the signal and is more spread out when compared to the case when none of the elements diffuse. When some or all of the local signal crosses beyond the critical value of $S$, the profile of $X^*$ has very weak spatial variation. Moreover the switch-like behaviour seen in the spatial profile in the case when none of the elements diffuse is absent here and the profile does not reach a zero value (Fig. B.1). When a localized signal input is applied, the profile of $X^*$ is smoothly localized. For signals with amplitudes below and above the critical value, $X^*$ always remains non-zero- unlike the previous case for the same signals (Fig. B.1). Thus there is no manifestation of the switch-like behaviour

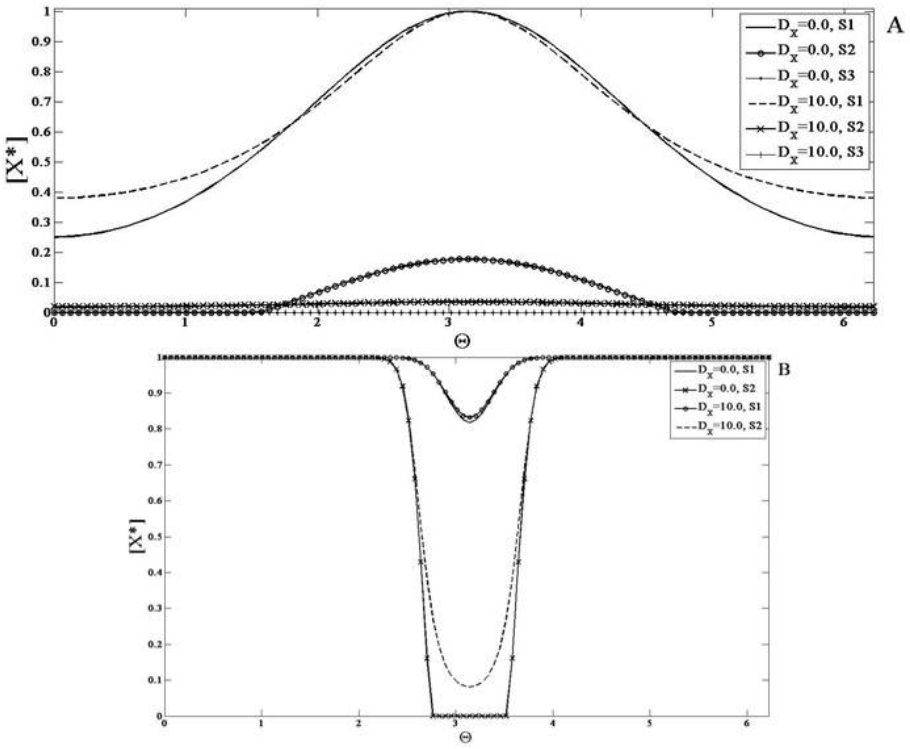


Figure B.1: **Response of the Transcritical Bifurcation switch module.** The response of the module to different (A) gradient signals $S1$, $S2$ and $S3$ and (B) localized signals $S1$ and $S2$ (see supplementary materials for S values) for the non-diffusible and highly diffusible cases is shown. (A) Non-diffusible case: S1- is above the switch threshold (i.e. it is small enough for a non-zero steady state output: see text) in the entire domain (solid line), S2 is partially above and below the switching threshold (solid line with circles) and S3 is below the switch threshold in the entire region (solid line with dots at zero), Diffusible case: S1 (dashed line), S2 (solid line with x markers) and S3 (solid line with plus signs at zero). (B) Non-diffusible case: S1 is above the switch threshold in the entire domain (solid line), S2 is partially above and below the switching threshold (solid line with x markers), Diffusible case: S1 (solid line with circles) and S2 (dashed line). For the non-diffusible case, in the spatial regions where the signal value crosses the "switch" threshold, the response exhibits a switch. This can be seen for S2 in (A) and in (B), where a part of the concentration profile shows non-zero spatial variation, and the other part is at zero or switched off. These plots clearly illustrate the presence of a spatial switch. Note that for S3 in (A) the profiles are at zero steady state in the entire domain. In the highly diffusible case, the spatial concentration profile of $X^*$ has weaker spatial variation and the switching nature of the response is not observed here.

in the spatial profile. If a signal is everywhere above a certain threshold (see below) then a spatially uniform zero response is observed, even with a gradient input.

It is worth pointing out that the diffusible element Y has the effect of preserving the switch-like behaviour in the steady state response to homogeneous signals, but negates the effect of this switch in spatial signal transduction in response to gradient signals.

These results are explained analytically in Alam-Nazki and Krishnan (2012).

## Parameter values for Figures

In this section, the signal and parameter values in each module are outlined. In all the simulations, unless otherwise mentioned, the initial conditions used are steady state values for a basal signal.

### Fig. 3.2 - Parameters for the Coherent Feedforward module

(A) $S = 1 + 0.3cos\theta$ and (B) $S = A * exp((x - x_o)/\alpha)$ where $A = 1.0$ and $\alpha = 0.1$, here and everywhere below, unless otherwise mentioned, $x_o = \pi$ (centre of domain) Parameter values: $k_{sx} = 1.0, k_{sy} = 1.0, k_x = 0.0, k_{-x} = 1.0, D_X = 0.0, k_{xr} = 10.0, k_y = 0.0, k_{-y} = 1.0, k_{yr} = 1.0, D_Y = 0.0, k_r = 0.0, k_{-r} = 1.0, X_{tot} = 1.0, Y_{tot} = 1.0, R_{tot} = 1.0$. $D_X = 10.0$ and $D_Y = 10.0$ for the highly diffusible cases. In this module $k_{xr}$ and $k_{yr}$ were varied to modulate the strength of the associated pathways.

### Fig. 3.3 - Parameters for the Incoherent Feedforward module

A: $S = 1 + 0.3cos\theta$; B:$S = a + A * exp((x - x_o)/\alpha)$ where $A = 1.0$, $a = 0.1$ and $\alpha = 0.1$. The parameter values are: $k_{sx} = 1.0; k_{-x} = 2.0; k_{xr} = 1.0; k_{sy} = 1.0; k_{-y} = 1.0; k_{yr} = 1.0;\ k_x = 0.0; D_X = 0.0; k_y = 0.0; D_Y = 0.0; k_r = 0.0; k_{-r} = 0.0; X_{tot} = 1.0; Y_{tot} = 1.0; R_{tot} = 1.0$. $D_X = 10.0$ and $D_Y = 10.0$ for the highly diffusible cases. C: The parameter values are: $k_{sy} = 2.0; k_{-y} = 0.5; k_{xr} = 1.0; k_{sx} = 1.0; k_{-x} = 0.0; k_{yr} = 1.0;\ k_y = 0.0; D_Y = 0.0; k_x = 1.0; D_X = 0.0; k_r = 0.0; k_{-r} = 1.0; X_{total} = 1.0; Y_{total} = 1.0; R_{total} = 10.0$.

## Fig. 3.4- Parameters for the Positive Feedback module

A: $S = 0.5 + 0.3cos\theta$; B: $S = a + A * exp((x - x_o)/\alpha)$ where $A = 1.0$, $a = 0.1$ and $\alpha = 0.1$. The parameters are $k_{sx} = 1.0, k_x = 0.0, k_{-x} = 1.0, D_X = 0.0, k_{ry} = 1.0, k_y = 0.0, k_{-y} = 1.0, D_Y = 0.0, k_{xr} = 1.0, k_r = 0.0, k_{-r} = 1.0, D_r = 0.0; X_{tot} = 1.0; Y_{tot} = 1.0; R_{tot} = 1.0$. $D_Y = 10.0$ for the highly diffusible case. $k_{yx}$ is varied here to modulate the effect of the feedback strength.

## Fig. 3.5 - Parameters for the Negative Feedback module

A: $S = 0.5 + 0.3cos\theta$; B: $S = A * exp((x - x_o)/\alpha)$ where $A = 1.0$ and $\alpha = 0.1$. The parameters for this module are: $k_{sx} = 1.0, k_x = 0.0, k_{-x} = 1.0, D_X = 0.0, k_{yr} = 5.0, k_y = 0.0, k_{-y} = 1.0, D_Y = 0.0, k_{xr} = 1.0, k_r = 0.0, k_{-r} = 1.0, D_R = 0.0; X_{tot} = 1.0; Y_{tot} = 1.0; R_{tot} = 1.0$. $D_Y = 10.0$ for the highly diffusible case. $k_{yx}$ is varied here to modulate the effect of the feedback strength.

## Fig. 3.6- Parameters for the Cyclic Reaction network module

A case with n=4 species in the module was analysed. A. $S = 1 + 0.3cos\theta$ and B. $S = A * exp((x - x_o)/\alpha)$ (where $A = 1.0, a = 0.1$ and $\alpha = 0.1$) The parameters for this module are: $k_s = k_2 = k_3 = k_4 = 1.0, D_{X1} = D_{X2} = D_{X3} = D_{X4} = 0.0$.

## Fig. 3.7 - The Cyclic Reaction network module with highly diffusible elements

$D_{X1} = 10.0$, $D_{X3} = 10.0$, when each of those elements was made highly diffusible. The parameters and the signal input are the same as outlined in Fig. 6.

## Fig. 3.8- Parameters for the Monostable Switch Module

(A,C). $S = 1 + 0.3sin\Theta$ and (B,D). $S$ is a square pulse: $S_{basal} = 0.1$ and $S_{maximum} = 5.0$. The parameters for this module are: $k_{sx} = 0.5, U = 0.5, K_{M1} = 0.01, K_{M2} = 0.01, D_X = 0.0, D_{X^*} = 0.0, [X] + [X^*](initially) = 0.2$. $D_X = 10.0$ when considering the diffusible case.

## Fig. 3.9 - Parameters for the Mutual Inhibition Bistable switch module

Note that in the analysis of this module different initial conditions have been used for the cases analysed and are outlined below. The effect of weak diffusion was also examined in this module. A. $S = 1 + 0.3cos\Theta$, B. $S = 1.6 + 0.3cos\Theta$. (C,D). $S = a + A * exp((x - x_o)/\alpha)$, where $a = 1.69$, (C) $A = 0.05$ and (D) $A = 0.1$. The parameters for this module are: $k_o = 0.0, k_1 = 0.05, k_2 = 0.1, k_{21} = 0.5, D_X = 0.0, k_3 = 0.2, K_{M3} = 0.05, k_4 = 1.0, K_{M4} = 0.05, D_Y = 0.0$. $X_{initial} = 0.1554$ and $Y_{initial} = 0.8617$ (E) For the weakly diffusible case $S = 1.27 + 0.3cos\Theta$ and $D_Y = 0.01$. $X^*_{initial} = 0.5632$ and $Y^*_{initial} = 0.02551$ at $\theta = 0$ to $0.46\pi$ and $1.52\pi$ to $2\pi$. $X_{initial} = 0.111$ and $Y_{initial} = 0.9443$ at $\theta = \pi/2$ to $3\pi/2$. $Y_{tot} = 1$ everywhere.

## Fig. 3.10 - Parameters for the Mutual Inhibition Bistable switch module with highly diffusible elements

$D_Y$=10.0 and the other parameters and the signal input are the same as outlined in Fig. 9. Note that in (E) $S = 1.3 + 0.3cos\Theta$ and $X^*_{initial} = 0.8855$ and $Y^*_{initial} = 0.01361$.

## Fig. 3.11 - Parameters for the Negative Feedback Oscillator module

Note that in this module, a case with a weakly diffusible species was also analysed. (A,B,C) $S = 0.3 + 0.2cos\theta$ (D) $S = A * exp((x - x_o)/\alpha)$, where $A = 4.0$. The parameters for this module are: $k_o = 0.0, k_1 = 1.0, k_2 = 0.01, k_{21} = 10.0, D_X = 0.0, k_3 = 0.1, k_4 = 0.2, k_5 = 0.1, k_6 = 0.05, K_{M3} = K_{M4} = K_{M5} = K_{M6} = 0.01, D_Y = 0.0$. (E,F) For the weakly diffusible case $S = 0.3 + 0.2cos\theta$ and $D_Y = 0.5$.

## Fig. 3.12 - Parameters for the Negative Feedback Oscillator module with highly diffusible elements

$D_Y$=10.0 and the other parameters and the input signals are the same as in Fig. 11.

## Fig. B.1 - Parameters for the Transcritical Bifurcation module

The parameters for this module are: $k_{sx} = 1.0, k_1 = 1.0, D_{X^*} = 0.0, k_2 = 1.0, k_{-y} = 1.0, D_{Y^*} = 0.0, X_{tot} = 1.0; Y_{tot} = 1.0$. A. $S1 = 0.3 + 0.3cos\theta$, $S2 = 1.0 + 0.3cos\theta$ and

$S3 = 2.0 + 0.3cos\theta$. B. $S = A * exp((x - x_o)/\alpha)$ where $\alpha = 0.1$, $S1$: $A = 0.1$ and $S2$: $A = 5.0$.

# Appendix C

# Covalent modification cycles through the spatial prism: Selection of Analytical Results, Discussion of Model Setting and Parameter values

In this section, we discuss a number of aspects in turn: (i)Signal Imposition and Boundary conditions (ii) Analytical explanation of certain results (reproduced from (Alam-Nazki and Krishnan, 2013)) (iii) Connection between temporal and spatial behaviour and (iv) The choice and effect of parameters. We start by discussing the model equations. The computational results presented in the main text are complemented by analytical work, which is presented in (Alam-Nazki and Krishnan, 2013) and reproduced in this section.

## Input Spatial Signal

In this paper we have investigated spatial aspects of signal transduction in a reversible covalent modification cycle. In this cycle the modification of protein X to $X^*$ is catalyzed by an enzyme K and the reverse reaction is catalyzed by the enzyme P. XK and $X^*P$ are the intermediate enzyme-substrate complexes. We first discuss how spatial input signals are introduced into the model. A spatial input signal may be introduced into the system by either assigning appropriate spatially varying initial conditions to the enzymes K and P or by explicitly adding production and degradation terms into the enzyme concentration

equation. The former corresponds to a "closed" system model of the cycle and the latter to an "open" system (we have presented results from the latter in the main text). This is because this allows for a continuous and reversible variation of the input.

When the input signal is imposed via the production and degradation of the free enzyme, the spatial concentration profile of the free enzyme remains fixed even when the substrate modification cycle contains diffusible components, as long as the enzyme-substrate complex is non-diffusible. This can be understood by looking at how the sum of the concentrations of K and XK changes in time:

$$\frac{\partial([XK]+[K])}{\partial t} = k_{f1}S(\theta) - k_{b1}[K] + D_K\frac{\partial^2[K]}{\partial\theta^2} \quad \text{(C.1)}$$

At steady state the L.H.S is equal to 0 and the free enzyme concentration is determined by an inhomogeneous linear differential equation, completely independent of the substrate cycle. For a simple linear cosine input, we employ $S = a + bcos\theta$, to obtain

$$[K] = k_{f1}a/k_{b1} + k_{f1}bcos\theta/(k_{b1} + D_K) \quad \text{(C.2)}$$

The diffusion of the enzyme does dampen its gradient, and as the diffusion of the enzyme becomes larger, the gradient of the enzyme is diminished. Similar conclusions hold when P is imposed in this way. Naturally, in other situations involving non-negligible diffusion of the complexes, the free enzyme profile can be perturbed by the diffusion of components of the substrate cycle.

In contrast to the kind of signal imposition we have considered above, when the gradient of the free enzyme is imposed via initial conditions its profile is perturbed (sometimes significantly).

## Effects of different signal imposition

We considered two ways in which the input signal can be imposed- via initial conditions and through the production and degradation of the free enzyme. While the results presented were through the latter scenario, it is worth examining what the effect of different kinds of signal imposition is. The effects of these differences are seen transparently in the mass action parameter regime (where enzyme sequestration is essentially absent). In this regime, investigation of the reference case (when none of the species diffuse), tells us that

the response is similar for both types of signal imposition. However this is not the case when diffusing species are present. When the input signal is imposed through the production and degradation of the free enzyme and if the enzyme itself diffuses, its spatial profile weakens as the diffusion coefficient increases but remains graded. However, if the signal is imposed by initial conditions and if the enzyme itself diffuses, its steady state spatial profile would be homogenous for any value of its diffusion coefficient (seen in Eqn. 2: the free enzyme satisfies a homogeneous diffusion equation). Thus signal imposition through production/degradation allows a continuous and reversible modulation of the enzyme which is not neutralized by diffusion.

On the other hand, one of the consequences of signal imposition through production/degradation is that the concentration of the free enzyme is fixed at steady state (especially in the absence of diffusion, see Seaton and Krishnan (2011)), thus any potential sequestration effects of enzyme in complexes, reducing free enzyme concentration cannot be properly examined through this type of imposition. For the most part, the sequestration effects on the free enzyme play a tangential role to the focus of interest except in the "ultrasensitive" parameter regime.

## Model equations for the "Ultrasensitive" case

As described above, the consequence of the "open" model employed is that the concentration of the free enzyme is fixed at steady state. This prevents the model from producing a switch-like output. This can be seen from an analysis of the equations in the temporal case itself (in that situation the model reduces to a series of first order mass action kinetic reactions with constant rates at steady state). We employ a modification of the "open" model above which incorporates the sequestration effect of the enzyme in the complex (this aspect is necessary for "ultrasensitive" behaviour in the cycle).

This is done by incorporating production of the free enzyme and degradation of free enzyme and complex (assumed equal). In addition we incorporate a "production" of substrate species (X, without loss of generality) and equal degradation of all species in the substrate cycle. This ensures that the total enzyme and substrate are fixed locally under homogenous conditions, as can be seen from a straightforward analysis of this (open) model, which in turn allows for significant sequestration effects of enzymes (in complexes) to be manifested.

The model equations are:

$$\begin{aligned}
\frac{\partial[X]}{\partial t} &= k_o - k_1[X][K] + k_{-1}[XK] + k_4[X^*P] \\
&\quad -k_{bx}[X] + D_X\frac{\partial^2 X}{\partial\theta^2} \\
\frac{\partial[X^*]}{\partial t} &= -k_3[X^*][P] + k_{-3}[X^*P] + k_2[XK] \\
&\quad -k_{bxs}[X^*P] + D_{X^*}\frac{\partial^2 X^*}{\partial\theta^2} \\
\frac{\partial[K]}{\partial t} &= -k_1[X][K] + k_{-1}[XK] + k_2[XK] + k_{f1}S(\theta) \\
&\quad -k_{b1}[K] + D_K\frac{\partial^2 K}{\partial\theta^2} \\
\frac{\partial[P]}{\partial t} &= -k_3[X^*][P] + k_{-3}[X^*P] + k_4[X^*P] + k_{f2}I(\theta) \\
&\quad -k_{b2}[P] + D_P\frac{\partial^2 P}{\partial\theta^2} \\
\frac{\partial[XK]}{\partial t} &= k_1[X][K] - k_{-1}[XK] - k_2[XK] - k_{xk}[XK] \\
&\quad +D_{XK}\frac{\partial^2 XK}{\partial\theta^2} \\
\frac{\partial[X^*P]}{\partial t} &= k_3[X^*][P] - k_{-3}[X^*P] - k_4[X^*P] - k_{xp}[X^*P] \\
&\quad +D_{X^*P}\frac{\partial^2 X^*P}{\partial\theta^2}
\end{aligned} \tag{C.3}$$

where $k_o$ is the generation of X and $k_{bx}$ and $k_{bxs}$ are the degradation rate constants for X and X$^*$, respectively. $k_{xk}$ and $k_{xp}$ are the degradation rate constants for XK and X$^*$P, respectively. The degradation rate constants are assumed to be equal. The remaining constants are: $k_1$ and $k_3$ are the forward rate constants for the binding of the enzyme and its substrate, $k_{-1}$ and $k_{-3}$ are the rate constants for the dissociation of the enzyme substrate complex and $k_2$ and $k_4$ are the rate constants for product formation. $\theta$ represents the domain space and $D_j$ is the diffusion coefficient for any species "j" in the cycle. The input equation rate constants are the same as mentioned in the 'Input Spatial Signal' section. Our results explore spatial signal transduction through this model, and show, in particular, that ultrasensitive behaviour can be observed in response to spatial signals.

## Boundary conditions

In our exploration of the spatial aspects of signalling, we cast the basic covalent modification model in one spatial dimension. This is because many of the basic spatial aspects of signal transduction are seen in this case. We also apply periodic boundary conditions for all (diffusing) components. This amounts to casting the model in a circular domain. It is worth pointing out that since in all cases involving a graded signal, any signal imposition respects a $\theta \to 2\pi - \theta$ symmetry (the signal is symmetric about the middle of the domain), the scenario considered is exactly equivalent to signal transduction in a domain of half the size with no-flux boundary conditions. A similar conclusion also holds good when enzymes signals are localized. Thus in the cases we analyze, boundary conditions play a minor role. There may be instances in specific contexts of spatial signalling, where boundary conditions play an important role and the analysis in those situations can build on the basic analysis here, along with a specific analysis of boundary effects in that context.

## Cycle Responses in the "Generic" parameter regime

We show some basic analysis here (reproduced from (Alam-Nazki and Krishnan, 2013)) to supplement the analysis presented in the text.

### Diffusion of a single species

In the main text, we have discussed the results for the "generic" parameter regime. Here we shed light on certain findings. Firstly it is straightforward to see that when $X$ or $X^*$ diffuse, it will attain a homogeneous profile at steady state. For instance in the case of $X$ diffusing, this is seen by noting that

$$\frac{\partial([X] + [XK] + [X^*] + [X^*P])}{\partial t} = D_X \frac{\partial^2 [X]}{\partial \theta^2} \tag{C.4}$$

This shows that at steady state X attains a homogeneous profile. This result is interpreted as follows: when only one species is significantly diffusible and others (for instance equally) weakly diffusible, then that species will attain a profile which is essentially homogeneous.

We now present an analysis of the results in scenario 2 (S2). In S2, the enzymes are counter-aligned with one another, i.e. the maximum of one coincides with the minimum

of the other in the domain. Thus while the enzymes still have opposing effects temporally, they cooperate from the perspective of spatial signalling. We employ model parameters so that K is stronger than P (see Parameter Values section for exact values). The reference case when none of the species diffuse is discussed in the main text. We discuss the response when the cycle is perturbed by diffusion of individual species. If $X^*$ diffuses, the complex profiles "flip" and become qualitatively opposite to K, while the amplitude of $X$ increases. $X^*$ itself becomes homogenous. A closer look at the relationship between the species of the cycle brings forth an underlying pattern that explains these results. In the reference case, the profiles of $X^*$ and both complexes mirror the profile of K while the X profile mirrors that of P. Furthermore, the "semi-irreversibility" of the cycle ensures that the spatial profiles of the complexes mirror one another. This can be shown mathematically:

$$\frac{\partial([XK]+[X])}{\partial t} = -k_2[XK] + k_4[X^*P] \tag{C.5}$$

At steady state the L.H.S of the equation is equal to zero. Thus:

$$[XK] = k_4/k_2[X^*P] \tag{C.6}$$

This equation shows the relationship between the two complexes: under certain conditions (i.e. when species in the substrate cycle do not diffuse or only one species is diffusible), the concentrations of the complexes are proportional to each other at steady state. Therefore, when $X^*$ diffuses, it becomes uniform at steady state and the spatial distribution of $X^*P$ will be governed by that of P and thus its profile qualitatively changes and mirrors that of P. Due to the relationship between the complexes shown above, XK will parallel $X^*P$ and hence "flip" .

Next, if K alone diffuses, it was observed that the profiles of both complexes undergo a qualitative change- as $D_K$ increases the profiles change from having a variation similar to that of K to one which parallels P. This can be explained as follows: in S2, the enzymes are counter-aligned with one another and the spatial distribution of the rest of the species is governed by the spatial profiles of both enzymes. As the K profile becomes more spread out, the cycle is dominated by the spatial information from enzyme P. For high diffusivity of K, the cycle resembles Scenario 1, except here the profile of P is spatially distributed and that of K is very weak. As a result, the spatial profile of $X^*P$ (and hence XK, from

Equation C.6) mirrors P, thus explaining the qualitative change.

## Diffusion of two species

In the main text we have examined the effect of diffusion of two species in the cycle- the enzyme-substrate complex and the enzyme (or substrate). Here we analytically reason why we observe certain trends in a selection of results (reproduced from (Alam-Nazki and Krishnan, 2013)) .

**Diffusion of $X^*$ and $X^*P$:** When these species diffuse in S1, all species in the substrate cycle become homogenous except X. This is explained as follows. Firstly, we have

$$\frac{\partial([XK]+[X])}{\partial t} = -k_2[XK]+k_4[X^*P] \tag{C.7}$$

This indicates that at steady state, the two complexes are in proportion. Now, by adding the equations for all species in the substrate cycle, we have

$$\frac{\partial([XK]+[X]+[X^*]+[X^*P])}{\partial t} = k_d\frac{\partial^2([X^*]+[X^*P])}{\partial\theta^2} \tag{C.8}$$

where $k_d$ is equal to the diffusion coefficient of $X^*$ and $X^*P$ (which are equal to each other). This immediately indicates that at steady state $[X^*]+[X^*P]=C$ where C is a constant, independent of spatial location ($[X^*]+[X^*P]$ satisfies a homogenous diffusion equation with periodic boundary conditions). The equation for $X^*$ can be written as

$$\frac{\partial([X^*])}{\partial t} = k_2[XK]-k_3[X^*][P]-k_{-3}[X^*P]+k_d\frac{\partial^2[X^*]}{\partial\theta^2} \tag{C.9}$$

Also, by adding the equation for $P$ and $X^*P$, we have

$$\frac{\partial([P]+[X^*P])}{\partial t} = k_{f2}I(\theta)-k_{b2}[P]+k_d\frac{\partial^2X^*P}{\partial\theta^2} \tag{C.10}$$

Note that I($\theta$) is a constant independent of $\theta$. Finally

$$\begin{aligned}\frac{\partial([X^*P])}{\partial t} &= k_3[X^*][P] - k_{-3}[X^*P] - k_4[X^*P] \\ &\quad + k_d\frac{\partial^2[X^*P]}{\partial\theta^2}\end{aligned} \tag{C.11}$$

Now at steady state, from Equations C.10 and C.11, eliminating the diffusion term and using $[X^*] + [X^*P] = C$, we have at steady state $[P] = g([X^*])$, where g is an algebraic function which can be obtained explicitly and is a ratio of linear functions. Substituting into the equation for $[X^*]$ at steady state , using $k_2[XK] = k_4[X^*P]$ and eliminating $[X^*P]$, we have

$$f([X^*]) + k_d\frac{\partial^2[X^*]}{\partial\theta^2} = 0 \tag{C.12}$$

The function f can be explicitly obtained and depends on C. The key point here is that the equation for $X^*$ has spatially homogenous coefficients and that this is completely independent of spatial information from K. Analysis shows that a spatially homogeneous steady state is readily obtained. This explains why $X^*$ is spatially homogeneous, from which the homogeneity of $X^*P$ follows. Since the complexes are proportional to one another this shows that XK is also spatially homogeneous. In fact only X and K are spatially inhomogeneous.

Overall, this analysis shows how $X^*$ is homogeneous even when K is not. This highlights some subtleties underlying the interplay between a spatial signal, diffusion and sequestration. It is clear that in the absence of enzyme sequestration in a complex (the mass action model of the modification cycle), that $X^*$ would have a spatially varying profile similar to K.

**Diffusion of XK and K or $X^*$P and P:** When either of these pairs of species diffuse, in all scenarios the complexes flatten out. This may again be understood by observing the relationship between both complexes (Equation C.6). XK (or $X^*$P) is the only species diffusing in the substrate cycle. Thus, at steady state, its profile will flatten out (Equation C.4). We note that by writing out the equation for both $[X] + [XK]$ and $[X^*] + [X^*P]$ we find that a proportional relationship holds good between complexes. Due to the proportional relationship between the complexes at steady state (which continues to hold good here), the profile of the other complex will also flatten out.

**Both X and X$^*$ diffuse equally:** Along with diffusion of a single substrate species in the cycle we have also explored the effects of diffusion of two substrate species. In the main text, we have studied cases where both the complex and enzyme (or substrate) diffuse. We have also studied the case when both the X and X$^*$ diffuse and discuss the results here. In S1-3: as the diffusion increases, the spatial profiles of both become weaker. This is in contrast to the case when one of the species alone diffuses (in that case the profile of the diffusing species will be flatten and the spatial amplitude of the other would be enhanced). If both species diffuse unequally, for e.g. if X is highly (or moderately) diffusible and X$^*$ is weakly diffusible, X$^*$ will achieve greater spatial variation and X will become very weak or flat. In general, we can say that the diffusion of X and X$^*$ has counteracting effects (Fig. C.1) and this can be understood in terms of the effects of individual species diffusion studied in the main text. The effect of X, X$^*$ and the complexes diffusing can likewise be studied.

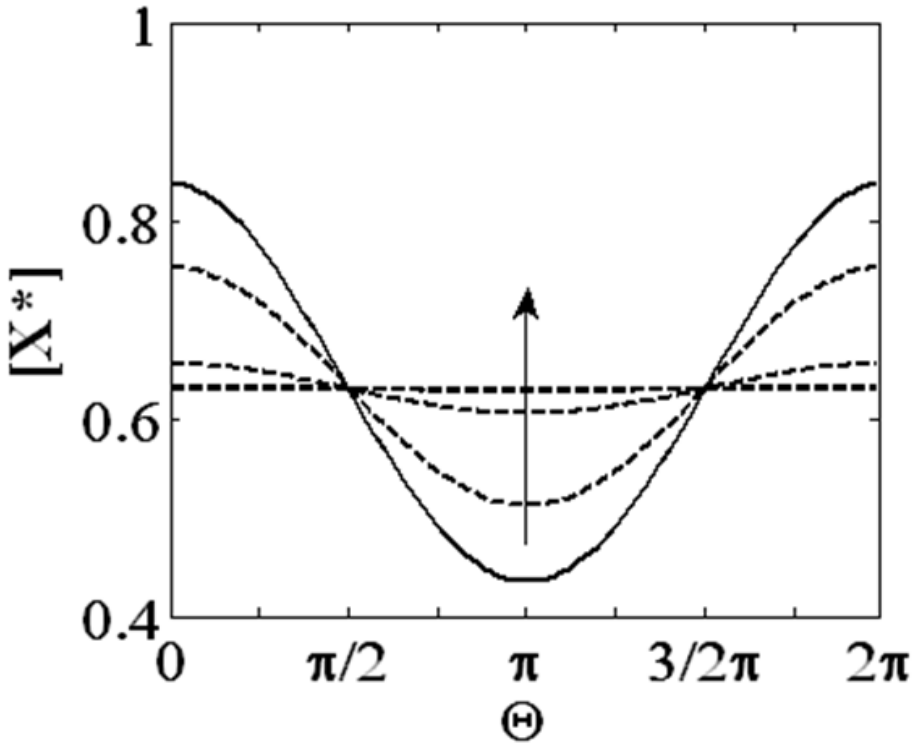


Figure C.1: This figure shows the effect of both X and X$^*$ diffusing (equally) on the profile of X$^*$. As the diffusivity increases, the spatial amplitude of the profile decreases. The arrow indicates the direction of increasing diffusion coefficient.

## Spatial and temporal signalling and the reference case

Our study has started with a reference case where all species are essentially non-diffusible, and we perturb this reference case by introducing diffusion of selected species. This has allowed us to examine the effects of diffusion of individual species. In this regard a few points are worth mentioning (i) While our basal case has species being (essentially) non-diffusible, we do not actually require them to be strictly non-diffusible. In fact all the essential trends we observe carry through, even if the species involved are weakly diffusible. Further, as discussed in the text, when all species in the substrate cycle are equally weakly diffusible, their steady state approaches that of the non-diffusible case. As a specific instance, our single species diffusion case may be interpreted as considering the situation where only one species is not weakly diffusible, and other species are weakly diffusible. We find the same trends with the minor change that the species under consideration has a spatial profile which is essentially but not exactly homogeneous (also see Fig. C.2). Since our analysis focusses on varying the diffusion coefficient over a fairly broad range, we see that the trend we observed remains essentially the same. (ii) While we could have used a reference state where multiple species were diffusible, and perturbed it in a similar way, we believe that the basal scenario we have considered, allows us to investigate the effects of diffusion of individual entities and complexes in a systematic and controlled way. It has the advantage of being a common unbiased platform which can be perturbed in multiple ways (note that our reference case does not require us to specify diffusivity of complexes vis a vis enzyme and substrate). Further discussion of this point is made in the text.

## Choice of Parameters

In this minimal model of the covalent modification cycle, we identify the kinetic rate constants, diffusion coefficients, total enzyme concentration and total substrate concentration as the model parameters. The possibilities of parameter sets that could be utilized vary substantially in the literature. This is because this module is a general one, in the sense that it is encountered ubiquitously as a key component of large and complex networks such as those of MAPK cascades, spatial GTPase cycles and multisite phosphorylation. A survey of the literature shows that numerous and varied parameter sets are employed in the investigation of covalent modification in a wide range of contexts. Some studies use parameter values that are obtained by experimental methods and make conclusions directly pertaining

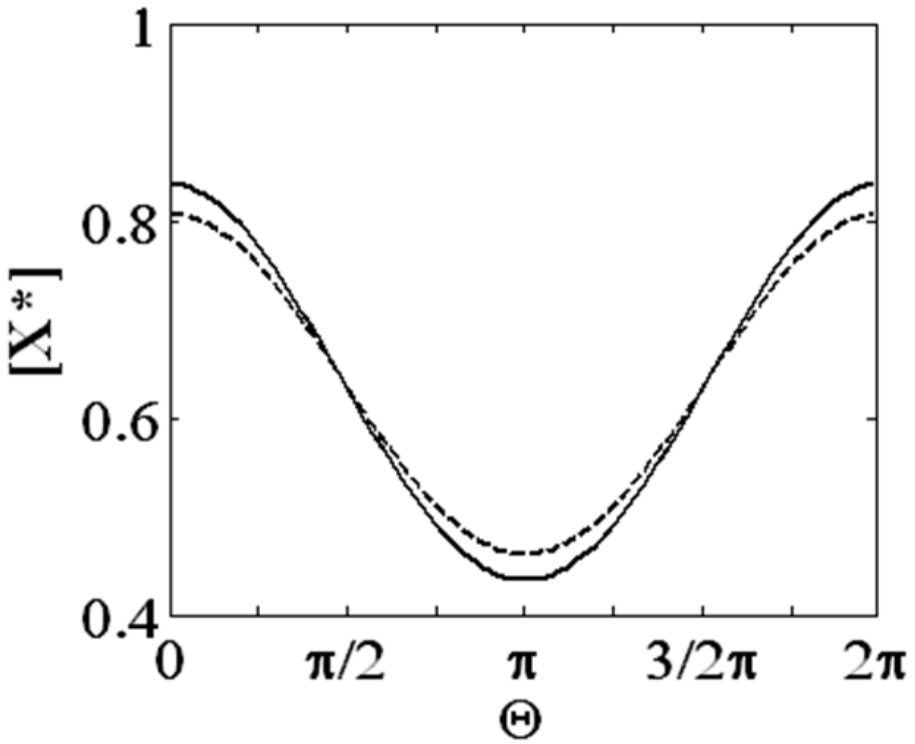


Figure C.2: This figure shows the profiles of $X^*$ for the reference case (solid line) and for a case where all species in the substrate cycle are very weakly diffusible (dashed line). The profiles shown here are for scenario 2. There is negligible difference in the profile of $X^*$ in both cases and no qualitative difference. This is an example of how observed trends apply even if all species are very weakly diffusible.

to a particular concrete system or pathway, while other studies utilize an arbitrary set of parameter values and the conclusions relate to general or non-system specific models (which may be physiologically relevant). A common obstacle encountered is the lack of available information on parameters (particularly transport related ones) in specific biological systems. Our search reveals that there is no single standard set of parameters that one can find in the literature to utilize in the study of our minimal model.

Our choice of parameter sets is dictated by the main goal of the study. This study revolves around the spatial aspects of signal transduction in this minimal module. Spatial effects are introduced into the cycle through diffusion of species and through spatial distribution of enzymes (either graded or localized). We would like to examine how diffusion and localization effects spatial signal processing in the cycle.

We perform analysis of the covalent modification cycle in three different kinetic parameter regimes (cast in non-dimensional terms): mass action, "ultrasensitive" and "generic" parameter regimes. The first two scenarios are commonly invoked in the study of covalent

modification cycles. We then study spatial signal transduction in the cycle by examining effects of diffusion of one or more species under a range of diffusivities which can be characterized as weak, moderate or strong.

Thus for the purposes of our study we perform analysis on models in different kinetic parameter regimes and study spatial aspects therein. This approach accounts for the qualitatively different kinetic regimes in the covalent modification cycle and studies spatial aspects in each of the cases. The values of individual kinetic rate constants in these regimes fall into the range of those seen in the literature Ferrell (1996); Huang and Ferrell (1996). The chosen diffusion coefficients are based on values in the literature as well.

As part of preliminary analysis of the cycle, we have also varied individual kinetic parameters (while keeping others fixed) and examined the effect on the response of the cycle. The sensitivity to transport parameters is directly accounted for in our analysis. Since the focus of this investigation is the distortion of a temporal cycle by spatial effects, the trends we observe when diffusing species are present are largely independent of the particular values of individual parameters. In fact, similar patterns are actually observed across the different parameter regimes, lending further credence to our approach.

The typical size of a eukaryotic cell is $10\mu$m in diameter and we based diffusion coefficients on estimates for proteins in the membrane (corresponding to weakly diffusing) (0.1 $\mu\text{m}^2/s$) and cytosol (corresponding to highly diffusible) (10 $\mu\text{m}^2/s$) Postma and Van Haastert (2001). We considered the total substrate concentration to be greater than that of the total enzyme concentration.

## Enzyme Localization

Our analysis in the main text showed that the average spatial concentration of $X^*$ shows a biphasic response with respect to the diffusion coefficient (when X and $X^*$ diffuse equally) for the case when K and P are separated. In order to rule out effects due to enzyme sequestration by the complex, we also considered a reduced model described by mass action

kinetics:

$$\begin{aligned}
\frac{\partial[X]}{\partial t} &= -k_1[X][K] + k_2[X^*][P] + D_X\frac{\partial^2 X}{\partial\theta^2} \\
\frac{\partial[X^*]}{\partial t} &= -k_2[X^*][P] + k_1[X][K] + D_{X^*}\frac{\partial^2 X^*}{\partial\theta^2} \\
\frac{\partial[K]}{\partial t} &= k_{f1}S(\theta) - k_{b1}[K] + D_K\frac{\partial^2 K}{\partial\theta^2} \\
\frac{\partial[P]}{\partial t} &= k_{f2}I(\theta) - k_{b2}[P] + D_P\frac{\partial^2 P}{\partial\theta^2}
\end{aligned}$$

where $k_1$ and $k_2$ are the forward kinetic rate constants for the binding of the enzyme and its substrate. $k_{f1}$ and $k_{f2}$ are the "production" constants and $k_{b1}$ and $k_{b2}$ are the "degradation" rate constants for the free enzymes K and P, respectively. $S(\theta)$ and $I(\theta)$ are parameters associated with the spatial distribution of the enzymes (non-diffusible) which are localized in this case. We found that when X and $X^*$ equally diffuse, in this model as well, the average spatial concentration of $X^*$ shows a biphasic response with respect to an increase in the diffusion coefficient. This results indicates that the biphasic effect is independent of any contribution of enzyme sequestration by enzyme-substrate complexes.

## Parameter values

Here we list the dimensionless kinetic and transport parameters.

### "Generic" parameter regime

$k_1 = 0.1; k_{-1} = 1.0; k_2 = 0.05; k_3 = 0.1; k_{-3} = 1.0; k_4 = 0.1$. The parameters used to define the production/degradation of free enzyme were: $k_{f1} = 1.0; k_{b1} = 1.0; k_{f2} = 1.0; k_{b2} = 1.0$. The initial conditions assigned to the variables in the generic regime simulations were: $X_i = 2.0; K_i = 1.0; XK_i = 0.001; X_i^* = 0.001; P_i = 1.0; X^*P_i = 0.001$.

### Enzyme distribution in Scenarios 1 to 3

In cases where the enzymes are graded S($\theta$) which corresponds to K and I($\theta$)) which corresponds to P, are a+bcos($\theta$) if co-aligned. If counter-aligned S($\theta$)=a+bcos($\theta$) and I($\theta$)=a+bcos($\theta+\pi$). In both cases: a=1.0 for both and b=0.3 for (K) and 0.2 for (P). In scenario 1, only K is graded, therefore a=1.0 for both and b=0.3 for (K) and 0.0 for (P).

## "Ultrasensitive" parameter regime

$k_1 = 10.0; k_{-1} = 1.0; k_2 = 1.0; k_o = 0.03; k_3 = 10.0; k_{-3} = 1.0; k_4 = 1.0; k_{f1} = 0.01; k_{b1} = 0.01; k_{f2} = 0.01; k_{b2} = 0.01; k_{fx} = 0.0; k_{bx} = 0.01; k_{fxs} = 0.0; k_{bxs} = 0.01; k_{xk} = 0.01; k_{xp} = 0.01$. The initial conditions assigned to the variables in the "ultrasensitive" regime simulations were: $X_i = 2.0; K_i = 0.05; XK_i = 0.001; X_i^* = 0.01; P_i = 0.06; X^*P_i = 0.001;$ The enzymes signal inputs are: for K: S($\theta$)=0.05+0.03cos($\theta$) and P: I($\theta$)=0.03.

## Enzymes Localization Case

The parameters used to model the localization of enzymes were: $k_1 = 0.1; k_{-1} = 1.0; k_2 = 0.05; k_3 = 0.1; k{-}3 = 1.0; k_4 = 0.1; k_{f1} = 1.0; k_{b1} = 1.0; k_{f2} = 1.0; k_{b2} = 1.0$ and K and P were square pulses ranging from 0.0 to 1.0 and 0.01 to 1.0, respectively. The initial conditions for the species when enzymes are localized were: $X_i = 2.0; K_i = 0.0; XK_i = 0.0; X_i^* = 0.0; P_i = 0.0; X^*P_i = 0.0$.

## Range of Diffusion Coefficients

For all the simulations the diffusion coefficients used were as follows (in dimensionless terms): D=0 for the no diffusion case; D=0.01 for the weak diffusion case; D=0.1 for the moderate diffusion cases and D=1 and 10 for the strong diffusion cases.

## Parameter values used in the Figures in the main text

### Fig. 4.1

In (B) parameter values and initial conditions from the "generic" parameter regime were used.

### Fig. 4.2

In (A) and (B) parameter values and initial conditions from the "generic" parameter regime were used. The enzymes are counter-aligned and co-aligned in (A) and (B), respectively. The range of diffusion values used is mentioned previously.

## Fig. 4.3

In (A) and (B) parameter values and initial conditions from the "generic" parameter regime were used. The enzymes are both counter- and co-aligned in (A) and co-aligned only in (B). The range of diffusion values used is mentioned previously and both complex and enzyme/substrate diffuse equally.

## Fig. 4.4

In this figure parameter values and initial conditions from the "ultrasensitive" parameter regime were used. In (A) D=0 and in (B) and (C) a range of diffusion values (mentioned before) is used.

## Fig. 4.5

Parameter values and initial conditions for the 'Enzymes Localization Case' (see above) are used here. In (A) the spatial concentration profiles are shown for: D=0.00005, 0.0005, 0.005, 0.05, 0.5 and 1.0. In (C) the range of diffusion coefficients tested in both cases are D=0.00001, 0.00005, 0.0001, 0.0005, 0.001, 0.005, 0.01, 0.05, 0.1, 0.5, 1.0, 5.0 and 10.0. In Case I K ranges from 0.0 to 1.0 and P ranges from 0.01 to 1.0 and in Case II K ranges from 0.0 to 2.0 and P ranges from 0.01 to 1.0.

# Appendix D

# Spatial control of biochemical modification cascades and pathways: Further discussion, analysis of models, additional cascades and parameter values

In this document, we present analysis of a number of aspects of topics presented in the main text. We present, in turn: (i) The models of the modification cascades (ii) Analysis of different aspects of enzymatic cascades with localization (iii) The effect of localization on multisite modifications (iv) The effect of localization on phosphotransfer mechanisms (v) Spatial aspects of open signalling cascades. (vi)Analysis of a single tier of a modification cascade with multiple diffusible entities. The computational results presented here are complemented by analytical work, which is presented in (Alam-Nazki and Krishnan, 2014, *manuscript under revision*) and reproduced in this section.

## D.1 Models

### D.1.1 Cascade

We present the various models which we will study. We first start with an enzymatic 2-step cascade, extended to incorporate spatial aspects. We first describe a general spatial model of a 2-step cascade. We then discuss how we adapt this to describe a 2-step cascade with spatial localization.

A general spatial model of a 2-stage enzymatic cascade (in one spatial dimension, with the spatial variable being denoted by $\theta$) is described by the following equations:

$$\begin{aligned}
\frac{\partial[X]}{\partial t} &= -k_1[X][K] + k_{-1}[XK] + k_4[X^*P1] + D_X\frac{\partial^2 X}{\partial\theta^2} \\
\frac{\partial[X^*]}{\partial t} &= -k_3[X^*][P1] + k_{-3}[X^*P1] + k_2[XK] - k_5[Y][X^*] \\
&\quad +k_{-5}[YX^*] + k_6[YX^*] + D_{X^*}\frac{\partial^2 X^*}{\partial\theta^2} \\
\frac{\partial[K]}{\partial t} &= -k_1[X][K] + k_{-1}[XK] + k_2[XK] + D_K\frac{\partial^2 K}{\partial\theta^2} \\
\frac{\partial[P1]}{\partial t} &= -k_3[X^*][P1] + k_{-3}[X^*P1] + k_4[X^*P1] + D_{P1}\frac{\partial^2 P1}{\partial\theta^2} \\
\frac{\partial[XK]}{\partial t} &= k_1[X][K] - k_{-1}[XK] - k_2[XK] + D_{XK}\frac{\partial^2 XK}{\partial\theta^2} \\
\frac{\partial[X^*P1]}{\partial t} &= k_3[X^*][P1] - k_{-3}[X^*P1] - k_4[X^*P1] + D_{X^*P1}\frac{\partial^2 X^*P1}{\partial\theta^2} \\
\frac{\partial[Y]}{\partial t} &= -k_5[Y][X^*] + k_{-5}[YX^*] + k_8[Y^*P2] + D_Y\frac{\partial^2 Y}{\partial\theta^2} \\
\frac{\partial[Y^*]}{\partial t} &= -k_7[Y^*][P2] + k_{-7}[Y^*P2] + k_6[YX^*] + D_{Y^*}\frac{\partial^2 Y^*}{\partial\theta^2} \\
\frac{\partial[P2]}{\partial t} &= -k_7[Y^*][P2] + k_{-7}[Y^*P2] + k_8[Y^*P2] + D_{P2}\frac{\partial^2 P2}{\partial\theta^2} \\
\frac{\partial[YX^*]}{\partial t} &= k_5[Y][X^*] - k_{-5}[YX^*] - k_6[YX^*] + D_{YX^*}\frac{\partial^2 YX^*}{\partial\theta^2} \\
\frac{\partial[Y^*P2]}{\partial t} &= k_7[Y^*][P2] - k_{-7}[Y^*P2] - k_8[Y^*P2] + D_{Y^*P2}\frac{\partial^2 Y^*P2}{\partial\theta^2}
\end{aligned} \tag{D.1}$$

The substrate species are X, $X^*$ (and corresponding complexes XK and $X^*P1$) in the

first level of the cascade and in the second level of the cascade, the substrate species (and relevant complexes) are $Y, YX^*, Y^*$ and $Y^*P2$. The enzymes for the first stage of the cascade are K (kinase) and P1 (phosphatase). $X^*$ acts as a kinase for the second level of the cascade and $P2$ is the phosphatase. The model encapsulates a fairly standard and broadly used description of the catalytic conversion of substrate by enzyme, explicitly incorporating enzyme substrate binding/unbinding and irreversible conversion. This kinetic description of the cascade has been used in multiple studies of signalling cascades.

The rate constants of binding of enzyme to substrate are $k_1$ (K to X), $k_3$ (P1 to $X^*$), $k_5$ ($X^*$ to Y) and $k_7$ (P2 to $Y^*$), while the corresponding unbinding constants are denoted by $k_{-1}, k_{-3}, k_{-5}$ and $k_{-7}$ respectively. The relevant catalytic rate constants for these reactions are denoted by $k_2, k_4, k_6$ and $k_8$ respectively. The diffusion coefficients are $D_X$, $D_K$, $D_{XK}$, $D_{X^*}$, $D_{P1}$, $D_{X^*P1}$, $D_Y$, $D_{YX^*}$, $D_{Y^*}$, $D_{P2}$ and $D_{Y^*P1}$, where the subscript denotes the species under consideration.

While this is a general spatial model of a 2 step cascade, we now discuss how we employ this in the context of our results.

## Response to a gradient

When we aim to study the response of the model to a spatial gradient we incorporate an explicit description of the input, which is the kinase $K$. There are different ways in which this can be incorporated. One way is to impose a particular free kinase concentration, described by an equation of the form

$$\frac{\partial[K]}{\partial t} = -k_1[X][K] + k_{-1}[XK] + k_2[XK] + k_{f1}S(\theta) - k_{b1}[K] + D_K\frac{\partial^2 K}{\partial\theta^2} \tag{D.2}$$

This describes a production of K by an external signal $S$ and removal of K (rate constants $k_{f1}$ and $k_{b1}$) in addition to the other reactions it is involved in. A similar input has been used in (Alam-Nazki and Krishnan, 2013).

## Localization

The primary focus of the paper is to study the effects of localization (and separation) of different steps of the cascade. Thus, we describe localization in the two step cascade as

follows. For simplicity, we will assume that all species are essentially non-diffusible apart from the species conveying the information from one location to the other. Other variants such as those where all localized species also diffuse in the individual locations (but confined there) can also be employed but we will not require these additional details for the purposes of our investigations here. We thus have K, P1 and X in location 1, while Y, $Y^*$ and P2 are in location 2. All relevant enzyme substrate complexes are in the respective locations, and these are assumed non-diffusible. $X^*$ is the diffusible species and thus it is present everywhere in the domain.

We employ the model in a periodic domain with the two locations symmetric and diametrically opposite to one another (see Fig. 1). This also exactly corresponds to no-flux boundary conditions in a domain of half the size.

When we study localization, we thus localize $K$ in the first location (and the relevant complex is contained here as well). The total concentration of kinase (free + complex) is automatically conserved. The total concentration of $K$ (free +complex) can be regarded as the input to the cascade.

### D.1.2 Three Step Cascade

A three step cascade may be described in an analogous manner. The only difference here is that there is more than one way to spatially partition a three step cascade. For instance, one possibility is that the first two steps are localized in location 1 and the last step is localized in location 2. Alternatively it is possible that the first step is in location 1 (just like the two step cascade above) and the next two steps is in location 2. In each case the only diffusing species is the communicating species, and the relevant models can be easily described by a simple expansion of the model considered above. We therefore do not explicitly describe these equations. A third case also considered is when the first and third steps are in location 1 and the second step is in location 2. This involves two communicating species. Again, this is described in an analogous manner.

**Multisite Modification** We now describe a spatial model of a 2-site ordered modification of substrate X. Here the modification of $X$ to $X^*$ is mediated by the kinase K1 and phosphatase P1, and the modification of $X^*$ to $X^{**}$ is mediated by the kinase K2 and the phosphatase P2. Note that, in an ordered multisite modification, there is a specific order to the modifications, in contrast to a random modification mechanism.

We first present a general spatial model of this two ordered site modification system.

This is described by the equations:

$$\begin{aligned}
\frac{\partial[X]}{\partial t} &= -k_1[X][K1] + k_{-1}[XK1] + k_4[X^*P1] + D_X\frac{\partial^2 X}{\partial\theta^2} \\
\frac{\partial[X^*]}{\partial t} &= -k_3[X^*][P1] + k_{-3}[X^*P1] + k_2[XK1] - k_5[X^*][K2] \\
&\quad +k_{-5}[X^*K2] + k_8[X^{**}P2] + D_{X^*}\frac{\partial^2 X^*}{\partial\theta^2} \\
\frac{\partial[X^{**}]}{\partial t} &= k_7[X^{**}][P2] - k_{-7}[X^{**}P2] + k_6[X^*K2] + D_{X^{**}}\frac{\partial^2 X^{**}}{\partial\theta^2} \\
\frac{\partial[K1]}{\partial t} &= -k_1[X][K1] + k_{-1}[XK1] + k_2[XK1] + D_{K1}\frac{\partial^2 K1}{\partial\theta^2} \\
\frac{\partial[P1]}{\partial t} &= -k_3[X^*][P1] + k_{-3}[X^*P1] + k_4[X^*P1] + D_{P1}\frac{\partial^2 P1}{\partial\theta^2} \\
\frac{\partial[K2]}{\partial t} &= -k_5[X^*][K2] + k_{-5}[X^*K2] + k_6[X^*K2] + D_{K2}\frac{\partial^2 K2}{\partial\theta^2} \\
\frac{\partial[P2]}{\partial t} &= -k_7[X^{**}][P2] + k_{-7}[X^{**}P2] + k_8[X^{**}P2] + D_{P2}\frac{\partial^2 P2}{\partial\theta^2} \\
\frac{\partial[XK1]}{\partial t} &= k_1[X][K1] - k_{-1}[XK1] - k_2[XK1] + D_{XK1}\frac{\partial^2 XK1}{\partial\theta^2} \\
\frac{\partial[X^*P1]}{\partial t} &= k_3[X^*][P1] - k_{-3}[X^*P1] - k_4[X^*P1] + D_{X^*P1}\frac{\partial^2 X^*P1}{\partial\theta^2} \\
\frac{\partial[X^*K2]}{\partial t} &= k_5[X^*][K2] - k_{-5}[X^*K2] - k_6[X^*K2] + D_{X^*K2}\frac{\partial^2 X^*K2}{\partial\theta^2} \\
\frac{\partial[X^{**}P2]}{\partial t} &= k_7[X^{**}][P2] - k_{-7}[X^{**}P2] - k_8[X^{**}P2] + D_{X^{**}P2}\frac{\partial^2 X^{**}P2}{\partial\theta^2}
\end{aligned} \tag{D.3}$$

The substrate species are X, $X^*, X^{**}$, while the relevant complexes are XK1, $X^*P1$, $X^*K2$ and $X^{**}P2$. The enzymes are K1 and P1 (first modification step) and K2 and P2 (second modification step). The forward association rate constants of the relevant enzyme to substrate are $k_1, k_3, k_5$ and $k_7$, the dissociation rate constants of the relevant enzyme substrate complexes are $k_{-1}, k_{-3}, k_{-5}$ and $k_{-7}$ and the corresponding catalytic constants are $k_2, k_4, k_6$ and $k_8$. The diffusion coefficients are $D_X$, $D_{K1}$, $D_{XK1}$, $D_{X^*}$, $D_{P1}$, $D_{X^*P1}$, $D_{X^*K2}$, $D_{X^{**}}$, $D_{K2}$, $D_{X^{**}P2}$ and $D_{P2}$, where the subscript denotes the species under consideration.

We focus on the effects of localization in the cascade. We do this as follows. All species relevant to the first modification (and "demodification") are in the first location, while those

relevant to the second modification (and demodification) are present in the second location. The only species which is diffusible is $X^*$. Thus the model describes a situation which is an analogue of the two step cascade considered above: the only difference is that the modified species acts as a substrate in the second stage.

### D.1.3 Phosphorelay

We now consider a different kind of modification sequence: a phosphorelay. We describe a spatial model of 4 step phosphorelay with phosphatases at each step. We present a more general model which allows the output of any of the stages to be the communicating species. All other species are assumed non-diffusible. The 4 step phosphorelay is described by the following equations:

$$
\begin{aligned}
\frac{\partial[X1]}{\partial t} &= -k_s[X1][K] + k_2[X1^*X2] + k_{p2}[X1^*P1] \\
\frac{\partial[X1^*]}{\partial t} &= k_s[X1][K] - k_1[X1^*][X2] + k_{-1}[X1^*X2] - k_{p1}[X1^*][P1] \\
&\quad + k_{-p1}[X1^*P1] + D_{X1^*}\frac{\partial^2 X1^*}{\partial\theta^2} \\
\frac{\partial[X2]}{\partial t} &= -k_1[X1^*][X2] + k_{-1}[X1^*X2] + k_4[X2^*X3] + k_{p4}[X2^*P2] \\
\frac{\partial[X2^*]}{\partial t} &= -k_3[X2^*][X3] + k_{-3}[X2^*X3] - k_{p3}[X2^*][P2] + k_{-p3}[X2^*P2] \\
&\quad + k_2[X1^*X2] + D_{X2^*}\frac{\partial^2 X2^*}{\partial\theta^2} \\
\frac{\partial[X3]}{\partial t} &= -k_3[X2^*][X3] + k_{-3}[X2^*X3] + k_{p6}[X3^*P3] + k_6[X3^*X4] \\
\frac{\partial[X3^*]}{\partial t} &= -k_5[X3^*][X4] + k_{-5}[X3^*X4] + k_4[X2^*X3] - k_{p5}[X3^*][P3] + k_{-p5}[X3^*P3] \\
&\quad + D_{X3^*}\frac{\partial^2 X3^*}{\partial\theta^2} \\
\frac{\partial[X4]}{\partial t} &= -k_5[X3^*][X4] + k_{-5}[X3^*X4] + k_{p8}[X4^*P4] \\
\frac{\partial[X4^*]}{\partial t} &= -k_{p7}[X4^*][P4] + k_{-p7}[X4^*P4] + k_6[X3^*X4] + D_{X4^*}\frac{\partial^2 X4^*}{\partial\theta^2} \\
\frac{\partial[X1^*X2]}{\partial t} &= k_1[X1^*][X2] - (k_{-1} + k_2)[X1^*X2] \\
\frac{\partial[X2^*X3]}{\partial t} &= k_3[X2^*][X3] - (k_{-3} + k_4)[X2^*X3] \\
\frac{\partial[X3^*X4]}{\partial t} &= k_5[X3^*][X4] - (k_{-5} + k_6)[X3^*X4] \\
\frac{\partial[X1^*P1]}{\partial t} &= k_{p1}[X1^*][P1] - (k_{-p1} + k_{p2})[X1^*P1] \\
\frac{\partial[X2^*P2]}{\partial t} &= k_{p3}[X2^*][P2] - (k_{-p3} + k_{p4})[X2^*P2] \\
\frac{\partial[X3^*P3]}{\partial t} &= k_{p5}[X3^*][P3] - (k_{-p5} + k_{p6})[X3^*P3] \\
\frac{\partial[X4^*P4]}{\partial t} &= k_{p7}[X4^*][P4] - (k_{-p7} + k_{p8})[X4^*P4] \\
\frac{\partial[P1]}{\partial t} &= -k_{p1}[X1^*][P1] + (k_{-p1} + k_{p2})[X1^*P1] \\
\frac{\partial[P2]}{\partial t} &= -k_{p3}[X2^*][P2] + (k_{-p3} + k_{p4})[X2^*P2] \\
\frac{\partial[P3]}{\partial t} &= -k_{p5}[X3^*][P3] + (k_{-p5} + k_{p6})[X3^*P3] \\
\frac{\partial[P4]}{\partial t} &= -k_{p7}[X4^*][P4] + (k_{-p7} + k_{p8})[X4^*P4]
\end{aligned}
\tag{D.4}
$$

In the above model, the substrate species are X1, X2, X3, X4, $X1^*, X2^*, X3^*$ and $X4^*$. The substrate complexes are $X1^*X2, X2^*X3$ and $X3^*X4$. The phosphatase substrate complexes are $X1^*P1, X2^*P2, X3^*P3$ and $X4^*P4$. The enzymes are K1 (the kinase for the first stage), and the phosphatases for the four stages are P1, P2, P3 and P4 respectively. The forward binding rate constants are $k_s, k_1, k_3, k_5$ (for the relevant forward modifications of each stage) and $k_{p1}, k_{p3}, k_{p5}, k_{p7}$ (for the reverse modifications of each stage). The dissociation/unbinding rate constants are $k_{-1}, k_{-3}, k_{-5}, k_{-p1}, k_{-p3}, k_{-p5}, k_{-p7}$ and the catalytic rate constants are $k_2, k_4, k_6, k_{p2}, k_{p4}, k_{p6}$ and $k_{p8}$. The diffusion coefficients of the substrate species are $D_{X1^*}, D_{X2^*}, D_{X3^*}$ and $D_{X4^*}$, where the subscript denotes the species under consideration. The first step of the phosphorelay is assumed to occur through mass action kinetics.

The above model is a simple model of a phosphorelay, where each elementary step is modelled by mass action kinetics; the binding/unbinding of the species is described explicitly. The main difference between this model and that of the cascade arises in the fact when the output at one stage (say $X1^*$) transfers a phosphate group to a species in the next stage (say $X2$), it gets converted back (to $X1$).

As before, we will consider different scenarios where some steps are localized in one location and other steps are localized in the other location. For instance if $X_2^*$ is the only diffusible species, this describes a scenario where the first two steps are in one spatial location and the last two are in a second location. The relevant communicating species is the sole diffusing species in such cases. Thus such a model describes a phosphotransfer mechanism with spatial localization.

A two step phosphotransfer model is obtained by considering only the first two steps in the model above. Making $X_1^*$ the only diffusible species and localizing the first stage in one location and the second stage in another location results in the two step phosphotransfer model with localization.

### D.1.4 Open cascade

For completeness, we also consider open models of modification sequences. For instance, we consider a 3 step modification sequence (assumed irreversible, for simplicity: reversible analogues have also been studied). Here $X_1$ is modified to $X_2$ which is modified to $X_3$. The only difference here is that there is a constant production of $X_1$ and a removal of $X_3$, proportional to its concentration. This is described by the model

$$\begin{aligned}
\frac{\partial[X1]}{\partial t} &= k_o - k_s[S][X1] \\
\frac{\partial[X2]}{\partial t} &= k_s[S][X1] - k_2[X2] + D_{X2}\frac{\partial^2 X2}{\partial \theta^2} \\
\frac{\partial[X3]}{\partial t} &= k_2[X2] - k_d[X3]
\end{aligned} \tag{D.5}$$

The signal S enters the chain of reactions between X1 and X2, catalyzing the conversion of $X_1$ to $X_2$. $k_o$ is the generation term for X1 and $k_s$ is the rate constant associated with the signal converting X1 to X2. $k_2$ is the rate constant associated with the conversion of X2 to X3 and $k_d$ is the degradation constant for X3. We will assume that $X_2$ is the communicating species and that $X_1$ is in the first location and $X_3$ is in the second location. $D_{X2}$ is the diffusion coefficient for X2. It should be noted that by making $X_2$ non-diffusible and by localizing all species in the same location, we recover the ODE model of this modification sequence (with input and removal). All reactions are described by mass-action kinetics for simplicity.

One can consider a minor variation of the above structure, where the signal is associated with the conversion from $X_2$ to $X_3$. This is described by the model

$$\begin{aligned}
\frac{\partial[X1]}{\partial t} &= k_o - k_1[X1] \\
\frac{\partial[X2]}{\partial t} &= k_1[X1] - k_s[S][X2] + D_{X2}\frac{\partial^2 X2}{\partial \theta^2} \\
\frac{\partial[X3]}{\partial t} &= k_s[S][X2] - k_d[X3]
\end{aligned} \tag{D.6}$$

Here, $k_o$ is the generation term for X1 and $k_1$ is the rate constant associated with the degradation of X1 or production of X2. $k_s$ is the rate constant for X2 being converted to X3 by the signal and $k_d$ is the degradation constant for X3. $D_{X2}$ is the diffusion coefficient for X2.

## D.2 Analysis of models

### D.2.1 Diffusion and retroactivity in cascades

Although most of our focus was on effects of localization, we also discuss some aspects of the response of cascades to spatially graded signals when there is no localization. Thus, we consider the same model of the two step cascade, with all components present everywhere in the domain. The input is provided in the form of a spatial gradient. When none of the signalling components diffuse, then the signal transduction is purely local, and can be studied using ODEs. On the other hand, as we have shown previously (Alam-Nazki and Krishnan, 2013), diffusion of individual components can significantly alter and distort signal transduction. When we examine signal transduction in such a cascade, the effects of diffusion of multiple components can be studied, some which can be simply understood from an equivalent study of a single covalent modification cycle and others which rely on the interplay of the two cycles. We discuss one example of the latter.

When the species in the second step Y and $YX^*$ (the substrate and relevant complex) diffuse while all other species are weakly diffusible, (Fig. D.1), we find that the spatial profile of $Y^*$ weakens. Further, the profiles of the species in the upstream cycle change- X becomes sharper, $X^*$ becomes flatter and profiles of complexes in the first cycle are also affected. The underlying reason for the change in profiles of species upstream is that $X^*$ is sequestered in the complex $YX^*$. Thus in this case diffusion affects the profile of $X^*$ having a ripple effect on the remaining species in the first step. This demonstrates how diffusion of species in a signalling cascade can significantly affect species upstream and illustrates one example of the spatial dimension to retroactivity. In the above example the reference case chosen was one where all other species were weakly diffusible, but the broader conclusion of the back propagating effects of species diffusion remains valid in other scenarios as well. This highlights one aspect of the effect of diffusion in signalling cascades.

### D.2.2 Spatial effects on a Goldbeter Koshland type switch

In the main text, we have discussed the consequences of localization and diffusion on switch-like responses arising in the Goldbeter Koshland parameter regime. The effect of separation of the stages of the cascade is shown in Fig. D.2.

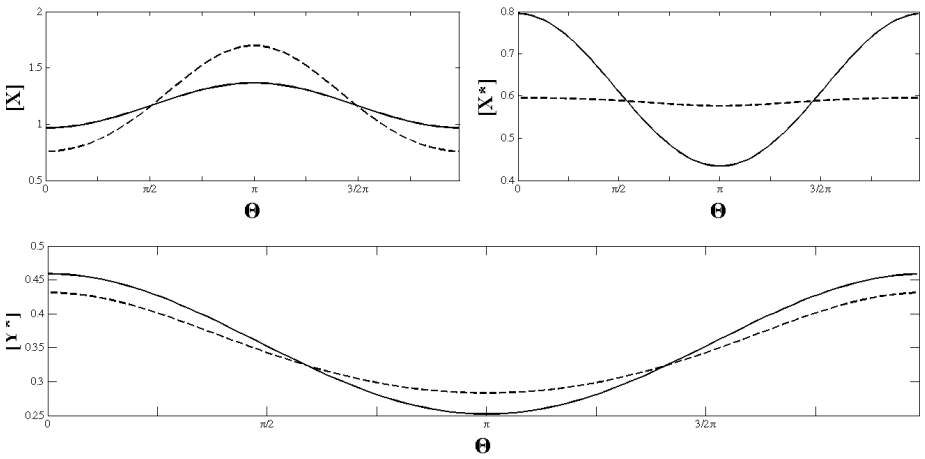


Figure D.1: **Two step covalent modification cascade subject to a gradient.** The enzymes are graded and of the form a+bCos($\theta$). The case depicted here is for when the phosphatase enzymes are counter-aligned with the input kinase profile. Spatial concentration profiles of species are shown for two cases- 1) All the species weakly diffuse (solid line) and 2) Y and YX$^*$ both diffuse strongly (dashed line) (other species are weakly diffusing). In the latter case, the spatial concentration profiles of all species, including the species in the upstream step are modified. The spatial profile of X becomes enhanced and that of X$^*$ becomes weaker. The spatial profile of Y$^*$ becomes weaker as well. The effect of diffusion propagates upstream causing a modification of spatial profiles both upstream and downstream. Schematic diagrams of modules employed.

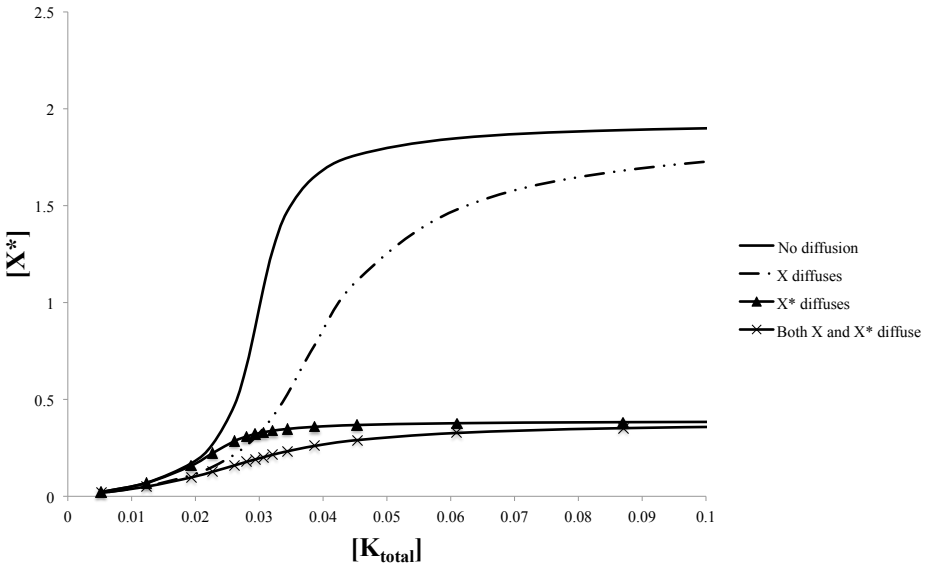


Figure D.2: **Effect of diffusion on the steady state Input/output curve.** A two-step modification cascade where the first step is in the ultrasensitive regime, and the second step occurs via mass action kinetics is considered. We focus on the first step. The steady state input/output curve of [X$^*$] is shown. When none of the species diffuse (solid line), the module shows an ultrasensitive response. If X$^*$ itself diffuses (solid line with triangle markers) the sensitivity of the input-output curve is greatly reduced. Therefore if $X^*$ is the communicating species in a spatially separated cascade, the switch-like effect is severely attenuated.

### D.2.3 Double site modification with a single enzyme pair

Spatial control in multisite modification can also occur through localization of kinase(s) and phosphatase(s) at different locations. We briefly consider a two site ordered mechanism of multisite modification by the same kinase and phosphatase pair (see Fig. D.3). We examine two cases. If the kinase is colocalized with the unmodified substrate and the doubly modified substrate is the only substrate species diffusing, then it diffuses to the location of the phosphatase and is completely converted back to the unmodified substrate. If both unmodified and doubly modified substrates diffuse (and the singly modified substrate does not), then the cycle can be completed. This is an example of spatial localization in multisite phosphorylation different from the ones considered above and is a simple multisite analogue of spatially separated kinase phosphatase pairs in covalent modification cycles seen in bacteria (Shapiro et al., 2009). We find here, that even though the cycle is complete, the behaviour is not a simple analogue of that situation. In fact we observe that singly modified substrate accumulates along with the kinase as well as phosphatase and both modified and double modified substrates exhibit weakly graded profiles. If all modified and unmodified substrates diffuse, then this is no longer the case. This points to another facet of the interplay between spatial control, localization and chemical modification sequences.

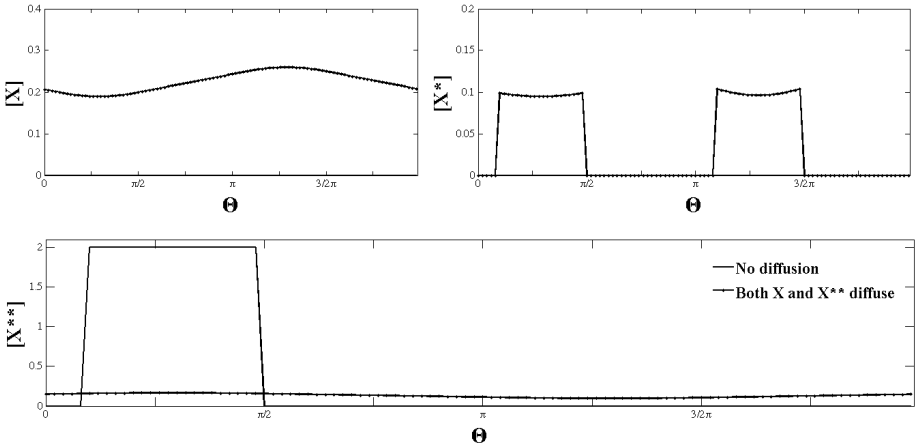


Figure D.3: **Double site modification with a single enzyme pair.** The enzymes are are localized in opposite patches in the domain (K is localized on the left in the domain and P is on the right). All substrate is initially localized alongside the kinase.The spatial concentration profiles of species X, $X^*$ and $X^{**}$ are shown. When there is no diffusion (solid line), $X^{**}$ profile is present where K is localized, X and $X^*$ are zero at steady state. If both X and $X^{**}$ diffuse (line with dots) then both spatial profiles are spread in the domain and $X^*$ is localized in both locations.

### D.2.4 Cascades

We first consider a two step enzymatic cascade for concreteness. For simplicity of notation, we will refer to the species in the first tier as $X_1$, (with active form $X_1^*$, complexes $K_1X_1, P_1X_1^*$) and likewise the species in the second tier as $X_2$ (with active form $X_2^*$, complexes $X_1 * X_2, P_2X_2^*$) Note that here $X1^*$ is the communicating species between the two compartments and also the only diffusible species. By adding up all the equations of all the species, we find that all kinetic terms cancel out leaving, at steady state,

$$\frac{\partial^2 X1^*}{\partial \theta^2} = 0$$

This shows that this species has a spatially uniform profile. We now deduce some facts based on this.

#### Spatial separation can result in reduction of the output of the cascade

We start by noting that the steady state of the cascade corresponds to the standard kinetic equations (i.e. those resulting from the ODEs) in each compartment, along with the conservation condition. The conservation of total substrate implies that $L_1(X1+KX1+X1^*P1+X1^*X2) + LX1^* = L_1X1_{tot}$. Note that $X1_{tot}$ corresponds to the total concentration of $X1$ species present initially and that $L_1X1_{tot}$ hence corresponds to the total amount of this species in the system. Similarly, $X2 + X1^*X2 + X2^* + P_2X2^* = X2_{tot}$. $X2_{tot}$ corresponds to the total concentration of $X2$ species present initially and that $L_1X2_{tot}$ hence corresponds to the total amount of this species in the system. The species 2 remains localized in the second compartment, and hence the sum of concentrations of all the species involving X2 is constant. In the above, $L_1$ corresponds to the size of the compartments (assumed equal) and $L$ corresponds to the size of the overall domain. Clearly $L > 2L_1$ if the two patches are disjoint and separated. $L = L_1$ corresponds to the situation where the two patches are coincident. Writing $L = L_1 + L_e$ we see from the conservation equation above, that in effect the available total amount of $X1$ species in compartment 1 is reduced by a factor $L_eX1^*$. For simplicity we will assume that dephosphorylation in the second step occurs via mass action kinetics.

We will approach this in two stages. Suppose there was no retroactivity (i.e. the phosphorylation in the second stage occurred via mass action kinetics). Then, we see that the

conservation equation for species $X_1$ results in $L_1(X1 + K_1X1 + X1^*P1) + LX1^* = L_1X1_{tot}$. In other words $X1 + K_1X1 + X1^* + P1X1^* \leq X1_{tot}$: the total concentration of $X1$ species in the first compartment is reduced due to its spreading in the domain.

We now show that at steady state in the ODE kinetic model $dX1^*/dX1_{tot} > 0$. In other words, the steady state output of the first tier of the cascade is an increasing function of the total amount of $X_1$ species. Clearly this is the case for small $X1_{tot}$, so if this condition were violated, we must require $dX1^*/dX1_{tot} = 0$ for some value of parameters. Now analyzing the model of the first level of the cascade, we see from conservation of enzymes that $K_1X1 = \alpha_1 K_{tot}X1/(1 + \alpha X1)$, $PX1^* = \beta_1 P_{tot}X1^*/(1 + \beta X1^*)$ for suitable constants $\alpha, \alpha_1, \beta, \beta_1$. Furthermore the concentrations of these complexes are proportional to each other at steady state. Now if $dX1^*/dX1_{tot} = 0$, then it follows immediately that $dPX1^*/dX1_{tot} = 0$ and from above that $dKX1/dX1_{tot} = 0$ (proportionality of complexes). It then follows that $dX1/dX1_{tot} = 0$. These conditions violate the conservation of species, and hence we conclude for a single covalent modification cycle $dX1^*/dX1_{tot} > 0$. Now if we consider this in light of a spatial cascade with no retroactivity, we find that the spreading of $X1^*$ in the domain reduces the total $X1$ species in compartment 1. This immediately means that $X1^*$ is reduced as a result, and since the kinetics in the second cycle is mass action, it means that $X2^*$ is also reduced (it being an increasing function of the concentration of $X1^*$).

We now examine a situation where the phosphorylation in the second cycle is not necessarily mass action (the dephosphorylation is still assumed to occur via mass action kinetics). Here we employ conservation of species 2 to impose $X2 + X2^* + X1^*X2 = X2_{tot}$. Now the steady state for the second cycle means $\gamma_1 X2^* = \gamma_2 X1^*X2 = \gamma_3(X1^*)(X2)$ for suitable constants $\gamma_1, \gamma_2, \gamma_3$. From this and the fact that the steady state concentration of the complex $X1^*X2$ is proportional to the product of concentrations of $X1^*$ and $X2$, we can infer that at steady state, the functional relationship between $X2^*$ and $X1^*$ is of the form

$$\begin{aligned} X2^* &= \frac{X2_{tot}X1^*}{a_1 + b_1X1^*} \\ X1^*X2 &= \frac{aX2_{tot}X1^*}{a_1 + b_1X1^*} \end{aligned} \tag{D.7}$$

Here $a, a_1, b_1$ are constants.

Now in this case, the steady state for $X1^*$ is governed by the same kinetic equations in the first location, along with the modified conservation condition $L_1(X1 + KX1 +$

$X1^*P1 + X1^*X2) + LX1^* = X1_{tot}$.

We now reason as follows. In the ODE model of the two step cascade, we see (under the conditions above) that $dX1^*/dX1_{tot} > 0$. Clearly this is the case for small $X1_{tot}$ so if this condition were violated, we must require $dX1^*/dX1_{tot} = 0$ for some value of parameters. We show that this is not possible. To do this we follow the exact same procedure above. We note that in the conservation relationship for species $X1$, there is an extra term corresponding to the concentration of the complex $X1^*X2$, which as noted above is related to $X1^*$ in the manner described. Thus if $dX1^*/dX1_{tot} = 0$, then it automatically follows that the derivative of this term with respect to $X1_{tot}$ is also zero. Thus the above argument carries through exactly. It is impossible to satisfy the conservation condition if $dX1^*/dX1_{tot} = 0$. Thus $dX1^*/dX1_{tot} > 0$.

Now the distributed system at steady state, the species of tier-1 satisfies the same steady state equation as the ODEs with a reduced $X1_{tot}$ (corresponding the extra $X1^*$ in the medium). Therefore at steady state $X1^*$ is reduced when compared to the situation where all species are localized together. From above it immediately follows that the same is true for $X2^*$. This shows how the separation of steps leads to a reduction in the output of the cascade.

**Retroactivity:** The above analysis can be used to examine the amount of $X1$ species contained in the downstream complex $X1^*X2$ which is a measure of the retroactivity. We see from the above analysis that the $X1^*X2$ concentration is related to the $X1^*$ concentration via a monotonic function. Since the separation leads to a reduction in $X1^*$ (relative the ODEs), we find that the $X1^*X2$ concentration is also reduced. In other words, the separation leads to a reduction in the retroactivity.

**Buffering against dilution:** The above analysis also provides insights into how the dilution effects can be buffered against in cascades. We see that the dilution effect occurs through $X1^*$ spreading in the medium. There are different ways to reduce the dilution. One way is to reduce the length of the medium. A second way, also seen from above, is to increase phosphatase $P1$ concentration. This leads to a reduction in $X1^*$. Now a low $X1^*$ will also result in a lower amount of dilution in the medium with the result that the effective total amount of X1 in location 1 will be modified only slightly. Thus the characteristics of the cascade are affected in only a minor way. While this of course involves operating the cascade in a regime of relatively low $X1^*$, Table D.1 shows how the effect of dilution in both absolute and relative terms is buffered against.

| [P1] | Dx*=0 (Together) | | Dx*=0.1 (Apart) | |
|---|---|---|---|---|
| | $X^*$ | $Y^*$ | $X^*$ | $Y^*$ |
| 0.3 | 1.177 | 1.074 | 0.3461 | 0.5318 |
| 0.7 | 0.7548 | 0.8702 | 0.2996 | 0.478 |
| 1 | 0.5908 | 0.7578 | 0.2715 | 0.4434 |
| 1.5 | 0.4324 | 0.6214 | 0.2342 | 0.3948 |
| 2 | 0.3406 | 0.5256 | 0.2055 | 0.3551 |
| 3 | 0.2389 | 0.401 | 0.1645 | 0.2949 |
| 10 | 0.07719 | 0.15 | 0.06778 | 0.1329 |

Table D.1: **Mitigating against the dilution effect.** The effect of varying P1 concentrations in a two step spatially cascade, when both steps are localized in the same location (columns 2 and 3) and when they are separated (columns 4 and 5). Increasing P1 concentrations results in the steady state output of the separated cascade, becoming close to that of the completely localized cascade, both in absolute and relative terms.

### D.2.5 Multisite modification and phosphotransfer

We briefly examine aspects of the multisite modification. Again, since $X^*$ is the only species which is diffusing, we find by adding all the equations that at steady state

$$\frac{\partial^2 X^*}{\partial \theta^2} = 0$$

In other words the concentration of $X^*$ is uniform in the domain. The conservation condition for substrate is altered by the fact that $X^*$ spreads in the medium. The equation becomes $L_1(X + K1X + P1X^* + K2X^* + X^{**} + P2X^{**}) + LX^* = X_{tot}$.

We will show that in the ODE model of the two site modification $dX^{**}/dX_{tot} > 0$. This can be seen by examining the two cycles sequentially. Firstly we see that by applying the conservation conditions for all the enzymes we have $P1 = P1_{tot}/(1 + \gamma_1 X^*)$ $K1 = K1_{tot}/(1 + \gamma_2 X)$, $K2 = K2_{tot}/(1 + \gamma_3 X^*)$, $P2 = P2_{tot}/(1 + \gamma_4 X^{**})$, where $\gamma_i$ are constant. Furthermore, all complex concentrations are simply proportional to the product of those of the corresponding free enzyme and substrate.

We note that $dX^{**}/dX_{tot} > 0$, for small $X_{tot}$. Suppose the inequality does not hold, we must require that $dX^{**}/dX_{tot} = 0$ at some parameter value. From an analysis of the second covalent modification cycle, since the concentrations of the two complexes are proportional at steady state, and the fact that each complex is related to the substrate concentration as a function of the form $a[S]/(1 + b[S])$, we immediately see that $dX^{**}P2/dX_{tot} = 0$, $dK1X^*/dX_{tot} = 0$. From this it follows that $dX^*/dX_{tot} = 0$.

Now, we use this and repeat the same analysis in the first cycle, to find that the derivative of concentrations of all substrate and complex species with respect to $X_{tot}$ is zero. This leads to a contradiction since this violates the conservation condition for substrate species. This shows therefore that $dX^{**}/dX_{tot} > 0$. Now if we contrast the separated model of the multisite modification model to that where all modifications occur together, we see that the formal equations satisfied in both cases is the same. The only difference arises in the conservation conditions. The steady state for the spatially distributed model corresponds to the steady state of a model with co-localized modifications (i.e. an ODE model) with reduced $X_{tot}$. Since $dX^{**}/dX_{tot} > 0$, we find that the spatially distributed modification results in reduced $X^{**}$.

We now turn to a different aspect of multisite modification. We examine the total and average concentration of $X^*$ in the situation when all modifications occur in the same location (patch of size $L_1$) and when the modifications are separated as examined above. For simplicity we will assume that all modifications occur via mass action kinetics (i.e. effectively very large catalytic constants for all modifications). In this case we have at steady state $X^*/X = \alpha K1_{tot}/P1_{tot}$ and $X^{**}/X^* = \beta K2_{tot}/P2_{tot}$, where $\alpha, \beta$ are the equilibrium constants for the two reactions. Now the conservation condition reads $L_1(X + X^{**}) + LX^* = X_{tot}$. To make a comparison between the two scenarios we write $X_{tot} = L_1X_o$. Thus $X_o$ would correspond to the total concentration of all substrate species (a conserved quantity) when the reaction occurred in the same location. From this it simply follows that

$$\begin{aligned} X^* &= \frac{L_1X_o}{L_1(P1_{tot}/(\alpha K1_{tot}) + \beta K2_{tot}/P2_{tot}) + L} \\ X^{**} &= \frac{\beta L_1X_oK2_{tot}/P2_{tot}}{L_1(P1_{tot}/(\alpha K1_{tot}) + \beta K2_{tot}/P2_{tot}) + L} \end{aligned}$$

It is clear from above that steady state concentrations of $X^*$ and $X^{**}$ are decreasing functions of $L$. If we consider the total amount of $X^*$ species in the domain, that is given

by $LX^*$, we find that this is a function which actually increases with L. We thus see that separated modification and increased separation does indeed decrease the doubly modified phosphoform concentration but in fact increases the total amount of phosphoform species in the domain.

**Shared Phosphatase** It is clear to see in the case of multisite modification with shared phosphatase, that a situation of separated modifications will result in all the $X$ species in the second domain to be converted to the unmodified form X. Further, at steady state the concentration of $X^*$ (which is uniform in the domain) is 0. This is simply seen by considering the second location. Firstly we know from above that the concentration of $X^*$ is spatially uniform. Now in the second location, by examining the kinetics of conversion we see that all available $X^*$ is converted to X. In other words, by examining the steady state condition for X, we see that $X^* = 0$ (since there is nothing to remove X and what is produced is produced via $X^*$). From this it follows that $X^{**} = 0$ and in fact the only species in location 2 is X. In fact all the substrate species ends up as X in the second location. In such a situation, an extra mechanism would be needed to transfer the X back to the original location.

### D.2.6 Phosphorelay

We briefly discuss a couple of aspects of the phosphorelay mechanism. We asserted that a 2 step separated model of the phosphorelay would result in 0 concentration of the output at steady state. We therefore consider a two step phosphorelay mechanism. Again we find similar to before that the spatial concentration of the communicating species $X1^*$ is uniform at steady state. This is obtained by adding all the equations of the species. Now, we notice that owing to the phosphotransfer mechanism, $X1^*$ is converted to $X1$ at the second location. By examining the equation for $X1$ at the second equation at steady state, we find that $X1^* = 0$ at steady state. This is because $X1$ is produced by $X1^*$ and not removed by any other mechanism. Therefore $X1^* = 0$, from which it follows that $X2^* = 0$. Naturally $X2^*$ may transiently increase from 0. We see a reasoning very similar to the situation above.

Finally, we briefly examine a 4 step phosphorelay, where the phosphatase is a bifunctional kinase (capable of triggering the phosphorelay). We see that if the phosphorelay is separated after the first step (i.e. the communicating species is $X2^*$ or $X3^*$) then by exactly the same reasoning as above, we find that $X4^*$ at steady state is 0. If however the commu-

nicating species is $X1^*$ then this is not necessarily the case: this is because the bifunctional kinase can effect a conversion from $X1$ (created in the second location) back to $X1^*$. Naturally, this pre-supposes the fact that the bifunctional kinase is capable of functioning as a kinase in the second location. This justifies what we mentioned in the text.

### D.2.7 Irreversible cascade with inflow and outflow

We now examine the 3 species irreversible cascade with inflow and outflow. By placing the entire cascade in one location, we find that at steady state, by adding all the equations of species, $X3 = k_o/k_d$. This shows how at steady state the output of the cascade recovers to pre-stimulus values (it is independent of S), exhibiting an adaptive response. We now consider spatial models of such a cascade. For specificity, we consider a situation where $X2$ is the diffusing species, and the signal mediates the conversion of $X2$ to $X3$. Now by adding all the equations and integrating over the full domain, we find that $k_o L_1 = k_d \int_0^{L_1} X_3 d\theta$. This shows that the spatially averaged concentration of the output of the cascade, X3 is in fact constant at a level independent of the stimulus, at steady state.

In order to obtain the steady state for X3, we need to find the steady state for $X2$. The steady state for X2 is governed by

$$\begin{aligned} k_0 + D_{X2}\frac{\partial^2 X2}{\partial \theta^2} &= 0, 0 \leq \theta < L_1/2 \\ D_{X2}\frac{\partial^2 X2}{\partial \theta^2} &= 0, L_1/2 \leq \theta < (L - L_1)/2 \\ -k_s S X2 + D_{X2}\frac{\partial^2 X2}{\partial \theta^2} &= 0, (L - L_1)/2 \leq \theta < L/2 \end{aligned} \tag{D.8}$$

The first equation has been written, eliminating $X1$. This is supplemented by no-flux boundary conditions at the two ends (for simplicity the problem is analytically solved in half the domain, applying no flux boundary conditions).

The solution to these equations can be obtained by solving them in a piece-wise manner

and matching them at the two interfaces. Thus the solution is obtained as

$$\begin{aligned} X2 &= -(k_o/2D_{X2})\theta^2 + C_1\theta + C_2, 0 \leq \theta < L_1/2 \\ X2 &= c_3\theta + c_4, L_1/2 \leq \theta < (L - L_1)/2 \\ X2 &= c_5 exp(-\sqrt{(}k_s S/D_{X2})x) + c_6 exp(\sqrt{(}k_s S/D_{X2})x, (L - L_1)/2 \leq \theta < L/2 \end{aligned} \tag{D.9}$$

The net steady state solution can be obtained by matching the concentration and flux at the two interfaces. We will not present the detailed expression here, as the main observations can be obtained from the expression above. We note that the overall profile (in each of the locations) depends on all the parameters in the above equation (through the matching conditions).

We see here that $X3$ can be easily obtained from the $X2$ concentration in the last subdomain, and is in fact proportional to it, with a proportionality factor depending on S. The point to note is (i) The solution is dependent on the absolute value of S and (ii) The solution also depends on the absolute value of the diffusion coefficient. We can therefore say that even though the average concentration of X3 exhibits an adaptive response, the local concentration of X3 at any specified location in the second location does not, in fact, adapt. In fact many characteristics of X3, such as the slope of the profile, do depend on S. Secondly, if the diffusion coefficient of X2 is very high, then the profile of X2 equilibrates at a level equal to $k_0/(k_s[S])$. This can be seen from the original equation in the limit of high $D_{X2}$ by using a perturbation expansion in $1/D_{X2}$. In this case the steady state profile of $X3$ is spatially uniform at a level $k_o/k_d$. We therefore see how spatial separation can distort the local adaptive response, and how a high diffusion of communicating species can make the response close to adaptive.

In general we find that step changes in S result in over-adaptive responses for $X3$ in some parts of the second domain (for instance in the middle, as shown in Fig. D.4) and in under-adaptive responses in others.

Now if we examine an analogous situation to the one above, but where the signal mediates the modification from $X1$ to $X2$, we find that $X2$ attains a profile independent of the signal, irrespective of the diffusion coefficient. Therefore, we find that $X3$ actually adapts to a step change in S, even though it does not have a uniform profile in the second compartment. This is seen by noting that the steady state profile of the diffusing species is

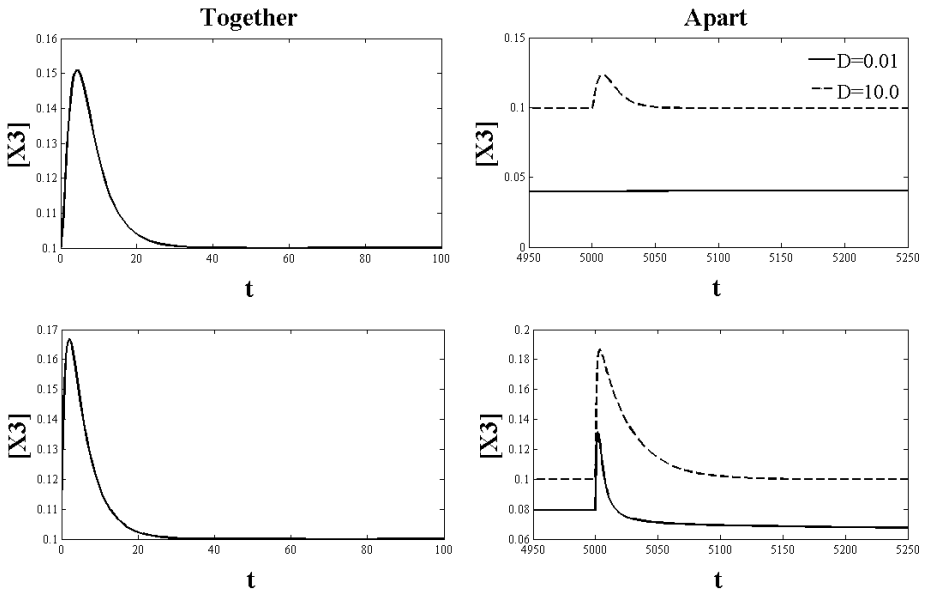


Figure D.4: **Open cascade.** The transient behaviour of X3 is shown in response to a step change in signal. The first row shows the case where the signal S enters the cascade between X1 and X2 and the second row shows the case where S enters the cascade between X2 and X3. The column on the left shows the case when all the species are localized together; X3 shows an adaptive response. The plots in the right column show the case where X1 and X3 are in two different compartments. [X3] in the middle of the second domain is shown. (Top RHS plot) X3 does exhibit an adaptive response and it's amplitude is higher for higher diffusivities of X2 (dashed line) and low when X2 diffusion is weak (solid line). In contrast, in the second case, for low diffusion coefficients (solid line) X3 does not perfectly adapt while it does for high diffusion coefficients (dashed line).

independent of S. This is seen immediately by inspecting the equations for $X2$ in this case:

$$\begin{aligned} k_0 + D_{X2}\frac{\partial^2 X2}{\partial\theta^2} &= 0, 0 \leq \theta < L_1/2 \\ D_{X2}\frac{\partial^2 X2}{\partial\theta^2} &= 0, L_1/2 \leq \theta < (L - L_1)/2 \\ -k_2 X2 + D_{X2}\frac{\partial^2 X2}{\partial\theta^2} &= 0, (L - L_1)/2 \leq \theta < L/2 \end{aligned} \tag{D.10}$$

Note that $X1$ has been eliminated in the first equation. We see that this equation is independent of S and hence so is $X2$, even though the profile is not homogeneous. Therefore step changes in S result in locally adaptive responses for $X3$.

Overall, we see how, depending on the position of the signal in an open spatial cascade,

one can maintain adaptive responses in some cases, and distort it in others. In contrast, exact adaptive responses result when the entire cascade is spatially localized in one location, irrespective of the position of the signal in the cascade. Numerical results for the open irreversible cascade are shown in Fig. S4.

### D.2.8 Communicating layer of cascade with multiple diffusing entities

While examining spatially separated model of cascades, we examined situations where the output of one level of the cascade acted as the communicating species. We now examine a variant of this scenario where both the modified and unmodified form are diffusible. In this case the two segments of the cascade may be regarded as being connected via a global layer.

We therefore examine the dynamics of this global layer. For simplicity we will assume that all relevant reactions involving the interconversion of these species act via mass action kinetics, and there is negligible retroactivity in the downstream reaction. We will refer to the species as $X$ and $X^*$ and assume both have the same diffusion coefficient $D$. At steady state we have

$$\begin{aligned} -k_f K(\theta) X + k_r P(\theta) X^* + D\frac{\partial^2 X}{\partial \theta^2} &= 0, \\ k_f K(\theta) X - k_r P(\theta) X^* + D\frac{\partial^2 X^*}{\partial \theta^2} &= 0 \end{aligned} \tag{D.11}$$

Here $K(\theta), P(\theta)$ refer to the kinase and phosphatase profiles. When we consider cascades of the kind examined earlier, $K(\theta)$ will be non-zero only in the first location.

By adding the above equations we find that at steady state $X + X^*$ is a constant, uniform in space. We call this constant $X_T$. Therefore the equation simplifies to

$$k_f K(\theta)(X_T - X^*) - k_r P(\theta) X^* + D\frac{\partial^2 X^*}{\partial \theta^2} = 0 \tag{D.12}$$

We will focus on some specific aspects of the profile of $X^*$. In general, in such a scenario, we may expect different possibilities for where the phosphatase is located. It may be located everywhere in the domain, it may be located in the second location, or it may be

located in the first location.

In the case where the phosphatase is present everywhere in the domain, the above steady state can be obtained, and the resulting profile depends on the diffusion coefficient (see Fig. D.5). Similarly when the phosphatase is in the second location only, the profile obtained, depends on all parameters, and depends on the diffusion coefficient. In both cases, when the diffusion coefficient becomes high, $X^*$ attains a profile which is uniform.

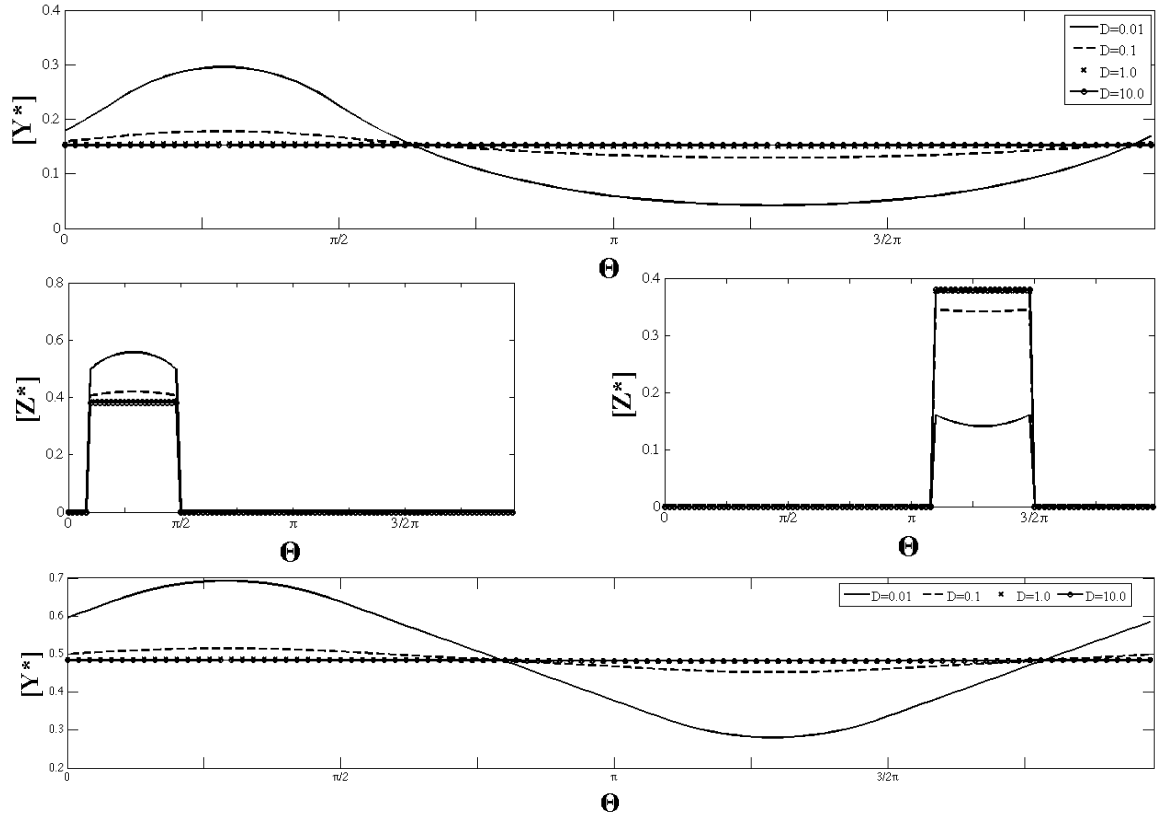


Figure D.5: **A three step cascade with a global second step.** Y and Y$^*$ both diffuse: the spatial concentration profiles of Y$^*$ (second step) and Z$^*$ (last step) are shown for different scenarios. (A) P2 is uniform and present everywhere in the domain. In the bottom LHS plot Z$^*$ is in location 1 and in the bottom RHS plot Z$^*$ is in the opposite location. The profile of the Z$^*$ is determined by the diffusion coefficient values of Y and Y$^*$ and its own position in the domain. The arrow denotes the direction of increasing diffusion coefficient for Y and Y$^*$. (B) P2 is in the second location and the resultant profile of Y$^*$ is shown. The spatial profile of Z$^*$ behaves in a similar fashion as in (A). Increasing the diffusion coefficient flattens the profile of $Y^*$.

In the case where the phosphatase is co-localized with the kinase, in the first location, we notice something different. When the kinase and phosphatase profile is uniform in this location, we have

$$X^* = X_T \frac{K/P}{k_r/k_f + K/P} \tag{D.13}$$

The point to note is that this concentration profile is uniform in space, and this is independent of the diffusion coefficient value. Thus we find that co-localizing the kinase and phosphatase of a global communicating layer can insulate the cascade from the effects of diffusivity or size of the domain. This points to another aspect of design and spatial organization of cascades.

## D.3 Parameter Values

Parameters and Additional Information about the Models:

In this section details about parameter values used in individual figures are presented. All equations are non-dimensionalized, and the appropriate parameter values are dimensionless. Most of the essential trends seen here are seen for other parameter values (domain lengths, diffusion coefficients).

### Two Step Cascade (Fig. 5.2)

The parameters are: $k_1 = k_3 = k_5 = k_7 = 0.1, k_{-1} = k_{-3} = k_{-5} = k_{-7} = 1.0, k_2 = k_6 = 0.05, k_4 = k_8 = 0.1$; Total Substrate = 2.0; Total Kinase= 1.0, Total Phosphatase P1=0.3, Total Phosphatase P2=0.5. A range of diffusion coefficients were tested from low $D_{X*} = 0.01$. to intermediate $= 0.1, 1.0$ to high $10.0$ for all figures. A: width of localized patches is 1/5th of domain length.

### Three Step Cascade (Fig. 5.2)

Parameter values are based on Huang and Ferrell. The association rate constants for step 1 (X and $X^*$) of the cascade are: $k_1 = k_3 = 1000$; for step 2 (Y to $Y^*$) are $k_5 = k_7 = 1000$; and for step 3 (Z to $Z^*$) are $k_9 = k_{11} = 1000$. The dissociation rate constants for each step are $k_{-1} = k_{-3} = 150$ (step 1); $k_{-5} = k_{-7} = 150$ (step 2) and $k_{-9} = k_{-11} = 150$ (step 3), and the catalytic constants are (step 1) $k_2 = k_4 = 150$; (step 2) $k_6 = k_8 = 150$ and (step 3) $k_{10} = k_{12} = 150$. Total Substrates $X^* = 0.003, Y^* = Z^* = 1.2$, Total Phosphatases

$P1 = P2 = 0.0003, P3 = 0.12$. A: width of localized patches is 1/5 th of of domain length. B: width of patches is 1/50th of domain length.

## Three Step Cascade with a transient input (Fig. 5.3)

For this analysis, the first reaction in the first step (X is converted to X*) in the three step cascade model is modified. For simplicity, the reaction is in the mass action regime. This allowed us to directly regulate the free/total Kinase concentration [K] (which is the transient input). $[K] = 0.1$, forward rate constant associated with K $k_1 = 1.0$. Spatial width of the patch was varied (as a fraction of domain length) and temporal duration of the pulse is t=10. Rest of the parameters are same as in Figure 3 (in this case $k_{-1}$ and $k_2 = 0$).

## Multisite phosphorylation (Fig. 5.4)

The parameters are: A and B: $k_1 = k_3 = k_5 = k_7 = 0.1, k_{-1} = k_{-3} = k_{-5} = k_{-7} = 1.0, k_2 = k_6 = 0.05, k_4 = k_8 = 0.1$; Total Substrate = 2.0; Total Kinase K1= 1.0, Total Phosphatase P1=0.3, Total Kinase K2= 1.0; Total Phosphatase P2=0.5. C:$k_1 = k_3 = k_7 = 1.0 k_5 = 0.2, k_{-1} = k_{-3} = k_{-5} = k_{-7} = 1.0, k_2 = k_6 = 0.05, k_4 = k_8 = 0.1$; Total Substrate = 2.0; Total Kinase K1= 0.5, Total Phosphatase P=0.3, Total Kinase K2= 0.5; C: width of localized patches is 1/5th of domain length. Diffusion coefficient shown is 0.01.

## Phosphorelay (Fig. 5.4)

Parameters are: A, B and D: $k_s = 1.0 = k_1 = k_3 = k_5 = k_{p1} = k_{p3} = k_{p5} = k_{p7} = 0.1$, the dissociation rate constants are $k_{-1} = k_{-3} = k_{-5} = k_{-p1} = k_{-p3} = k_{-p5} = k_{-p7} = 1.0$ and the catalytic rate constants are $k_2 = k_4 = k_6 = 0.05, k_{p2} = k_{p4} = k_{p6} = k_{p8} = 0.1$. Total Substrates $X1 = X2 = X3 = X4 = 2.0$; Input signal $K = 1.0$, Total Phosphatase $P1 = P3 = P4 = 0.3$, Total Phosphatases $P2 = P3 = 0.5$; C: Same as above except $k_{-p7} = k_{p8} = 0.0$. Total Substrate $X1 = X2 = X3 = X4 = 2.0$; Total Phosphatases $P1 = P3 = 0.3$, Total Phosphatases $P2 = 0.5$ A, B and C: width of localized patches is 3/10th of domain length.

## Fig. D.1

The parameters are: $k_1 = k_3 = k_7 = 0.1, k_5 = 0.2, k_{-1} = k_{-3} = k_{-5} = k_{-7} = 1.0, k_2 = k_6 = 0.05, k_4 = k_8 = 0.1$; Total Substrate $X = 2.0$; Total Kinase $K = 1.0 + 0.3cos\theta$, Total Substrate $Y = 1.0$; Total Phosphatase $P1 = P2 = 1 + 0.2Cos(\pi + \theta)$. All upstream X species are weakly diffusing at $D_{X*} = 0.001$ and Y and YX$^*$ diffuse at $D = 1.0$.

## Fig. D.2

$k_1 = k_3 = 10.0, k_{-1} = k_{-3} = 1.0, k_2 = k_4 = 0.1$ Total Substrate $= 2.0$, Total Phosphatase $P = 0.03$. Width of the localized patch is 1/5th of domain length. A range of diffusion coefficients were tested from low $D_{X*} = 0.01$ to intermediate $= 0.1 and 1.0$ to high $10.0$. The diffusion coefficient shown here is D$= 1.0$.

## Fig. D.3

$k_1 = k_3 = k_7 = 0.1, k_5 = 0.2, k_{-1} = k_{-3} = k_{-5} = k_{-7} = 1.0, k_2 = k_6 = 0.05, k_4 = k_8 = 0.1$; Total Substrate $= 2.0$; Total Kinase K$= 0.5$, Total Phosphatase P$= 0.5$. The width of localized patches is 1/5 th of domain length. A range of diffusion coefficients were tested from low $D_{X*} = 0.01$ to intermediate $= 0.1 and 1.0$ to high $10.0$. The diffusion coefficient shown here is D$= 0.01$.

## Fig. D.4

Top row: $k_o = 0.1; S = 0.2; k_s = 1.0; k_2 = 0.5; k_d = 1.0$, Total Substrates $X1 = 0.2, X2 = 1.0, X3 = 0.1$. Row 2: $k_o = 0.1; S = 0.2; k_1 = 0.5; k_s = 1.0; k_d = 1.0$, Total Substrates $X1 = 0.2, X2 = 1.0, X3 = 0.1$. RHS plots: $D_{X2} = 0.01$ (solid line) and $D_{X2} = 10.0$ (dashed line) Width of localized patches is 1/5th of domain length.

## Fig. D.5

(A and B) $k_1 = k_3 = k_7 = k_{11} = 0.1, k_5 = 0.2$ and $k_9 = 0.3$, the dissociation rate constants are $k_{-1} = k_{-3} = k_{-5} = k_{-7} = k_{-9} = k_{-11} = 1.0$, and the catalytic constants are $k_2 = k_6 = k_{10} = 0.05, k_4 = k_8 = k_{12} = 0.1$. Total Substrates $X^* = 2.0, Y^* = 1.0; Z^* = 1.2$, Total Phosphatases $P1 = 0.5; P2 = 1.0, P3 = 0.5$, Total Kinase $K = 1.0$. The diffusion coefficients of Y and Y$^*$ are equal and are D=0.01 (solid line), D=0.1 (dashed

line), D=1.0 (crosses) and D=10.0 (solid line with circles). Width of localized patches is 1/5th of domain length.

# Appendix E

# *Caulobacter* Cell Signalling networks: Bifunctional enzymes, bistable models and parameters values.

## E.1 Brief synopsis of bifunctional enzymes

Bifunctional enzymes are found in most organisms from prokaryotes to eukaryotes. In bacteria, widely occurring signal transduction networks generally known as Two-component systems (TCSs) and phosphorelays often contain bifunctional enzymes (Marks et al., 2009). These enzymes may either function as kinases or phosphatases. TCSs and phosphorelays form building blocks of a wide range of regulatory processes (such as osmotic regulation and nitrogen fixation) that allow bacterial cell to function and survive (Marks et al., 2009). In eukaryotes, bifunctional enzymes occur in different contexts for example in metabolic pathways and biosynthesis pathways (Michels and Rigden, 2006; Paul et al., 2010).

Many aspects of bifunctional enzymes are the focus of recent experimental and modeling efforts. The focus of many modeling efforts (especially in the context of TCSs and phosphorelays) is to understand how signal from the environment of the cell is received by a bifunctional kinase and transduced to other components in the network (Straube, 2013, 2014). Other modelling studies revolve around what types of mechanisms of signal flow combined with particular enzyme structures may (or may not) lead to special temporal behaviours (for e.g. ultrasensitive behavior or robustness against noise) (Shinar and Feinberg, 2010). Other studies model individual networks in detail where bifunctional enzymes are

present (Chen et al., 2011; Subramanian et al., 2013; Tropini and Huang, 2012). The focus of these studies is mainly the temporal aspects of signaling. Experimental studies on bifunctional enzymes are varied and context dependent- from understanding specific interactions between enzyme and substrates to unearthing the structure of particular enzymes to capturing the role of bifunctional enzymes in different biological systems (Paul et al., 2010; Stewart, 2010; Zheng and Jia, 2010).

## E.2 Discussion on the number of catalytic sites in a bifunctional enzyme

In our investigation we assumed that the enzyme has a single catalytic site. This assumption was based on based on the hypothesis that in many known bifunctional sensor kinases enzymes found in bacteria the forward and reverse modifications occur on a single catalytic site (Jiang et al., 2000; Stewart, 2010; Zheng and Jia, 2010). Bifunctional enzymes with two distinct catalytic sites have also been observed in experiments (Ventura et al., 2010) and have been modelled accordingly (Shinar and Feinberg, 2010). These enzymes may form dimers or ternary complexes with the substrates. We did not consider these possibilities in our analysis; since our main aim was to study the effects of spatial perturbations we kept the models as simple as possible to ascertain a fundamental understanding without invoking such effects. The study of these interactions in conjunction with spatial effects could be the goal of a separate future study).

## E.3 Modification of Building Block Model II

Model II was modified slightly in order to achieve a sharper sensitivity or input-output curve. The modification was based on the model in (Straube, 2014)). This model takes the conservation of the ligand or signal (which in this case regulates the conversion of $E^*$ to E) into explicit consideration:

$$[S_{total}] = [S] + E + X^*E \tag{E.1}$$

The sensitivity curve was obtained by plotting $X^*$ against the total concentration of the signal $S_{total}$. This is shown in Fig. 6.6.

## E.4 A second model for the bistable response

Model IV.II: This model is capable of exhibiting a bistable response which arises due to the presence of the cooperative positive feedback interaction between $X^*$ and $E^*$. The equations governing this model are:

$$\begin{aligned} \frac{\partial[X^*]}{\partial t} &= k_1[X][E^*] - k_2[X][E] + D_{X^*}\frac{\partial^2 X^*}{\partial\theta^2} \\ \frac{\partial[E^*]}{\partial t} &= k_3[S][E] - k_4[E^*] + k_{pf}[X]^2[E] + D_{E^*}\frac{\partial^2 E^*}{\partial\theta^2} \end{aligned} \tag{E.2}$$

where $k_1$ and $k_2$ are the forward and backward rate constants associated with the conversion of E to $E^*$. $k_3$ and $k_4$ are the rate constants for the binding of the signal to E and the basal conversion of $E^*$ to E. $k_{pf}$ is the feedback rate constant from $X^*$ to $E^*$.) A summary of the main results is shown in Fig. E.1.

## E.5 Phosphotransfer mechanism in the building block model combinations

In the second part of the analysis where interaction in different building block combinations BBC1 and BBC2 were examined- the modification cycles were modelled as phosphor-signalling pathways. The associated kinases (DivJ and CckA) carry out phosphotransferase reactions (as opposed to covalent modifications of the substrate). The basic reactions for the phosphotransfer mechanism are:

$$X + E^* \underset{k_{-1}}{\overset{k_1}{\rightleftharpoons}} XE^* \xrightarrow{k_2} X^* + E$$

$$X^* + E \underset{k_{-3}}{\overset{k_3}{\rightleftharpoons}} X^*E \xrightarrow{k_4} X + E$$

For the purposes of this analysis, the second reaction is the dephosphorylation reaction (that is the same as in covalent modification mechanism). The "reverse phosphorelay" reaction where $X^*$ transfers its phosphate group to E form of the enzyme in the reverse reaction (resulting in X and $E^*$) is not considered in this study. This is simply because in the biological networks under consideration the relevant enzymes are believed to dephosphorylate the product. The equations for this mechanism are given by:

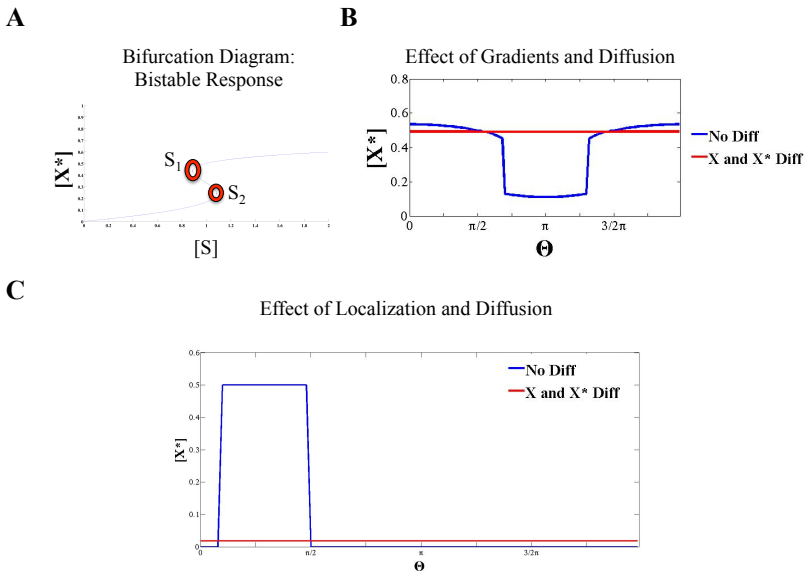


Figure E.1: **Spatial effects in Model IV.II: distortion of the bistable response.** (A) A bifurcation curve is shown for $X^*$ with respect to the parameter [S]. Critical values S1 and S2 are labeled. (B) The bistable response is perturbed by a graded external signal: The concentration profile of $X^*$ shows a spatial switch-like characteristic when none of the species diffuse (blue line). When both X and $X^*$ diffuse (red line) this switch-like character is lost and the profile is homogenous. (C) Perturbation by localization and diffusion: All species are localized together in one patch of the spatial domain. When none of the species diffuse (blue line) the profile of $X^*$ has an amplitude commensurate with the higher steady state branch. If both X and $X^*$ diffuse (red line), the concentration of $X^*$ reduces and the bistable response is lost.

$$\begin{aligned}
\frac{\partial[E^*]}{\partial t} &= -k_s[S][E^*] + k_{fb}[E] - k_{bb}[E^*] - k_1[X][E^*] + k_{-1}[XE^*] + D_{E^*}\frac{\partial^2 E^*}{\partial\theta^2} \\
\frac{\partial[E]}{\partial t} &= k_s[S][E^*] - k_{fb}[E] + k_{bb}[E^*] - k_3[X^*][E] + k_{-3}[X^*E] + k_4[X^*E] \\
&\quad + k_2[XE^*] + D_E\frac{\partial^2 E}{\partial\theta^2}
\end{aligned} \tag{E.3}$$

The difference between this mechanism and the covalent modification mechanism may seen in the PDE for [E*]. In the phosphotransfer mechanism the $k_2[XE^*]$ term is excluded in the equation; it is now present in the PDE for [E]. The modules in BBC1 and BBC2 were modelled accordingly.

## E.6 Parameters values

### Fig. 6.5

(A,B) Model I: $k_1 = 0.1, k_{-1} = 1.0, k_2 = 0.05, k_3 = 0.1, k_{-3=1.0}, k_4 = 0.1$, $S(\theta) = 1 + 0.3Cos\theta$ (C,D) Model II: $k_s = 1.0, k_1 = 0.01, k_2 = 0.5$, $k_3 = 0.1, k_{-3} = 1.0, k_4 = 0.05$, $k_5 = 0.1, k_{-5} = 1.0, k_6 = 0.1$, $S = 1 + 0.3Cos\theta$ (A,B,C,D) A range of diffusion coefficients are tested in each case: D=0,0.01,0.1,1.0,10. $[X_{TOTAL}] = 2.0, [E_{TOTAL}] = 1.0$

### Fig. 6.6

(A,B) $k_s = 1.0, k_2 = 0.001$, $k_3 = 20.0, k_{-3} = 1.0, k_4 = 1.0$, $k_5 = 20.0, k_{-5} = 1.0, k_6 = 1.0$, $S(\theta) = 0.05 + 0.02Cos\theta$ A range of diffusion coefficients are tested in each case: D=0,0.01,0.1,1.0,10. $[X_{TOTAL}] = 10.0, [E_{TOTAL}] = 0.1$ (B) Shown: D=0.1

### Fig. 6.7

(A,B,C) $k_s = 1.0, k_1 = 1.0, k_{-1} = 1.0, k_2 = 10.0$, $k_3 = 1.0, k_{-3} = 1.0, k_4 = 10.0$, $k_{pf} = 0.05$ $[X_{TOTAL}] = 2.0, [E_{TOTAL}] = 1.0$ $S_{critical} = 0.1$ A range of diffusion coefficients are tested in each case: D=0,0.01,0.1,1.0,10. (B) CASE1: $S = 0.07 + 0.03Cos\theta$ CASE3: $S = 0.1 + 0.03Cos\theta$ (C) $S = 0.05$ $W = 20\%$ (LHS), $W = 90\%$ (RHS)

### Fig. 6.8

(A) $S_1 = 0.4551, S_2 = 0.802$ $k_s = 1.0, k_1 = 0.00, k_2 = 0.0$, $k_3 = 1.0, k_{-3} = 1.0, k_4 = 10.0$, $k_5 = 1.0, k_{-5} = 1.0, k_6 = 10.0$, $k_{pf} = 8.0, k_7 = 2.0, k_8 = 1.0, k_b = 0.001$, (B) $[X_{TOTAL}] = 1.0, [E_{TOTAL}] = 10.0$ CASE1: $S = 0.5 + 0.2Cos\theta$ CASE3: $S = 0.6 + 0.1Cos\theta$ A range of diffusion coefficients are tested in each case: D=0,0.01,0.1,1.0,10. (C) $[X_{TOTAL}] = 1.0, [E_{TOTAL}] = 5.0$ LHS: $S = 0.6$ $W = 20\%$ RHS: $k_{pf} = 8.6, S = 0.6, W = 90\%$

### Fig. 6.9

(A,B) $k_1 = 0.1, k_{-1} = 1.0, k_2 = 0.05, k_3 = 0.1, k_{-3=1.0}, k_4 = 0.1$, $k_{s1} = 2.0, k_{b1} = 1.0, k_{s2} = 1.0, k_{b2} = 1.0$, $[X_{TOTAL}] = 2.0, [E_{TOTAL}] = 0.1$ A range of diffusion co-

efficients are tested in each case: D=0,0.01,0.1,1.0,10. (A) $S1 = 1 + 0.3Cos\theta$ , $S2 = 1 + 0.2Cos(\theta + \pi)$ (B) $S1 = 0.5, S2 = 0.5, W = 20\%$

## Fig. 6.10

(A,B) Upstream module: $k1 = 0.1, k_{-1} = 1.0, k_2 = 0.05$, $k_3 = 0.2, k_{-3} = 1.0, k_4 = 0.1$, $k_j = 1.0, k_{fj} = 1.0$, Downstream Module $k_a = 0.1, k_{-a} = 1.0, k_b = 0.05$, $k_c = 0.2, k_{-c} = 1.0, k_d = 0.1$, $k_{ff} = 1.0, k_{bb} = 1.0$, Intermediate: $k_i = 1.0, k_f i = 1.0, k_b i = 1.0, k_5 = 2.0$ $[DivK_{TOTAL}] = 2.0, [PleC_{TOTAL}] = [DivJ_{TOTAL}] = 1.0$ $[CtrA_{TOTAL}] = 1.0, [CckA_{TOTAL}] = 1.0, [DivL_{TOTAL}] = 1.0$ (B)A range of diffusion coefficients are tested in each case: D=0,0.01,0.1,1.0,10. Shown: D=0,0.01. (C) Upstream module,Intermediate and Downstream are the same as (A) except: $k_6 = 1.0$ Parameter $k_5$ is varied=1.0,2.0,5.0,10.0 Shown:D=0,0.01.

## Fig. 6.11

Same as Fig. 6.10 (A) Parameter $k_i$ is varied=1.0,2.0,5.0,10.0 Shown:D=0.01.

## Fig. 6.12

(A,B) Upstream module: $k1 = 1.0, k_{-1} = 1.0, k_2 = 10.0$, $k_3 = 1.0, k_{-3} = 1.0, k_4 = 10.0$, $k_{fxp} = 2.0, k_{bxp} = 1.0$,(Inhibition of X on E) $k_{pf} = 8.8$, (Positive feedback between $X^*$ and $E^*$ $k_{ba} = 1.0, k_{bba} = 0.001$, ($E^*$ and E conversion) $[DivK_{TOTAL}] = 1.0, [E_{TOTAL}] = 5.0$ $[CtrA_{TOTAL}] = 1.0, [CckA_{TOTAL}] = 1.0, [DivL_{TOTAL}] = 1.0$ Intermediate and Downstream are the same as (A) in Fig. 6.11 except: $k_5 = 1.0, k_6 = 1.0$ [S]=1.0. Shown:D=0,0.01.

## Fig. 6.13

(A) Model A: $k_j(\theta)$ =20.0, $k_k$=1.0, $k_c(\theta)$=20.0, $k_p$=1.0, $k_b$=1.0, $k_u$=0.5. sw($\theta$)=1.0; D=2.0, $k_{po}$=0.1; $[DivK_{TOTAL}] = 2.0$, (B)Model B: $k_{ph}$=100; and $k_{dp}$=10; $k_{pho}$ and $k_{do}$=0.1, Sw($\theta$) and St($\theta$)=1.0; $D_C$=2.0; $[CtrA_{TOTAL}] = 1.0$

## Fig. 6.14

(A,B) Upstream and Downstream same as Fig. 6.13 (A) and (B), respectively. Intermediate interaction: $k_{bi} = 1.0; k_5 = 1.0; k_{fi} = 1.0; K_{total} = 1.0; k_f = 1.0; k_r = 0.01;$ $[DivL_{TOTAL}] = 2.0$ Parameter $k_5$ is varied=1.0,2.0,5.0,10.0 (C) Same as (A,B) except: $k_6$=1.0

## Fig. 6.15

(A) Same as (A) in Fig. 6.13 and $k_f$=20, $k_{-f}$=2.0, $k_e$=20, $k_p$=20.0; $D_P$=10.0; $t_a$=4000, $t_b$=8000; $t_f$=20,000 (B) Same as in (A) except $k_k$=$k_p$=40.0, (C) Delocalized Mutant: $k_j(\theta)$ is now $k_j$ =20.0 and on everywhere (D) Mislocalized Mutant: $k_j(\theta)$ is on at the opposite pole.

# References

Agapakis, C. M., Boyle, P. M., and Silver, P. A. (2012). Natural strategies for the spatial optimization of metabolism in synthetic biology. *Nature Chemical Biology*, 8(6):527–535.

Aguda, B. D. (1999). A quantitative analysis of the kinetics of the g(2) dna damage checkpoint system. *Proceedings of the National Academy of Sciences of the United States of America*, 96(20):11352–11357.

Alam-Nazki, A. and Krishnan, J. (2010). A mathematical modelling framework for understanding chemorepulsive signal transduction in dictyostelium. *Journal of Theoretical Biology*.

Alam-Nazki, A. and Krishnan, J. (2012). An investigation of spatial signal transduction in cellular networks. *BMC Systems Biology*, 6(1):83.

Alam-Nazki, A. and Krishnan, J. (2013). Covalent modification cycles through the spatial prism. *Biophysical Journal*, 105(7):1720–1731.

Alam-Nazki, A. and Krishnan, J. (2014). Spatial control of chemical modification cascades and pathways, *Biophysical Journal, (under revision*).

Albeck, J. G., Burke, J. M., Spencer, S. L., Lauffenburger, D. A., and Sorger, P. K. (2008). Modeling a snap-action, variable-delay switch controlling extrinsic cell death. *PLoS Biol*, 6(12):2831–2852.

Alberts, B. et al. (2002). Molecular biology of the cell.

Alon, U. (2006a). *An Introduction to Systems Biology: Design Principles of Biological Circuits*. Chapman and Hall/CRC.

Alon, U. (2006b). *An Introduction to Systems Biology: Design Principles of Biological Circuits*. Chapman and Hall/CRC.

Altschuler, S. J., Angenent, S. B., Wang, Y., and Wu, L. F. (2008). On the spontaneous emergence of cell polarity. *Nature*, 454(7206):886–889.

Arrieumerlou, C. and Meyer, T. (2005). A local coupling model and compass parameter for eukaryotic chemotaxis. *Developmental Cell*, 8(2):215–227.

Ausmees, N. and Jacobs-Wagner, C. (2003). Spatial and temporal control of differentiation and cell cycle progression in caulobacter crescentus. *Annual Reviews in Microbiology*, 57(1):225–247.

Barkai, N. and Leibler, S. (1997). Robustness in simple biochemical networks. *Nature*, 387(6636):913–917.

Bashor, C. J., Helman, N. C., Yan, S., and Lim, W. A. (2008). Using engineered scaffold interactions to reshape map kinase pathway signaling dynamics. *Science*, 319(5869):1539–1543.

Bastein D. Gomperts, IJsbrand M. Kramer, P. E. T. (2009). *Signal Transduction*. Academic Press, 2nd Edition.

Behar, M., Hao, N., Dohlman, H. G., and Elston, T. C. (2007). Mathematical and computational analysis of adaptation via feedback inhibition in signal transduction pathways. *Biophysical Journal*, 93(3):806–821.

Berridge, M. J., Lipp, P., and Bootman, M. D. (2000). The versatility and universality of calcium signalling. *Nature Reviews Molecular Cell Biology*, 1(1):11–21.

Blenis, J. and Resh, M. D. (1993). Subcellular localization specified by protein acylation and phosphorylation. *Current Opinion in Cell Biology*, 5(6):984–989.

Brown, G. C. and Kholodenko, B. N. (1999). Spatial gradients of cellular phospho-proteins. *FEBS letters*, 457(3):452–454.

Buchler, N. E. and Louis, M. (2008). Molecular titration and ultrasensitivity in regulatory networks. *Journal of Molecular Biology*, 384(5):1106–1119.

Calabrese, E. J. (2001). Cell migration/chemotaxis: biphasic dose responses. *Critical Reviews in Toxicology*, 31(4-5):615–624.

Calabrese, E. J. (2005). Hormetic dose-response relationships in immunology: occurrence, quantitative features of the dose response, mechanistic foundations, and clinical implications. *Critical Reviews in Toxicology*, 35(2-3):89–295.

Caudron, M., Bunt, G., Bastiaens, P., and Karsenti, E. (2005). Spatial coordination of spindle assembly by chromosome-mediated signaling gradients. *Science*, 309(5739):1373–1376.

Chen, A. H. and Silver, P. A. (2012). Designing biological compartmentalization. *Trends in Cell Biology*, 22(12):662–670.

Chen, Y. E., Tropini, C., Jonas, K., Tsokos, C. G., Huang, K. C., and Laub, M. T. (2011). Spatial gradient of protein phosphorylation underlies replicative asymmetry in a bacterium. *Proceedings of the National Academy of Sciences of the United States of America*, 108(3):1052–1057.

Chen, Y. E., Tsokos, C. G., Biondi, E. G., Perchuk, B. S., and Laub, M. T. (2009). Dynamics of two phosphorelays controlling cell cycle progression in caulobacter crescentus. *Journal of Bacteriology*, 191(24):7417–7429.

Collier, J. and Shapiro, L. (2007). Spatial complexity and control of a bacterial cell cycle. *Current Opinion in Biotechnology*, 18(4):333–340.

Conchonaud, F., Nicolas, S., Amoureux, M.-C., Ménager, C., Marguet, D., Lenne, P.-F., Rougon, G., and Matarazzo, V. (2007). Polysialylation increases lateral diffusion of neural cell adhesion molecule in the cell membrane. *Journal of Biological Chemistry*, 282(36):26266–26274.

Cyert, M. S. (2001). Regulation of nuclear localization during signaling. *Journal of Biological Chemistry*, 276(24):20805–20808.

Daniels, B. R., Perkins, E. M., Dobrowsky, T. M., Sun, S. X., and Wirtz, D. (2009). Asymmetric enrichment of pie-1 in the caenorhabditis elegans zygote mediated by binary counterdiffusion. *The Journal of Cell Biology*, 184(4):473–479.

Dawes, A. T. and Edelstein-Keshet, L. (2007). Phosphoinositides and rho proteins spatially regulate actin polymerization to initiate and maintain directed movement in a one-dimensional model of a motile cell. *Biophysical Journal*, 92(3):744–768.

Del Vecchio, D., Ninfa, A. J., and Sontag, E. D. (2008). Modular cell biology: retroactivity and insulation. *Molecular Systems Biology*, 4(1).

Drubin, D. G. (2000). *Cell polarity*, volume 28. Oxford University Press, USA.

Eijkelenboom, A. and Burgering, B. M. (2013). Foxos: signalling integrators for homeostasis maintenance. *Nature reviews Molecular cell biology*, 14(2):83–97.

Eisenbach, M., Lengeler, J. W., Varon, M., Gutnick, D., Segall, J. E., Meilli, R., Firtel, R. A., Omann, G. M., Murakami, F., and Tamada, A. (2004). *Chemotaxis*. Imperial College Press.

Etoc, F., Lisse, D., Bellaiche, Y., Piehler, J., Coppey, M., and Dahan, M. (2013). Subcellular control of rac-gtpase signalling by magnetogenetic manipulation inside living cells. *Nature Nanotechnology*, 8(3):193–198.

Feliu, E. and Wiuf, C. (2012). Enzyme-sharing as a cause of multi-stationarity in signalling systems. *Journal of The Royal Society Interface*, 9(71):1224–1232.

Ferrell, J. E. (1996). Tripping the switch fantastic: how a protein kinase cascade can convert graded inputs into switch-like outputs. *Trends in Biochemical Sciences*, 21(12):460–466.

Ferrell, J. E. and Machleder, E. M. (1998). The biochemical basis of an all-or-none cell fate switch in xenopus oocytes. *Science*, 280(5365):895–898.

Ferrell, J. E. and Xiong, W. (2001). Bistability in cell signaling: How to make continuous processes discontinuous, and reversible processes irreversible. *Chaos*, 11(1):227–236.

García Véscovi, E., Sciara, M. I., and Castelli, M. E. (2010). Two component systems in the spatial program of bacteria. *Current Opinion in Microbiology*, 13(2):210–218.

Gierer, A. and Meinhardt, H. (1972). A theory of biological pattern formation. *Kybernetik*, 12(1):30–39.

Goldbeter, A. and Koshland, D. E. (1981). An amplified sensitivity arising from covalent modification in biological systems. *Proceedings of the National Academy of Sciences of the United States of America*, 78(11):6840–6844.

Goley, E., Toro, E., McAdams, H., and Shapiro, L. (2009). Dynamic chromosome organization and protein localization coordinate the regulatory circuitry that drives the bacterial cell cycle. In *Cold Spring Harbor symposia on quantitative biology*, pages sqb–2009. Cold Spring Harbor Laboratory Press.

Goley, E. D. (2013). Tiny cells meet big questions: a closer look at bacterial cell biology. *Molecular Biology of the Cell*, 24(8):1099–1102.

Good, M. C., Zalatan, J. G., and Lim, W. A. (2011). Scaffold proteins: hubs for controlling the flow of cellular information. *Science*, 332(6030):680–686.

Griffin, E. E., Odde, D. J., and Seydoux, G. (2011). Regulation of the mex-5 gradient by a spatially segregated kinase/phosphatase cycle. *Cell*, 146(6):955–968.

Howell, A. S., Savage, N. S., Johnson, S. A., Bose, I., Wagner, A. W., Zyla, T. R., Nijhout, H. F., Reed, M. C., Goryachev, A. B., and Lew, D. J. (2009). Singularity in polarization: rewiring yeast cells to make two buds. *Cell*, 139(4):731–743.

Huang, C.-Y. and Ferrell, J. E. (1996). Ultrasensitivity in the mitogen-activated protein kinase cascade. *Proceedings of the National Academy of Sciences of the United States of America*, 93(19):10078–10083.

Hurtley, S. (2009). Location, location, location. *Science*, 326:1205.

Huttenlocher, A. and Poznansky, M. C. (2008). Reverse leukocyte migration can be attractive or repulsive. *Trends in Cell Biology*, 18(6):298–306.

Iglesias, P. and Devreotes, P. N. (2008). Navigating through models of chemotaxis. *Current Opinion in Cell Biology*, 20:35–40.

Iniesta, A. A., Hillson, N. J., and Shapiro, L. (2010a). Cell pole–specific activation of a critical bacterial cell cycle kinase. *Proceedings of the National Academy of Sciences of the United States of America*, 107(15):7012–7017.

Iniesta, A. A., Hillson, N. J., and Shapiro, L. (2010b). Polar remodeling and histidine kinase activation, which is essential for caulobacter cell cycle progression, are dependent on dna replication initiation. *Journal of Bacteriology*, 192(15):3893–3902.

Jacobs, C., Hung, D., and Shapiro, L. (2001). Dynamic localization of a cytoplasmic signal transduction response regulator controls morphogenesis during the caulobacter cell cycle. *Proceedings of the National Academy of Sciences of the United States of America*, 98(7):4095–4100.

Janetopoulos, C., Ma, L., Devreotes, P. N., and Iglesias, P. A. (2004). Chemoattractant-induced phosphatidylinositol 3, 4, 5-trisphosphate accumulation is spatially amplified and adapts, independent of the actin cytoskeleton. *Proceedings of the National Academy of Sciences of the United States of America*, 101(24):8951–8956.

Jiang, P., Atkinson, M. R., Srisawat, C., Sun, Q., and Ninfa, A. J. (2000). Functional dissection of the dimerization and enzymatic activities of escherichia coli nitrogen regulator ii and their regulation by the pii protein. *Biochemistry*, 39(44):13433–13449.

Jilkine, A., Marée, A. F. M., and Edelstein-Keshet, L. (2007). Mathematical model for spatial segregation of the rho-family gtpases based on inhibitory crosstalk. *Bulletin of Mathe*, 69(6):1943–1978.

Kam, L., Shen, K., and Dustin, M. (2013). Micro-and nanoscale engineering of cell signaling. *Annual Review of Biomedical Engineering*, 15:305.

Karsenti, E. (2008). Self-organization in cell biology: a brief history. *Nature Reviews Molecular Cell Biology*, 9(3):255–262.

Katz, E. (2012). *Biomolecular Information Processing: From Logic Systems to Smart Sensors and Actuators*. John Wiley & Sons.

Keizer-Gunnink, I., Kortholt, A., , and Van Haastert, P. (2007). Chemoattractants and chemorepellents act by inducing opposite polarity in phospholipase C and PI3K signalling. *Journal of Cell*, 177:579–585.

Kholodenko, B. N. (2006). Cell-signalling dynamics in time and space. *Nature Reviews Molecular Cell Biology*, 7(3):165–176.

Kholodenko, B. N., Hancock, J. F., and Kolch, W. (2010). Signalling ballet in space and time. *Nature Reviews Molecular Cell Biology*, 11(6):414–426.

Klipp, E., Liebermeister, W., Wierling, C., Kowald, A., Lehrach, H., and Herwig, R. (2013). *Systems biology*. John Wiley & Sons.

Knudsen, M., Feliu, E., and Wiuf, C. (2012). Exact analysis of intrinsic qualitative features of phosphorelays using mathematical models. *Journal of Theoretical Biology*, 300:7–18.

Kondoh, K., Torii, S., and Nishida, E. (2005). Control of map kinase signaling to the nucleus. *Chromosoma*, 114(2):86–91.

Krauss, G. (2008). *Biochemistry of Signal Transduction and Regulation*. Wiley.

Krishnan, J. (2009). Signal processing through a generalized module of adaptation and spatial sensing. *Journal of Theoretical Biology*, 259(1):31–43.

Krishnan, J. (2011). Effects of saturation and enzyme limitation in feedforward adaptive signal transduction. *IET. Systems Biology*, 5(3):208.

Krishnan, J. and Alam-Nazki, A. (2011). An investigation of design principles underlying repulsive and attractive gradient sensing and their switching. *Journal of Theoretical Biology*, 273(1):80–99.

Krishnan, J. and Iglesias, P. (2007). Receptor-mediated and intrinsic polarization and their interaction in chemotaxing cells. *Biophysical journal*, 92(3):816–830.

Laloux, G. and Jacobs-Wagner, C. (2014). How do bacteria localize proteins to the cell pole? *Journal of Cell Science*, 127(1):11–19.

Lasker, K. and Shapiro, L. (2014). Towards optically reversible spatial mutations for dissecting the asymmetric developmental program of a bacterium.

Levchenko, A. and Iglesias, P. A. (2002). Models of eukaryotic gradient sensing: application to chemotaxis of amoebae and neutrophils. *Biophysical Journal*, 82(1 Pt 1):50–63.

Levskaya, A., Weiner, O. D., Lim, W. A., and Voigt, C. A. (2009). Spatiotemporal control of cell signalling using a light-switchable protein interaction. *Nature*, 461(7266):997–1001.

Li, S., Brazhnik, P., Sobral, B., and Tyson, J. J. (2008). A quantitative study of the division cycle of caulobacter crescentus stalked cells. *PLoS Computational Biology*, 4(1):e9.

Li, S., Brazhnik, P., Sobral, B., and Tyson, J. J. (2009). Temporal controls of the asymmetric cell division cycle in caulobacter crescentus. *PLoS Computational Biology*, 5(8):e1000463.

Li, S., Huang, N. F., and Hsu, S. (2005). Mechanotransduction in endothelial cell migration. *Journal of Cellular Biochemistry*, 96(6):1110–1126.

Lim, W. A. (2010). Designing customized cell signalling circuits. *Nature Reviews Molecular Cell Biology*, 11(6):393–403.

Lipkow, K. and Odde, D. J. (2008). Model for protein concentration gradients in the cytoplasm. *Cellular and Molecular Bioengineering*, 1(1):84–92.

Lipshtat, A., Jayaraman, G., He, J. C., and Iyengar, R. (2010). Design of versatile biochemical switches that respond to amplitude, duration, and spatial cues. *Proceedings of the National Academy of Sciences of the United States of America*, 107(3):1247–1252.

Liu, A. P. and Fletcher, D. A. (2009). Biology under construction: in vitro reconstitution of cellular function. *Nature Reviews Molecular Cell Biology*, 10(9):644–650.

Loose, M., Fischer-Friedrich, E., Ries, J., Kruse, K., and Schwille, P. (2008). Spatial regulators for bacterial cell division self-organize into surface waves in vitro. *Science*, 320(5877):789–792.

Ma, L., Janetopoulos, C., Yang, L., Devreotes, P. N., and Iglesias, P. A. (2004). Two complementary, local excitation, global inhibition mechanisms acting in parallel can explain the chemoattractant-induced regulation of pi (3, 4, 5) p¡ sub¿ 3¡/sub¿ response in dictyostelium cells. *Biophysical journal*, 87(6):3764–3774.

Maly, I. V., Steven Wiley, H., and Lauffenburger, D. A. (2004). Self-organization of polarized cell signaling via autocrine circuits: computational model analysis. *Biophysical journal*, 86(1):10–22.

Markevich, N. I., Tsyganov, M. A., Hoek, J. B., and Kholodenko, B. N. (2006). Long-range signaling by phosphoprotein waves arising from bistability in protein kinase cascades. *Molecular Systems Biology*, 2(1).

Marks, F., Klingmüller, U., and Müller-Decker, K. (2009). *Cellular signal processing: an introduction to the molecular mechanisms of signal transduction*. Garland Science New York, NY, USA.

Meyer, T. and Stryer, L. (1988). Molecular model for receptor-stimulated calcium spiking. *Proceedings of the National Academy of Sciences of the United States of America*, 85(14):5051–5055.

Michels, P. A. and Rigden, D. J. (2006). Evolutionary analysis of fructose 2, 6-bisphosphate metabolism. *IUBMB life*, 58(3):133–141.

Moore, T. I., Chou, C.-S., Nie, Q., Jeon, N. L., and Yi, T.-M. (2008). Robust spatial sensing of mating pheromone gradients by yeast cells. *PloS ONE*, 3(12):e3865.

Mori, Y., Jilkine, A., and Edelstein-Keshet, L. (2008). Wave-pinning and cell polarity from a bistable reaction-diffusion system. *Biophysical Journal*, 94(9):3684–3697.

Moseley, J. B., Mayeux, A., Paoletti, A., and Nurse, P. (2009). A spatial gradient coordinates cell size and mitotic entry in fission yeast. *Nature*, 459(7248):857–860.

Mueller, B. K. (1999). Growth cone guidance: first steps towards a deeper understanding. *Annual RevIew Neuroscience*, 22:351–388.

Muñoz-García, J., Neufeld, Z., and Kholodenko, B. N. (2009). Positional information generated by spatially distributed signaling cascades. *PLoS Computational Biology*, 5(3):e1000330.

Murray, J. D. (2008). *Mathematical Biology*. Springer.

Nakano, T., Eckford, A. W., and Haraguchi, T. (2013). *Molecular communication*. Cambridge University Press.

Narang, A. (2006). Spontaneous polarization in eukaryotic gradient sensing: a mathematical model based on mutual inhibition of frontness and backness pathways. *Journal of Theoretical Biology*, 240(4):538–553.

Nelson, W. J. (2003). Adaptation of core mechanisms to generate cell polarity. *Nature*, 422(6933):766–774.

Nishiyama, M. e. a. (2003). Cyclic AMP/GMP dependent modulation of calcium channels sets the polarity of nerve growth-cone turning. *Nature*, 423:990–995.

Ortega, F., Acerenza, L., Westerhoff, H. V., Mas, F., and Cascante, M. (2002). Product dependence and bifunctionality compromise the ultrasensitivity of signal transduction cascades. *Proceedings of the National Academy of Sciences of the United States of America*, 99(3):1170–1175.

Othmer, H. G. and Schaap, P. (1998). Oscillatory camp signaling in the development of dictyostelium discoideum. *Comments on Theoretical Biology*, 5:175–282.

Padte, N. N., Martin, S. G., Howard, M., and Chang, F. (2006). The cell-end factor pom1p inhibits mid1p in specification of the cell division plane in fission yeast. *Current Biology*, 16(24):2480–2487.

Park, C. S., Schneider, I. C., and Haugh, J. M. (2003). Kinetic analysis of platelet-derived growth factor receptor/phosphoinositide 3-kinase/akt signaling in fibroblasts. *Journal of Biological Chemistry*, 278(39):37064–37072.

Paul, D., Chatterjee, A., Begley, T. P., and Ealick, S. E. (2010). Domain organization in candida glabrata thi6, a bifunctional enzyme required for thiamin biosynthesis in eukaryotes. *Biochemistry*, 49(45):9922–9934.

Paul, R., Jaeger, T., Abel, S., Wiederkehr, I., Folcher, M., Biondi, E. G., Laub, M. T., and Jenal, U. (2008). Allosteric regulation of histidine kinases by their cognate response regulator determines cell fate. *Cell*, 133(3):452–461.

Peters, R. J., Marguet, M., Marais, S., Fraaije, M. W., van Hest, J., and Lecommandoux, S. (2014). Cascade reactions in multicompartmentalized polymersomes. *Angewandte Chemie International Edition*, 53(1):146–150.

Postma, M. and Van Haastert, P. (2001). A diffusion-translocation model for gradient sensing by chemotactic cells. *Biophysical journal*, 81(3):1314.

Poznansky, M. C., Olszak, I. T., Foxall, R., Evans, R. H., Luster, A. D., and Scadden, D. T. (2000). Active movement of t cells away from a chemokine. *Nature Medicine*, 6(5):543–548.

Purnick, P. E. and Weiss, R. (2009). The second wave of synthetic biology: from modules to systems. *Nature reviews Molecular cell biology*, 10(6):410–422.

Rappaport, R. (1971). Cytokinesis in animal cells. *International Review of Cytology*, 31:169–213.

Reisinger, S. J., Huntwork, S., Viollier, P. H., and Ryan, K. R. (2007). Divl performs critical cell cycle functions in caulobacter crescentus independent of kinase activity. *Journal of Bacteriology*, 189(22):8308–8320.

Rocks, O., Gerauer, M., Vartak, N., Koch, S., Huang, Z.-P., Pechlivanis, M., Kuhlmann, J., Brunsveld, L., Chandra, A., Ellinger, B., et al. (2010). The palmitoylation machinery is a spatially organizing system for peripheral membrane proteins. *Cell*, 141(3):458–471.

Rosse, C., Linch, M., Kermorgant, S., Cameron, A. J. M., Boeckeler, K., and Parker, P. J. (2010). Pkc and the control of localized signal dynamics. *Nature Reviews Molecular Cell Biology*, 11(2):103–112.

Rudner, D. Z. and Losick, R. (2010). Protein subcellular localization in bacteria. *Cold Spring Harbor Perspectives in Biology*, 2(4):a000307.

Rudner, D. Z., Pan, Q., and Losick, R. M. (2002). Evidence that subcellular localization of a bacterial membrane protein is achieved by diffusion and capture. *Proceedings of the National Academy of Sciences of the United States of America*, 99(13):8701–8706.

Sachdeva, G., Garg, A., Godding, D., Way, J. C., and Silver, P. A. (2014). In vivo co-localization of enzymes on rna scaffolds increases metabolic production in a geometrically dependent manner. *Nucleic Acids Research*, 42(14):9493–9503.

Saini, D. K., Chisari, M., and Gautam, N. (2009). Shuttling and translocation of heterotrimeric g proteins and ras. *Trends in Pharmacological Sciences*, 30(6):278–286.

Schwarz-Romond, T. and Gorski, S. A. (2010). Focus on the spatial organization of signalling. *THE EMBO Journal*, 29:2675–2676.

Seaton, D. and Krishnan, J. (2012). Effects of multiple enzyme-substrate interactions in basic units of cellular signal processing. *Physical Biology*, 9(4):045009.

Seaton, D. D. and Krishnan, J. (2011). The coupling of pathways and processes through shared components. *BMC systems biology*, 5(1):103.

Shahrezaei, V. and Swain, P. S. (2008). The stochastic nature of biochemical networks. *Current opinion in biotechnology*, 19(4):369–374.

Shannon, C. E. (1948). A mathematical theory of communication. *The Bell System Technical Journal*, 27:379–423.

Shapiro, L., McAdams, H. H., and Losick, R. (2009). Why and how bacteria localize proteins. *Science*, 326(5957):1225–1228.

Shinar, G. and Feinberg, M. (2010). Structural sources of robustness in biochemical reaction networks. *Science*, 327(5971):1389–1391.

Skupsky, R., Losert, W., and Nossal, R. J. (2005). Distinguishing modes of eukaryotic gradient sensing. *Biophysical Journal*, 89(4):2806–2823.

Soh, S., Byrska, M., Kandere-Grzybowska, K., and Grzybowski, B. A. (2010). Reaction-diffusion systems in intracellular molecular transport and control. *Angewandte Chemie International Edition*, 49(25):4170–4198.

Song, H., Ming, G., He, Z., Lehmann, M., McKerracher, L., Tessier-Lavigne, M., and Poo, M. (1998). Conversion of neuronal growth cone responses from attraction to repulsion by cyclic nucleotides. *Science*, 281:1515–18.

Stelling, J. and Kholodenko, B. N. (2009). Signaling cascades as cellular devices for spatial computations. *Journal of Mathematical Biology*, 58(1-2):35–55.

Stewart, R. C. (2010). Protein histidine kinases: assembly of active sites and their regulation in signaling pathways. *Current Opinion in Microbiology*, 13(2):133–141.

Straube, R. (2012). Comment on "load-induced modulation of signal transduction networks": reconciling ultrasensitivity with bifunctionality? *Science signaling*, 5(205):lc1.

Straube, R. (2013). Sensitivity and robustness in covalent modification cycles with a bifunctional converter enzyme. *Biophysical journal*, 105(8):1925–1933.

Straube, R. (2014). Reciprocal regulation as a source of ultrasensitivity in two-component systems with a bifunctional sensor kinase. *PLoS Computational Biology*, 10(5):e1003614.

Sturrock, M., Terry, A. J., Xirodimas, D. P., Thompson, A. M., and Chaplain, M. A. J. (2011). Spatio-temporal modelling of the hes1 and p53-mdm2 intracellular signalling pathways. *Journal of Theoretical Biology*, 273(1):15–31.

Subramanian, K., Paul, M., Tyson, J., and Rao, C. V. (2013). Potential role of a bistable histidine kinase switch in the asymmetric division cycle of caulobacter. *PLoS Computational Biology*.

Swaney, K. F., Huang, C.-H., and Devreotes, P. N. (2010). Eukaryotic chemotaxis: a network of signaling pathways controls motility, directional sensing, and polarity. *Annual Review of Biophysics*, 39:265–289.

Takahashi, K., Tănase-Nicola, S., and Ten Wolde, P. R. (2010). Spatio-temporal correlations can drastically change the response of a mapk pathway. *Proceedings of the National Academy of Sciences of the United States of America*, 107(6):2473–2478.

Thanbichler, M. (2009). Spatial regulation in caulobacter crescentus. *Current Opinion in Microbiology*, 12(6):715–721.

Tharp, W. G., Yadav, R., Irimia, D., Upadhyaya, A., Samadani, A., Hurtado, O., Liu, S.-Y., Munisamy, S., Brainard, D. M., Mahon, M. J., Nourshargh, S., van Oudenaarden, A., Toner, M. G., and Poznansky, M. C. (2006). Neutrophil chemorepulsion in defined interleukin-8 gradients in vitro and in vivo. *Journal of Leukocyte Biology*, 79(3):539–554.

Tindall, M., Maini, P., Porter, S., and Armitage, J. (2008). Overview of mathematical approaches to model bacterial chemotaxis 1: The single cell. *Bulletin of Mathema*, 70:1526–69.

Tropini, C. and Huang, K. C. (2012). Interplay between the localization and kinetics of phosphorylation in flagellar pole development of the bacterium caulobacter crescentus. *PLoS Computational Biology*, 8(8):e1002602.

Tsokos, C. G., Perchuk, B. S., and Laub, M. T. (2011). A dynamic complex of signaling proteins uses polar localization to regulate cell-fate asymmetry in caulobacter crescentus. *Developmental Cell*, 20(3):329–341.

Turing, A. M. (1952). The chemical basis of morphogenesis. *Philosophical Transactions of the Royal Society of London*, 237(1-2):37–72.

Turner, N. and Grose, R. (2010). Fibroblast growth factor signalling: from development to cancer. *Nature Reviews Cancer*, 10(2):116–129.

Tyson, J. J., Chen, K. C., and Novak, B. (2003). Sniffers, buzzers, toggles and blinkers: dynamics of regulatory and signaling pathways in the cell. *Current Opinion in Cell Biology*, 15(2):221–231.

Tyson, J. J. and Novák, B. (2010). Functional motifs in biochemical reaction networks. *Annual Review of Physical Chemistry*, 61:219.

Van Albada, S. B. and Ten Wolde, P. R. (2007). Enzyme localization can drastically affect signal amplification in signal transduction pathways. *PLoS Computational Biology*, 3(10):e195.

Vartak, N. and Bastiaens, P. (2010). Spatial cycles in g-protein crowd control. *The EMBO journal*, 29(16):2689–2699.

Ventura, A. C., Jiang, P., Van Wassenhove, L., Del Vecchio, D., Merajver, S. D., and Ninfa, A. J. (2010). Signaling properties of a covalent modification cycle are altered by a downstream target. *Proceedings of the National Academy of Sciences of the United States of America*, 107(22):10032–10037.

Ventura, A. C., Sepulchre, J.-A., and Merajver, S. D. (2008). A hidden feedback in signaling cascades is revealed. *PLoS Computational Biology*, 4(3):e1000041.

Vianello, F., Olszak, I. T., and Poznansky, M. C. (2005). Fugetaxis: active movement of leukocytes away from a chemokinetic agent. *Journal of Molecular Medicine*, 83(10):752–763.

Vilela, M., Morgan, J. J., and Lindahl, P. A. (2010). Mathematical model of a cell size checkpoint. *PLoS Computational Biology*, 6(12):e1001036.

Walsh, C. (2006). *Posttranslational modification of proteins: expanding nature's inventory*. Roberts and Company Publishers Englewood, CO.

Welf, E. S. and Haugh, J. M. (2012). Stochastic models of cell protrusion arising from spatiotemporal signaling and adhesion dynamics. *Methods in cell biology*, 110:223.

Wheeler, R. T. and Shapiro, L. (1999). Differential localization of two histidine kinases controlling bacterial cell differentiation. *Molecular Cell*, 4(5):683–694.

Xu, J., Wang, F., Keymeulen, A. V., Herzmark, P., Straight, A., Kelly, K., Takuwa, Y., Sugimoto, N., Mitchison, T., and Bourne, H. R. (2003). Divergent signals and cytoskeletal assemblies regulate self-organizing polarity in neutrophils. *Cell*, 114(2):201–214.

Yudushkin, I. A., Schleifenbaum, A., Kinkhabwala, A., Neel, B. G., Schultz, C., and Bastiaens, P. I. (2007). Live-cell imaging of enzyme-substrate interaction reveals spatial regulation of ptp1b. *Science Signalling*, 315(5808):115.

Zhao, M., Song, B., Pu, J., Wada, T., Reid, B., Tai, G., Wang, F., Guo, A., Walczysko, P., Gu, Y., et al. (2006). Electrical signals control wound healing through phosphatidylinositol-3-oh kinase-$\gamma$ and pten. *Nature*, 442(7101):457–460.

Zhao, Q., Yi, M., and Liu, Y. (2011). Spatial distribution and dose-response relationship for different operation modes in a reaction-diffusion model of the mapk cascade. *Physical Biology*, 8(5):055004.

Zheng, J. and Jia, Z. (2010). Structure of the bifunctional isocitrate dehydrogenase kinase/phosphatase. *Nature*, 465(7300):961–965.